An aptamer-based sensor for the detection of antimalarial drugs



Erin Sutton Coonahan

Linacre College

University of Oxford

A thesis submitted for the degree of

Doctor of Philosophy

Trinity 2019

Declaration of work

This dissertation is my own work and includes nothing which is the outcome of work done in collaboration except as declared in the text. No part of my dissertation has already been submitted, or is being concurrently submitted for any such degree, diploma, or other qualification at the University of Oxford or any other University or similar institution. It does not exceed the prescribed 50,000 word limit.

Acknowledgements

I first owe thanks to my supervisors for supporting this research. Carole Long, for taking on this project and for the encouragement, guidance, and confidence in me to allow me to keep failing until we finally created a working aptamer sensor. Maarten De Vos, for his continued support as the project goals evolved. Joel Tarning, for sharing his expertise and advice from the other side of the world and the PK lab at MORU for welcoming me during my short stints in Bangkok. Rick Fairhurst, for first supporting the project and guiding the initial project aims. Tom Wellems for his time, advice, and my own corner of bench space in his lab.

Thank you to my many colleagues at the Laboratory of Malaria and Vector Research at the National Institutes of Health. Kristin Lane, for patiently teaching me how to grow and transform E. coli and John Andersen, for his advice on the Biacore measurements. Thank you to everyone in the Long Lab, especially Kazutoyo for his invaluable advice.

I am very grateful to the Stojanovic lab at Columbia University. Thank you to Stevan Pecic for his synthetic chemistry help. Thank you, especially, to Kyung-Ae Yang whose aptamer selection protocol and advice were essential for the success of this project.

I would like to acknowledge the NIH Oxford Cambridge Scholars Program, whose support made this project possible. Thank you to the program leaders and the Biomedical Research Alliance. Thank you to all of my peers in the program and the mentors and role models whose advice and encouragement helped me succeed.

To the friends I made over the last four years, Megan Ansbro, Jessica Hostetler, Chanaki Amartagunta, and Kim Breglio, I am so grateful to have had your company in the lab. Kim and the rest of the Breglios, thanks for housing me and answering my many questions. Chanaki, thank you for being my teacher, friend, and cheerleader.

Finally, thank you to all of my friends and family who supported me over the last twenty-eight years. Mom and Michael, thank you for everything you did to get me to this point and thank you for always being proud of me. Dad and the boys, thank you for all that you've done, especially your frequent calls of encouragement. Scott, you are my best supporter of all. Thank you for inspiring me to be confident and encouraging me to follow my dreams. You are the best teammate and advocate and I can't wait for our future adventures together.

Abstract

Artemisinin-based combination therapies (ACTs) have begun to fail as first-line therapies for the treatment of *Plasmodium falciparum* malaria in Southeast Asia. Preventing the further spread of drug-resistant parasites is a top priority for global malaria elimination campaigns. A low-cost, field-based assay to detect slow-clearing ACT compounds from patient samples could allow for improved tracking of antimalarial drug use, monitoring of treatment adherence, and evaluation of therapeutic efficacy and resistance. It could also provide sensitive detection of active components in assessments of tablet quality. This research reports the development of a low-cost, rapid, fluorescent sensor for the specific detection of piperaquine and mefloquine. In order to do this, DNA aptamers were identified that bind and differentiate between small molecule partner drugs. These aptamers were selected from a library of single-stranded DNA molecules for their selectivity and binding affinity. Following their isolation by a capture-SELEX method, a structure-switching aptamer fluorescent sensor was developed.

The sensor performance was optimized for the detection of drug from crushed tablets and from human serum, resulting in two fluorescent sensing platforms. The sensors were evaluated for their sensitivity and specificity in relevant sample matrices and the serum sensor was validated against an LC-MS gold standard drug detection method. Feedback from potential assay end-users was collected to inform the assay development and it is believed that these aptamer sensors will be useful tools for monitoring antimalarial drug quality and studying antimalarial drug use.

Contents

List of Figures **ix**

List of Tables **xii**

List of Abbreviations **xiv**

1 Introduction **1**

1.1 Malaria . . . 1

1.1.1 History and burden of Malaria . . . 2

1.2 Antimalarial drugs . . . 4

1.2.1 Mechanisms of action of antimalarial drugs . . . 8

1.3 History of antimalarial resistance . . . 9

1.3.1 Looking ahead . . . 11

1.4 Methods for the detection of antimalarial drugs . . . 12

Detection methods to monitor drug use and efficacy . . . 12

Detection methods to assess medicine quality . . . 13

1.5 Aptamers . . . 14

1.5.1 Aptamer selection . . . 14

1.5.2 Aptamers against small molecule targets . . . 18

1.5.3 Aptamer applications . . . 20

1.6 Thesis aims . . . 22

2 Needs Assessment Survey **24**

2.1 Introduction . . . 24

2.1.1 Chapter 2 aims . . . 25

2.2 Methods . . . 25

2.2.1 Study design . . . 25

Interviews . . . 26

Web-based questionnaire . . . 26

2.3 Results . . . 27

2.3.1 Web-based questionnaire responses . . . 27

2.3.2 In-person interview responses . . . 29

2.3.3 Development of target product profiles (TPPs) . . . 32

2.4 Discussion . . . 32
2.4.1 Overview . . . 32
2.4.2 Limitations . . . 34
2.4.3 Conclusions . . . 35

3 Aptamer Selection **37**
3.1 Introduction . . . 37
3.1.1 Chapter 3 aims . . . 39
3.2 Methods . . . 39
3.2.1 Lumefantrine SELEX protocol . . . 39
Reagent preparation . . . 41
Library immobilization . . . 42
Negative selection . . . 43
Positive selection . . . 43
Amplification via PCR . . . 44
Generation of ssDNA via lambda exonuclease . . . 45
Purification of ssDNA . . . 45
SELEX conditions . . . 46
Sequencing . . . 46
3.2.2 Piperaquine and mefloquine SELEX protocol . . . 47
Piperaquine SELEX targets . . . 47
Synthesis of molecule 190 . . . 48
Reagent preparation . . . 50
Library immobilization . . . 51
Negative selection . . . 51
Positive selection . . . 52
Amplification via PCR . . . 52
ssDNA generation via NaOH . . . 53
Purification of ssDNA . . . 54
Cloning after selection . . . 55
Sequencing . . . 58
Clone SELEX elution profiles . . . 58
3.2.3 Binding affinity assays . . . 59
ITC analysis of lumefantrine sequences . . . 59
Fluorescent-binding assay analysis of piperaquine and mefloquine sequences . . . 60
Optimizing quencher ratios and length . . . 61
Assessing sensitivity and specificity . . . 64
Biacore methods . . . 64

3.3 Results . . . 72
3.3.1 SELEX summary . . . 73
3.3.2 Sequence analysis results . . . 76
Lumefantrine SELEX sequence analysis . . . 76
Piperaquine and mefloquine SELEX sequence analysis . . . 78
3.3.3 Binding affinity results . . . 80
Lumefantrine ITC results . . . 86
Piperaquine and mefloquine fluorescent-binding assay results 86
Biacore analysis of lumefantrine sequences . . . 94
Biacore analysis of model kanamycin aptamer and SELEX tracking method . . . 95
Biacore characterization of aptamers PQ4 and MQ2 . . . 98
3.4 Discussion . . . 103
3.4.1 Overview . . . 103
3.4.2 SELEX . . . 103
3.4.3 Sequencing . . . 105
3.4.4 Affinity analysis . . . 105
3.4.5 Limitations and conclusion . . . 108

4 Fluorescent Sensor Development 110
4.1 Introduction . . . 110
4.1.1 Chapter 4 aims . . . 111
4.2 Methods . . . 111
4.2.1 Characterization of tablet sensors . . . 112
Sensor functional range . . . 113
Cross-reactivity . . . 113
Testing a crushed tablet . . . 114
4.2.2 Sensor function in serum versus buffer . . . 115
4.2.3 Serum sensor troubleshooting . . . 116
Measuring the effects of serum carrier proteins . . . 116
Adjusting pH . . . 117
Adding surfactant/solvent . . . 119
Increasing the sensor concentration . . . 119
Serum dilutions . . . 120
Higher wavelength fluorophores . . . 121
4.2.4 Characterization of serum sensors . . . 125
Limit of detection and limit of quantification . . . 125
Cross-reactivity . . . 125
Accuracy/Precision testing . . . 126

Matrix effects . . . 126
Validation against LC-MS reference standard . . . 127
4.3 Results . . . 127
4.3.1 Characterization of tablet sensors . . . 127
Sensor functional range . . . 127
Cross-reactivity . . . 128
Testing a crushed tablet . . . 129
4.3.2 Sensor function in serum vs. buffer . . . 132
Initial sensor testing in serum . . . 132
4.3.3 Serum sensor troubleshooting results . . . 134
Measuring effects of serum carrier proteins . . . 134
Adjusting pH . . . 136
Adding surfactant/solvent . . . 137
Increasing the concentration of sensor . . . 138
Serum dilutions . . . 138
Higher wavelength fluorophores . . . 139
4.3.4 Characterization of serum sensors . . . 143
Limit of detection and limit of quantification . . . 143
Cross-reactivity . . . 145
Accuracy/Precision testing . . . 145
Matrix effects . . . 145
Assay validation against LC-MS reference standard . . . 149
4.4 Discussion . . . 153
4.4.1 Overview . . . 153
4.4.2 Tablet sensors . . . 154
4.4.3 Serum optimization . . . 155
4.4.4 Serum sensors . . . 156
4.4.5 Limitations and conclusion . . . 158

5 Conclusion **160**
5.1 Overview . . . 160
5.2 Cost analysis . . . 161
5.3 Limitations and future work . . . 161
5.4 Summary of findings . . . 164

References **166**

List of Figures

1.1 Malaria life cycle . . . 3
1.2 Chloroquine structure . . . 5
1.3 Artemisinin structure . . . 5
1.4 SELEX workflow . . . 15
1.5 Capture SELEX . . . 17
1.6 Structure switching sensor format . . . 22

2.1 Reported drug target preference from interviews . . . 30
2.2 Reported sample preference from interviews . . . 30
2.3 Reported preference for quantitative versus qualitative readout from interviews . . . 31
2.4 Reported potential assay applications from interviews . . . 31

3.1 Lumefantrine structure . . . 39
3.2 Lumefantrine SELEX method . . . 40
3.3 Structure of molecule 190 versus piperaquine . . . 48
3.4 Piperaquine and mefloquine SELEX method . . . 49
3.5 Synthesis of molecule 190 . . . 49
3.6 Small scale PCR elution profile example . . . 53
3.7 Fluorescent sensor design . . . 61
3.8 SELEX PQ2 conditions and elution profiles . . . 74
3.9 SELEX MQ1 conditions and elution profiles . . . 75
3.10 Lumefantrine sequences of interest . . . 77
3.11 SELEX PQ1 sequence results . . . 79
3.12 SELEX PQ1 sequences of interest . . . 81
3.13 SELEX PQ1 clone SELEX elution profiles . . . 82
3.14 SELEX PQ2 sequence results . . . 82
3.15 SELEX PQ2 sequences of interest . . . 83
3.16 SELEX PQ2 clone SELEX elution profiles . . . 84
3.17 SELEX MQ1 sequence results . . . 84
3.18 SELEX MQ1 sequences of interest . . . 85
3.19 SELEX MQ1 clone SELEX elution profiles . . . 85

3.20 Lumefantrine ITC results . . . 87
3.21 SELEX PQ1 quencher dilution curves . . . 89
3.22 SELEX PQ2 quencher dilution curves . . . 90
3.23 SELEX MQ1 quencher dilution curves . . . 91
3.24 SELEX PQ1 fluorescent-binding assay results . . . 92
3.25 Aptamer 18.18 specificity testing via fluorescent-binding assay . . . 93
3.26 Aptamer 18.18 affinity to molecule 190 versus whole piperaquine via fluorescent-binding assay . . . 93
3.27 SELEX PQ2 fluorescent-binding assay results . . . 94
3.28 SELEX MQ1 fluorescent-binding assay results . . . 95
3.29 Biacore assessment of model kanamycin aptamer . . . 97
3.30 Biacore method to track SELEX enrichment . . . 98
3.31 Aptamer PQ4-capture sensorgrams . . . 99
3.32 Aptamer MQ2-capture sensorgrams . . . 100
3.33 Aptamer PQ4-drug sensorgrams . . . 101
3.34 Aptamer MQ2-drug sensorgrams . . . 102

4.1 Serum autofluorescence . . . 121
4.2 Piperaquine tablet sensor LOD, LOQ . . . 128
4.3 Mefloquine tablet sensor LOD, LOQ . . . 129
4.4 Piperaquine tablet sensor cross-reactivity . . . 130
4.5 Mefloquine tablet sensor cross-reactivity . . . 131
4.6 Piperaquine crushed tablet (Eurartesim) dilutions . . . 132
4.7 Piperaquine crushed tablet (Eurartesim) test . . . 133
4.8 Aptamer 18.18 in serum versus buffer test . . . 134
4.9 Aptamer PQ4 in serum versus buffer test . . . 134
4.10 Aptamer MQ2 in serum versus buffer test . . . 135
4.11 Serum protein effects on sensor PQ4 . . . 135
4.12 Serum protein effects on sensor MQ2 . . . 135
4.13 Effects of altering pH on sensor PQ4 . . . 136
4.14 Effects of SDS on serum sensor function . . . 137
4.15 Effects of DMSO on serum sensor function . . . 138
4.16 Effects of increased sensor concentration on serum sensor function . 139
4.17 Effects of serum dilution on serum sensor function . . . 139
4.18 PQ4 new quencher dilution curves . . . 140
4.19 PQ4 with new fluorophores in serum vs buffer . . . 141
4.20 PQ4 with all new fluorophores in serum for comparison . . . 141
4.21 MQ2 new quencher dilution curves . . . 142
4.22 MQ2 with select new fluorophores in serum for comparison . . . 143
4.23 Piperaquine serum sensor LOD, LOQ . . . 144

4.24 Mefloquine serum sensor LOD, LOQ 144
4.25 Piperaquine serum sensor cross-reactivity 146
4.26 Mefloquine serum sensor cross-reactivity 147
4.27 Piperaquine serum sensor accuracy and precision plots 149
4.28 Mefloquine serum sensor accuracy and precision plots 150
4.29 Piperaquine and mefloquine sensor matrix effects 150
4.30 Piperaquine serum sensor comparison to LC-MS reference standard 151
4.31 Mefloquine serum sensor comparison to LC-MS reference standard . 152

5.1 Aptamers PQ4 and MQ2. 163

List of Tables

1.1 Artemisinin combination therapy (ACT) data 7

2.1 Reported assay utility from web-based survey 28
2.2 Reported operational requirements from web-based survey 29
2.3 Lab-based assay target product profile 33
2.4 Point-of-care assay target product profile 34

3.1 Binding and washing buffer components 41
3.2 Lumefantrine SELEX library 41
3.3 Lumefantrine SELEX primers 41
3.4 Target molecule stock solutions 42
3.5 Lumefantine SELEX 1 protocol 43
3.6 Lumefantine SELEX 2 protocol 44
3.7 Optimized lumefantine SELEX PCR conditions 45
3.8 Selection buffer components 50
3.9 Piperaquine and mefloquine SELEX library 50
3.10 Piperaquine and mefloquine SELEX primers 51
3.11 Optimized piperaquine and mefloquine SELEX PCR conditions . . 52
3.12 Piperaquine SELEX 1 protocol (SELEX PQ1) 54
3.13 Piperaquine SELEX 2 protocol (SELEX PQ2) 55
3.14 Mefloquine SELEX 1 protocol 56
3.15 Fluorescent sensor templates 61
3.16 Quencher optimization of SELEX PQ1 sequences 62
3.17 Quencher optimization of SELEX PQ2 sequences 62
3.19 Quencher dilutions 63
3.18 Quencher optimization of SELEX MQ1 sequences 63
3.20 Lumefantrine sequences assessed via Biacore 66
3.21 Kanamycin sequences assessed via Biacore 68
3.22 Piperaquine and mefloquine sequences assessed via Biacore 71
3.23 Lumefantrine SELEX sequence data 78
3.24 SELEX PQ1 optimized quencher conditions 88
3.25 SELEX PQ2 optimized quencher conditions 88

3.26 SELEX MQ1 optimized quencher conditions 89
3.27 Biacore assessment of lumefantrine sequences 96
3.28 Aptamer PQ4-capture affinity analysis 100
3.29 Aptamer PQ4-capture affinity analysis 100
3.30 Aptamer PQ4-drug affinity analysis 102
3.31 Aptamer MQ2-drug affinity analysis 102

4.1 Tablet sensor sequences 112
4.2 Serum sensor sequences 113
4.3 Stock solutions of drug targets and potentially cross-reactive compounds 114
4.4 Typical serum protein concentrations 117
4.5 Conditions for varying pH assay 118
4.6 Higher wavelength fluorophores and quenchers 122
4.7 Optimized excitation/emission wavelengths 123
4.8 Quencher optimization conditions for new fluorophores 124
4.9 QC samples for accuracy and precision testing 126
4.10 PQ4 new quencher optimized ratios 140
4.11 MQ2 new quencher optimized ratios 142
4.12 Piperaquine serum sensor accuracy and precision testing 148
4.13 Mefloquine serum sensor accuracy and precision testing 148
4.14 Comparison of piperaquine sensor to LC-MS reference standard . . 153
4.15 Comparison of mefloquine sensor to LC-MS reference standard . . . 153

5.1 Sensor cost analysis 162

List of Abbreviations

ACT . . . . . Artemisinin based combination therapy

AGP . . . . . Alpha-acid glycoprotein

AQ . . . . . Amodiaquine

BHQ . . . . . Black hole quencher

BSA . . . . . Bovine serum albumin

B+W . . . . . Binding and washing

CE-SELEX . . Capillary electrophoresis SELEX

CQ . . . . . Chloroquine

Cy3 . . . . . Cyanine3 fluorophore

DAB . . . . . Dabcyl quencher

DMSO . . . . . Dimethyl sulfoxide

DNA . . . . . Deoxyribonucleic acid

DDT . . . . . Dichlorodiphenyltrichloroethane

EDC . . . . . 1-Ethyl-3-(3-dimethylaminopropyl) carbodiimide hydrochloride

ELISA . . . . . Enzyme-linked immunosorbent assay

FAM . . . . . Fluorescein fluorophore

HSA . . . . . Human serum albumin

IAB . . . . . Iowa black quencher

IDT . . . . . Integrated DNA technologies

IgG . . . . . Immunoglobulin G

ITC . . . . . Isothermal titration calorimetry

LC-MS . . . . Liquid chromatography-mass spectrometry: an analytical chemistry technique used to detect drug compounds from human samples

LF . . . . . Lumefantrine

LOD . . . . . Limit of detection

LOQ . . . . . Limit of quantification

MQ . . . . . Mefloquine

190 . . . . . Molecule 190 (1/2 piperaquine)

M-SELEX . . Microfluidics-SELEX

NGS . . . . . Next generation sequencing

NHS . . . . . N-hydroxysuccinimide

Oligo . . . . . Oligonucleotide

PBS . . . . . Phosphate buffered saline

PQ . . . . . Piperaquine

PCR . . . . . Polymerase chain reaction

RDT . . . . . Rapid diagnostic test

RFU . . . . . Relative fluorescence units

RNA . . . . . Ribonucleic acid

SDS . . . . . Sodium dodecyl sulfate

SELEX . . . . Systematic Evolution of Sequences by EXponential enrichment: the process used for identifying new aptamer sequences

SOMAmer . . Slow Off-rate Modified Aptamer

SPR . . . . . Surface plasmon resonance

ssDNA . . . . Single stranded DNA

TPP . . . . . Target product profile

TYE563 . . . . small molecule fluorophore replacement for cyanine5

1 Introduction

Contents

1.1 Malaria 1
1.1.1 History and burden of Malaria 2
1.2 Antimalarial drugs 4
1.2.1 Mechanisms of action of antimalarial drugs 8
1.3 History of antimalarial resistance 9
1.3.1 Looking ahead 11
1.4 Methods for the detection of antimalarial drugs 12
1.5 Aptamers 14
1.5.1 Aptamer selection 14
1.5.2 Aptamers against small molecule targets 18
1.5.3 Aptamer applications 20
1.6 Thesis aims 22

1.1 Malaria

Malaria is a tropical infectious disease with over 200 million recorded instances of infection each year, resulting in around a half-million deaths[1]. The disease is caused by single-celled eukaryotic parasites of the genus *Plasmodium*. *Plasmodium* parasites have infected humans, other mammals, birds, and reptiles for thousands of years. There are six malaria species known to infect humans, *P. falciparum, P. vivax, P. knowlesi, P. malariae*, and two sub-species of *P. ovale*, though the

vast majority of cases are caused by *P. falciparum* and *P. vivax*. In the middle ages, the symptoms of malaria infection were termed "mal'aria" by the Romans for their belief that disease was caused by "bad air" found in swamps. In the late 19thcentury, the parasites were first discovered in blood samples and described by Alphonse Laveran[2]. Several years later, Sir Patrick Manson and Sir Ronald Ross suggested that the mode of transmission to humans was via mosquitos[3, 4]. Since then, the combined efforts of many researchers have elucidated the details of malaria transmission and its complex life cycle (shown in Figure 1.1).

In the last hundred years, significant progress has been made to understand parasite biology and its effects on hosts. Using this knowledge, interventions such as vector control and antiparasitic drugs have been developed, successfully reducing, but not eliminating the burden of disease in humans.

1.1.1 History and burden of Malaria

Over the course of the 20th century, effective drugs and vector control significantly reduced the global distribution of malaria, eliminating parasites from Europe and the United States. The beginning of the 21st century saw targeted approaches to eliminate malaria globally and it is estimated that the incidence rate of malaria decreased by 41% between 2000 and 2015[6]. Despite this progress, more than one billion people worldwide still live at risk of malaria infection by either *P. falciparum* or *P. vivax*[7].

P. falciparum is the most prevalent malaria species, occurring primarily in Africa. In 2017, 92% of all malaria cases occurred in Africa and 99% of these cases were caused by *P. falciparum*. The same year, in Southeast Asia, where 5% of global malaria cases occurred, 63% of cases were *P. falciparum* and 37% *P. vivax*[1]. In addition to being the most prevalent, *P. falciparum* malaria is also the deadliest.

Clinical symptoms of malaria infection most commonly include cyclic fever, anemia, headache, nausea, vomiting, and myalgia[8]. Without medication, these symptoms can progress to severe malaria characterized by the dysfunction of vital organs due to sequestration of parasitized red cells. These immobilized red blood

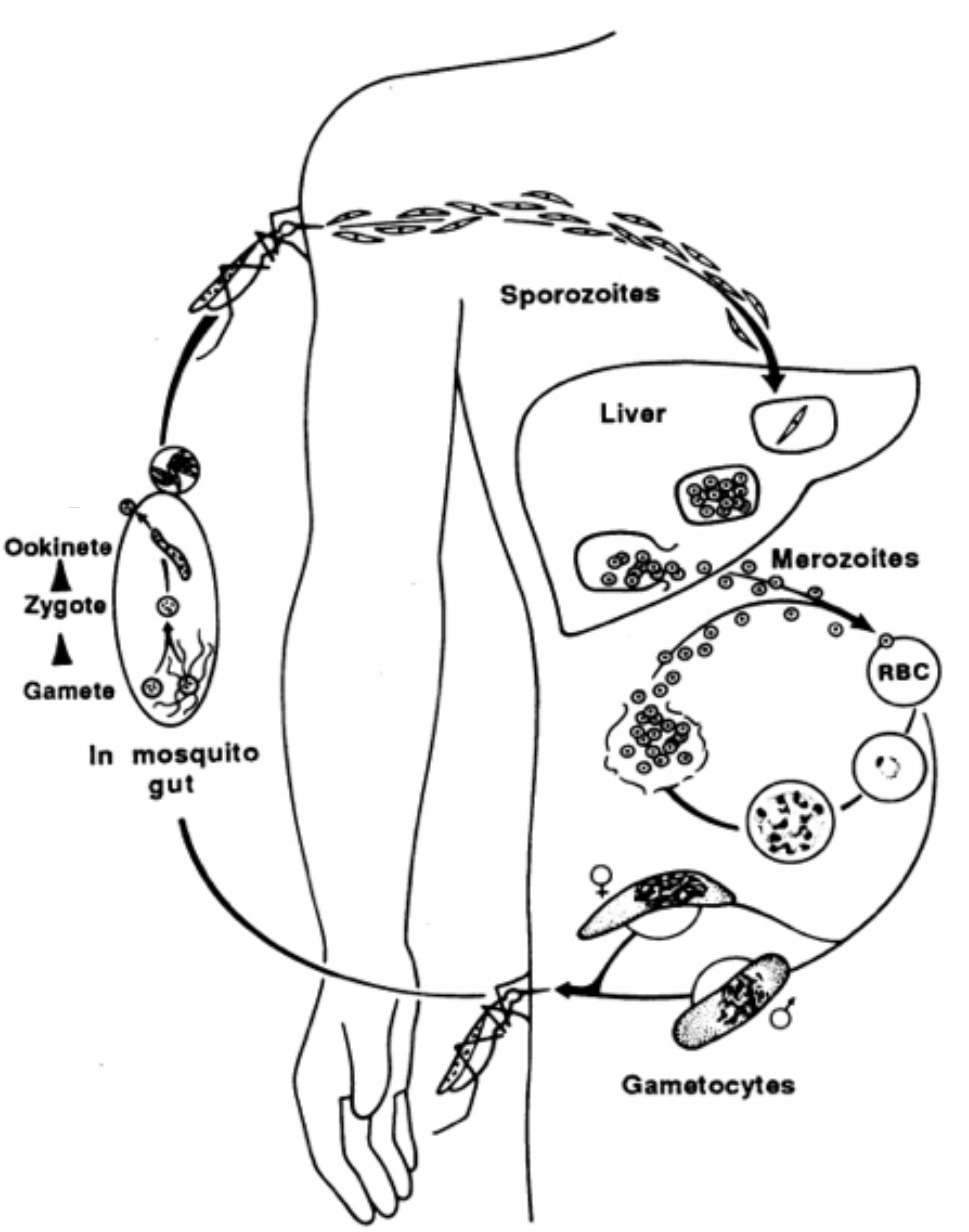


Figure 1.1: Malaria life cycle[5]. Human infection begins when an infected female Anopheles mosquito injects malaria sporozoites while taking a blood meal. Sporozoites travel to the liver where they infect hepatic cells, multiply, and rupture releasing merozoites into blood circulation. Merozoites invade red blood cells, progressing from a ring stage to a schizont which ruptures, releasing more merozoites which invade new red blood cells. Some of the blood stage parasites will enter a sexual life cycle, developing into gametocytes. Male and female gametocytes are ingested by a new female *Anopheles* mosquito during a subsequent blood meal. Gametocytes join to form zygotes in the mosquito midgut, developing into oocysts. Oocysts rupture releasing sporozoites which travel to the mosquito salivary glands, ready to be injected to a new host. Figure reprinted with permission from AAAS and adapted with permission from Louis Miller.

cells inhibit circulation and damage vascular endothelium. Symptoms of severe malaria vary by age but typically include pulmonary edema[9], severe anemia[10], metabolic acidosis, acute renal failure[11], and coma (cerebral malaria) due to sequestration of parasites in the brain endothelial tissue[12]. A failure to treat severe malaria results in death in the majority of cases[13]. Severe malaria and death mainly result from cases of *P. falciparum* malaria, although *P. vivax* and *P. knowlesi* have also been reported to lead to severe disease[14]. Over half of all malaria-related deaths each year occur in children under the age of five[1].

1.2 Antimalarial drugs

The first known medicine for the treatment of malaria was powdered bark of the cinchona tree. Quinine, a quinoline alkaloid isolated from this bark, is still used to treat both *P. falciparum* and *P. vivax* infections. A search for new compounds during World War II, when the Allies lost access to quinine supplies, resulted in the widespread use of the 4-aminoquinoline, chloroquine[15], which had been previously discovered but believed to be too toxic. Chloroquine was the first majorly successful synthetic molecule used to treat malaria and its worldwide distribution during the 20th century contributed to the elimination of malaria from many countries (chloroquine structure shown in Figure 1.2).

However, by the late 20^{th} century, the emergence and spread of chloroquine resistance rendered it largely ineffective worldwide. Again, it was a time of war that motivated the search for new treatments. In the late 1960's, Ho Chi Minh requested the help of Chairman Mao to supply new and effective drugs to the North Vietnamese soldiers dying of malaria on the battlefield. Chairman Mao initiated 'Project 523,' enlisting Chinese scientists to screen compounds to identify new antimalarial drugs. One of the compounds to emerge from this project was qinghaosu, later called artemisinin (shown in Figure 1.3). Artemisinin was extracted from the qinghao (*Artemisia annua*) plant which had been used for centuries to treat fever in rural China[16]. Chinese scientist Youyou Tu won the Nobel Prize for Medicine or Physiology in 2015 for her contribution to the discovery of artemisinin.

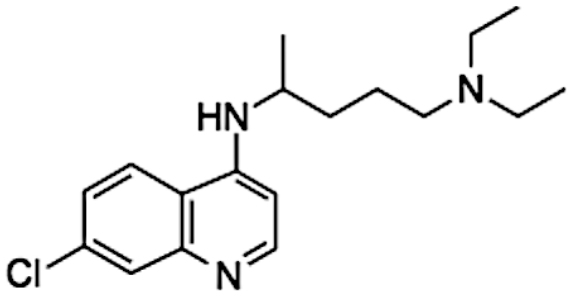


Figure 1.2: Structure of chloroquine molecule.

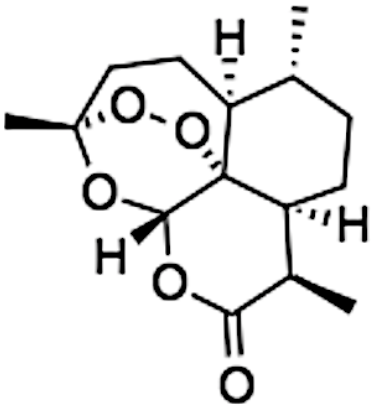


Figure 1.3: Structure of artemisinin molecule.

Although the effects of artemisinin were discussed and published in China in the 1970's[17], drug trials with artemisinin outside of China were not conducted until the 1990's. In 2006, the World Health Organization (WHO) first recommended Artemisinin Combination Therapies (ACTs) as a first-line therapy[18, 19].

Artemisinin has proven to be a very effective drug with high tolerability and rapid action against all blood-stage parasites. Artemisinin compounds are metabolized to their active metabolite, dihydroartemisinin (DHA) in several hours and then cleared by the liver. DHA also has a very short half-life (1-2 hours) which limits the drug's efficacy as a monotherapy. Although artemisinins rapidly alleviate clinical symptoms, their fast clearance inhibits removal of all parasites, resulting in recrudescence and the recurrence of symptoms as parasites repopulate the blood. Artemisinin monotherapy courses of three to five days report recrudescence rates above 25% and

seven day courses report recrudescence rates of 10-20%[16]. Patient adherence during long courses of antimalarial drugs has proven challenging, especially when symptoms rapidly resolve[20]. In order to address the low cure rates of artemisinin monotherapy and to further protect against the development of resistance, artemisinins were combined with slower clearing antimalarial compounds with differing chemical structures and predicted mechanisms of action[21, 22]. Several artemisinin derivatives were co-formulated with other promising antimalarial compounds to create the ACT class of drugs. ACTs have been the first-line treatment for *P. falciparum* malaria worldwide for the last 13 years. Between the years of 2010-2017, an estimated 2.74 billion courses of ACTs were delivered to countries worldwide[1]. The most commonly used ACTs include DHA-piperaquine, artesunate-mefloquine, artemether-lumefantrine, and artesunate-amodiaquine. The structures of the partner drugs used in these ACTs along with their recommended dosing, typical C_{max}, plasma $t^{1/2}$, and day seven plasma concentrations are shown in Table 1.1.

Piperaquine was first synthesized in France in the 1950's. It was rediscovered in China in the 1960's and was widely used in China throughout the late 1970's and 1980's. However, after widespread use as a monotherapy, resistance to piperaquine developed and piperaquine was mostly abandoned until the 1990's when it was first used in a combination therapy. CV8®, a combination of DHA-piperaquine, was first used in Vietnam in 2000. Since then, the dosing of DHA and piperaquine has been adjusted and DHA-piperaquine has been rebranded as Artecom®, Artekin®, Duo-Cotecxin®, and Euratesim®[32, 33].

Mefloquine was originally introduced as a treatment option for chloroquine-resistant parasites in the 1970's[34]. It was identified by the US Army during a screen for new effective drugs during the Vietnam War. Mefloquine was first sold in 1985 under the brand name Lariam®. It has been used in combination with sulfadoxine-pyrimethamine, as a monotherapy, and was first combined with artesunate in the mid 1990's[35].

Lumefantrine was first discovered in China in the 1970's through project 523, along with artemisinin. Artemether-lumefantrine (brand-name Coartem®) was

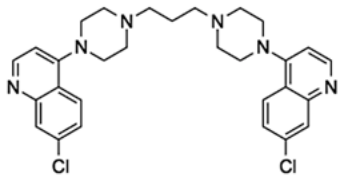
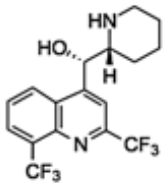
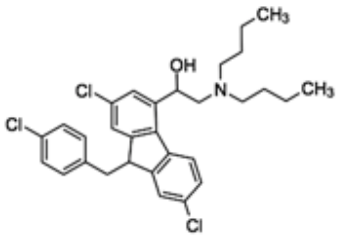
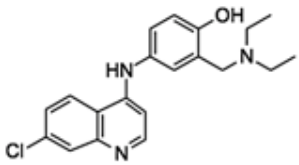
	Piperaquine	Mefloquine
		
Recommended dosing	16-27 mg/kg, (children <25 kg: 20 mg/kg); Once daily for 3 days	5-11 mg/kg; Once daily for 3 days
$t^{1/2}$	~22-28 days	8-20 days
C_{max}	300-1000 ng/mL	1500-3800 ng/mL
Day 7 plasma conc.	50-100 ng/mL	600 ng/mL
Paired artemisinin derivative	Dihydroartemisinin (DHA) Dosing: 2-10 mg/kg, (children <25 kg: 2.5 mg/kg); Once daily for 3 days	Artesunate Dosing: 2-10 mg/kg; Once daily for 3 days
	Lumefantrine	**Amodiaquine**
		
Recommended dosing	29-144 mg/kg; Twice daily for 3 days	7.5-15 mg/kg; Once daily for 3 days
$t^{1/2}$	3-4 days	Amodiaquine (10h-16h) Desethylamodiaquine (10-12.5 days)
C_{max}	~6,000-7,000 ng/mL	Amodiaquine (16-54 ng/mL) Desethylamodiaquine (250-550ng/mL)
Day 7 plasma conc.	~280 ng/mL	Amodiaquine (---) Desethylamodiaqine (~80 ng/mL)
Paired artemisinin derivative	Artemether Dosing: 5-24 mg/kg; Twice daily for 3 days	Artesunate Dosing: 2-10 mg/kg; Twice daily for 3 days

Table 1.1: ACT data. Recommended dosing from WHO guidelines for malaria treatment[13]. This study is mainly concerned with the slow clearing compounds, often referred to as partner compounds. Paired artemisinin derivates are also listed for reference. Pharmacokinetic data from the following studies: Piperaquine[23–26], Mefloquine[27, 28], Lumefantrine[29, 30], Amodiaquine[31].

listed on the WHO's list of essential medicines in 2002 and by 2009 was approved for use in 90 countries[36]. Lumefantrine is highly lipophilic and absorption is variable, but improved, when taken with a fatty meal.

Amodiaquine (Camoquin®) is a derivative of chloroquine originally introduced for its moderate activity against chloroquine resistant parasites. It was first added to the WHO's list of essential medicines in 1977 but removed in 1988 due to fatal adverse drug reactions when used for prophylaxis. In the late 1990's, after further safety testing, it was reinstated as a monotherapy for the treatment of uncomplicated *P. falciparum* malaria[37]. In 2008, artesunate-amodiaquine (ASAQ Winthrop®) was prequalified by the WHO and it is now approved for use in 33 countries[38].

1.2.1 Mechanisms of action of antimalarial drugs

Despite their success and widespread use, the mechanisms of action of most antimalarial compounds are not fully understood. It is hypothesized that the aminoquinolines such as chloroquine inhibit the parasite's ability to safely digest hemoglobin. Upon entering the red blood cell, the parasite produces proteases to degrade the protein components of hemoglobin for its own amino acid needs. Amino acids are transported to the cytoplasm of the parasite but the heme (ferriprotoporphyrin) groups remain in the digestive vacuole[39]. When the iron atom in heme is oxidized, it forms hematin (ferriprotoporphyrin IX) causing oxidative stress and toxicity to the parasite in high concentrations. Hematin is quickly polymerized by the parasite to generate insoluble, nontoxic hemozoin[40]. It is hypothesized that the chloroquine molecule binds hematin and inhibits this polymerization. Similarly, it has been shown that piperaquine[32], mefloquine[41], amodiaquine[37], and lumefantrine[42] inhibit the formation of hemozoin. Although there remains some debate over the exact mechanisms of interaction, it is understood that a resulting build-up of toxic heme in the presence of these drugs ultimately results in parasite death. It has been suggested that mefloquine and lumefantrine may target other processes as well[43, 44].

The mechanism of action of artemisinin is also disputed. However, it has been shown that the endoperoxide bridge, unique to artemisinin among current antimalarial drugs, is necessary for its function[45]. This endoperoxide bridge is reportedly cleaved when the drug interacts with hemoglobin digestion products, releasing damaging free radicals[46]. Additionally, artemisinin has been shown to bind heme and inhibit the formation of hemozoin[47]. More recently, artemisinin has been shown to bind a variety of parasite proteins suggesting mechanisms of action targeting a wide range of parasite functions[48]. Many studies to further elucidate the mechanisms of action of antimalarial compounds are ongoing in research groups around the world.

1.3 History of antimalarial resistance

The widespread use of chloroquine and dichlorodiphenyltrichloroethane (DDT) in the 1940's and 1950's led to predictions of rapid worldwide malaria elimination[49]. However, these hopes were lost by the 1960's with the report of chloroquine resistant parasites emerging in both Southeast Asia and South America[50]. The development of resistance was blamed on widespread and unregulated use of chloroquine as well as the distribution of poor-quality tablets. By the 1970's, chloroquine resistant parasites had spread across South America and Southeast Asia to India, and during the 1980's, they spread across the African continent[51]. As chloroquine resistance spread, global malaria deaths almost doubled from about 1 million in 1980 to over 1.8 million in 2004[52].

Genetic analysis of the chloroquine resistance marker, *pfcrt*[53], revealed a migration of chloroquine resistant parasites from Southeast Asia to Africa. Microsatellite analysis of loci on chromosome 7 flanking *pfcrt*, confirms that chloroquine resistant parasites initially emerged in Southeast Asia and spread to Africa rather than emerging separately in Asia and then Africa. This pattern was also observed in the spread of sulfadoxine-pyramethamine resistance, a combination therapy used initially to treat chloroquine resistant parasites. Genetic analysis of the resistance markers for pyrimethamine (*dhfr*) and sulfadoxine (*dhps*) both reveal that resistance

in Africa can be traced back to the migration of parasites from Southeast Asia[54, 55]. This trend highlights the need for increased vigilance of drug efficacy monitoring and use practices in Southeast Asia to prevent the emergence and spread of new resistance in the region and its likely spread to Africa.

In the mid-2000's, the hope of world-wide malaria elimination was restored through the introduction of artemisinins and the widespread use of ACTs. The number of global malaria deaths dropped by 48% from the year 2000 to the year 2015, in large part due to the efficacy of ACTs[56]. However, surveillance efforts revealed that by 2009, parasites in Western Cambodia showed reduced sensitivity to artemisinin[57, 58]. Research is ongoing to characterize artemisinin resistance, which so far has been observed as a delayed parasite killing rather than a complete loss of function, as well as to elucidate the mechanism of resistance. Although the definition of artemisinin resistance is currently controversial, its potential implications for the effective treatment of malaria are a widely accepted concern.

Reduced susceptibility to artemisinin places more of the parasite killing burden on the ACT partner drug, increasing the likelihood of resistance against both compounds and the complete failure of an ACT[59, 60]. Shortly after its adoption as a first-line therapy in 2008, the efficacy of DHA-piperaquine in Cambodia began to decline due to a reduced efficacy of both DHA and piperaquine[61, 62]. High DHA-piperaquine failure rates led the WHO to change its recommended first-line therapy for Cambodia from DHA-piperaquine to artesunate-mefloquine in 2015[63]. Although effective in 2015, previous resistance to mefloquine in Cambodia suggests that parasites with reduced sensitivity to artemisinin will swiftly regain resistance to mefloquine, leading to the failure of this ACT[24].

Reduced sensitivity to artemisinin and resistance to various partner drugs has spread throughout the majority of Southeast Asia[63–65]. While this is of serious concern for malaria control efforts in the region, perhaps even more concerning is the likely spread of these resistant parasites from Southeast Asia to Africa. A repetition of this trend would result in a surge of deaths in Africa and a huge setback for global malaria elimination goals.

1.3.1 Looking ahead

The emergence of ACT resistance has spurred investigation into new compounds. Over the last decade, various compounds with new or unknown mechanisms of action have been assessed. Potential new drugs include variations of aminoquinolines, imidazolopiperazines, and synthetic endoperoxides among others[66, 67]. It is unclear if promising new candidates will emerge and how long it will take for them to reach the market (without a new war to motivate the governments of developed countries). In the meantime, to maintain drug efficacy in Southeast Asia, countries are rotating between available drugs. As resistance to one partner drug emerges, the first-line therapy is altered to a new partner drug which has regained sensitivity through the absence of drug pressure[13]. Another proposed short-term solution currently undergoing clinical testing is the combination of multiple partner drugs, called triple ACTs[68]. The hope is that, in combining two partner drugs with an artemisinin derivative, efficacy will be maintained, but only until the ultimate emergence of parasites resistant to all three compounds.

As researchers work to optimize current treatment regimens to delay the spread of resistance in Southeast Asia, more information on patterns of drug use will be needed. Frequently alternating first-line therapies requires logistical organization, monitoring, and enforcement. Regulation of drug access in private sector pharmacies in Southeast Asia is difficult and essentially nonexistent[69]. As reported in a recent study from Cambodia, many pharmacies receive drug supplies from unregulated channels, illegally sell prescription medicines without prescriptions, and continue to distribute monotherapies that are no longer effective or approved for treatment of *P. falciparum*[70]. Monitoring drug adherence will also be important. Directly observed therapy is used to ensure adherence, but this is challenging with multi-day drug regimens, as many patients are lost to follow up. Monitoring adherence of treatment is important for understanding drug habits and how they contribute to resistance and is especially important in the roll out of mass drug administration campaigns. Adherence for antimalarial treatment regimens is reportedly variable and often poor[71, 72].

There currently exists very little data on drug use and adherence in Southeast Asia. The most straightforward way to obtain this information is through patient interviews. However, the accuracy of patient recall is limited and many confounding factors affect reporting. In a recent report from Cambodia, patients with *P. falciparum* were enrolled in a drug monitoring study. Although patients enrolled reported no recent treatment with antimalarial drugs or no knowledge of recent treatment, 52% of patients had detectable piperaquine or mefloquine in their plasma[73]. A similar study in Tanzania reported detectable antimalarial drug levels in 74% of patients enrolled, all of whom had reported no antimalarial drug use for the previous 28 days[74]. Several studies have assessed the reporting accuracy of mothers or caretakers for children and found consistent underreporting of previous treatment[75, 76]. Many factors contribute to the unreliability of reporting and this, combined with an absence of health records and poor regulation of drug distribution in pharmacies, results in a large gap in knowledge about antimalarial drug use and drug pressure in regions of study.

The most reliable method for tracking drug use is direct measurement of drug levels from patient samples[77]. Accurate data on country-wide drug use is important for governments and researchers to report and improve the efficacy of enforcement strategies. Understanding drug pressure in a region will be helpful to study patterns that lead to the emergence of resistance. This data could not only help slow the spread of current resistance but also help to prevent the emergence of resistance to new therapies that are greatly needed for malaria elimination in Southeast Asia.

1.4 Methods for the detection of antimalarial drugs

Detection methods to monitor drug use and efficacy

The gold standard for measuring antimalarial drug levels for pharmacokinetic analysis, surveillance, and therapeutic efficacy studies is liquid chromatography-mass spectrometry (LC-MS). Over the last 20 years, methods to extract and measure antimalarial drugs from plasma samples have been optimized in several laboratories around the world. Specific methods for the detection of most antimalarial drugs

have been developed[78–83]. These methods can be very sensitive and accurate. However, they are time consuming and typically require shipping frozen blood or plasma to a central lab capable of performing the analysis. Quality assessment and control for these methods requires regimented protocols to assess consistent extraction efficiency, sample handling, and equipment performance. Design and implementation of quality control measures is essential to ensure consistent and reliable results. Additionally, sample stability during shipment is variable and cold chain shipments can be prohibitively expensive and logistically challenging.

In order to address some of these issues, several methods to extract antimalarial drugs from dried blood spots have been developed[77, 84]. These methods negate the need for shipping frozen samples but they still require access to LC-MS equipment and highly trained technicians. There are very few labs worldwide with the expertise to run optimized and properly controlled methods for the LC-MS detection of antimalarial drugs from patient samples.

Detection methods to assess medicine quality

Poor quality medicines are believed to play a role in the development of antimalarial drug resistance by exposing parasites to subtherapeutic levels of active compounds. Reports of both falsified (identity, composition, or source is deliberately misrepresented) and substandard (authorized products that do not meet quality standards or specification) medicines are common across all continents[85, 86]. Medicines have been falsified for hundreds of years with devastating effects for individual patients and for global disease control. A 2012 review of almost 3,000 drug samples from Southeast Asia and Africa reported 35% of samples in both regions were either falsified or substandard[87]. Other reviews estimate this number to be closer to 10%[88] or higher than 35%[89] with discrepancies due to purportedly biased reporting and a lack of reliable and consistent methods to evaluate tablet quality.

A recent review[90] of available methods to measure tablet quality assessed methods ranging from thin layer chromatography[91], spectroscopy methods[92, 93], and colorimetric dipstick tests[94, 95] to self-contained kits like the GPHF

MiniLab®[96] . While there are an abundance of published methods to assess the presence of many different compounds, the majority of these tools are prohibitively expensive, difficult to maintain, or require a level of training that is challenging to maintain in low and middle income countries[97]. Simple colorimetric and dipstick methods aim to provide access to quality testing in the absence of well-equipped laboratories[98]. However, they are limited by their small repertoires of detectable targets. Many of these tests have not been validated in field-settings or in the hands of minimally trained users. Detecting falsified and substandard drugs is a worldwide challenge and is especially difficult in malaria endemic countries.

1.5 Aptamers

Oligonucleotides are typically known for their role in storing genetic information, but the target-binding ability of riboswitches has led researchers to explore the selective binding potential of DNA and RNA. In 1990, two research groups identified target-binding oligonucleotide sequences, called aptamers, *in vitro* from a pool of synthetic RNA molecules[99, 100]. In the last 30 years, the process of identifying new aptamers has evolved as molecular biology techniques advanced. Both DNA and RNA aptamers have now been developed to bind numerous small molecules, proteins, and even whole cell targets. Like protein antibodies, aptamers demonstrate target binding sensitivity and specificity useful for a variety of biosensing and therapeutic applications.

1.5.1 Aptamer selection

The process of identifying new aptamer sequences against desired targets is called Systematic Evolution of Ligands by EXponential enrichment (SELEX). Although there are many variations of SELEX protocols, the basic principle is shown in Figure 1.4. A library of synthetic DNA or RNA sequences is prepared with conserved primer regions flanking 20-80 random bases. The random region provides the variability in folding and charge distribution to allow binding to various targets, while the primer regions allow for amplification of the library via PCR. This starting library, usually

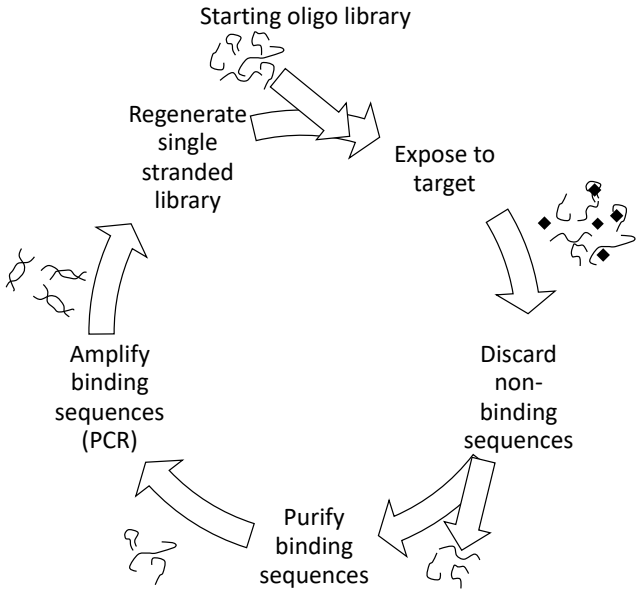


Figure 1.4: General SELEX workflow. A starting oligo library containing a region of random bases flanked by conserved primer regions is exposed to a desired target. Sequences that bind the target are separated from non-binding sequences which are discarded. The binding sequences are amplified, made single-stranded, and purified to become the starting library of the next round. This is repeated until a final round when the enriched library is sequenced and the binding properties of the identified sequences are evaluated.

containing around 10^{15} sequences each with a unique random region, is exposed to the desired target. Any sequences from the library that bind the target are purified from the non-binding sequences. The binding sequences are amplified via PCR, then regenerated to a single stranded pool to be carried forward to the next round of target exposure. This cycle is repeated several or many rounds until the library evolves to contain copies of sequences with the desired binding characteristics. After the final round, the remaining library constituents are sequenced and characterized.

Many variations of SELEX protocols have been devised to function with various targets, to improve aptamer sensitivity and specificity, and to reduce required time and labor. Protocol variations include the addition of counter SELEX steps to sort out sequences that bind undesired similarly structured molecules, changes to buffer conditions, changes in the stringency of wash steps, new methods for separating binding from non-binding sequences, adaptations to SELEX libraries, and improved methods to track library evolution. There are several common classes

of SELEX protocols. Cell-SELEX[101] is a method in which an aptamer library is incubated with cell components or whole cells and sequences that bind cellular components are collected via filtration through a protein-binding matrix or identified via fluorescent-activated cell sorting[102]. Capillary electrophoresis (CE)-SELEX, is a variation in which binding sequences are sorted from nonbinding sequences via capillary electrophoresis, improving the separation stringency and reducing the necessary number of rounds[103]. Microfluidics (M)-SELEX techniques have been developed in which miniature fluid channels are designed to assist the separation of binding and non-binding sequences[104].

Capture-SELEX is a technique in which the aptamer library is immobilized to a solid support using a short complementary oligo. Aptamer sequences that change structure when binding target, releasing the short complementary oligo, are collected and advanced to further rounds. This ability of aptamers to break free from hybridization with a short complementary oligo to bind a non-nucleotide target allows for the selection of aptamers that can easily be adapted into fluorescent sensors[105]. Capture-SELEX is especially appealing for the selection of aptamers against small molecule targets. Most SELEX protocols require the immobilization of targets to a solid support in order to separate binding sequences from non-binding sequences. The immobilization of small molecules requires chemical modifications which are typically more challenging than protein immobilization and can alter the target so that the binding of selected aptamers to immobilized target does not translate to binding targets free in solution. Several variations of capture-SELEX protocols were used in this research and the general principle is described in Figure 1.5.

In addition to the SELEX protocol, the design of the aptamer library is an important factor for selection. Most SELEX libraries are composed of sequences with a random region of 8-60 nucleotides. The number of possible unique sequences for any library is 4^n, where (n) represents the length of the random region. Longer random regions allow for more diversity but are more expensive to synthesize and more challenging to work with. When selecting small-molecule binding aptamers,

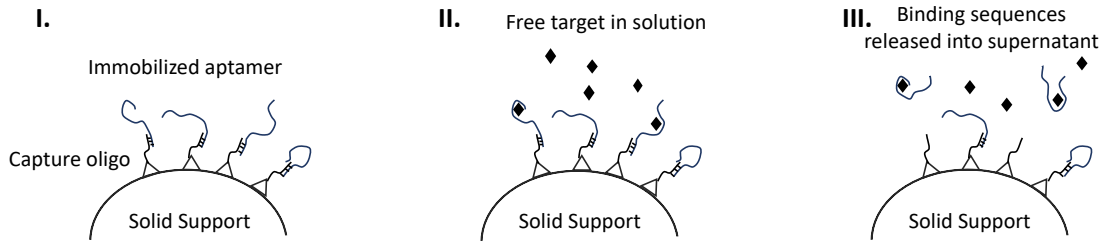


Figure 1.5: Capture SELEX. **I.** The aptamer is immobilized to a streptavidin coated solid support via a short biotinylated complementary (capture) oligo. **II.** A solution of target is introduced to the immobilized library. **III.** Any aptamer sequences that fold to bind target, releasing from the complementary oligo can be collected in the supernatant. Any non-structure switching sequences remain tethered to the solid support and can be discarded.

it is likely that few bases will interact with the molecule and shorter sequences may be sufficient to provide effective binding pockets[106]. Especially in the case of structure-switching libraries, a very long random region may allow for more instances of binding that does not force the aptamer to release from its complementary oligo. In any case, most protocols start with a library containing around 10^{15} sequences which corresponds to roughly the number of unique sequences generated from a library with only 25 random bases.

Another library consideration is the nucleic acid type. While RNA aptamers were more frequently selected in the early days of aptamers, DNA aptamers are now commonly preferred. RNA is believed to have the potential for higher affinity binding aptamers due to complex 3D folding, and an extra hydroxyl group available to interact with targets[107]. However, due to increased stability, DNA libraries are easier to handle and often favored for applications involving biological materials. For aptamer use in high DNAse/RNAse environments, such as *in vivo* sensors or therapeutics, modifications to bases have been made to enhance stability. The most common is the addition of fluoro or amino groups to the 2' position of pyrimidine nucleotides[108]. Modifications to enhance library diversity have also been devised, most notably in the case of SOMAmers (Slow Off-rate Modified Aptamers) which contain 5'-modified synthetic nucleotides[109]. The ability of polymerases to recognize and incorporate modified nucleotides is a concern and often requires optimization since PCR amplification is an important step in the

SELEX process. Researchers have also attempted to design libraries with built-in secondary structure or ones that are initially enriched for predicted binding motifs[110]. To date, efficacy of sequence predictions and algorithms to identify aptamers *in situ* has been limited and the majority of new aptamers are selected from random libraries. Despite all of the advances in molecular biological techniques and SELEX protocols, SELEX remains a fairly laborious and uncertain process[109].

1.5.2 Aptamers against small molecule targets

While aptamers have been selected against a variety of targets, some molecules make more accessible targets than others. Ideal targets are large molecules with structural diversity and varied charge distribution. Proteins, with larger surface area and more binding motifs available for conformational fits and electrostatic interactions accounted for more than 70% of all published aptamer targets from their invention in 1990 until 2015, while small molecule targets made up less than 20%[111, 112]. As previously mentioned, target immobilization is an added technical challenge for small molecule SELEX. In order to immobilize target to a solid support, as is required of most SELEX protocols, the target must be chemically modified which introduces the likelihood that the selected aptamer will not recognize the native target. In addition, some small molecule targets do not have functional groups that can be easily adapted for immobilization.

Another challenge is that many of the standard binding affinity measurement techniques are not amenable to small molecule binding aptamers[112]. Many require target labelling or filtration by size exclusion, which work well for the measurement of protein-aptamer complexes, but are not easily translated to small molecules. Isothermal titration calorimetry (ITC) is a technique that measures the heat released or absorbed when two molecules interact in solution. This method is well-suited for small molecule aptamer affinity measurements as long as enough material can be generated and target solubility is not an issue. Surface plasmon resonance (SPR) techniques have also been successfully used to assess small molecule-aptamer binding. SPR measures the accumulation of mass on a chip surface when an immobilized

ligand binds an analyte. Typically, a target is immobilized and aptamer is injected over the chip surface[113]. Upon target-aptamer binding, mass accumulation at the chip surface is measured. However, by inverting this, if aptamer is immobilized to the surface of the chip, small molecule accumulation can be measured, although sensitivity may be low due to small molecular weights. Binding affinity measurements are an important step in the characterization of resulting aptamers and have to be carefully optimized to accommodate small molecule targets.

Despite these challenges, small molecule-binding aptamers have many promising qualities that make them worth pursuing. Studies of various aptamers against small molecules report similar or better binding affinities when compared to antibodies against the same targets[114]. However, even more impressive is their capacity for selectivity. A classic example demonstrating the discriminatory capacity of aptamers is the theophylline aptamer which is able to distinguish between caffeine and theophylline - small molecules differing only by one methyl-group[115]. Aptamers have also been selected to differentiate between enantiomers[116, 117], including L-versus D-amino acids[118].

Compared to antibodies, the ability to select aptamers *in vitro* is also a notable advantage. To generate antibodies against small molecules, the targets must be conjugated to a carrier molecule in order to elicit an immune response. Again, immobilization chemistry may be challenging or impossible and may result in an antibody that only recognizes the carrier-bound small molecule. Another notable advantage to aptamers is the stability of oligonucleotides, especially DNA. DNA molecules can be denatured by pH, temperature, or salts and unlike antibodies, can regain their native structure and binding properties when returned to original conditions[111]. Also unlike antibodies, once an aptamer sequence is elucidated, the large scale synthesis of that aptamer is quick and inexpensive with no batch to batch variability. Although many of the applications requiring target-recognition are now built around antibody technology, many researchers believe that aptamers will begin to replace antibodies as their potential is further explored.

1.5.3 Aptamer applications

Therapeutics

Aptamers have been developed for a variety of therapeutic and sensing applications. The first therapeutic aptamer to receive FDA approval is a VEGF antagonist used to treat macular degeneration, called pegaptanib (Macugen)[119]. Other RNA and DNA based aptamers targeting the treatment of cancers, inflammation, and blood disorders are currently in clinical trials[120]. Most therapeutic aptamers work as antagonists, blocking a disease-state interaction via target binding. The ability of aptamers to deliver drugs to cell targets has also been investigated, exploiting their target specificity and uptake by cells. Aptamer-mediated drug delivery has been achieved by conjugating aptamers directly to drug molecules[121, 122] and by conjugating them to drug containing nanoparticles such as liposomes[123].

Sensors

The largest field for aptamer applications is biosensing. The demand for new biosensors is growing as databases of biomarkers expand and improved indicators of disease are understood. Aptamers have been selected against targets for the detection of infectious diseases including *P. falciparum*[113] as well as for tracking chronic conditions such as cardiovascular disease[124].

In addition to their use in biological sensors once targets have been identified, aptamers are employed for biomarker discovery by using healthy tissue samples as a negative selection target and disease state tissue as a positive selection target[125]. Aptamers that bind disease state but not healthy tissues can be partitioned and their targets elucidated. This way, aptamers have been selected to identify various cancerous tissues[126, 127] and even to differentiate between metastatic and non-metastatic tissue[128].

Aptamers have been adapted into numerous sensing platforms. The most common include electrochemical sensors[129], fluorescent sensing platforms[130], and colorimetric readouts[131]. The most simple format is the direct labelling

of aptamers with a reporter molecule such as a fluorophore. The visualization of reporter-tagged aptamers can be used to localize targets during *in vivo* imaging[125].

Aptamer-based colorimetric sensors using gold nanoparticles were developed after the observation that unmodified single stranded DNA adsorbs to the surface of these particles in solution. Gold nanoparticles aggregate in the presence of salt, causing a color change in solution. The negatively charged DNA backbone adsorbs to the surface of gold nanoparticles, inhibiting their aggregation. Once aptamer target is introduced to this system, the aptamers bind the target, leaving the gold nanoparticles which aggregate inducing a visible color change. This approach has been tested for many different small molecule and protein-binding aptamers and provides a simple, visual readout. However, the system must be properly calibrated to induce color change upon target addition and some targets or sample matrices may interfere with nanoparticle aggregation or the visible readout[132, 133]. Aptamers have also been adapted to mimic the enzyme-linked immunosorbent assay (ELISA) that is commonly used in antibody sensing technology[134]. In this approach, one immobilized aptamer (or antibody) binds the target to attach it to a solid support and then, following wash steps, a second labeled aptamer is introduced. The binding of this reporter aptamer indicates the presence of target. Fluorescent or colorimetric dye labelled aptamers are commonly used in this approach. However, it can be challenging for small molecule targets which may not have the surface area to allow for the binding of two ligands simultaneously.

Another successful sensing platform involves target induced structure-switching aptamers. Aptamers that fold when binding their target, forcing the release of a complementary DNA strand were first reported in 2003[105]. This property has been adapted into various sensing platforms, mainly electrochemical[135, 136], and fluorescent[137, 138] sensors as shown in Figure 1.6.

The adaptation of binding aptamers into reporter molecules after selection can require a detailed understanding of the binding interaction and careful optimization to tailor the aptamer molecule. Moreover, it is not always generalizable as some sequences may not be able to create effective sensors[139]. By requiring enriched



Figure 1.6: Structure switching sensor format. **I.** Shows a simple structure-switching electrochemical sensor. The aptamer is initially hybridized to a complementary oligo that maintains a rigid format in which the electroactive reporter molecule is far from the electrode. Once target is introduced, the aptamer releases the complementary oligo to bind target, folding and bringing the reporter molecule closer to the electrode generating a measurable signal. **II.** Shows a structure-switching fluorescent aptamer sensor. Initially, the fluorophore labeled aptamer is bound to a quencher-tagged complementary oligo. Once target is introduced, the aptamer releases the quencher strand to fold and bind target and the fluorescent signal can be measured.

aptamers to bind the target and also undergo a significant secondary structure change or release from a capture oligo in the selection, the likelihood that selected aptamers can be adapted to sensors is increased. As discussed further in Chapter 3, this is another important advantage to capture-SELEX protocols.

1.6 Thesis aims

Much of the recent progress towards malaria elimination has been credited to effective medications and ongoing research continues to prioritize drug interventions. The majority of malaria R&D funding since 2010 was spent on medications over vaccine development, vector control, basic research, or diagnostics[1]. However, without effective implementation, regulation, and monitoring, drug compounds are vulnerable to resistance. The spread of resistance to current first-line ACTs has become a major concern for malaria elimination efforts, especially its spread westward towards Africa. As malaria parasites in Southeast Asia lose sensitivity to first-line ACTs, countries are alternating mandated therapies between combinations trying to preserve efficacy. This has led to challenging regulation and difficulties restricting access to compounds that are no longer approved for use.

A lack of information regarding drug access and adherence inhibits the ability to enforce regulation and to study factors affecting the emergence and spread

of resistance. The current reality of health-seeking behavior where patients visit pharmacies rather than health centers and in which they are frequently unaware of the specific drugs they are sold, results in an absence of information regarding drug use and adherence. Current methods to track drug use by detection from patient samples are expensive and time consuming. It was suggested that a low-cost field-based assay to measure ACT compounds from patient samples could be a useful tool to track drug use, quality, and adherence. This information could help resolve how these factors contribute to resistance and increase the ability to propose new policies to improve drug regulation and adherence.

My first aim in this thesis research was to confirm the utility of a field-based assay to detect slow-clearing ACT partner drugs. Our team of malaria researchers believed that this would be a helpful tool. However, I wanted to confirm that this belief was shared by members of key groups in the intended environment of use. I aimed to collect feedback on a potential new drug detection tool by conducting in-person interviews and an online survey of malaria clinicians, researchers, and experts at government bodies and funding institutions. This feedback would advise whether assay development should be pursued and if so, would inform the assay's operational characteristics.

My second aim was to select single stranded DNA aptamers capable of binding and differentiating between small molecule ACT partner drugs. To do this, I would use a capture-SELEX protocol, selecting aptamers that could easily be adapted into a fluorescent sensing platform without requiring immobilization of my drug targets. After selection, I would characterize the resulting sequences, selecting the most promising aptamers for sensor development.

My third aim was to develop a fluorescent sensor, following the feedback collected in aim 1 and using aptamers selected in aim 2. Ideally, the sensor would be easy to use, inexpensive, and only require access to basic bench top equipment. My final goal was to optimize the sensor function in relevant samples and characterize its performance.

2

Needs Assessment Survey

Contents

2.1 Introduction 24
2.1.1 Chapter 2 aims 25
2.2 Methods 25
2.2.1 Study design 25
2.3 Results 27
2.3.1 Web-based questionnaire responses 27
2.3.2 In-person interview responses 29
2.3.3 Development of target product profiles (TPPs) 32
2.4 Discussion 32
2.4.1 Overview 32
2.4.2 Limitations 34
2.4.3 Conclusions 35

2.1 Introduction

The emergence and spread of drug resistant malaria in Southeast Asia threatens to reverse progress made towards malaria elimination in the region and globally [64, 65]. In order to assist the study of drug use and regulation in Southeast Asia, a low-cost, field-based assay to detect slow clearing ACT partner compounds from patient samples was envisioned as a method of tracking drug use, adherence, and treatment failures. It was believed this would be a useful tool to study the

spread of drug resistance and to ascertain previous treatment information that could inform future treatment. However, in order to confirm the utility of the assay, it was necessary to collect feedback from potential end users and those familiar with the assay's intended environment of use.

New point-of-care tools have led to improved access to diagnosis and treatment of disease globally, and especially in the case of tropical diseases in rural settings. The efficacy and value of malaria rapid diagnostic tests (RDTs) have led to their vast adoption, with RDT use in Africa alone increasing from 25 million in 2008 to 125 million sold in 2014 [140]. However, many new tools for the diagnosis and study of disease are never adopted due to a lack of clinical need or operational feasibility. In order to ensure the prioritization of research efforts to develop effective new tools, proper market research and feedback collection should be performed prior to design [56]. This chapter discusses methods to perform a clinical needs assessment to determine the utility of an assay to detect ACT partner drugs from patient samples. Feedback on the most realistic applications of the assay and ideal design characteristics are reported and two separate target product profiles are developed.

2.1.1 Chapter 2 aims

1. Develop methods to collect feedback from malaria researchers, members of government/funding organizations, and field-based clinicians about the utility and desired operational characteristics of a drug detection assay.

2. Determine if this assay development is worth pursuing and if so create a target product profile from the survey feedback.

2.2 Methods

2.2.1 Study design

In-person interviews and a web-based survey were conducted in 2017 and 2018, targeting individuals working in malaria research, in funding or governmental organizations, and as clinicians in malaria endemic regions. In-person interviews

allowed for in-depth discussions, question follow-up, and inclusion of individuals without access to a web-based survey. The web-based survey allowed for inclusion of participants from more diverse geographies. University of Oxford social science professors Marco Haenssgen and Phaikyeong Cheah advised the design of the questionnaire and the structure of in-person interviews. Both qualitative and quantitative data were collected and both types of data informed the development of the target product profiles.

Interviews

Semi-structured interviews were performed one-on-one in Bangkok and Mae Sot, Thailand and Phnom Penh, Cambodia. Interviews were all conducted in English with translation help when necessary. They ranged from 20 to 60 minutes and were conducted at the interviewee's place of work. The interviews were transcribed and data was analyzed manually using qualitative analysis and coding by topic. Twenty-eight total interviews were conducted over the course of two months.

Web-based questionnaire

A web-based questionnaire was developed to target malaria researchers and those working at funding or government agencies focused on malarial control in broader geographic settings. The questionnaire was developed using Survey Monkey's online platform. It was adapted and optimized through in-person pretesting, as well as pilot testing with members of the study population. Pretesting was performed at the Mahidol Oxford Tropical Medicine Research Unit (MORU) in Bangkok, Thailand. Members of the study population were recruited to complete the web-based questionnaire under supervision. They were asked to verbalize all thoughts, questions, and concerns as they completed each question. This in-person pretesting revealed points of confusion or variable interpretation of questions prior to pilot testing. Participants of in-person pretesting were excluded from the final questionnaire data set. Pilot testing consisted of sending the questionnaire first to a small subset of the study population. Once these results were received and

evaluated, the questionnaire was sent to the rest of the targeted study population. The questionnaire was sent to 30 selected individuals.

2.3 Results

2.3.1 Web-based questionnaire responses

A total of 18 participants completed the web-based questionnaire. Of these participants, 17 reported being employed by a university or research institute and one reported being employed by a public health program. Participants reported working in Brazil (3), Cambodia (4), Colombia (1), Kenya (2), Laos (1), Mali (1), Myanmar (3), Peru (1), Senegal (3), Switzerland (2), Thailand (5), Uganda (1), The United Kingdom (1), The United States, (3), Vietnam (1), and Zambia (1). Several participants work in more than one country.

Of the 18 participants, 17 reported working in a setting where rapid diagnostics or point-of-care assays are used and 10 reported having a need for a point-of-care assay to detect antimalarial drugs from human samples in the last year. The most relevant applications of such an assay were reported to be surveillance of drug use in a region, inclusion/exclusion to a research protocol, and monitoring adherence during mass drug administration campaigns. The most relevant drugs for detection were reported to be piperaquine, lumefantrine, artemisinin-derivatives, primaquine, and mefloquine and preferences aligned with the most common therapies in the country where the respondent worked. The majority of respondents (67%) reported that there are scenarios where it would be useful to detect only one drug but all reported the likelihood of scenarios where it would be necessary to detect more than one drug (Table 2.1).

Regarding the operational characteristics of the assay, the majority of respondents believed that the assay should cost no more than $1 in order for it to be feasible for use. On average, about half of the respondents felt that it was not important that the assay provide any sort of quantitative output, and that a qualitative (yes/no) response indicating the presence or absence of drug would be sufficient. The in-person interviews helped clarify this perspective. During the interviews, several malaria

Question	Answer Options	% (N)
Does your work involve settings where rapid diagnostics or point-of-care assays are used?	Yes	94.4 (17)
	No	5.6 (1)
In the past year, have you had a need for a point-of-care assay to detect antimalarial drugs from patient samples?	Yes	55.6 (10)
	No	44.4 (8)
What antimalarial drugs are relevant to your research goals/clinical responsibilities? Please select all that apply.	Artemisinin/artemisinin derivatives	100 (18)
	Piperaquine	77.8(14)
	Mefloquine	61.1 (11)
	Amodiaquine	44.4 (8)
	Lumefantrine	77.8 (14)
	Chloroquine	61.1 (11)
	Primaquine	88.9 (16)
	Sulfadoxine/pyrimethamine	50 (9)
	Other (please specify)	5.6 (1)
What do you think would be the most relevant applications for a field-based drug detection assay? Please select all that apply.	Detecting previous treatment failures	61.1 (11)
	Inclusion/exclusion to a research protocol	72.2 (13)
	Surveillance of drug use in a region	77.8 (14)
	Measuring drug levels as an indicator of drug absorption and treatment efficacy	66.7 (12)
	Monitoring adherence during mass drug administration campaigns	72.2 (13)
	Detecting falsified/substandard drugs (from crushed tablets)	61.1 (11)
	Other (please specify)	16.7 (3)
Based on the applications you envision, what drugs do you think would be most useful to detect in a point-of-care setting? Please select all that apply.	Artemisinin/artemisinin derivatives	66.7 (12)
	Piperaquine	77.8 (14)
	Mefloquine	55.6 (10)
	Amodiaquine	50 (9)
	Lumefantrine	77.8 (14)
	Chloroquine	27.8 (5)
	Primaquine	66.7 (12)
	Sulfadoxine/pyrimethamine	33.3 (6)
	Other (please specify)	0.0% (0)
Is there a scenario where it would be useful to detect just one drug?	Yes	66.7% (12)
	No	33.3% (6)
Is there a scenario where you would need to be able to detect more than one drug in order to be useful?	Yes	100% (18)
	No	0% (0)

Table 2.1: Reported assay utility from web-based survey. The questions, possible answer choices, and responses in both absolute number and percent of total responses are reported. The survey was completed by 18 participants.

Question	Answer Options	% (N)
How much could this assay cost in order for it to be feasible for use?	Less than $1	66.7% (12)
	Between $1 and $5	22.2% (4)
	More than $5	11.1% (2)
	Other (please specify)	0% (0)
On a scale of 0-100, how important is it that the assay be semi-quantitative (provide a range of concentrations) versus qualitative (appearance of line indicates some drug present).	Average of responses 0 = semi-quantitative 100 = qualitative.	54 Score from 0-100 (N=13)
What sample type would be the easiest to use in this point-of-care assay? Please rank most practical (1) to least practical (4).	Sample Type	Average Rank (N=17)
	Finger stick blood	1.8
	Saliva	1.9
	Urine	2.9
	Venus blood	3.3

Table 2.2: Reported operational requirements from web-based survey. The questions, possible answer choices, and responses in both absolute number and percent of total responses are reported. The survey was completed by 18 participants. The question regarding semi-quantitative versus qualitative readouts reports an average score from preferentially semi-quantitative (0) to preferentially qualitative (100). A score of 54 indicates that there was no clear preference. This topic was further clarified in the interviews.

clinicians and those familiar with clinic work in rural malaria-endemic settings explained a preference for a qualitative assay due to ease of interpretation. However, in the case of a lab-based assay used by malaria researchers, a semiquantitative readout was indicated as preferred since this information could be useful and the environment would allow for more complex interpretation of results. Respondents ranked four possible sample types, from most to least practical, with finger stick blood being the most practical and venous blood being the least practical (Table 2.2).

2.3.2 In-person interview responses

Of the twenty-eight interviews conducted, nine interviewees were identified as malaria researchers, nine as people working at funding/development or government agencies, and ten as field-based clinicians. All interviewees reported working in Thailand, Cambodia, or both and several also worked in other Southeast Asian countries. After transcription, the interview content was sorted into main questions and further into the profession of the interviewee. This allowed for the identification

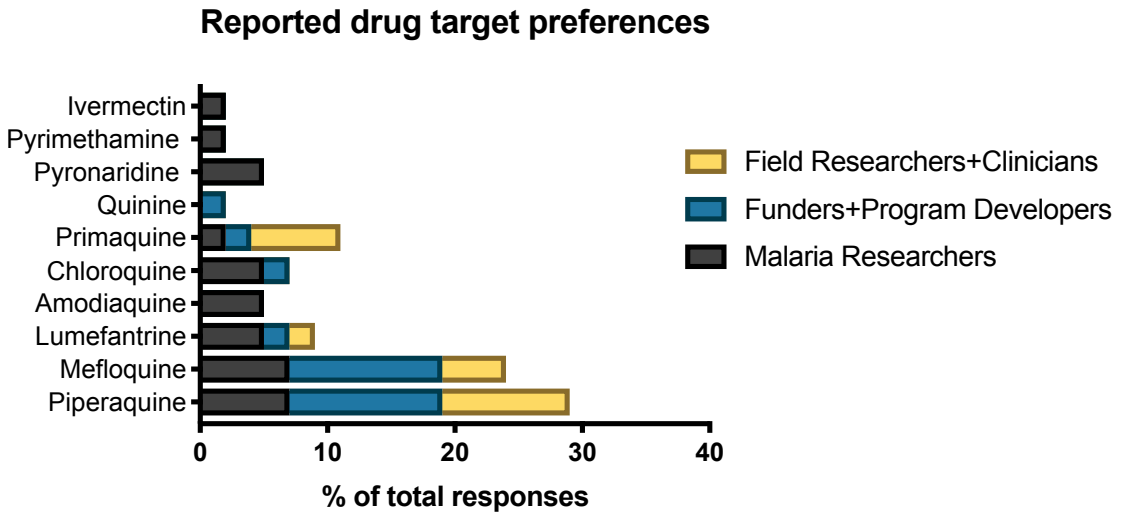


Figure 2.1: Reported drug target preference from interviews. The majority of interviewees responded considering their experience and knowledge of drug use in Southeast Asia. However, lumefantrine was also cited due to its well-known issues with absorption.

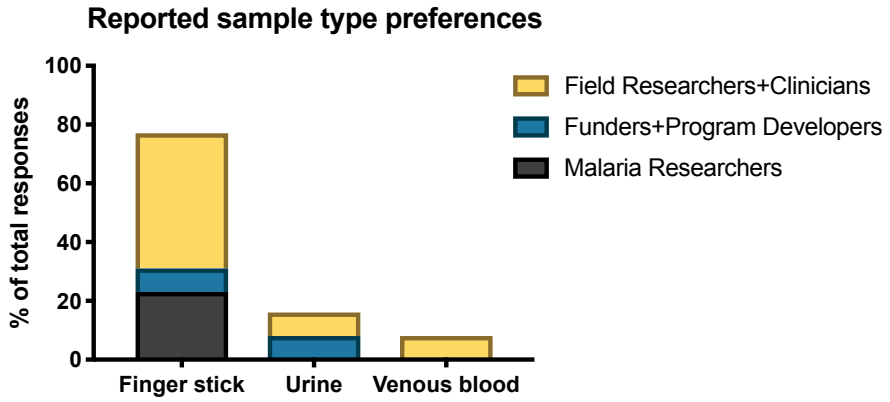


Figure 2.2: Reported sample preference from interviews. It should be noted that the preference for venous blood samples was in reference to a scenario where a venous draw had already been done. In this case, it would be desirable to use the venous blood rather than to have to perform an additional finger stick.

of trends in answers based on work environment and experience such as the difference in quantitative versus qualitative readout preference described previously and shown in Figure 2.3. The preferred drug targets reported in interviews followed the trend from the web-based survey response that the respondent's area of work and the current first-line therapy in that region primarily determined drug target preferences (Figure 2.1). Regarding the preferred sample type for the assay, a majority responded that a finger stick sample would be most practical (Figure 2.2). The most reported

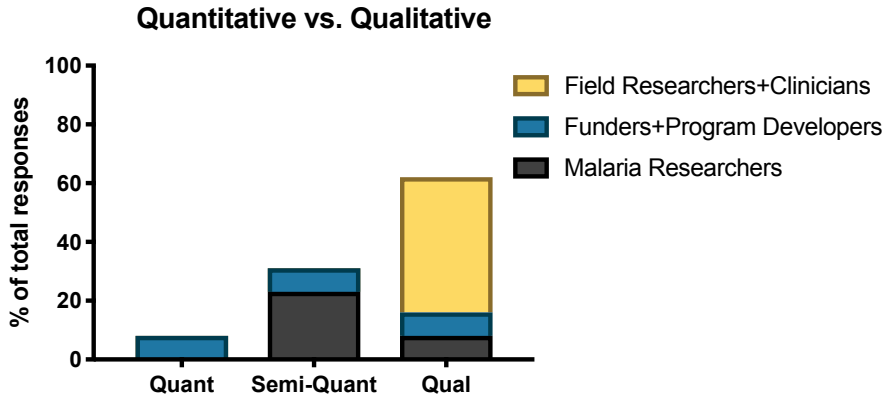


Figure 2.3: Reported preference for quantitative versus qualitative readout from interviews. All field researchers and clinicians reported a preference for a qualitative assay and explained that this was due to the challenging interpretation of semi-quantitative or quantitative assays in such environments.

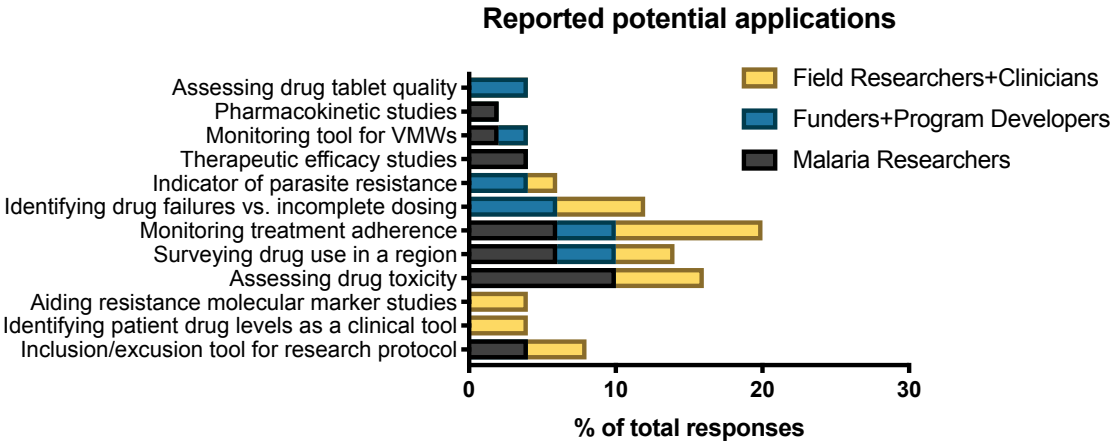


Figure 2.4: Reported potential assay applications from interviews. The trend in answers reported in the interviews follows that of the web-based survey. The most common responses suggest the use of this assay as a research tool that could operate in a laboratory to collect data on drug use and treatment adherence. However, several reported applications such as assessing drug toxicity and measuring patient drug levels in the clinic or for MDA monitoring could require a point-of-care assay format.

applications of a drug detection assay were monitoring adherence during mass drug administration, assessing drug toxicity, and surveying drug use in the region (Figure 2.4). Since the in-person interviews were conducted in Southeast Asia, this data should be interpreted mainly as preferences for an assay to be used in Southeast Asia.

2.3.3 Development of target product profiles (TPPs)

Based on the information collected via the web-based survey and the in-person interviews, an interest in two different tools was reported and thus two target product profiles were developed. A major point of feedback was an interest in this tool primarily as a research assay. An affordable assay that could be used in small labs in Southeast Asia requiring only standard lab equipment would allow researchers to collect information on drug use in a more timely and cost-effective manner as compared to shipping samples for liquid chromatography-mass spectrometry (LC-MS) analysis. This lab-based assay would ideally be quantitative or semi-quantitative and detect multiple drugs to increase its utility for a variety of applications. The consumables should be those readily affordable and accessible and cost no more than $5 per sample. The assay could require access to standard bench top equipment, though this may limit its accessibility. The details of the target product profile are shown in Table 2.3.

The second target product profile describes a point-of-care assay where it would be useful to have information on drug use while the clinician is still in contact with or making treatment decisions for the patient. This assay should be qualitative and would require an easier to use format without access to bench top equipment for analysis. The assay should cost no more than $5 per test, including all necessary components, and would ideally run on small volumes of either finger stick or venous blood. The details of the target product profile are reported in Table 2.4.

2.4 Discussion

2.4.1 Overview

The creation of new point-of-care tools is often motivated by technological advancement rather than a defined clinical need. This approach can result in misguided design and the use of resources to develop tools that will not be adopted in the clinic as they were envisioned in the lab. Initial attempts to develop an ACT partner drug detection assay described in this thesis began after discussions with peers in

Target Product Profile 1: Inexpensive lab-based assay			
Parameter	**Ideal**	**Acceptable**	**Comments**
Cost	< $1	$1-5	This refers to the cost of consumables. The assay may require access to bench top equipment.
Sample type	Finger stick or venous blood (or dissolved tablets)	Plasma or serum from finger stick or venous blood (or dissolved tablets)	Preference for smallest possible blood volume. Preference for unprocessed blood but centrifugation to isolate plasma accepted.
Drug Target	All partner drugs in use in the region	One first-line partner drug	Depends on region and desired application.
Quant vs. Qual	Quantitative	Semi-quantitative	
Limit of detection	3-30 days	3-7 days after	
Access to equipment	Portable and inexpensive fluorimeter or spectrophotometer. All consumables included in kit.	Bench top fluorimeter or spectrophotometer, may require access to standard lab consumables such as well-plates.	

Table 2.3: Lab-based assay target product profile.

the malaria research field. During initial development, a lack of clarity regarding the operational characteristics of the tool and the feasibility of its envisioned use led to a pause in assay development to prioritize a study to understand the realistic utility of the assay and how it might be adopted before further design.

Three stakeholder groups were identified to survey: 1) malaria researchers to gather wider and more in-depth feedback from peers, 2) malaria clinicians and field workers to understand the opinions and desired assay characteristics of those who are envisioned to be the end-users of the assay, and 3) government officials and funding agencies believed to be decision makers about the adoption of new tools in target countries. The use of both an online web-based survey and in-person interviews was planned in order to ensure access to members of stakeholder groups and to collect thorough responses. The in-person interviews provided useful context which helped interpret responses from the web-based questionnaire and the two data

Target Product Profile 2: Point-of-care clinical assay			
Parameter	**Ideal**	**Acceptable**	**Comments**
Cost	< $1	$1-5	Refers to entire kit
Sample type	Finger stick and venous blood	Finger stick blood	Ideally would work similarly with finger stick and venous blood
Drug Target	All partner drugs in use in the region	One first-line partner drug	
Quant vs. Qual	Qualitative	Qualitative	Qualitative was reportedly preferred over quantitative for field-based POC settings
Limit of detection	3-30 days after	3-7 days after	30 days after treatment would identify more people if using for surveillance and could identify failed treatments
Access to equipment	No bench top equipment required, all components packaged together	No bench top equipment required, all components packaged together	

Table 2.4: Point-of-care assay target product profile.

sets served to reinforce findings. Responses from members of different stakeholder groups were found to be mostly similar. A notable difference was the discussed example where clinicians and field workers' experience of RDT use in rural clinics allowed them to suggest operational characteristics to improve utility that may not have been obvious to malaria researchers or government officials.

2.4.2 Limitations

The conclusions of this survey are limited by the number of participants. Only eighteen participants responded to the online survey and twenty-eight individuals were surveyed in person. The majority of participants were based in Southeast Asia, though some reported working in other regions as well. In order to increase confidence in the conclusions drawn from the surveys, more participants should be included. Additionally, if the results are to be interpreted for environments outside of Southeast Asia, more participants familiar with other settings should

be included. For the purpose and scope of this research, the data collected improved understanding of realistic assay applications and necessary operational characteristics to improve the assay's feasibility.

Another limitation in this survey is possible bias in reporting which would likely skew the results towards a more positive representation of the usefulness of the assay. It is likely that participants of both the survey and in-person interviews felt encouraged to report a need for the assay based simply on the fact that they were being asked by a researcher who was considering developing such an assay. In order to try to avoid this, the survey responses were kept anonymous except in the instance where respondents provided their contact information to receive a report of the results (which was made clear at the beginning of the survey). In-person interviews were clearly not anonymous and more likely influenced by this type of reporting bias. The interviewer made extra effort to establish at the beginning of each interview that the goal was to determine whether such a tool would be useful and gather honest feedback to inform assay development. However, to reduce bias, perhaps a better method would be to have the interviews conducted by a third person who was not invested in assay development.

2.4.3 Conclusions

The feedback from this survey helped inform subsequent assay development efforts. The feedback reported that the initial assay idea, where a point-of-care drug detection tool would report previous treatment in order to inform future treatment was likely not feasible. However, participants reported an interest in an affordable lab-based drug detection assay. An alternative method to LC-MS for measuring drug levels from patient samples that could be performed by researchers in their own labs in Thailand and Cambodia would allow them to expand their research capabilities to study drug use, regulation, and patterns that contribute to emerging resistance.

Prior to this survey, a lab-based assay platform had not been considered and only a point-of-care format was envisioned. Based on the feedback collected, there appears to be a use-case for a point-of-care assay to detect antimalarial drugs.

However, in order for the point-of-care assay to be useful, it will need to be very inexpensive, easy to interpret, and adaptable for the detection of various drugs. The greater interest in an affordable lab-based assay as well as the relatively lower technological hurdles of a lab-based assay, as compared to a point-of-care assay, led to the prioritization of the lab-based format. Without conducting the survey, only a point-of-care format would have been pursued.

Collecting feedback to assess need and required operational characteristics should be performed before time and resources are used to develop new point-of-care tools. This type of research is especially important before the development of new tools for low-resource settings where there is an incorrect opinion that a general lack of access to technology will result in the more liberal adoption of new tools. In fact, tools designed for rural or low-resource settings often encounter large and unpredictable barriers to use. In conclusion, the feedback collected in this chapter allowed for the development of target product profiles that informed the development of a new drug detection sensor.

3
Aptamer Selection

Contents

3.1 Introduction 37
3.1.1 Chapter 3 aims 39
3.2 Methods 39
3.2.1 Lumefantrine SELEX protocol 39
3.2.2 Piperaquine and mefloquine SELEX protocol 47
3.2.3 Binding affinity assays 59
3.3 Results 72
3.3.1 SELEX summary 73
3.3.2 Sequence analysis results 76
3.3.3 Binding affinity results 80
3.4 Discussion 103
3.4.1 Overview 103
3.4.2 SELEX 103
3.4.3 Sequencing 105
3.4.4 Affinity analysis 105
3.4.5 Limitations and conclusion 108

3.1 Introduction

The ability to generate single-stranded oligonucleotide sequences that bind specific target molecules via electrostatic interactions and conformational fit was first discovered in 1990 [99, 100]. These single-stranded molecules, called aptamers,

are developed in an evolutionary process called SELEX (Systematic Evolution of Ligands by EXponential enrichment). The SELEX protocol begins with a pool of many random-sequence single stranded DNA or RNA oligonucleotides, which are repetitively exposed to target molecules. Binding sequences are separated and carried forward for subsequent rounds until the pool evolves to be enriched for target-binding sequences. Aptamer applications include therapeutics, biosensors, and the identification of biomarkers. They have been selected to bind protein, whole cell, and small molecule targets.

Aptamer selection against small molecule targets has unique challenges due to the inability to immobilize targets while retaining their native structure and charge distribution. Several methods to work around this issue have been developed including protocols in which the aptamer library itself is immobilized allowing the target to be introduced to the library in solution. The immobilization of either library or target is important for separating binding sequences from non-binding sequences. A capture-SELEX method, first described in 2012, introduced the use of a short 'capture' or 'binding' oligonucleotide to weakly bind the aptamer library via hybridization [141]. In this method, the introduction of target molecules in solution forces the aptamer library to compete between binding the short complementary oligo to which it is immobilized and the small molecule target. This model negates the need for small molecule immobilization and, in selecting structure switching aptamers that release a complementary oligo upon target binding, facilitates the development of simple sensors to report aptamer-target interaction.

This chapter describes methods to select single-stranded DNA aptamers capable of specifically binding small molecule ACT partner drug compounds. Two different capture-SELEX protocols were attempted and the results are reported. Selected sequences were assessed for binding affinity using three different binding assays, isothermal titration calorimetry (ITC), a fluorescent-binding assay, and surface plasmon resonance (SPR) via Biacore.

3.1.1 Chapter 3 aims

1. Select aptamers against ACT partner drugs with sufficient sensitivity to detect drugs at least seven days after dosing and specificity to distinguish between partner drugs.

2. Characterize the binding affinity of selected aptamers.

3.2 Methods

3.2.1 Lumefantrine SELEX protocol

The first SELEX experiment in this project was performed against the target lumefantrine. Lumefantrine is typically co-formulated with the artemisinin derivative artemether and branded as Coartem®, Riamet®, and Falcynate-LF®, among others [36]. Lumefantrine was chosen as the first ACT partner drug for aptamer selection due to its widespread use as well as its unique structure (Figure 3.1). Lumefantrine is the only commonly used partner drug that is not comprised of one or more quinoline rings. It was hypothesized that lumefantrine's unique structure would improve the likelihood of successfully selecting aptamers without cross-reactivity to other partner drugs.

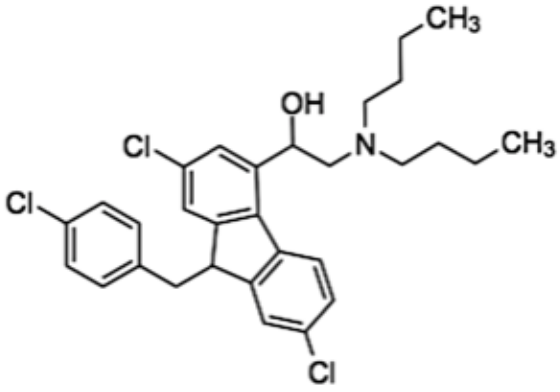


Figure 3.1: Lumefantrine structure

The first attempted SELEX experiment was adapted from a protocol published by Stoltenburg et al. [141]. Changes to the published protocol were made in

the single-stranded DNA generation, purification, and sequencing steps. The library design from the protocol was used, in which two random regions surround a conserved docking sequence (Figure 3.2). This library design had been reported to successfully select DNA aptamers against small molecule aminoglycoside antibiotics. The rationale behind this library structure is the belief that inserting the conserved docking region between the random regions will improve the likelihood that binding will result in a structure change that forces the sequences to release from the capture oligo upon binding. The details of the protocol are reported here and depicted in Figure 3.2.

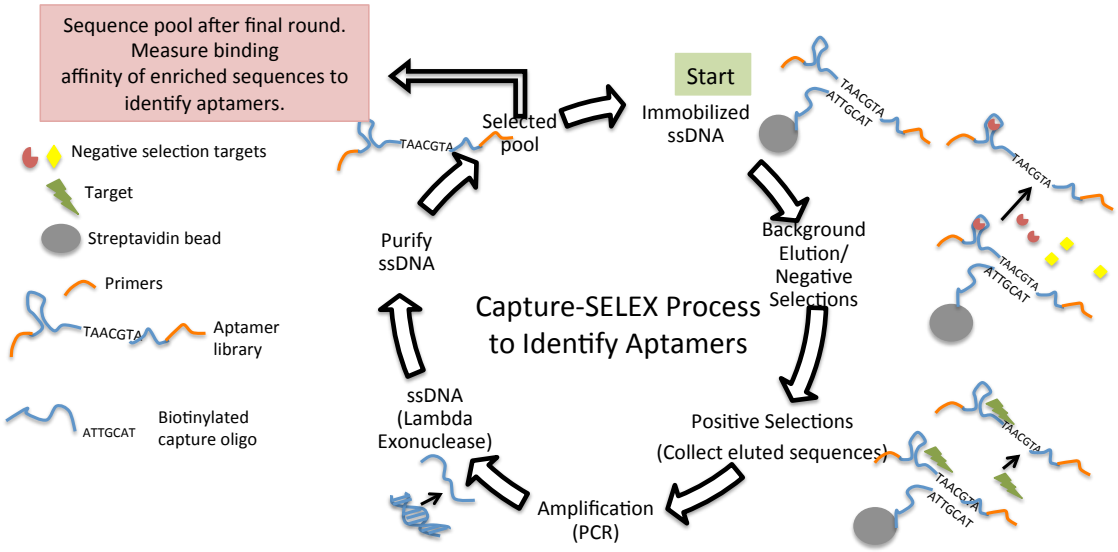


Figure 3.2: Describes the steps of the lumefantrine SELEX protocol. To start, the aptamer library is immobilized to streptavidin coated magnetic beads via hybridization to a short biotinylated capture oligo. Next, background elution washes and negative selection steps are performed in which the immobilized library is washed with buffer and with solutions of negative selection targets (in this case, amodiaquine, piperaquine, and mefloquine). Any sequences that release during these steps are removed from the pool and discarded. Next, the positive selection target (lumefantrine) is added to the library in solution. Any sequences that release during this step are collected in the supernatant and carried forward to be amplified via PCR. After PCR, a single stranded library must be made from the amplified sequences which are now double stranded. The double stranded sequences are exposed to a lambda exonuclease which degrades the reverse strand. The remaining strand is purified from discarded nucleotides and enzyme and resuspended in buffer, ready to begin the next cycle. These steps are repeated until the library pool evolves to contain enriched sequences with desired binding characteristics. After the final round, the library is sequenced and the enriched sequences are identified and characterized.

Binding and Washing (B+W) Buffer	
Contents	**Final concentration**
Tris Buffered Saline (Sigma Aldrich, cat. no. T5912)	50 mM
NaCl (Sigma-Aldrich, ca. no. S9888)	137 mM
$MgCl_2$ (Invitrogen, cat. no. AM9530G)	5 mM
KCl (Fluka, cat. no. 60142)	5 mM

Table 3.1: Binding and washing (B+W) buffer components.

Reagent preparation

Binding and Washing (B+W) buffer was prepared according to Table 3.1. The pH was adjusted to 7.4 with 1N NaOH (Sigma Aldrich, cat. no. S2770) and 1N HCl (Sigma Aldrich, cat. no. H98982). The buffer was filtered through a 0.2-µm filter (EMD Millipore, cat. no. SCGVU01RE) and stored at room temperature.

The aptamer library, capture oligo, and primers (Tables 3.2 and 3.3) were synthesized and HPLC purified by Integrated DNA Technologies (IDT, Coralville, IA). All oligonucleotides were suspended in DNase/RNase-free water at a stock concentration of 100 µM and stored at -20°C until use.

Aptamer Library	5'-ATACCAGCTTATTCAATT-(N10)-TGAGGCTCGATC-(N40)-AGATAGTAAGTGCAATCT-3'
Capture Oligo	5'-Bio- GTC/iSp9/GATCGAGCCTCA

Table 3.2: Lumefantrine library and capture sequence format. Note: iSp9 is a triethylene glycol spacer. Conserved regions in grey.

Forward Primer	5'-ATACCAGCTTATTCAATT-3'
Reverse Primer	5'-phospho-AGATTGCATTACTATCT-3'

Table 3.3: Lumefantrine SELEX primer sequences. Note: 5' phosphorylation is required for lambda exonuclease activity.

Table 3.4 shows positive and negative target stock solutions, prepared in methanol, dimethyl sulfoxide (DMSO), or water depending on solubility. All stock solutions were stored at 4°C until use.

Target	Stock
Lumefantrine	10 mM, 100% DMSO
Amodiaquine	50 mM, 100% MeOH
Desethyl-Amodiaquine	50 mM, 100% MeOH
Mefloquine	50 mM, 100% MeOH
Piperaquine	1 mM, 5% MeOH
Chloroquine	50 mM, H_2O
190 (1/2 piperaquine)	50 mM, 100% MeOH
BSA	1 mM, H_2O

Table 3.4: Positive and negative target molecule stock solutions. Lumefantrine, amodiaquine, desethyl-amodiaquine, and chloroquine were obtained as reference stocks from the WorldWide Antimalarial Resistance Network (WWARN) malaria drug reference material programme. Piperaquine (cat. no. C7874), mefloquine (cat. no. M2319), and bovine serum albumin (BSA, cat. no. 05470) were obtained from Sigma Aldrich. The purity of all compounds and standards was reported to be $\geq$ 98%. Molecule 190 was synthesized as described in Section 3.2.2, purity > 95%.

Before selection, the biotinylated capture oligo was immobilized on Invitrogen M-270 Dynabeads™(cat. no. 65306). These streptavidin coated magnetic beads have a binding capacity of 0.2 nmol single stranded (ss)DNA/100 µL bead solution. A 500 µL aliquot of beads was washed twice with 750 µL B+W Buffer, mixed gently, and the supernatant was discarded after concentrating beads on a magnetic tube rack. The washed beads were incubated with 500 µL 5 µM biotinylated capture oligo in B+W buffer for 10 min with gentle agitation at room temperature. The beads were washed twice in 500 µL B+W buffer to remove any weakly bound molecules and stored at 4°C. A 10 µM aptamer library solution was prepared in B+W buffer from 100 µM aptamer library stock, incubated in boiling water for five minutes, then cooled to room temperature to promote consistent secondary structure after thawing.

Library immobilization

To immobilize the library on the capture oligo treated beads, 300 µL capture oligo-immobilized beads were transferred to a new tube and the supernatant was discarded. A 200 µL aliquot of 10 µM aptamer library in B+W buffer was added to the beads and incubated for 30 minutes at room temperature with gentle agitation. After 30 minutes, the supernatant was removed and the beads were washed twice with 500 µL 1% DMSO, B+W buffer.

Lumefantrine SELEX 1 protocol			
Round	**Washes**	**Negative Selection**	**Positive Selection**
1	**1:** 500 µL B+W Buffer **2:** 500 µL B+W Buffer	---	30-min B+W buffer, 1% DMSO, 100 µM LF
2	**1:** 500 µL B+W Buffer, 1% DMSO	---	30-min B+W buffer, 1% DMSO, 100 µM LF
3	**1:** 500 µL B+W Buffer, 1% DMSO	30-min B+W buffer, 1% DMSO	30-min B+W buffer, 1% DMSO, 100 µM LF
4	**1:** 500 µL B+W Buffer, 1% DMSO	30-min B+W buffer, 1% DMSO, 10 µM AQ, MQ, PQ	30-min B+W buffer, 1% DMSO, 100 µM LF
5	**1:** 500 µL B+W Buffer, 1% DMSO	30-min B+W buffer, 1% DMSO, 10 µM AQ, MQ, PQ	30-min B+W buffer, 1% DMSO, 50 µM LF
6	**1:** 500 µL B+W Buffer, 1% DMSO	30-min B+W buffer, 1% DMSO, 10 µM AQ, MQ, PQ	30-min B+W buffer, 1% DMSO, 100 µM LF
7	**1:** 500 µL B+W Buffer, 1% DMSO	30-min B+W buffer, 1% DMSO, 10 µM AQ, MQ, PQ	30-min B+W buffer, 1% DMSO, 100 µM LF
8	**1:** 500 µL B+W Buffer, 1% DMSO **2:** 500 µL B+W Buffer, 1% DMSO	30-min B+W buffer, 1% DMSO, 10 µM AQ, MQ, PQ	30-min B+W buffer, 1% DMSO, 100 µM LF

Table 3.5: Lumefantrine SELEX experiment 1 (SELEX LF1). Eight rounds of SELEX were performed washing with B+W buffer, 1% DMSO and using amodiaquine (AQ), mefloquine (MQ), and piperaquine (PQ) as the negative selection targets. The lumefantrine concentration was maintained at 100 µM since a drop to 50 µM for round 5 resulted in very low DNA recovery (assessed via the number of PCR rounds required to produce a visible band).

Negative selection

For the first SELEX round, the negative selection step consisted of a 30-minute wash. The library-coated beads were resuspended in 100 µL 1% DMSO B+W buffer, mixed and incubated at room temperature for 30 minutes with gentle agitation. The supernatant was then removed and discarded. Washes with 1% DMSO were included in the negative selection steps to remove any sequences that might be affected by the solvent since lumefantrine buffer contains 1% DMSO in the positive selection step. The stringency of negative selection increased throughout SELEX rounds. The conditions of each round are described in Tables 3.5 and 3.6.

Positive selection

After negative selection, the beads were resuspended in 100 µL freshly made 100 µM lumefantrine (1% DMSO, B+W buffer). The beads were incubated for 30 minutes with gentle agitation. After 30 minutes, the supernatant was removed

Lumefantrine SELEX 2 protocol			
Round	**Washes**	**Negative Selection**	**Positive Selection**
1	**1:** 500 µL B+W Buffer, 1% DMSO **2:** 500 µL B+W Buffer, 1% DMSO	30-min B+W buffer, 1% DMSO	30-min B+W buffer, 1% DMSO, 100 µM LF
2	**1:** 500 µL B+W Buffer, 1% DMSO **2:** 500 µL B+W Buffer, 1% DMSO	30-min B+W buffer, 1% DMSO, 10 µM AQ, MQ, PQ	30-min B+W buffer, 1% DMSO, 100 µM LF
3	**1:** 500 µL B+W Buffer, 1% DMSO **2:** 500 µL B+W Buffer, 1% DMSO	30-min B+W buffer, 1% DMSO, 10 µM AQ, MQ, PQ	30-min B+W buffer, 1% DMSO, 100 µM LF
4	**1:** 500 µL B+W Buffer, 1% DMSO **2:** 500 µL B+W Buffer, 1% DMSO	30-min B+W buffer, 1% DMSO, 10 µM AQ, MQ, PQ	30-min B+W buffer, 1% DMSO, 50 µM LF
5	**1:** 500 µL B+W Buffer, 1% DMSO **2:** 500 µL B+W Buffer, 1% DMSO	30-min B+W buffer, 1% DMSO, 10 µM AQ, MQ, PQ	30-min B+W buffer, 1% DMSO, 50 µM LF
6	**1:** 500 µL B+W Buffer, 1% DMSO, **0.5% BSA** **2:** 500 µL B+W Buffer, 1% DMSO	30-min B+W buffer, 1% DMSO, 10 µM AQ, MQ, PQ	15-min B+W buffer, 1% DMSO, 50 µM LF
7	**1:** 500 µL B+W Buffer, 1% DMSO, **0.5% BSA** **2:** 500 µL B+W Buffer, 1% DMSO	15-min B+W buffer, 1% DMSO, 10 µM AQ, MQ, PQ	15-min B+W buffer, 1% DMSO, 50 µM LF

Table 3.6: Lumefantrine SELEX experiment 2 (SELEX LF2). Seven rounds of SELEX were performed. Bovine serum albumin (BSA, 0.5%) was added to the later wash steps to remove library components that might bind nonspecifically to protein. Amodiaquine (AQ), mefloquine (MQ), and piperaquine (PQ) were used as negative selection targets. With the goal of identifying higher affinity aptamers, the lumefantrine concentration was decreased to 50 µM for the final rounds and the target incubation time was decreased to 15 minutes.

and transferred to prepared PCR tubes. The lumefantrine concentration for each positive selection round is described in Tables 3.5 and 3.6.

Amplification via PCR

Before starting SELEX, the PCR annealing temperature, template concentration, and primer concentrations were optimized in order to limit amplification of non-specific products. Optimized conditions are shown in Table 3.7. Prior to each SELEX experiment, a PCR master mix was prepared by combining 4 mL Takara Taq Pre-mix (cat. no. R004A), 2.4 mL H_2O, 400 µL 10 µM forward primer, and 400 µL 10 µM reverse primer. Aliquots of 90 µL per PCR tube were prepared and frozen at -20°C. After each positive selection round, 10 pre-made PCR tubes were thawed and 10 µL of positive selection supernatant were added to each tube. A negative control tube was also run. First, a single tube was amplified 4 cycles and then loaded on a 3% Agarose, 0.02% ethidium bromide gel to check for a band. If no band was visible, 4 more cycles were run. This was repeated until a band

LF SELEX optimized PCR conditions			
1.	95°C	15 min	
2.	95°C	1 min	Repeat for X cycles
3.	59°C	30 sec	
4.	72°C	30 sec	
5.	72°C	2 min	

Table 3.7: Optimized PCR conditions for lumefantrine SELEX experiments.

was visible. Amplification was performed slowly with visual checks to avoid over amplification and the appearance of nonspecific product in the aptamer library. After the initial test, the rest of the PCR tubes were brought up to the minimum number of cycles required to produce a band.

Generation of ssDNA via lambda exonuclease

After amplification, a single stranded library was generated using lambda exonuclease (New England Biolabs cat. no. M0262L). Lambda is a 5' to 3' exonuclease with a preferred 5' phosphorylated double stranded DNA substrate. Each 100 µL of PCR product was combined with 10 µL lambda digestion buffer and 1 µL lambda exonuclease, incubated at 37°C for 30 minutes, then at 75°C for 10 minutes to inactivate the enzyme. After lambda digestion, the sample was run on a gel to confirm a decrease in band strength indicating proper enzyme function.

Purification of ssDNA

After lambda digestion, the ssDNA products were purified to remove digested DNA, enzymes, and salts from PCR amplification and exonuclease processing using Invitrogen's Chargeswitch® purification kit (cat. no. CS12000). The contents of two lambda-digested PCR tubes were combined with 200 µL purification buffer and 10 µL Chargeswitch® beads. The contents were mixed and incubated at room temperature for one minute. Beads were concentrated using a magnetic rack and the supernatant was discarded. The beads were washed twice with 150 µL of Chargeswitch® washing buffer. Rather than eluting DNA using the Chargeswitch® elution buffer, 100 µL B+W buffer was added to the washed beads, mixed, and incubated at room temperature for one minute. Elution in B+W buffer

was not as efficient as the kit's recommended elution buffer and this modification to the protocol resulted in a 25% loss of DNA, measured via Nanodrop. However, this was less than the loss measured during other forms of ssDNA purification (such as ethanol precipitation) and avoided the need of a buffer exchange step. After adding B+W buffer, the beads were concentrated with a magnetic rack and the supernatant was collected and saved for the next round.

SELEX conditions

The procedures for library immobilization, negative selection, positive selection, amplification, ssDNA generation, and purification were repeated for all SELEX cycles. Two separate SELEX experiments against lumefantrine were performed in parallel as described in Tables 3.5 and 3.6. The second lumefantrine selection (SELEX LF2) had more stringent washes, negative, and positive selection steps. It also included bovine serum albumin (BSA) as an additional negative target in later wash steps. These two experiments with varying conditions were performed side by side with the goal of studying the effects of increased stringency on SELEX success.

Sequencing

Library samples from one intermediate round and the final round of each SELEX experiment were PCR amplified and purified via Qiaquick PCR purification kit (Qiagen, cat. no. 28104). The samples were adapted and sequenced on an Illumina MiSeq by colleagues at the Rocky Mountain Laboratory (Research Technologies Branch, NIAID) in Montana, USA.

The results of both SELEX LF1 and LF2 experiments are described in Section 3.3.2. The obtained sequences were sorted based on enrichment. The predicted secondary structure of the most enriched sequences as well as their binding affinity to lumefantrine were evaluated.

3.2.2 Piperaquine and mefloquine SELEX protocol

After the lumefantrine SELEX experiments resulted in little enrichment and selected sequences showed no measurable binding affinity to target, several modifications to the protocol were proposed. In particular, it was determined that methods should be implemented to measure SELEX progress to better predict the ideal number of rounds to perform. Attempts to develop a Biacore method to achieve this are described in Section 3.3.3. Around this time, a methods paper was published reporting successful selection of aptamers against a variety of small molecule targets [142]. This approach retained most of the desired characteristics of the original lumefantrine SELEX protocol. The new protocol selected for structure switching aptamers that could be adapted to a simple fluorescent sensor and did not require the immobilization of positive and negative target molecules. This protocol also suggested a new method for single-stranded DNA generation and purification and included a simple method for tracking SELEX progress via small-scale elution profiles.

Before implementation of the new SELEX protocol, feedback from the survey described in Chapter 2 was collected and analyzed. Results of the survey suggested prioritizing new ACT partner drugs for detection. As the idea for the assay evolved, it was decided that the target partner drugs for detection should be those used most commonly in Southeast Asia – piperaquine and mefloquine. Using this new SELEX protocol, selection experiments were performed against both drug targets. The details of this new protocol are shown in Figure 3.4 and described in this section.

Piperaquine SELEX targets

Due to the limited aqueous solubility of piperaquine, it was not possible to make a 100 µM piperaquine solution in selection buffer. Based on the published protocol, there was concern that starting below a 100 µM target concentration would not allow for adequate selection. To address this, a half-piperaquine molecule with improved solubility was synthesized and used as the positive target. Molecule SP-III-190C (190), is one half of the full symmetrical piperaquine molecule as shown in Figure

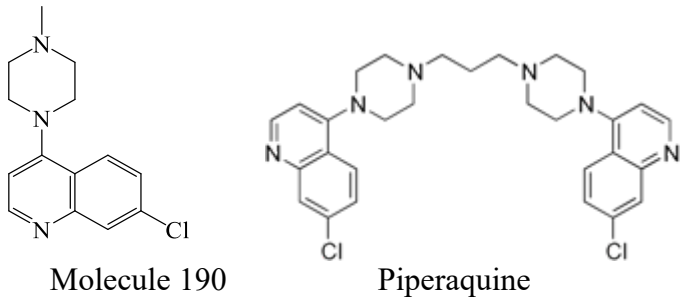


Figure 3.3: Structure of molecule 190 versus piperaquine

3.3. It was hypothesized that aptamers selected against the 190 half-molecule would also bind the full piperaquine molecule and that perhaps two aptamers could bind each piperaquine molecule improving sensitivity of the envisioned aptamer sensor. A 100 µM solution of molecule 190 in selection buffer was easily prepared from a 50 mM MeOH stock (Table 3.4) and piperaquine SELEX experiment 1 (SELEX PQ1) was performed using molecule 190 as the positive selection target. However, after testing of the selected aptamers revealed a decreased sensitivity to the full piperaquine molecule as compared to molecule 190, SELEX was repeated using the full piperaquine molecule at a starting concentration of 50 µM (SELEX PQ2).

Synthesis of molecule 190

All solvents and reagents were obtained from Sigma Aldrich and used without further purification. To start, 4,7-dichloroquinoline (500 mg, 2.5 mmol) in acetonitrile (5 mL) and 1-methyl piperazine (0.28 mL, 2.5 mmol) was added to a 100 mL round-bottom flask. The reaction mixture was cooled down to 0°C and 60% potassium carbonate (3 mL) was added. The reaction mixture was refluxed for 3 hours. After the reaction finished (monitored by thin layer chromatography (TLC)), it was concentrated and extracted with ethyl acetate (3 x 15 mL). Organic layers were combined and dried over anhydrous sodium sulfate, following silica gel chromatography using a 1:1 ethyl acetate/hexane solvent system. The pure product was a pale-yellow solid and 250 mg were produced (38% yield).

Analytical TLC was performed on aluminum plates pre-coated with silica gel (Sigma Aldrich, cat. no. 1167170001). Column chromatography was carried out

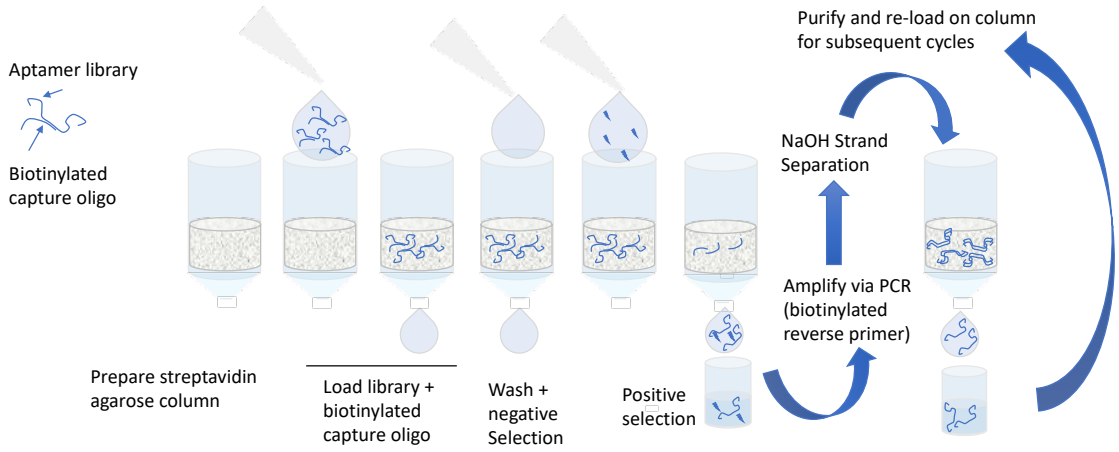


Figure 3.4: Piperaquine and Mefloquine SELEX method. An aptamer library is immobilized to a streptavidin agarose column via hybridization to a short biotinylated capture oligo. Washes, negative, and positive selection steps are performed by adding a constant volume (250 µL) of buffers to the column and collecting or discarding the column elutions. Negative selections are performed by adding a solution of negative targets (in this case, chloroquine, amodiaquine, or diluted serum) and discarding the elution volumes. Positive selection is performed by adding a solution of positive target (mefloquine or piperaquine) to the column and collecting the elutions to amplify via PCR. After PCR amplification using a biotinylated reverse primer, the double stranded products are loaded into a freshly prepared column. To separate the strands, 0.2 N NaOH is added to the column and the eluted strands are collected. The biotinylated strands remain immobilized to the column and are discarded. The collected strands are purified using molecular weight spin columns and resuspended in buffer ready to be loaded onto a new column for the subsequence selection round. After the final round, the remaining sequences are cloned and sequenced. The enriched sequences are characterized for their binding affinity and specificity.

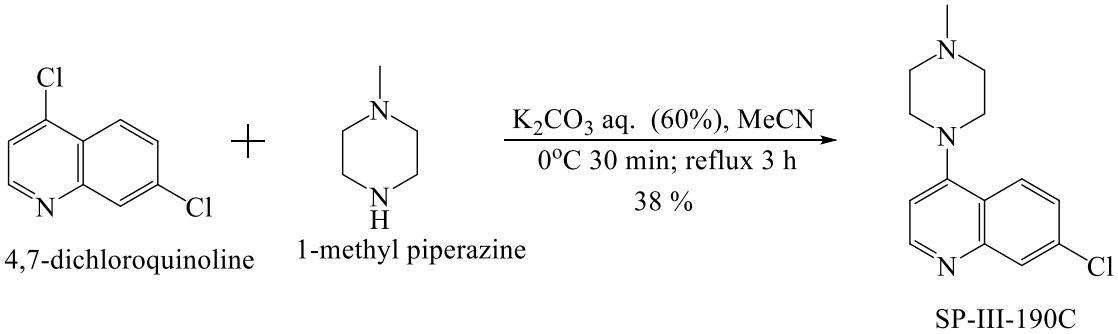


Figure 3.5: Synthesis of molecule 190. The procedure for the synthesis of molecule 190 was adapted from Shaikh et al.[143] and performed at Columbia University with the help and expertise of Dr. Stevan Pecic.

on Merck 938S silica gel. Purity was confirmed to be >95% by analytical LC/MS recorded with a Shimadzu system. Elution started with water (95%, +0.1% formic acid) and acetonitrile (5%, +0.1% formic acid) and ended with acetonitrile (95%, 0.1% formic acid) and water (5%, 0.1% formic acid) and used a linear gradient at a flow rate of 0.2 mL/min. The compound melting point was measured to be 90-92°C with a MEL-TEMP II melting point apparatus. Synthesis was performed at Columbia University with the help of Dr. Stevan Pecic.

Reagent preparation

All buffers were prepared according to Table 3.8

Contents	Final concentration
Selection Buffer	
$MgCl_2$ (Invitrogen, cat. no. AM9530G)	2 mM
PBS (Corning, cat. no. 21-040-CV)	1x
2x Selection Buffer	
$MgCl_2$ (Invitrogen, cat. no. AM9530G)	4 mM
PBS (Gibco Life Technologies, cat. no. 70011-044)	2x
Single Stranded Buffer	
PBS (Corning, cat. no. 21-040-CV)	1x

Table 3.8: Buffer recipes for piperaquine and mefloquine SELEX protocol.

The aptamer library, capture oligo, and primers were originally designed and optimized by Yang et al.[142] (Tables 3.9 and 3.10). This library contains a 30mer random region and the conserved docking sequence is included in one of the primer regions rather than in between random regions as was the case in the lumefantrine SELEX library. All oligos were synthesized by IDT (Coralville, IA). Oligo stock solutions were prepared at 100 µM in DNase/RNase free-water and stored at -20°C.

Aptamer Library (LibN30)	5'-GGAGGCTCTCGGGACGAC-(N30)-GTCGTCCCGATGCTGCAATCGTAA-3'
Capture Oligo	5'-GTCGTCCCGAGAGCCATA-BioTEG-3'

Table 3.9: Library and capture design for piperaquine and melfoquine SELEX experiments. Note: BioTEG is a biotin molecule with a triethylene glycol spacer

Forward Primer	5'-GGAGGCTCTCGGGACGAC-3'
Reverse Primer	5'-TTACGATTGCAGCATCGGGACG-3'
Reverse Biotinylated Primer	5'-Biotin-TTACGATTGCAGCATCGGGACG-3'

Table 3.10: Primers for piperaquine and melfoquine SELEX experiments. The reverse biotinylated primer is used for single-stranded DNA generation.

Library immobilization

For the initial SELEX round, 500 pmols LibN30 and 2,500 pmols capture oligo from stock solutions were combined in a total volume of 250 µL selection buffer. The aptamer-capture mixture was incubated in boiling water for five minutes then cooled to room temperature to maximize annealing. To prepare the streptavidin agarose column, 250 µL of streptavidin agarose resin (Pierce Biotech cat. no. 732-6204) was added to a micro bio-spin column (Bio-rad, cat. no. 732-6204) and washed six times with a volume of 250 µL selection buffer. Once the aptamer-capture mixture was cooled to room temperature, 5 µL were saved for small-scale PCR and the remainder was added to the streptavidin agarose column. The library was applied to the column three times by collecting the column flow-through and reapplying it to the top of the column. The flow-through from the third application was discarded.

Negative selection

The column was washed 10-24 times with 250 µL selection buffer to remove any weakly bound sequences. After washing, negative selection steps were performed following the conditions for each round listed in the Tables 3.12, 3.13, and 3.14. Piperaquine SELEX experiment 2 and Mefloquine SELEX experiment 1 included two sets of negative selections in later rounds. The first negative selection consisted of drug targets and the second of diluted pooled human serum (Interstate Blood Bank, Inc. Memphis, TN). Each negative selection step was followed by 12-24 wash steps before the positive selection.

PQ and MQ SELEX optimized PCR conditions			
1.	95°C	2 min	
2.	95°C	15 sec	Repeat for X cycles
3.	59°C	30 sec	
4.	72°C	45 sec	
5.	72°C	2 min	

Table 3.11: Optimized PCR conditions for piperaquine and mefloquine SELEX experiments.

Positive selection

For each round, three positive target elutions were performed at the concentrations described in Tables 3.12, 3.13, and 3.14. Each wash, positive elution, and negative elution used a volume of 250 µL and 5 µL of selected elutions were saved for the small-scale PCR described later. Each of the three positive selection elutions were collected and combined (total volume $\sim$ 750 µL). This volume was added, 350 µL at a time, to a 10K MWCO column (EMD Millipore, cat. no. UFC5003), and spun at 14,000 RPM, reloading and repeating until all 750 µL were added. To wash away remaining salts and target molecules, 400 µL of deionized H_2O was added to the column and the volume was reduced to 100 µL.

Amplification via PCR

The concentrated positive elution sample was added to a previously prepared large-scale 1 mL PCR mix (1 µM primers (biotinylated reverse primer), Takara Taq Premix). The library was gradually amplified (4-6 cycles at a time) and run on a 3% agarose, 0.02% ethidium bromide gel until bands were visible. Optimized PCR conditions are listed in Table 3.11.

In addition to the large-scale PCR, a small-scale PCR was run each round to generate an elution profile to track SELEX progress. A volume of 3-5 µL of the initial library, first and last washes, negative elutions, and positive elutions were saved during selection. These were each added to a 50 µL PCR reaction (2 µL sample into 50 µL volume of 1 µM primers, Takara Taq Premix) and gradually amplified, checking for the appearance of the positive elution bands. The small-scale PCR was analyzed to determine SELEX progress after each round and informed any

needed adjustments to subsequent selection conditions. Figure 3.6, shows elution profiles of an intermediate round (Round 7) compared to a final round (Round 17). As the library pool evolved to contain more sequences with binding specificity for the positive selection targets and fewer sequences that eluted during the wash steps or to negative selection targets, this progress was observed in the elution profiles. The small-scale PCR informed how many rounds of selection were performed.

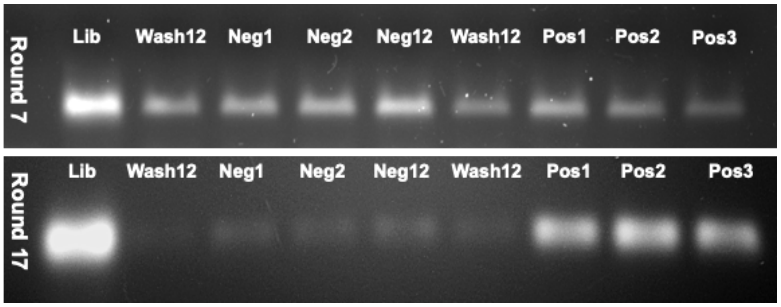


Figure 3.6: Small scale elution profile example. The evolution of an aptamer library from SELEX Round 7 to Round 17, as observed in the small-scale PCR elution profiles. The first column is a measure of how much DNA was loaded on the column that round. Subsequent columns show how much DNA eluted at each selection step. At Round 7, sequences appear to elute nonspecifically in the wash steps and the negative selection steps (Neg1, Neg2, Neg12). However, by Round 17, remaining sequences have a strong preference for elution to the positive selection target (Pos1, Pos2, Pos3). To generate the elution profiles, a sample of each elution volume was collected and amplified via PCR until visible on a 3% agarose, 0.2% ethidium bromide gel.

ssDNA generation via NaOH

After library amplification via large-scale PCR, the 1 mL volume of PCR product was loaded into a 10K MWCO column 350 µL at a time and spun at 14,000 RPM until all of the volume was added and reduced to $\sim$ 100 µL. The concentrated PCR product was collected from the spin column and ssDNA buffer was added to bring the volume up to 250 µL. A new column was prepared for single stranded DNA generation. Streptavidin agarose resin (250 µL) was added to the column and washed six times with 250 µL of single stranded buffer (no $MgCl_2$). The concentrated PCR product (with a biotinylated reverse strand) was added to the column three times by collecting the flow-through and reapplying it. The column was washed six more times with 250 µL of single stranded buffer. A cap was

Piperaquine SELEX 1 protocol			
Round	**Washes**	**Negative Selection**	**Positive Selection**
1	10x	---	100 µM
2	15x	---	100 µM
3	25x	---	100 µM
4	12x, 12x	10 µM CQ, 12x	100 µM
5	16x, 12x	10 µM CQ, 12x	100 µM
6	16x	---	25 µM
7	12x, 16x	25 µM CQ, 12x	25 µM
8	12x, 16x	25 µM CQ, 12x	25 µM
9	12x, 16x	25 µM CQ, 12x	25 µM
10	16x, 16x	25 µM CQ, 12x	25 µM
11	16x	---	15 µM
12	16x, 16x	20 µM CQ, 16x	8 µM
13	16x, 16x	20 µM CQ, 16x	8 µM
14	16x, 16x	50 µM CQ, 16x	8 µM
15	16x, 16x	50 µM CQ, 16x	8 µM
16	16x	---	4 µM
17	24x	---	2 µM
18	24x	---	1 µM
19	24x	---	0.5 µM

Table 3.12: Piperaquine SELEX experiment 1 (SELEX PQ1). Nineteen rounds of SELEX were performed, tracking progress via small scale PCR elution profiles. A volume of 250 µL was added for each wash, negative, or positive selection step. The number of washes was gradually increased and two separate wash steps were performed in rounds with negative selection, one before and one after the negative selection step. Chloroquine (CQ) was used as a representative quinoline-containing molecule for the negative selection target. The chloroquine concentration was gradually increased as well as the number of negative selection elutions. In rounds where the positive target concentration was significantly decreased, the negative selection step was skipped. Molecule 190 (half-piperaquine) was used as the positive selection target and its concentration was gradually decreased from 100 µM to 0.5 µM. Three positive selection elutions were performed every round.

applied to the bottom of the column and 250 µL of 0.2 N NaOH was added to the column and allowed to incubate for 10 minutes. After 10 minutes, the cap was removed and all of the flow-through was collected. The reverse biotinylated strands remained bound to the column and were discarded.

Purification of ssDNA

After collecting ssDNA in 0.2 N NaOH from the column, the pH was adjusted to 7.4 with 0.2 N HCl, measured using pH strips (Healthywiser, Santa Monica, CA) with a pH range of 4.5-9. The volume was doubled by adding 2X selection

Piperaquine SELEX 2 protocol				
Round	**Washes**	**Negative Selection 1**	**Negative Selection 2**	**Positive Selection**
1	10x	---	---	50 µM
2	15x	---	---	50 µM
3	24x	---	---	50 µM
4	12x, 12x	5µM AQ, 5µM CQ, 12x	---	50 µM
5	12x, 12x	5µM AQ, 5µM CQ, 16x	---	50 µM
6	12x, 16x	5µM AQ, 5µM CQ, 16x	---	25 µM
7	12x, 16x	10µM AQ, 10µM CQ, 16x	---	25 µM
8	12x, 16x	10µM AQ, 10µM CQ, 16x	---	25 µM
9	16x, 16x	20µM AQ, 20µM CQ, 16x	---	25 µM
10	16x, 16x	20µM AQ, 20µM CQ, 16x	---	20 µM
11	16x, 16x, 24x	20µM AQ, 20µM CQ, 16x	1/100 serum, 12x	20 µM
12	16x, 16x, 24x	20µM AQ, 20µM CQ, 16x	1/100 serum, 16x	10 µM
13	16x, 16x, 24x	20µM AQ, 20µM CQ, 16x	1/100 serum, 16x	4 µM
14	16x, 24x	---	1/100 serum, 16x	1 µM
15	16x, 24x	---	1/100 serum, 16x	0.5 µM
16	16x, 24x	---	1/100 serum, 16x	0.5 µM
17	24x	---	---	0.25 µM

Table 3.13: Piperaquine SELEX experiment 2 (SELEX PQ2). Seventeen rounds of SELEX were performed, tracking progress via small scale PCR elution profiles. Amodiaquine (AQ) was included in the negative selection steps since resulting aptamers from SELEX PQ1 showed cross-reactivity to amodiaquine. Also, in an effort to reduce potential cross-reactivity to serum components, 100-fold diluted serum was used in a second negative selection step. Washes were performed before and after each negative selection step. Since aptamers selected from SELEX PQ1 showed reduced binding to the full-piperaquine molecule as compared to the half-piperaquine molecule, full piperaquine was used as the positive target in SELEX PQ2. However, due to poor aqueous solubility, the starting concentration was 50 µM rather than 100 µM. The concentration of the piperaquine was reduced to 0.25 µM for the final SELEX round. Three positive selection elutions were performed every round.

buffer (Table 3.8) to readjust the salt concentrations. The product was then concentrated once again using a 10K MWCO column to a volume of 50-100 µL. The concentration of the final product was measured via Nanodrop (Denovix DS-11 FX+) and, with the exception of the first round in which all DNA was carried forward to the second round, 100 pmol of library was carried forward to the next round. The remainder was stored at -80°C.

Cloning after selection

After a satisfactory elution profile was observed via small-scale PCR (e.g. Round 17 in Figure 3.6), the target elutions (total volume $\sim$ 750µL) were concentrated

Mefloquine SELEX 1 protocol				
Round	**Washes**	**Negative Selection 1**	**Negative Selection 2**	**Positive Selection**
1	10x	---	---	100 µM
2	15x	---	---	100 µM
3	24x	---	---	10 µM
4	12x, 12x	5µM AQ, 5µM CQ, 12x	---	100 µM
5	12x, 12x	5µM AQ, 5µM CQ, 16x	---	100 µM
6	12x, 16x	5µM AQ, 5µM CQ, 16x	---	50 µM
7	12x, 16x	10µM AQ, 10µM CQ, 16x	---	50 µM
8	12x, 16x	10µM AQ, 10µM CQ, 16x	---	50 µM
9	16x	---	---	50 µM
10	16x, 16x	20µM AQ, 20µM CQ, 16x	---	50 µM
11	16x, 16x, 24x	20µM AQ, 20µM CQ, 16x	1/100 serum, 12x	50 µM
12	16x, 16x, 24x	20µM AQ, 20µM CQ, 16x	1/100 serum, 16x	20 µM
13	16x, 16x, 24x	20µM AQ, 20µM CQ, 16x	1/100 serum, 16x	8 µM
14	16x, 24x	---	1/100 serum, 16x	4 µM
15	16x, 24x	---	1/100 serum, 16x	1 µM
16	16x, 24x	---	1/100 serum, 16x	0.5 µM
17	24x	---	1/100 serum, 16x	0.5 µM
18	24x	---	---	0.25 µM

Table 3.14: Mefloquine SELEX experiment 1. Eighteen rounds of SELEX were performed, tracking progress via small scale PCR elution profiles. Washes and negative selection conditions followed those of piperaquine SELEX experiment 2 (Table 3.13). Mefloquine was used as the positive selection target and the concentration was decreased from 100 µM to 0.25 µM. Three positive selection elutions were performed every round.

via Amicon ultra 10K centrifugal filters to 100 µL, washed with 400 µL deionized water to remove excess drug target and buffer salts, and reduced again to 100 µL. A 400 µL volume PCR reaction was prepared (1 µM primers, Takara Taq Premix) to amplify 30 µL of the 100 µL concentrated target elution. The remaining 70 µL were stored at -20°C. After 8-10 rounds of PCR, with an extra 15-minute final extension phase, the products were run on a 3% agarose, 0.02% ethidium bromide gel to ensure successful amplification. The PCR product was ethanol precipitated to purify and concentrate DNA. All 400 µL of the PCR product were combined with 1 mL of 100% ethanol, 40 µL 3M Sodium Acetate, pH 5.5 (Ambion cat. no. 9740), and stored overnight at -80°C. The precipitate solution was then centrifuged at 20,000 rcf, 25 min, 4°C. The pellet was washed twice with 75% ethanol (1.4 mL), centrifuged at 20,000 rcf for five minutes, and decanted after each wash. After the final wash was decanted, the tube was left open at room temperature until the DNA pellet was visibly dry ($\sim$ 2 hours). The dried pellet was resuspended in 40 µL

water, the DNA concentration was measured via Nanodrop (Denovix DS-11 FX+), and the volume was adjusted to a concentration between 1-2 µg/µL.

Cloning and transformation were performed following the TOPO® TA Cloning Kit (Invitrogen cat. no 45-0641) protocol. A 6 µL reaction was prepared with ∼ 3 µL purified PCR product (depending on the concentration after EtOH precipitation), 1 µL salt solution provided by the kit, 1 µL TOPO® Vector, and 1 µL sterile water. This reaction mixture was gently mixed and incubated at room temperature for five minutes, then placed on ice. One vial of One Shot® E. coli cells was thawed on ice and 3 µL of the 6 µL TOPO® cloning reaction from the previous step were added to the thawed cells and gently mixed. The cells were incubated on ice for five minutes then heat-shocked for 30 seconds in a 42°C water bath. After heat shocking, 100 µL of SOC medium (Clontech, cat. no. 636766) at room temperature was added to the cells and the whole volume was spread onto room temperature nutrient agar plates containing X-gal and ampicillin under sterile conditions. Once the volume was absorbed by the agar, the plates were flipped and incubated at 37°C overnight.

Agar plates were prepared by combining 30 grams tryptic soy broth (Millipore cat. no. 22092), 15 grams agar (Millipore cat. no. 05040), 1 L water. The mixture was stirred, covered with tin foil, and autoclaved, then stirred while cooling. Once cooled to room temperature, 1mL of 200 mg/mL X-gal (Sigma-Aldrich cat. no. BG-3) and 1mL of 100 mg/mL ampicillin (Sigma Aldrich cat. no. A5354) were added (final concentrations: 200 µg/mL X-gal, 100 µg/mL amp). The mixture was poured into plates and stored at 4°C.

The day following transformation, 25-30 white colonies were picked with a 10 µL pipette tip, transferred to a new amp, X-gal, agar plate, and dipped in a 20 µL PCR reaction (1 µM M13 forward and reverse primers, Takara Taq Premix). PCR products were run on a 3% agarose, 0.02% ethidium bromide gel to screen for positive inserts. Positive samples were purified using the ExoSAP-IT™ kit from Applied Biosystems (cat. no. 78200). PCR product (30 µL) was combined with 3 µL ExoSAP-IT ™. The reaction was then incubated at 37°C for 15 minutes

to allow for degradation of single stranded primers and nucleotides. Tubes were then incubated at 80°C for 15 minutes to inactivate the enzyme.

Sequencing

Purified DNA was prepared following recommended concentration guidelines (20-40 ng/µL template, 2-10 pmol/µL primers) and Sanger sequenced by Eurofins Scientific (Louisville, KY). M13 primers were used for sequencing to ensure that the entire library, including library primers would be of good quality. Results were processed and sorted based on sequence enrichment and unique structure as hypothesized by Mfold (shown in Section 3.3.2). Several rounds of transformation, cloning, and sequencing were performed in order to obtain > 20 sequences per SELEX library.

Clone SELEX elution profiles

After sequence sorting and analysis, four-to-six clones were selected to be analyzed via clone specific SELEX elution profiles. ExoSAP-IT™ purified DNA from the selected clones was amplified again, now using aptamer library primers. A 500 µL PCR reaction was prepared (5 µL template, 1µM aptamer library primers (biotinylated reverse primer), Takara Taq Premix). After amplification, DNA was run on a 3% agarose, 0.02% ethidium bromide gel to confirm proper amplification. Single-stranded DNA was generated for each of the new clone libraries following the protocol previously described in SELEX methods. The amount of resulting ssDNA was measured via Nanodrop (Denovix DS-11 FX+). Just as during SELEX rounds, 100 pmol of ssDNA of each clone was incubated with 5x biotinylated capture oligo and immobilized to a column prepared from 250 µL of streptavidin agarose. The library was applied three times, then washed 12 times with 250 µL selection buffer. The 12^{th} wash was collected. A solution of a final SELEX concentration of negative target in selection buffer was applied to the column twice at a volume of 250 µL, both elution volumes were collected. The column was then washed 12 more times and the 12^{th} wash was collected. Finally, 250 µL of a final concentration of positive target in selection buffer was added to the column twice and both elutions were collected.

A small-scale PCR was performed and elution profiles were generated from the collected elutions, just as described previously in the SELEX methods. These clone-specific elution profiles were analyzed to select the most promising sequences for sensor development. The selected sequences, their Mfold[144] predicted structure, and their specific elution profiles are shown in Section 3.3.2.

3.2.3 Binding affinity assays

After selection, aptamer sequences were identified from each SELEX experiment for further analysis based on their level of enrichment and secondary structure. Sequences selected from the lumefantrine SELEX experiments were initially tested for their affinity to lumefantrine via isothermal titration calorimetry (ITC). These results were later repeated through Biacore SPR affinity measurements. Sequences from the piperaquine and mefloquine SELEX experiments were tested via Biacore as well as a fluorescent-binding assay. ITC testing, the fluorescent-binding assay, and several different approaches to Biacore testing are described in this section. Attempts to develop a Biacore method for tracking SELEX enrichment using a kanamycin model system are also described.

ITC analysis of lumefantrine sequences

DNA sequences of interest from SELEX LF1 and LF2 were synthesized at the University of Oxford Chemistry department and purified via PAGE gel extraction (LF2c7n2 and LF2c7n4) or by Integrated DNA Technologies (IDT) (LF1c8n1, LF1c8n2, and LF1c8n3). All experiments were run in B+W buffer (50 mM Tris, 137 nM NaCl, 5 mM $MgCl_2$, 5 mM KCl, pH 7.4) with 2.5% DMSO. A 250 µM solution of lumefantrine was prepared in B+W buffer, 2.5% DMSO. Aptamers were prepared at concentrations of 20 µM (LF2c7n2 and LF2c7n4), 8µM (LF1c8n1), 12µM (LF1c8n2), or 10µM (LF1c8n3) in B+W buffer. Concentrations were dictated by the maximum amount of oligonucleotide produced. DNA concentration was maximized to try to improve assay sensitivity.

Using a Malvern MicroCal VP-ITC apparatus, 2.5 µL of drug solution were injected for 17 total injections spaced three minutes apart at a temperature of 25°C. First, a blank heat of dilution was performed in which B+W buffer was loaded into the cell and the lumefantrine solution was injected to measure any heat exchange effects of the drug injections alone. This heat of dilution was subtracted from each aptamer run. Next, each aptamer was loaded into the cell and the thermograms were recorded. The heat of dilution subtracted thermograms from each aptamer are reported in Figure 3.20.

Fluorescent-binding assay analysis of piperaquine and mefloquine sequences

The capture-SELEX method described in this chapter used a biotinylated complementary capture oligo to weakly immobilize the aptamer library to facilitate the sorting of binding from non-binding sequences. This built-in selection criteria also allowed for the design of a simple fluorescent sensor. The 3' biotin on the capture oligo was replaced with a 3' dabcyl (DAB) quencher and a 5' fluorescein (FAM) fluorophore was attached to the potential aptamer sequences. This way, the release of aptamer from quencher upon binding its drug target results in the dissociation of fluorophore from quencher. Target binding is indicated by the measurement of a fluorescent signal at optimized FAM excitation/emission wavelength. The sensor mechanism is shown in Figure 3.7.

Clone SELEX elution profiles informed the selection of several aptamer sequences for which sensor development was attempted. For each selected aptamer sequence, the oligonucleotides shown in Table 3.15 were synthesized and purified via HPLC by IDT. The aptamers were labeled with a 5' fluorescein (FAM) tag and the capture strands were labeled with 3' dabcyl (DAB) molecules to become "quencher strands." After the biotin on the capture strand is replaced with a quencher it is referred to as a quencher strand. Quencher strands with both 13 and 14 complementary bases to the 5' end of the aptamer were tested to identify a complementary length that would ensure proper annealing of the quencher and aptamer strand.

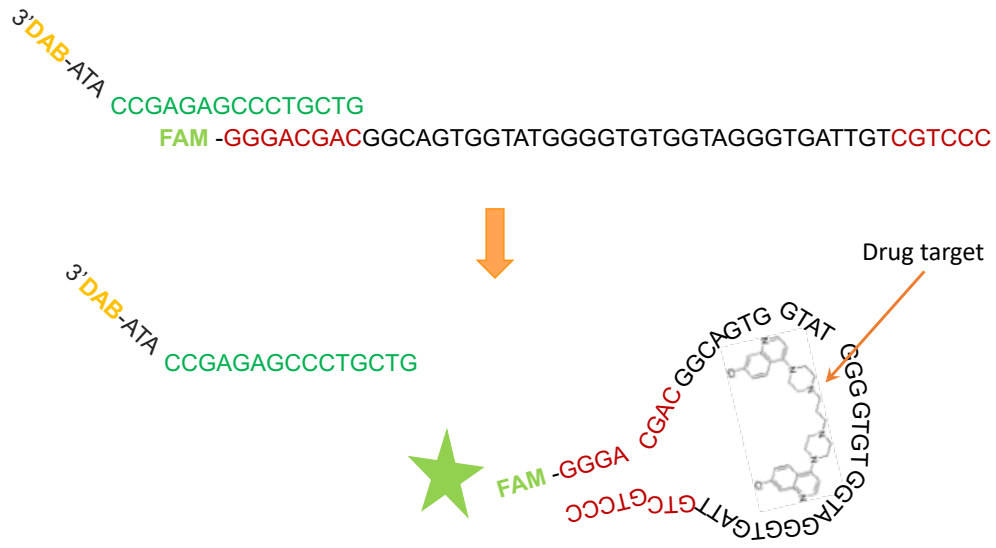


Figure 3.7: Fluorescent sensor design. The fluorophore (FAM) labeled aptamer sequence is hybridized to the capture strand which is tagged with a quencher (DAB). When target is introduced, the aptamer sequence releases the quencher strand to bind its target. Upon binding, the fluorophore releases from the quencher and binding can be measured via fluorescence.

Aptamer Template	5'-FAM-CTCTCGGGACGAC(N30)CGTCCC-3'
13mer Quencher	5'-GTCGTCCCGAGAG-DAB-3'
14mer Quencher	5'-NGTCGTCCCGAGAG-DAB-3'

Table 3.15: Oligonucleotide templates for each aptamer sequence and its corresponding quencher strands to be synthesized for testing via the fluorescent-binding assay. Conserved regions in grey.

Optimizing quencher ratios and length

To optimize function of the fluorescent sensor, multiple lengths and concentrations of quenching strands were tested. As described here, all selected sequences were tested with both 13mer and 14mer quenchers ranging in concentrations from a 1:0.156 ratio of aptamer:quencher to a 1:10 ratio of aptamer:quencher, as shown in Table 3.19. The sequences of interest and their corresponding 13mer and 14mer quencher strands are described here for SELEX PQ1, PQ2, and MQ1. The aptamer and quencher templates are shown in Table 3.15.

Piperaquine SELEX experiment 1 (SELEX PQ1):

Based on the elution profiles of specific sequences from the final aptamer library of SELEX PQ1, selected sequences were synthesized with 5' FAM labels by IDT as well as the corresponding 3' DAB labeled capture strand with 13 or 14 complementary bases as shown in Table 3.16.

Aptamer 18.18	
5'-FAM-CTCTCGGGACGACGGCAGTGGTATGGGGTGTGGTAGGGTGATTGTCGTCCC-3'	
13mer Quencher	**14mer Quencher**
5'-GTC GTC CCG AGA G-DAB-3'	5'-CGT CGT CCC GAG AG-DAB-3'
Aptamer 18.3	
5'-FAM-CTCTCGGGACGACCGTGTTTATTGTGCTCTGTCACACTAGTTTGTCGTCCC -3'	
13mer Quencher	**14mer Quencher**
5'-GTC GTC CCG AGA G-DAB-3'	5'-GGT CGT CCC GAG AG-DAB-3'
Aptamer 17.16	
5'-FAM- CTCTCGGGACGACCGGCTGTTGCAAACTCTCATTCGAGCGTAGGTCGTCCC -3'	
13mer Quencher	**14mer Quencher**
5'-GTC GTC CCG AGA G-DAB-3'	5'-GGT CGT CCC GAG AG-DAB-3'
Aptamer 17.21	
5'-FAM- CTCTCGGGACGACCCGGAGGGTATTGGCTATACCGCGTAATCGGTCGTCCC -3'	
13mer Quencher	**14mer Quencher**
5'-GTC GTC CCG AGA G-DAB-3'	5'-GGT CGT CCC GAG AG-DAB-3'

Table 3.16: Relevant sequences for quencher optimization from SELEX PQ1

Piperaquine SELEX experiment 2 (SELEX PQ2):

After SELEX PQ2, fluorophore-labelled aptamer sequences PQ4 and PQ19 and corresponding quenching strands were synthesized by IDT.

PQ4	
5'-FAM- CTCTCGGGACGACCACACGCTAGTTGCGCCGAATGGCCGTGAAAGTCGTCCC -3'	
13mer Quencher	**14mer Quencher**
5'-GTC GTC CCG AGA G-DAB-3'	5'-GGT CGT CCC GAG AG-DAB-3'
PQ19	
5'-FAM- CTCTCGGGACGACCCGCAGGAGCGTAGCTCGAACCGGAGGGAGGTCGTCCC -3'	
13mer Quencher	**14mer Quencher**
5'-GTC GTC CCG AGA G-DAB-3'	5'-GGT CGT CCC GAG AG-DAB-3'

Table 3.17: Relevant sequences for quencher optimization from SELEX PQ2

Melfoquine SELEX experiment 1 (SELEX MQ1):

For SELEX MQ1, the fluorophore-labelled aptamers MQ2 and MQ10 and corresponding quencher oligos were synthesized by IDT.

	Final [Aptamer] (nM)	Final [Quencher] (nM)	Ratio
1	50	0	1:0
2	50	7.8125	1:0.156
3	50	15.625	1:0.313
4	50	31.25	1:0.625
5	50	62.5	1:1.25
6	50	125	1:2.5
7	50	250	1:5
8	50	500	1:10

Table 3.19: The quencher dilutions tested against each aptamer sequence for aptamer:quencher ratio optimization.

MQ2	
5'-FAM-CTCTCGGGACGACGGCAGTCTATACCCCGTATCGCCGAAGGTTGTCGTCCC -3'	
13mer Quencher	**14mer Quencher**
5'-GTC GTC CCG AGA G-DAB-3'	5'-CGT CGT CCC GAG AG-DAB-3'
MQ10	
5'-FAM-CTCGGGACGACGGTGGTAACCTACTCGGAAGAGAAAGGTGCGTCGTCCC -3'	
13mer Quencher	**14mer Quencher**
5'-GTC GTC CCG AGA G-DAB-3'	5'-CGT CGT CCC GAG AG-DAB-3'

Table 3.18: Relevant sequences for quencher optimization from SELEX MQ1

Each fluorescently labelled aptamer sequence was tested with dilutions of both 13mer and 14mer quenchers to identify aptamer:quencher ratios that provided sufficient quenching of the fluorophore in selection buffer upon hybridization of aptamer and quenching strand. Stock solutions (100 µM) of the IDT synthesized FAM-labelled aptamer and dabcyl-labelled quencher strands were prepared in DNAse/RNAse free water. A 100 nM solution of FAM-labelled aptamer was prepared in selection buffer from the 100 µM stock. A 1 µM quencher solution of each quencher was prepared in selection buffer from the 100 µM stock and was serially diluted seven times. These dilutions and a buffer blank were combined with the 100 nM fluorophore labelled aptamer solution 1:1 (40 µL aptamer + 40 µL quencher) so that final concentrations of both aptamer and quencher were prepared as shown in Table 3.19.

The combined sensor and quencher mixtures were incubated in boiling water for five minutes, then cooled at room temp for $\geq$ 30 minutes to ensure proper annealing. The cooled sensing solutions were transferred (75µL) to a Corning

flat bottom black 384 well plate (cat. no. 3577). The dilutions were performed in triplicate and read by a Molecular Devices Spectramax 190 microplate reader, ex/em: 485/538. Ratios of aptamer:quencher that provided 80-90% quenching were selected for further sensor analysis. If both the 13mer and 14mer quencher strand provided 80-90% quenching at a certain concentration in the tested range, both quenchers were tested for target sensitivity and specificity. The results of the quencher optimization are described in Section 3.3.3.

Assessing sensitivity and specificity

Sensor solutions at the optimized quencher length and aptamer:quencher ratios were tested to assess sensitivity to desired target and to assess response to negative selection targets. To do this, 2X concentrated solutions of aptamer and quencher were prepared in selection buffer from 100 µM stocks. For example, to test a sensor solution with 50 nM aptamer and 500 nM quencher (a 1:10 ratio), a 100 nM sensor, 1 µM quencher solution was prepared in selection buffer from oligonucleotide stocks, incubated in boiling water for five minutes and allowed to cool to room temperature. This sensor solution was then combined 1:1 with drug spiked selection buffer (40 µL sensor + 40 µL sample). Sensor and sample were allowed to equilibrate for 30 minutes in the dark and then 75 µL of the sensor + target mixtures were transferred to a Corning flat bottom black 384 well plate. The dilutions were performed in triplicate and read by a Molecular Devices Spectramax 190 microplate reader, ex/em: 485/538. Serial dilutions of drug spiked selection buffer were prepared from drug stocks described in Table 3.4.

Biacore methods

A Biacore T100 instrument (GE Healthcare) was used to measure the binding affinity of selected aptamer sequences from both SELEX protocols. Several approaches to these measurements were attempted, first through aptamer immobilization to a biotinylated capture oligo then through biotinylation of the aptamer itself. In all cases, a Biacore chip was coated with NeutrAvidin to immobilize a biotinylated oligonucleotide ligand. Before each experiment, a Biacore CM5

chip (cat. no. BR-1000-12) was prepared for NeutrAvidin immobilization using the amine coupling kit from GE Healthcare Life Sciences (cat. no. BR-1000-50). 1-ethyl-3-(3-dimethylaminopropyl) carbodiimide hydrochloride (EDC) and N-hydroxysuccinimide (NHS) stock solutions were prepared in deionized water following the manufacturer's instructions and frozen at -80°C in 200 µL aliquots. NeutrAvidin (ThermoFisher Scientific, cat. no. 31000) stock aliquots were prepared at a concentration of 1 mg/mL in deionized water and frozen at -80°C until the day of chip preparation. In order to immobilize NeutrAvidin to the CM5 chip, the surface was first treated with 70 µL of 0.2 M EDC/0.05 M NHS per flow cell to convert carboxyl groups on the carboxymethyl dextran chip surface to reactive succinimide esters. These activated esters covalently attach to primary amines on the NeutrAvidin molecule. A 40 µg/mL solution of NeutrAvidin was prepared in 10 mM sodium acetate buffer pH 5 (GE Healthcare Life Sciences, cat. no. BR-1003-51) from the 1 mg/mL stock. NeutrAvidin immobilization to the activated ester requires an uncharged amine group and pH 5 acetate buffer was found to provide satisfactory NeutrAvidin solubility and immobilization. Followed by a 70 µL injection of 40 µg/mL NeutrAvidin, 70 µL of 1 M Ethanolamine-HCl pH 8.5 (included in the GE Healthcare amine coupling kit) was injected over the chip surface to inactivate any remaining succinimide esters. All injection flow rates for the chip surface preparation protocol were 10 µL/min.

After successful NeutrAvidin immobilization on the desired flow cells (note: CM5 chips have 4 parallel flow cells), 4x 30-second pulses of 50 mM NaOH (GE Healthcare Life Science cat. no. BR-1003-58) at 30 µL/min were performed to remove any traces of weakly, electrostatically bound NeutrAvidin ligand. Next, the biotinylated oligonucleotide of interest was immobilized to the NeutrAvidin treated surface. Each NeutrAvidin protein has four biotin binding sites and an extremely high biotin affinity. The specific conditions of each Biacore experiment are described here.

Lumefantrine Biacore measurements:

Lumefantrine capture and aptamer sequences for Biacore analysis	
Capture Oligo	5'-Bio- GTC*i*Sp9/GATCGAGCCTCA
Lib3	5'-ATACCAGCTTATTCAATT-(N10)-TGAGGCTCGATC-(N40)-AGATAGTAAGTGCAATCT-3'
LF1c8n2	ATACCAGCTTATTCAATTGGTTAGCGAATGAGGCTCGATCTTATAAGGTCG CCTAGCCAATGACAAGAGGGTATCACTTAAGATAGTAAGTGCAATCT
LF1c8n4	ATACCAGCTTATTCAATTACGCAATACCTGAGGCTCGATCATGACGTAATG AGGGTAAGCGGGGATGAAGATTGACTCTTAGATAGTAAGTGCAATCT
LF2c7n2	ATACCAGCTTATTCAATTATAATCTTATTGAGGCTCGATCATTATAATTGTA TCTTATATTAATTATAAATTAATATTTGAGATAGTAAGTGCAATCT
LF2c7n4	ATACCAGCTTATTCAATTATAAAGTCGCTGAGGCTCGATCACACGGGAGAC GTTATAATGGGCTGGGACGATTGTACGTAAGATAGTAAGTGCAATCT

Table 3.20: The sequences tested via Biacore for lumefantrine binding ability. The biotinylated capture oligo was used to immobilize aptamers to the chip and the library (Lib3) was used as a reference. Sequences LF1c8n2, LF2c7n2, and LF2c7n4 were previously tested via ITC and retested here to confirm the results. Sequence LF1c8n4 was a newly selected sequence that had not yet been assessed for binding ability.

Four aptamer sequences from SELEX LF1 and LF2 were tested via Biacore for their lumefantrine binding ability. Three of these sequences had already been tested via ITC and were repeated using the Biacore method to confirm results. The sequences as well as the capture oligonucleotide used to immobilize them to the Biacore chip are shown in Table 3.20.

A new CM5 chip was treated with NeutrAvidin as previously described. A 1 µM solution of biotinylated capture oligo in B+W buffer was prepared from a 100 µM stock solution, incubated in boiling water for five minutes, and cooled to room temperature. Biotinylated capture oligo was immobilized on the NeutrAvidin treated chip surface of both the test and reference flow cell in sequential injections at a flow rate of 30 µL/min until saturation (∼16,000 RU). The lumefantrine aptamers were synthesized and HPLC purified by IDT. Before immobilization, a 1 µM solution of the initial selection library (Lib3) as well as each aptamer was prepared in B+W buffer from a 100 µM stock solution, incubated in boiling water for five minutes, and cooled to room temperature.

The library solution was immobilized to the reference cell via hybridization to capture oligo until saturation (∼45,000 RU), using an injection flow rate of 10 µL/min. Aptamers LF1c8n2, LF1c8n4, LF2c7n2, LF2c7n4 were similarly

immobilized to the test cell. Each aptamer was immobilized and subjected to drug and buffer injections individually. The random library on the reference cell reported any background effects of injecting drug over a ssDNA molecule of similar size to the aptamers. The response of the reference cell was subtracted from the test cells for analysis. Initial injections of 10 µM lumefantrine in 1% MeOH, B+W buffer showed no signal response so the drug concentration was increased to 50 µM lumefantrine solution (5% MeOH, B+W buffer). Methanol was used as a solvent for lumefantrine in the Biacore experiments rather than DMSO due to concerns about DMSO effects on instrument tubing. Drug dilutions were prepared from a 1 mM stock solution. Each aptamer was subjected first to a 300s injection of 5% MeOH, B+W buffer to serve as a blank, and then a 300s injection of 50 µM LF in 5% MeOH, B+W buffer at a flow rate of 10 µL/min. Between each aptamer test, the aptamer was removed from capture oligo with 10 second regeneration pulses of 50 mM NaOH until all aptamer was removed and the RU no longer decreased. After regeneration, the next aptamer was added to saturation and tested. Several aptamers were also tested against a concentration of 100 µM lumefantrine (10% MeOH, B+W buffer). No aptamer response to lumefantrine was recorded during these test injections so the experiment was not continued.

Kanamycin Biacore measurements:

A previously published kanamycin aptamer [141] selected from the same starting library as the lumefantrine sequences was tested via Biacore in order to assess the accuracy and reproducibility of the method described in the previous section. The relevant sequences are shown in Table 3.21.

A new CM5 chip was treated with NeutrAvidin as previously described. A 1 µM solution of biotinylated capture oligo in B+W buffer was prepared from a 100 µM stock solution, incubated in boiling water for five minutes, and cooled to room temperature. Biotinylated capture oligo was injected over the NeutrAvidin treated chip surface in sequential injections at a flow rate of 10 µL/min until saturation (∼25,000 RU) of both the test and reference flow cell. Lib3 and aptamer 13_82

Kanamycin capture and aptamer sequences for Biacore analysis	
Capture Oligo	5'-Bio- GTC/iSp9/GATCGAGCCTCA
Lib3	5'-ATACCAGCTTATTCAATT-(N10)-TGAGGCTCGATC-(N40)-AGATAGTAAGTGCAATCT-3'
Aptamer 13-82	ATACCAGCTTATTCAATTCAGGGCGGTATGAGGCTCGATCAAGGTCGGA GCGAGAATTTTTTCGCGGAGTCGGCTGGATCAGATAGTAAGTGCAATCT

Table 3.21: The kanamycin sequences tested via Biacore as a positive control to confirm the efficacy of the method. The biotinylated capture oligo was used to immobilize aptamers to the chip and the library (Lib3) was used as a reference.

(Table 3.21) were synthesized and HPLC purified by IDT. Before immobilization, 1 µM solutions of library and aptamer 13_82 in B+W buffer were prepared from 100 µM stock solutions, incubated in boiling water for five minutes, and cooled to room temperature.

Aptamer library was immobilized to the reference cell and aptamer 13_82 to the test cell via a 5 µL/min injection for 300s (∼1,000 RU each). Initial injections of 50 µM kanamycin and 100 µM kanamycin showed a dose dependent response in the loss of mass at the surface of the test cell (unlike during the lumefantrine sequence testing). Kanamycin solubility allows for higher drug concentrations to be prepared in aqueous buffer than that of lumefantrine. A 1 mM kanamycin solution was prepared in B+W buffer and serially diluted down to 100 µM.

After satisfactory initial tests with kanamycin injections, a protocol was set using the Biacore control software to sequentially inject each drug concentration over the test and reference flow cell. Between each condition, both cells were regenerated to remove bound aptamer and library, and then Lib3 was reloaded on the reference cell and aptamer 13_82 was reloaded on the test cell via a 300s injection at a 5 µL/min flow rate. This ensured an even starting concentration of aptamer and library for each sequential drug injection. The binding data is shown in the results.

Biacore method development to track SELEX enrichment with kanamycin model aptamer:

After the lumefantrine SELEX experiment, an improved method to track SELEX progress was desired to better inform the number of selection rounds that should

be performed. A Biacore method to assess the affinity of intermediate libraries and thus track the progress of SELEX was tested using the model kanamycin aptamer. Varying percentages of 13_82 aptamer were spiked into Lib3 solutions to mimic partially enriched pools such as those found during intermediate SELEX rounds. These pools were immobilized on different flow cells of a Biacore chip and their response to kanamycin was measured.

After chip preparation and capture oligo immobilization was performed as previously described, a 100% Lib3 solution was immobilized to flow cell 1 (Fc1) to serve as the reference cell, 10% 13_82 in Lib3 was immobilized to flow cell 2 (Fc2) as a test cell, 5% 13_82 in Lib3 was immobilized to flow cell 3 (Fc3) as second a test cell, and 2% 13_82 in Lib3 was immobilized to flow cell 4 (Fc4) as a third test cell. Each library solution was immobilized via a 300s injection at a flow rate of 5 µL/min. A 2 mM solution of kanamycin was prepared in B+W buffer and serially diluted down to 50 µM. The same Biacore program to sequentially inject drug concentrations with a regeneration and re-loading of aptamer/library between each injection was run across all four flow cells. The binding curves are shown in Figure 3.30.

Piperaquine and mefloquine aptamer-capture affinity measurements:

A Biacore assay was performed to assess the binding affinities between the most promising aptamer sequences from the piperaquine and mefloquine selections (PQ4 and MQ2) and the capture oligo. The function of the aptamer sensor depends on both the aptamer-drug interactions and the aptamer-capture interactions. To measure the affinity between aptamers and their captures, the biotinylated 13mer capture oligo was immobilized to a new NeutrAvidin treated chip surface. Varying concentrations of each aptamer were then injected over the flow cell surface and aptamer binding was measured. Selection buffer from the piperaquine and mefloquine SELEX protocol (PBS + 2 mM $MgCl_2$) was used as the running buffer for chip preparation and binding assays. Fc1 was left with NeutrAvidin treatment only to serve as a reference cell. Biotinylated 13mer capture oligo was incubated in boiling water for five minutes then cooled to room temperature and immobilized on

Fc2 of the chip surface. Initially, a high concentration of capture oligo (around 900 RU) was immobilized to the surface of Fc2 by injecting 1 µM biotinylated 13mer capture for 30 seconds at a flow rate of 5 µL/min. After initial measurements, it was determined that less capture oligo should be immobilized on the test cell in order to reduce potential mass transfer effects for the MQ2 capture affinity assessment. To keep the R_{max} value low in order to reduce mass transfer effects, a new chip surface was prepared and only ∼150 RU of capture ligand was immobilized to the test cell. The theoretical R_{max} of a chip surface can be calculated as $R_{max} = R_{ligand}(MW_{analyte}/MW_{ligand})$. Using this calculation, around 150 RU of capture ligand should result in an R_{max} of about 405 RU (150(16,344/6,054) = 405 RU).

Once the amount of immobilized capture ligand had been optimized, the affinity measurements of aptamer PQ4 and the 13mer capture were repeated. A 2.5 µM solution of PQ4 aptamer was prepared in selection buffer from a frozen 100 µM stock, incubated in boiling water for five minutes and cooled to room temperature. Serial dilutions along with a blank and a replicate of the highest concentration were prepared. A blank and a replicate were included for reference and to show an absence of carry-over after regeneration, respectively. Using the Biacore T100 software, a protocol was set to sequentially inject each aptamer concentration for 10 minutes with a 10-minute dissociation time at a flow rate of 30 µL/min. A regeneration was performed between each condition via the injection of 50 mM NaOH for 60 seconds at a flow rate of 30 µL/min. This regeneration protocol was optimized to remove all of the immobilized aptamer without affecting binding characteristics or immobilization of the capture oligo ligand. The sensorgrams of this binding assay and the binding analysis are shown in Figures 3.31 and **??**.

The same procedure was performed for MQ2 aptamer. A new CM5 chip was prepared with NeutrAvidin only on the reference cell and biotinylated 13mer capture on the reference cell. The sensorgrams and binding analysis are shown in Figures 3.32 and **??**.

Piperaquine and mefloquine aptamer-drug affinity measurements:

Piperaquine and mefloquine aptamer sequences for Biacore analysis	
N32 Library	/5BiosG/CTCTCGGGACGACC-(N32)-CGTCCC
PQ4	/5BiosG/CTCTCGGGACGACCACACGCTAGTTGCGCCGAATGGCCGTGAA AGTCGTCCC
MQ2	/5BiosG/CTCTCGGGACGACGGCAGTCTATACCCCGTATCGCCGAAGGTTG TCGTCCC

Table 3.22: The sequences tested via Biacore for piperaquine (PQ4) and mefloquine (MQ2) aptamer binding analysis. The library (N32) was immobilized to the reference cell. Conserved regions are in grey.

A Biacore assay was performed to assess the binding affinities between the most promising aptamer sequences (PQ4 and MQ2) and their drug targets. A new CM5 chip was prepared with NeutrAvidin as previously described. A biotinylated aptamer library, consisting of the same conserved regions in PQ4 and MQ2 flanking 32 random bases was synthesized and HPLC purified by IDT. The random library was immobilized to the reference cell so that any non sequence-specific effects could be measured and subtracted from the sensorgram of the test cell. Biotinylated PQ4 and MQ2 aptamers were also synthesized and purified via HPLC by IDT. The sequences are shown in Table 3.22.

A 1 µM solution of both biotinylated PQ4 and biotinylated library were prepared in selection buffer from 100 µM stocks. The aptamers were incubated in boiling water for five minutes then cooled to room temperature. Using selection buffer as the running buffer, 1 µM biotinylated library was injected at a flow rate of 10 µL/min for one minute injections until around 3,000 RU of library was immobilized on Fc1. The same was repeated for biotinylated PQ4 aptamer on Fc2 until around 3,000 RU of aptamer was immobilized. Since the analyte in this assay was a small molecule drug compared to a large aptamer ligand, the ratio of $MW_{analyte}/MW_{ligand}$ was very low (535.5/16,345 = 0.0328). A large amount of ligand was immobilized to the flow cells in order to maximize the R_{max} to ensure measurable drug accumulation at the surface. After ligand immobilization, 30-second pulses of 50 mM NaOH were injected over the flow cells to release weakly bound ligands until the injections no longer resulted in a decrease in RU.

Serial dilutions of piperaquine from 10 µM to 39 nM were prepared in selection buffer from a 1 mM stock (water, 5% MeOH). Using the Biacore T100 software, a protocol was set to sequentially inject each drug concentration for 10 minutes with a 5-minute dissociation time at a flow rate of 30 µL/min. A blank and a replicate of the highest drug concentration were included for reference and to show an absence of carry-over after regeneration, respectively. A regeneration was performed between each condition via the injection of 50 mM NaOH for 60 seconds at a flow rate of 30 µL/min. This regeneration protocol was tested to ensure the removal of all bound drug without affecting binding characteristics of the aptamer.

The same procedure was repeated on Fc3 and Fc4 of the CM5 chip, immobilizing biotinylated library to the reference cell and biotinylated MQ2 aptamer to the test cell. Serial dilutions of mefloquine were prepared from 10 µM to 39 nM. The results of the drug affinity measurements are shown in Section 3.3.3.

3.3 Results

The SELEX attempts for each target and the methods used to characterize the resulting sequences are described in this section. The results are categorized into the lumefantrine SELEX experiment and the piperaquine and mefloquine SELEX experiments. First, a summary of the SELEX protocol for each target is referenced, including SELEX tracking data for the most successful piperaquine and mefloquine SELEX experiments (SELEX PQ2 and MQ1). The sorted sequence data resulting from each of the SELEX experiments is then reported.

Next, attempts to assess the binding characteristics of resulting sequences of interest are described. For the lumefantrine SELEX experiment, this was initially attempted via ITC. After ITC results showed no binding, analysis was also performed via Biacore to confirm the negative results. During this analysis, the Biacore method was validated using a model kanamycin aptamer. Also using the model kanamycin aptamer, a method was developed to track SELEX enrichment via Biacore analysis of intermediate libraries. However, as discussed in this chapter, it was later determined to be too difficult to synthesize enough intermediate library to efficiently use this

method. Instead of Biacore tracking, the piperaquine and mefloquine SELEX experiments used small scale elution profiles to monitor enrichment.

Several alternative assays were used to screen the piperaquine and mefloquine SELEX sequences. After sorting the resulting sequences, a clone SELEX elution profile was created to assess sequences of interest. The most promising sequences in the clone SELEX elution profile analysis were then tested via a fluorescent binding assay. To test sequences via the fluorescent binding assay, the quencher conditions needed to be optimized. This optimization included determining a quencher (capture strand with a 3' quencher) strand length and concentration that resulted in the majority of aptamer-bound fluorophore quenching in the absence of drug target but still allowed for the release of aptamer in the presence of drug. Once these conditions were optimized, the piperaquine and mefloquine aptamers were assessed for their sensitivity and specificity using the fluorescent binding assay. Finally, the most promising aptamers, PQ4 and MQ2, were characterized via Biacore binding analysis. Each aptamer's interaction with both its capture oligo and its drug target was assessed independently.

3.3.1 SELEX summary

A summary of optimized SELEX protocols includes the SELEX conditions themselves as well as SELEX tracking data. The SELEX protocol conditions for the lumefantrine SELEX experiment are thoroughly described in Section 3.2.1. Since this SELEX protocol did not include any methods for tracking the library evolution, there is no tracking data to report. The SELEX protocol conditions for the piperaquine and mefloquine SELEX protocols are thoroughly described in Section 3.2.2. The piperaquine and mefloquine SELEX protocols used small scale elution profiles to track SELEX enrichment. Figures 3.8 and 3.9 show the small scale elution profiles and SELEX conditions of odd numbered rounds for SELEX PQ2 and MQ1. This raw data was used to track enrichment to determine how many rounds should be performed and how to adjust the conditions of subsequent rounds.

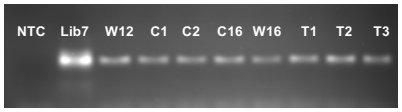
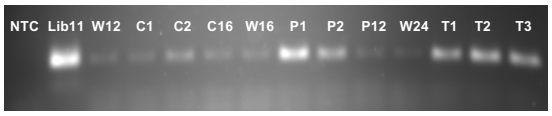
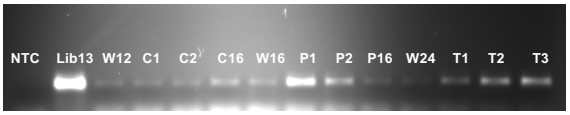
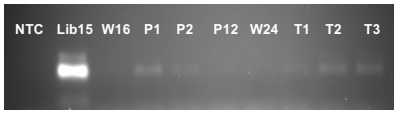
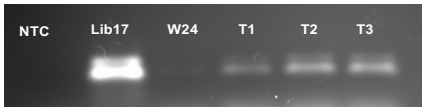
Round/Conditions	Piperaquine SELEX elution profile
Round 1: **Washes:** 10x **Target:** 50μM PQ	
Round 3: **Washes:** 24x **Target:** 50μM PQ	
Round 5: **Washes:** 12x **Counter:** 5μM CQ, 5μM AQ **Washes:** 12x **Target:** 50μM PQ	
Round 7: **Washes:** 12x **Counter:** 10μM CQ, 10μM AQ **Washes:** 16x **Target:** 25μM PQ	
Round 9: **Washes:** 16x **Counter:** 20μM CQ, 20μM AQ **Washes:** 16x **Target:** 25μM PQ	
Round 11: **Washes:** 16x **Counter:** 20μM CQ, 20μM AQ **Washes:** 16x **Plasma:** 12x **Washes:** 24x **Target:** 20μM PQ	
Round 13: **Washes:** 16x **Counter:** 20μM CQ, 20μM AQ **Washes:** 16x **Plasma:** 62x **Washes:** 24x **Target:** 4μM PQ	
Round 15: **Washes:** 16x **Plasma:** 16x **Washes:** 24x **Target:** 0.5μM PQ	
Round 17: **Washes:** 24x **Target:** 0.25μM PQ	

Figure 3.8: SELEX PQ2 conditions and elution profiles. The small scale elution profiles of odd numbered rounds are included here to visualize enrichment tracking. As rounds progress, less DNA elutes during the wash, counter SELEX, and plasma steps and more DNA elutes during the target steps. Also note that in later rounds, the concentration of counter targets are increased and the concentration of target is decreased. NTC = no template control, W1-24 = wash steps, C1-16 = counter elutions, P1-16 = plasma elutions, T1-3 = target elutions.

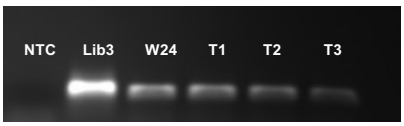
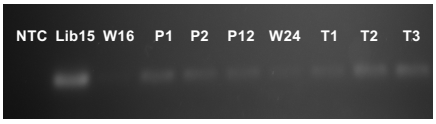
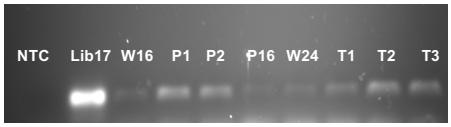
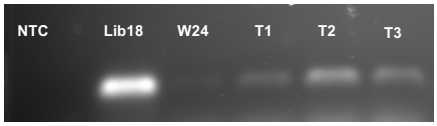
Round/Conditions	Mefloquine SELEX elution profile
Round 1: **Washes:** 10x **Target:** 100μM MQ	
Round 3: **Washes:** 24x **Target:** 100μM MQ	
Round 5: **Washes:** 12x **Counter:** 5μM CQ, 5μM AQ **Washes:** 12x **Target:** 100μM MQ	
Round 7: **Washes:** 12x **Counter:** 10μM CQ, 10μM AQ **Washes:** 16x **Target:** 50μM MQ	
Round 9: **Washes:** 16x **Counter:** 20μM CQ, 20μM AQ **Washes:** 16x **Target:** 50μM MQ	
Round 11: **Washes:** 16x **Counter:** 20μM CQ, 20μM AQ **Washes:** 16x **Plasma:** 12x **Washes:** 24x **Target:** 50μM MQ	
Round 13: **Washes:** 16x **Counter:** 20μM CQ, 20μM AQ **Washes:** 16x **Plasma:** 16x **Washes:** 24x **Target:** 8μM MQ	
Round 15: **Washes:** 16x **Plasma:** 16x **Washes:** 24x **Target:** 1μM MQ	
Round 17: **Washes:** 24x **Target:** 0.5μM MQ	
Round 18: **Washes:** 24x **Target:** 0.25μM MQ	

Figure 3.9: SELEX MQ1 conditions and elution profiles. Small scale elution profiles of odd numbered rounds as well as final SELEX round. A similar trend is observed as in the elution profiles for SELEX PQ2. Abbreviations explained in Figure 3.8.

3.3.2 Sequence analysis results

The sequencing results of all SELEX experiments are reported in this section. Sequencing of the lumefantrine SELEX protocol was performed via next generation sequencing (NGS) while sequencing of the piperaquine and mefloquine SELEX protocol was performed via cloning and Sanger sequencing. The sequencing results of the lumefantrine SELEX experiments are reported via the number of reported sequences from each cycle sequenced and the level of enrichment of the most enriched sequence from each cycle. For the piperaquine and mefloquine SELEX experiments, all of the sequenced clones are reported since there are less than 50 sequences per SELEX experiment. For each experiment, several of the most enriched sequences were selected for further analysis and their Mfold predicted secondary structure is reported.

Lumefantrine SELEX sequence analysis

Intermediate and final rounds of both lumefantrine SELEX experiments (SELEX LF1 and SELEX LF2) were sequenced via NGS. NGS provides in depth information about the level of enrichment of sequences throughout the selection. Table 3.23 shows that over two million reads were reported for each measured cycle and the frequency of the most enriched sequences increased from intermediate to final rounds. Although the frequency of the most enriched sequences remained low (50-70 reads per million) at the final SELEX rounds, the trend towards enrichment was somewhat encouraging. Of course, it is possible that enrichment could be due to PCR bias or other influences during the selection manipulation and may not reflect enrichment for sequences with a binding affinity for lumefantrine.

The most enriched sequences were analyzed for structural similarities. Several sequences with varying predicted secondary structures were assessed for potential lumefantrine binding affinity. The Mfold predicted structures of these sequences are shown in Figure 3.10.

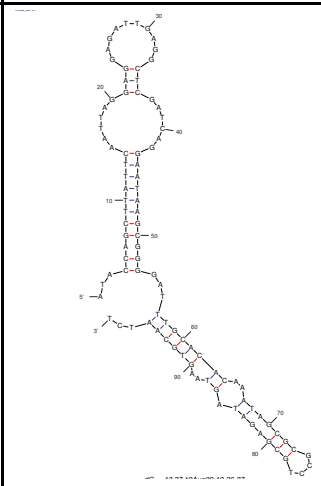
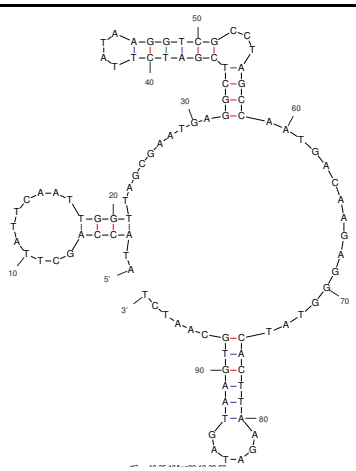
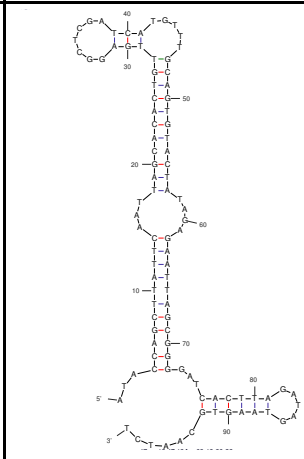
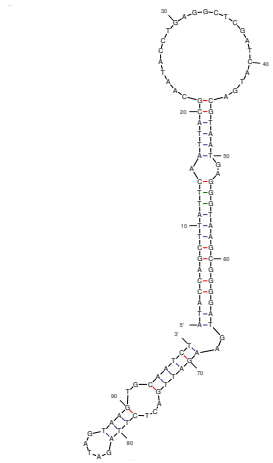
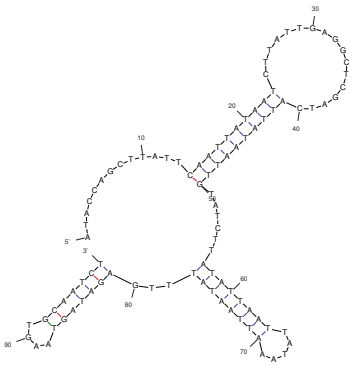
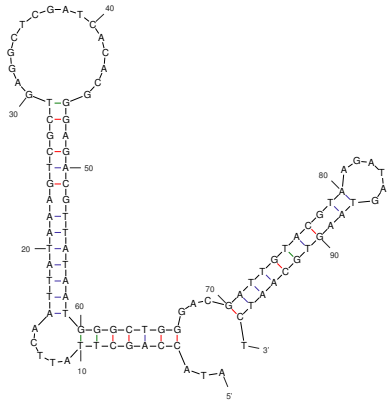
Sequence	**LF1c8n1**	**LF1c8n2**
Enrichment	55.9 RPM	42.4 RPM
Mfold structure		
Sequence	**LF1c8n3**	**LF1c8n4**
Enrichment	40.8 RPM	38 RPM
Mfold structure		
Sequence	**LF2c7n2**	**LF2c7n4**
Enrichment	55 RPM	24.6 RPM
Mfold structure		

Figure 3.10: Lumefantrine sequences of interest. Their enrichment data is reported in reads per million (RPM) and their potential secondary structure is predicted via Mfold.

Experiment and cycle number	Total number of successful reads	Most enriched sequence (copy number)	Most enriched sequence (reads per million (RPM))
LF1cycle3	2,459,640	3	1.21
LF1cylce8	2,189,208	141	55.85
LF2cycle5	2,234,339	12	5.26
LF2cylce7	2,501,938	147	65.76

Table 3.23: Lumefantrine SELEX sequence data. Libraries from an intermediate (LF1cycle3 and LF2cycle5) and final round (LF1cycle8 and LF2cycle7) of both lumefantrine SELEX experiments were sequenced via next generation sequencing. A trend towards increasing enrichment is observed from the intermediate to final rounds though enrichment remains low overall (this is especially apparent in comparison with levels of enrichment seen in piperaquine and mefloquine SELEX experiments).

Piperaquine and mefloquine SELEX sequence analysis

After piperaquine and mefloquine SELEX experiments, sequencing was performed via cloning and Sanger sequencing rather than next generation sequencing. Sanger sequencing, while faster and more affordable, did not provide the same depth of sequence information as next generation sequencing and did not allow for the tracking of sequences across rounds. However, the small-scale PCR elution profiles enabled the tracking of library evolution and sequencing was only performed once elution profiles suggested that the library was highly enriched for binding sequences. It was hypothesized that in a highly enriched library, sequencing of 20-50 clones would be sufficient to observe patterns in sequence enrichment.

Sequence results for SELEX PQ1:

After 19 rounds of selection, the final library pool from SELEX PQ1 was sequenced and the resulting 47 sequences were sorted based on enrichment and sequence similarities. Figure 3.11 shows the sequences aligned using Multalin online software [145].

Six sequences were selected for further analysis via clone SELEX in which a SELEX elution profile was generated from a library of only that sequence. The level of enrichment and predicted Mfold structure of the selected sequences are shown in Figure 3.12 and the results of the clone SELEX elution profiles are shown in Figure 3.13. Aptamers selected from a cluster of replicate sequences were named for a representative sequence in the cluster (e.g. 18.18 represents all

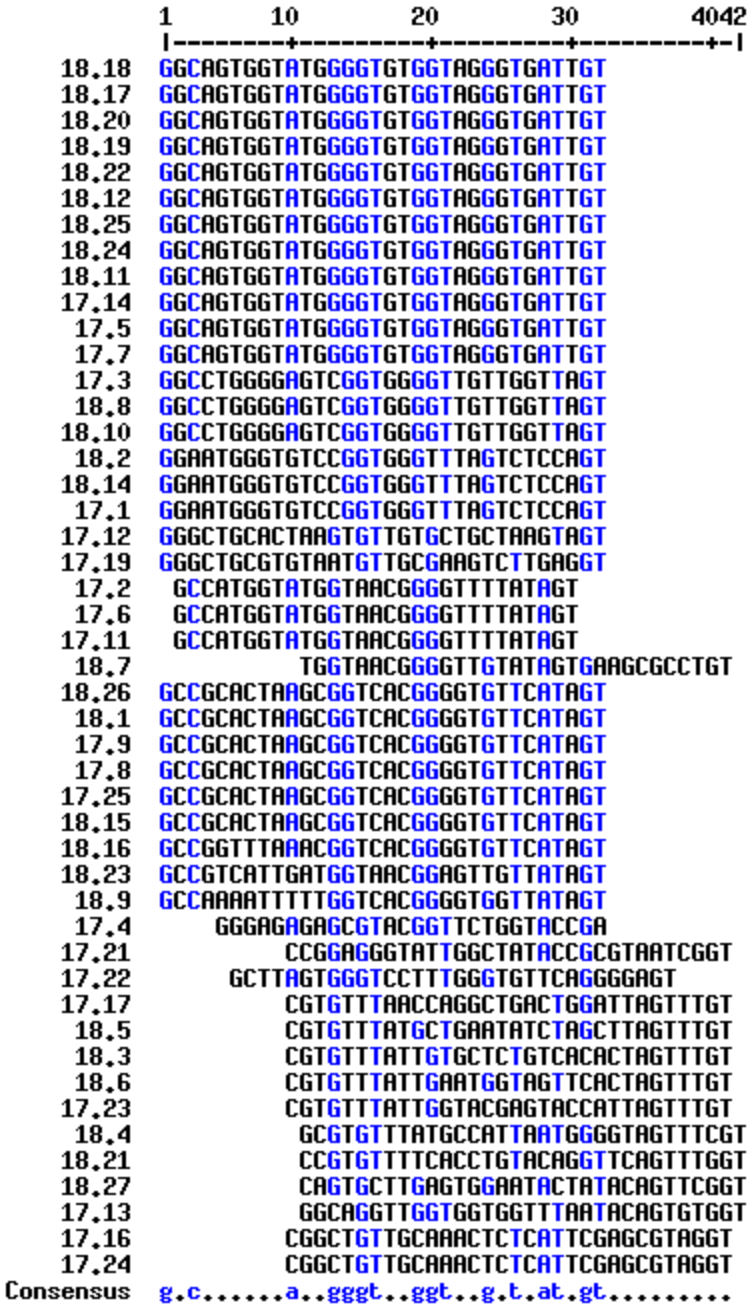


Figure 3.11: Alignment of SELEX PQ1 sequences using Multalin online software. Red indicates >90% base identity (none shown here), blue indicates >50% base identity. Repeats are clustered to show enrichment.

12 sequences identical to aptamer 18.18). From the clone SELEX elution profiles of SELEX PQ1 sequences of interest, four sequences were selected for further analysis via the fluorescent-binding assay.

Sequence results for SELEX PQ2:

After 17 rounds of selection, the final SELEX PQ2 library was cloned and sequenced. The sorted final sequences are shown in Figure 3.14. Four sequences were selected for further analysis via clone SELEX. Their predicted Mfold structures, level of enrichment, and clone SELEX elution profiles are shown in Figures 3.15 and 3.16.

Sequence results for SELEX MQ1:

After 18 selection rounds, the final SELEX MQ1 pool was sequenced and the sorted results are listed in Figure 3.17. Four sequences were selected from the sorted results for further analysis. Their predicted Mfold structures, level of enrichment, and clone SELEX elution profiles are shown in Figures 3.18 and 3.19.

3.3.3 Binding affinity results

Several sequences from the lumefantrine SELEX experiment (shown in Figure 3.10), were selected for binding analysis. Initially, ITC was used to measure potential binding of selected sequences to lumefantrine. ITC does not require immobilization or labelling of the aptamer or target and can provide accurate binding constant analysis via the measurement of heat released or absorbed upon analyte and ligand binding. However, ITC required large amounts of material for each measurement. Initial synthesis and purification of oligonucleotides only produced enough material to measure high affinity binding and to test each sequence once. Due to these constraints, experimental parameters could not be thoroughly optimized and any weak binding could not be accurately measured. Additionally, poor lumefantrine solubility was a concern during ITC testing. The concentration of DMSO was increased to try to improve solubility and a heat of dilution was performed to subtract out any background solvent effects.

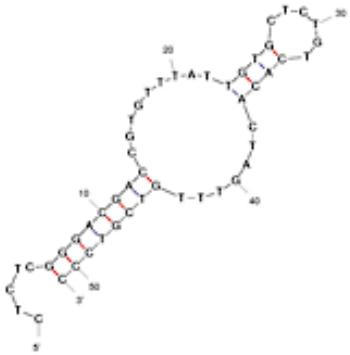
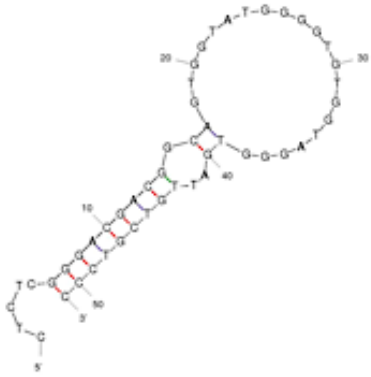
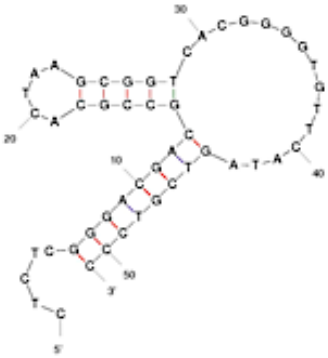
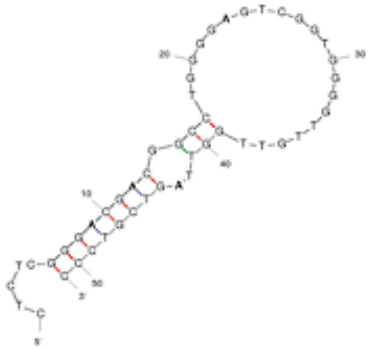
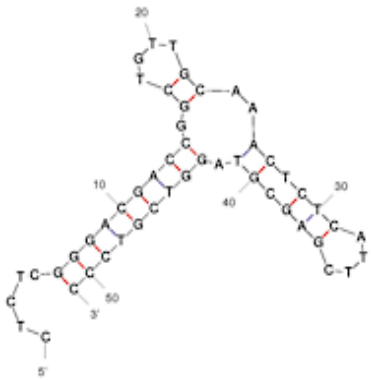
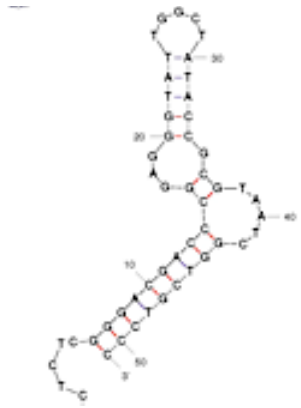
Aptamer name	**18.3**	**18.18**
Enrichment	1/47	12/47
Mfold structure		
Aptamer name	**18.26**	**17.3**
Enrichment	6/47	3/47
Mfold structure		
Aptamer name	**17.16**	**17.21**
Enrichment	2/47	1/47
Mfold structure		

Figure 3.12: The six sequences selected for further evaluation from SELEX PQ1. Their names, level of enrichment (reported as number of replicates/total # of sequences), and Mfold predicted secondary structure are reported.

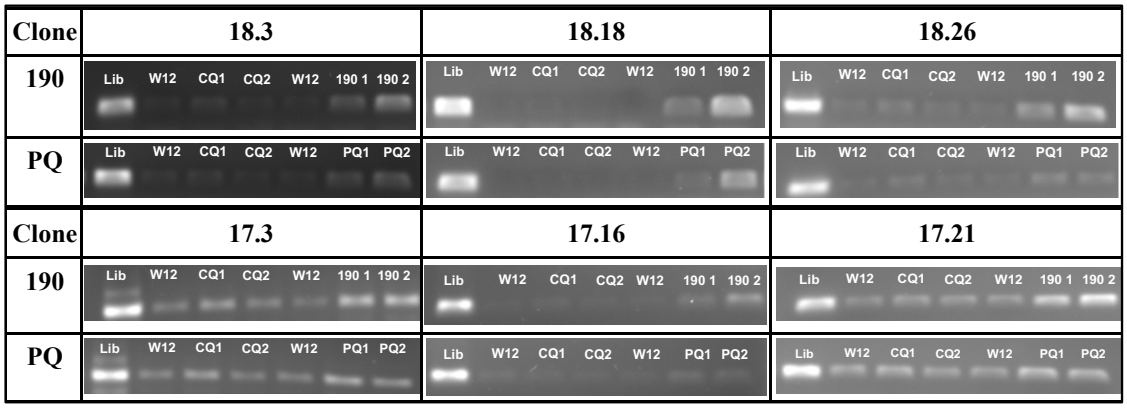


Figure 3.13: Clone SELEX elution profiles of the six sequences selected from SELEX PQ1. Since SELEX PQ1 was performed against molecule 190 rather than the full piperaquine molecule, elution profiles were generated against both 190 and piperaquine for evaluation. The positive targets (PQ and 190) were applied at a concentration of 1 µM and chloroquine in the counter target (CQ1, CQ2) was applied at a concentration of 1 µM. Sequence 18.18 shows an ideal elution profile with very little elution to wash or negative selection steps and strong elution to both 190 and piperaquine. In contrast, sequences 17.3 and 17.21 show nonspecific elution to chloroquine and during wash steps.

```
          1        10        20        30  34
          |--------+---------+---------+---|
PQ1        TCACGGGCATACGCCGCAACTAGCGTGTGGT
PQ19      CCGCAGGAGCGTAGCTCGAACCGGAGGGAGGT
PQ22        GGGCCACCATCCTGTGAAGGATCCGATAGGGT
PQ2       CACACG-TAGTTGCGGCGTATGCCCGTGTAAGT
PQ3       CACACG-TAGTTGCGGCGTATGCCCGTGTAAGT
PQ7       CACACG-TAGTTGCGGCGTATGCCCGTGTAAGT
PQ12      CACACG-TAGTTGCGGCGTATGCCCGTGTAAGT
PQ15      CACACG-TAGTTGCGGCGTATGCCCGTGTAAGT
PQ31      CACACG-TAGTTGCGGCGTATGCCCGTGTAAGT
PQ6       CACGCG-TAGCTGCGGCGTATGCCCGTGTAAGT
PQ4       CACACGCTAGTTGCGCCGAATGGCCGTGAAAGT
PQ5       CACACGCTAGTTGCGCCGAATGGCCGTGAAAGT
PQ10      CACACGCTAGTTGCGCCGAATGGCCGTGAAAGT
PQ18      CACACGCTAGTTGCGCCGAATGGCCGTGAAAGT
PQ21      CACACGCTAGTTGCGCCGAATGGCCGTGAAAGT
PQ33      CACACGCTAGTTGCGCCGAATGGCCGTGAAAGT
PQ29      CACACGCTAGTTGCGCCGAATGGCCGTGAAAGT
PQ24      CACACGCTAGTTGCGCCGAATGGCCGTGAAAGT
PQ14      CACACGCTAGTTGCGCTGAATGGCCGTGAAAGT
PQ28      CACACGCTAGTTGCGCTGAATGGCCGTGAAAGT
PQ32      CACACGCTAGTTGCGCTGAATGGCCGTGAAAGT
PQ27      CACACGCTAGTTGCGGCGTATGCCCGTGTAAGT
PQ30      CACACGCTAGTTGCGGCGTATGCCCGTGTAAGT
Consensus CaCaCGctagtTgCgccGaAtGgcCGTGaAaGt
```

Figure 3.14: The 23 sequences from the final PQ2 library are listed and sorted based on similarity using Multalin online software. Red indicates >90% base identity, blue indicates >50% base identity. Repeats are clustered to show enrichment.

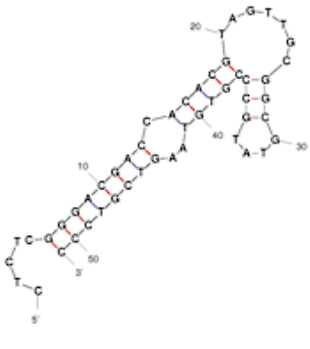
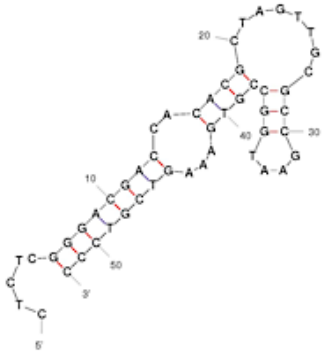
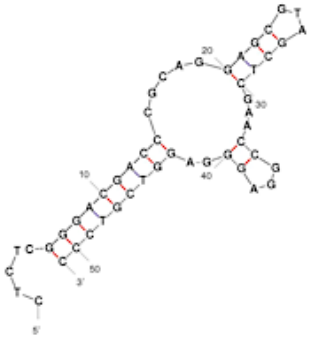
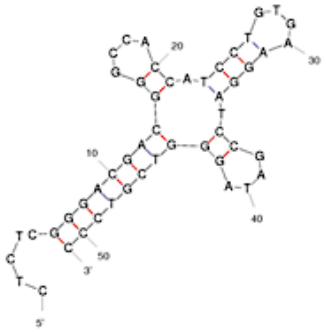
Aptamer name	PQ2	PQ4
Enrichment	6/23	11/23
Mfold structure		
Aptamer name	**PQ19**	**PQ22**
Enrichment	1/23	1/23
Mfold structure		

Figure 3.15: The four sequences selected for further evaluation from SELEX PQ2 via clone SELEX. Their names, level of enrichment (reported as number of replicates/total # of sequences), and Mfold predicted secondary structure are reported. Two highly enriched sequences (PQ2 and PQ4) and two unique sequences (PQ19 and PQ22) from the final sequence data were selected.

Because of concerns with solubility and difficulty generating enough material for ITC analysis, a second binding analysis method was tested to assess potential lumefantrine aptamers. Like ITC, Biacore SPR methods allow for the binding analysis of unlabeled analytes. In this method, a ligand is immobilized to a chip surface and analyte is injected over that surface. The accumulation of analyte mass on the chip surface as it binds ligand is measured via a change in refractive index at the chip surface reported as resonance units (RU). Two different Biacore methods were tested to assess potential aptamer binding. In the first method, lumefantrine sequences were immobilized to the chip surface via hybridization to

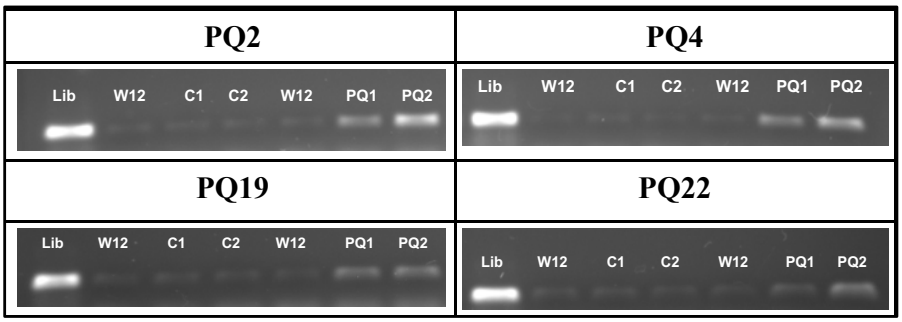


Figure 3.16: Clone SELEX elution profiles of the four sequences selected from SELEX PQ2. Since this SELEX was performed using the full piperaquine molecule as the positive target, the positive elution target (PQ1, PQ2) was the full piperaquine molecule at a concentration of 1 µM. The counter target (C1, C2) was a mixture of 1 µM amodiaquine and 1 µM chloroquine. Sequences PQ2, PQ4, and PQ19 show similar elution profiles and appear to have more selective elution than PQ22.

```
          1        10        20        30  34
          |--------+---------+---------+---|
MQ1        GGAACCGAACATAACTTGGAGGAAGTACTGAGT
MQ6       GAGGACGCACTGAAGCTTACTGGAACCGCAGT
MQ8       GAGGACGCACTGAAGCTTACTGGAACCGCAGT
MQ45      GAGGACGCACTGAAGCTTGCTGGAACCGCAGT
MQ11      GGGTACGTCAGTACTGGGACCTGTCGCTTAGT
MQ47       GGCACTTAGCAAACGCGGCTTCAGTGTGAGGT
MQ14       GGCAAGAATGGCATGGCAAAGATACTTCACGT
MQ15       GGCAAGAATGGCATGGCAAAGATACTTCACGT
MQ17       GGCAAGAATGGCATGGCAAAGATACTTCACGT
MQ18       GGCAAGAATGGCATGGCAAAGATACTTCACGT
MQ37        TAACAGACCTACCGTACCAACCACCTGATCGT
MQ2         GGCAGTCTATACCCCGTATCGCCGAAGGTTGT
MQ5         GGCAGTCTATACCCCGTATCGCCGAAGGTTGT
MQ12        GGCAGTCTATACCCCGTATCGCCGAAGGTTGT
MQ20        GGCAGTCTATACCCCGTATCGCCGAAGGTTGT
MQ48        GGCAGTCTATACCCCGTATCGCCGAAGGTTGT
MQ44        GGTGGTTGGTAGGGAAGCGTAGCGAAGGTTGT
MQ7       GAGGTGGTAACCTTATCGCGGAAGGTGCGAGT
MQ10        GGTGGTAACCTACTCGGAAGAGAAAGGTGCGT
MQ19        GGTGGTAACCTACTCGGAAGAGAAAGGTGCGT
MQ21        GGTGGTAACCTACTCGGAAGAGAAAGGTGCGT
MQ32        GGTGGTAACCTACTCGGAAGAGAAAGGTGCGT
Consensus  ..Gga.gta...aac.cg.a.g..a...gagtgt
```

Figure 3.17: The 22 sequences from the final MQ1 library are listed and sorted based on similarity using Multalin online software. Red indicates >90% base identity, blue indicates >50% base identity. Repeats are clustered to show enrichment.

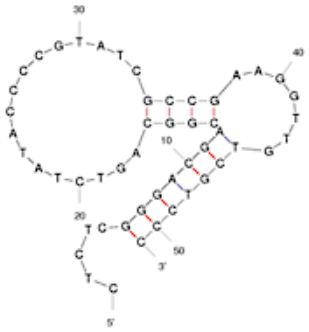
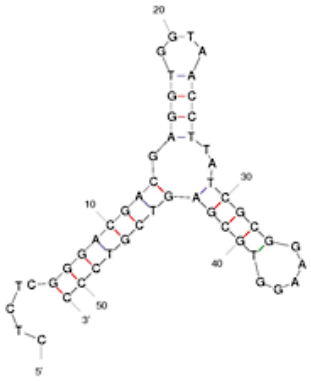
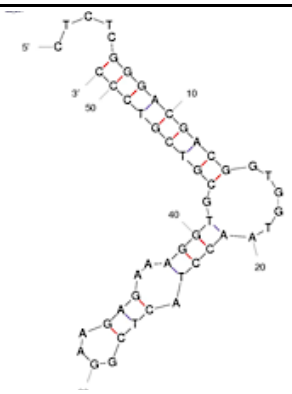
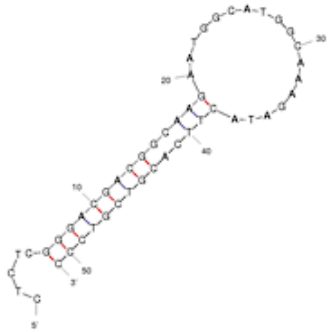
Aptamer name	MQ2	MQ7
Enrichment	5/22	1/22
Mfold structure		
Aptamer name	**MQ10**	**MQ14**
Enrichment	4/22	4/22
Mfold structure		

Figure 3.18: The names, level of enrichment, and Mfold predicted secondary structure of the sequences selected from SELEX MQ1 for further analysis. Three enriched sequences and one unique sequence were selected from the final sequence data for further analysis via clone SELEX elution profiles.



Figure 3.19: Clone SELEX elution profiles of the four sequences selected from SELEX MQ1. The positive elution target (MQ1, MQ2) was mefloquine at a concentration of 1 µM and the counter target (C1, C2) was a mixture of 1 µM amodiaquine and 1 µM chloroquine. Sequences MQ2 and MQ10 show specific elution to the positive target while sequences MQ7 and MQ14 show weak elution to the positive target and cross-reactivity.

a biotinylated capture oligo. Lumefantrine was then injected over the surface so that as sequences bound target and released from the capture oligo, a decrease in mass at the chip surface could be detected. This method was validated using a kanamycin model system. In the second method, piperaquine and mefloquine aptamers were biotinylated and directly immobilized to the chip surface and drug was injected. In this model, the accumulation of small molecule drug at the surface of the chip indicated aptamer-drug binding. In order to measure piperaquine and mefloquine aptamer binding affinity to their capture oligos, biotinylated capture oligo was immobilized to the chip surface and aptamer was injected over the chip. Accumulation of mass at the chip surface was measured when aptamer bound to capture. To first test the binding potential of piperaquine and mefloquine aptamers of interest, a simple fluorescent-binding assay was employed. The results of each of these experiments are described in the following sections.

Lumefantrine ITC results

Heat of dilution corrected isotherm plots of initial ITC results for five selected lumefantrine aptamers are shown in Figure 3.20. MicroCal Origin software was used to assess binding. However, no significant binding was observed in any of the tested sequences and no reliable binding curves were fit.

Piperaquine and mefloquine fluorescent-binding assay results

Optimizing quencher conditions:

A fluorescent-binding assay was used to screen piperaquine and mefloquine sequences for their sensitivity, specificity, and ability to be adapted into sensors. The first step in assessing aptamer binding affinity via the fluorescent-binding assay was to optimize the length and concentration of the quencher-tagged capture strand (quencher). In order to assess aptamer-target affinity, a quencher length and aptamer:quencher ratio that quenched most of the fluorescent signal via hybridization but still allowed for competition with target needed to be identified for each aptamer. To do this, dilutions of 13 base and 14 base quencher strands were tested with each aptamer

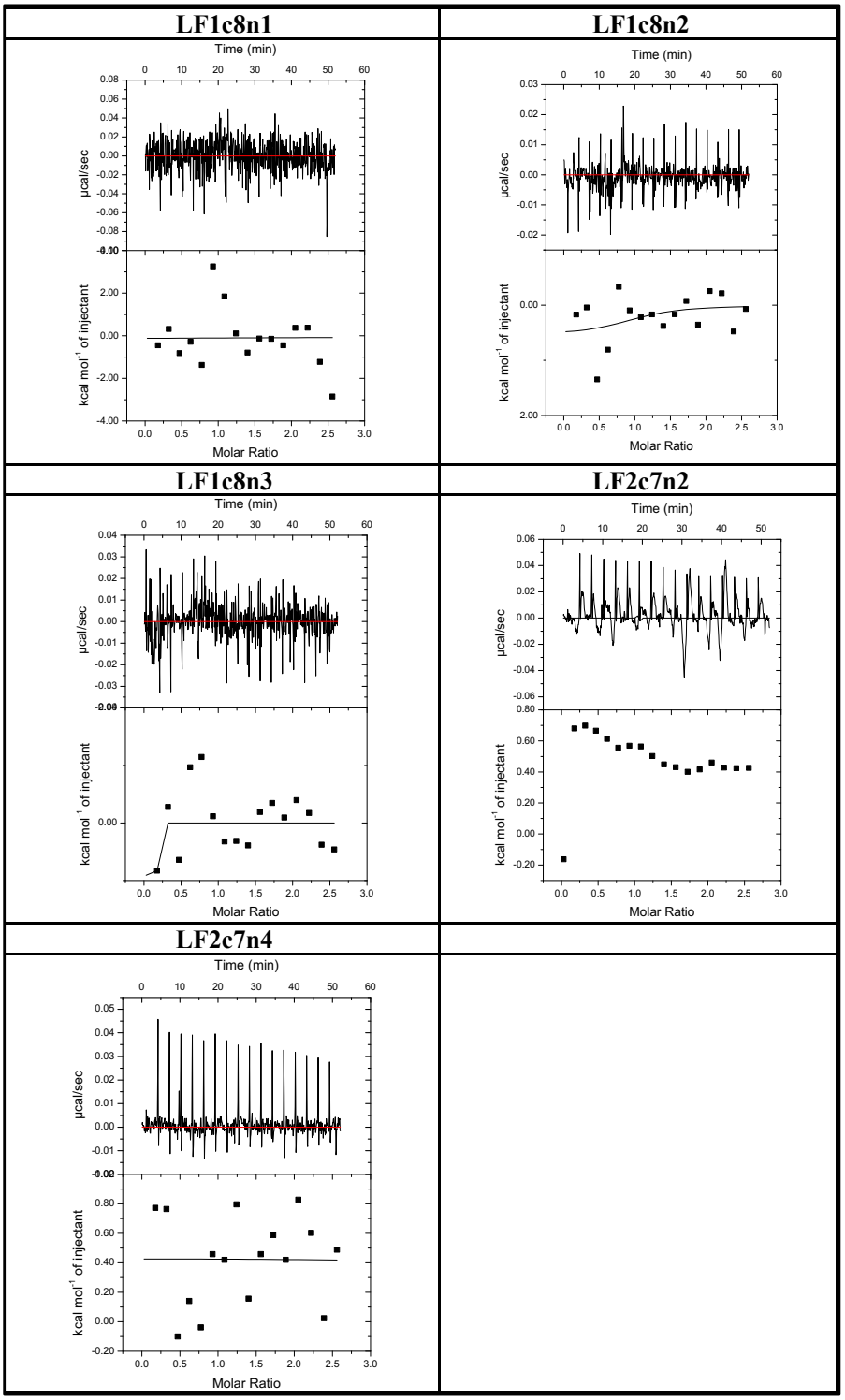


Figure 3.20: ITC binding results of selected lumefantrine sequences. Consecutive injections of 250 µM lumefantrine in B+W buffer (2.5% MeOH) into aptamer (8 µM to 20 µM) in B+W buffer are shown. For each aptamer, the raw data is reported above the heat of dilution corrected binding isotherm. However, no trends indicating binding are reported and no binding curves were able to be fit by MicroCal Origin software.

Aptamer	Selected 13mer ratio	Selected 14mer ratio
18.3	1:10	1:2.5
18.18	1:5	1:2.5
17.16	X	1:2.5
17.21	X	1:10

Table 3.24: The optimized aptamer:quencher ratios are reported for each of the selected aptamer sequences from SELEX PQ1. For aptamers 17.16 and 17.21, the highest aptamer:quencher ratio (1:10) did not provide close to 90% quenching so only the 14mer quencher ratio is reported and only the 14mer quencher was used.

Aptamer	Selected 13mer ratio	Selected 14mer ratio
PQ4	1:10	1:5
PQ19	X	1:10

Table 3.25: The optimized aptamer:quencher ratios are reported for each of the selected aptamer sequences from SELEX PQ2. For PQ19, only the 14mer provided close to 90% quenching.

sequence. The quencher length and ratio that provided roughly 90% quenching in the absence of target was selected for use in the fluorescent assay. If both 13mer and 14mer quencher strands provided close to 90% quenching at tested concentrations, then both quencher strands were assessed in the fluorescent-binding assay.

For SELEX PQ1, four sequences were selected for analysis via the fluorescent-binding assay based on clone SELEX elution profiles (18.18, 18.3, 17.16, and 17.21). Each of these aptamer sequences was tested with dilutions of 13mer and 14mer quenchers. The quencher dilution test is shown in Figure 3.21 and the selected quenchers and their aptamer:quencher ratios are listed in Table 3.24.

Two aptamer sequences from SELEX PQ2 (PQ4 and PQ19) were selected and tested against dilutions of 13mer and 14mer quenchers. The quencher dilution test is shown in Figure 3.22 and the selected quenchers and their aptamer:quencher ratios are listed in Table 3.25. Two aptamer sequences were selected from SELEX MQ1 and tested against dilutions of 13mer and 14mer quenchers. The quencher dilution test is shown in Figure 3.23 and the selected quenchers and their aptamer:quencher ratios are listed in Table 3.26.

Sensitivity and specificity assessment via fluorescent-binding assay:

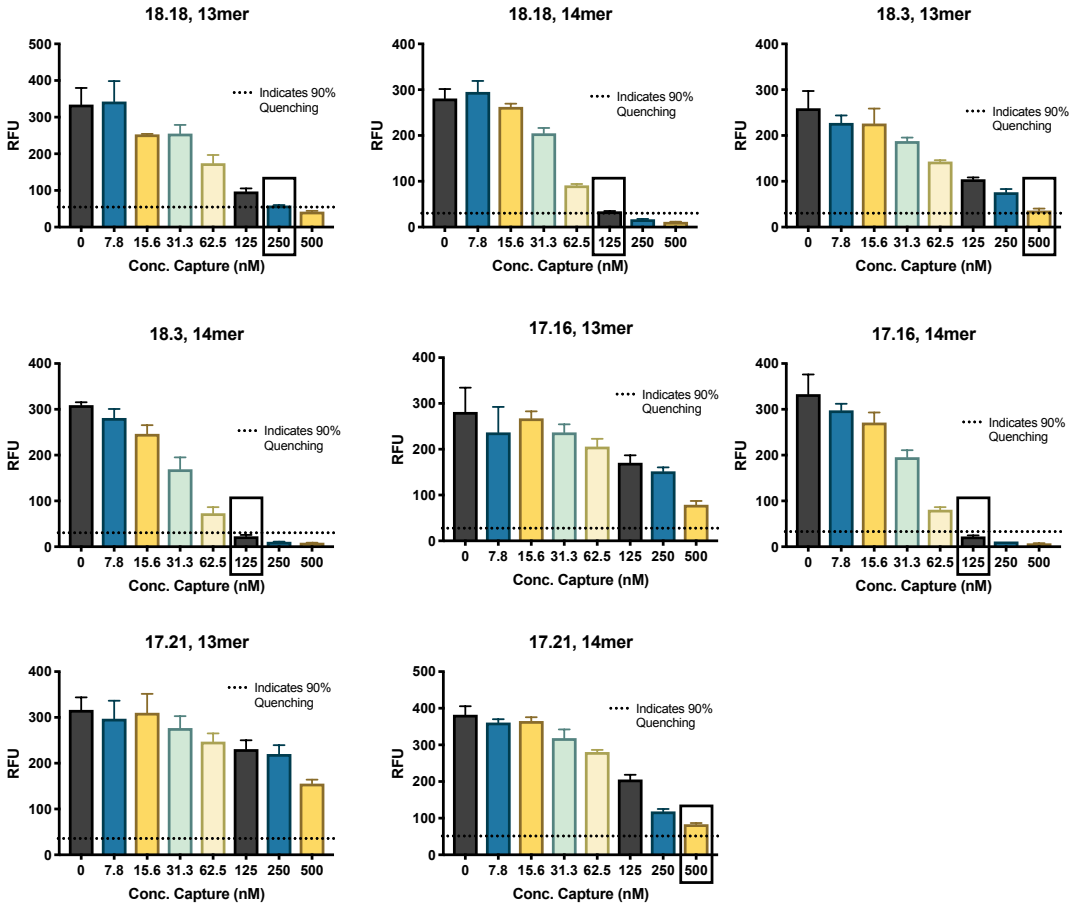


Figure 3.21: The dilution curves of SELEX PQ1 sequences with both 13mer and 14mer quenchers. Quencher concentrations are reported on the X-axis and relative fluorescent units (RFU) are reported on the Y-axis. The dotted line indicates 90% quenching and the box indicates the selected quencher concentrations. As expected, a longer complementary quencher decreases the sensitivity of the fluorescent response.

Aptamer	Selected 13mer ratio	Selected 14mer ratio
MQ2	1:10, 1:5	1:5
MQ10	X	1:10

Table 3.26: The optimized aptamer:quencher ratios are reported for each of the selected aptamer sequences from SELEX MQ1.

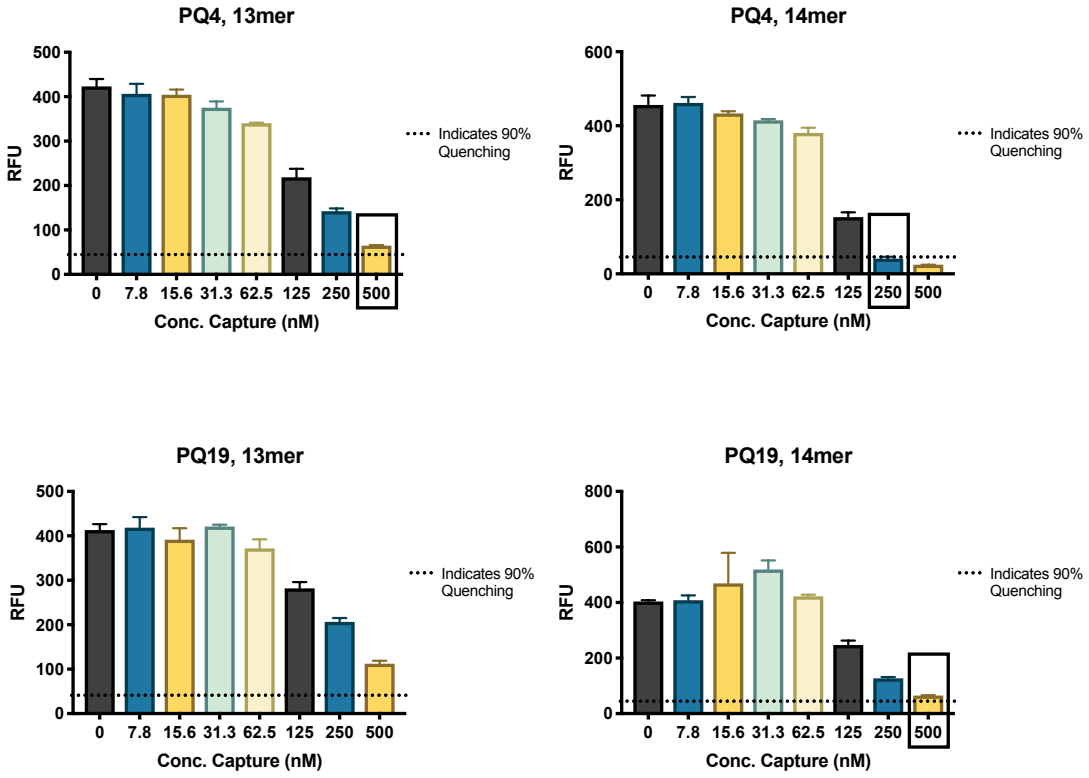


Figure 3.22: The dilution curves of SELEX PQ2 sequences with both 13mer and 14mer quenchers. Quencher concentrations are reported on the X-axis and relative fluorescent units (RFU) are reported on the Y-axis. The dotted line indicates 90% quenching and the box indicates the selected quencher concentrations.

Once the quencher strand lengths and concentrations were optimized, selected sensors from SELEX PQ1 were assessed for sensitivity and specificity via the fluorescent-binding assay. Piperaquine was used as the positive target and chloroquine as the negative target. Dilutions of both drugs were tested from around 5,000 ng/mL to about 5 ng/mL (dilutions were originally made in µM concentrations and then converted to ng/mL for consistency). All conditions were tested in triplicate. Results are shown in Figure 3.24. Based on these results, aptamer 18.18 with a 13mer capture was selected for further testing as the most promising aptamer.

Aptamer 18.18 was tested for cross-reactivity to other quinoline antimalarial drugs as well as other commonly used drugs and corn starch, a tablet filler. All drug dilutions were made in selection buffer and all conditions were tested in triplicate. These results are shown in Figure 3.25.

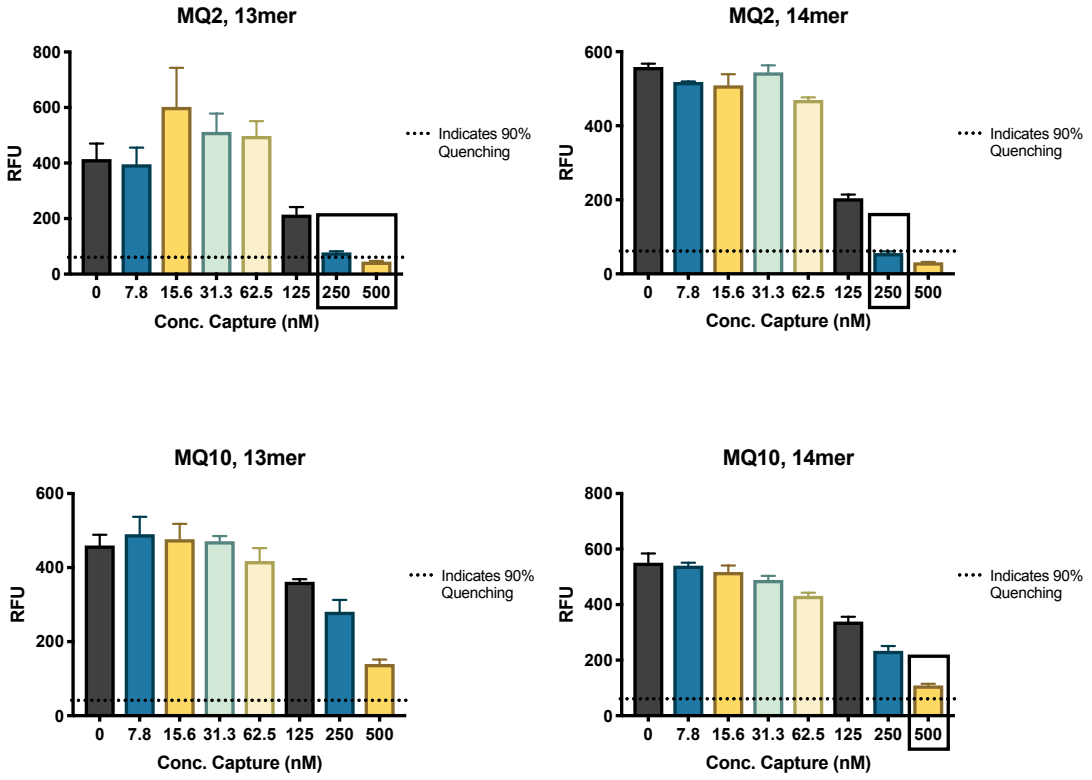


Figure 3.23: The dilution curves of SELEX MQ1 sequences with both 13mer and 14mer quenchers. Quencher concentrations are reported on the X-axis and relative fluorescent units (RFU) are reported on the Y-axis. The dotted line indicates 90% quenching and the box indicates the selected quencher concentrations.

SELEX PQ1 was performed using molecule 190 as the positive selection target so the sensitivity of sensor aptamer 18.18 against molecule 190 was compared to its sensitivity against the full piperaquine molecule. Dilutions of both compounds were prepared from 1 mM stock solutions and tested in triplicate. It was hypothesized that aptamers that bound molecule 190 would also bind the symmetrical piperaquine molecule and that they might be able to bind at an aptamer:drug ratio of 2:1, increasing the sensitivity of the resulting sensor. However, based on results shown in Figure 3.26, this did not appear to be the case.

The cross-reactivity, poor function in serum (discussed in Chapter 4), and weaker response to full piperaqiune as compared to molecule 190 motivated the decision to repeat a piperaquine SELEX experiment. SELEX PQ2 used both chloroquine and amodiaquine as the negative selection targets, included an extra

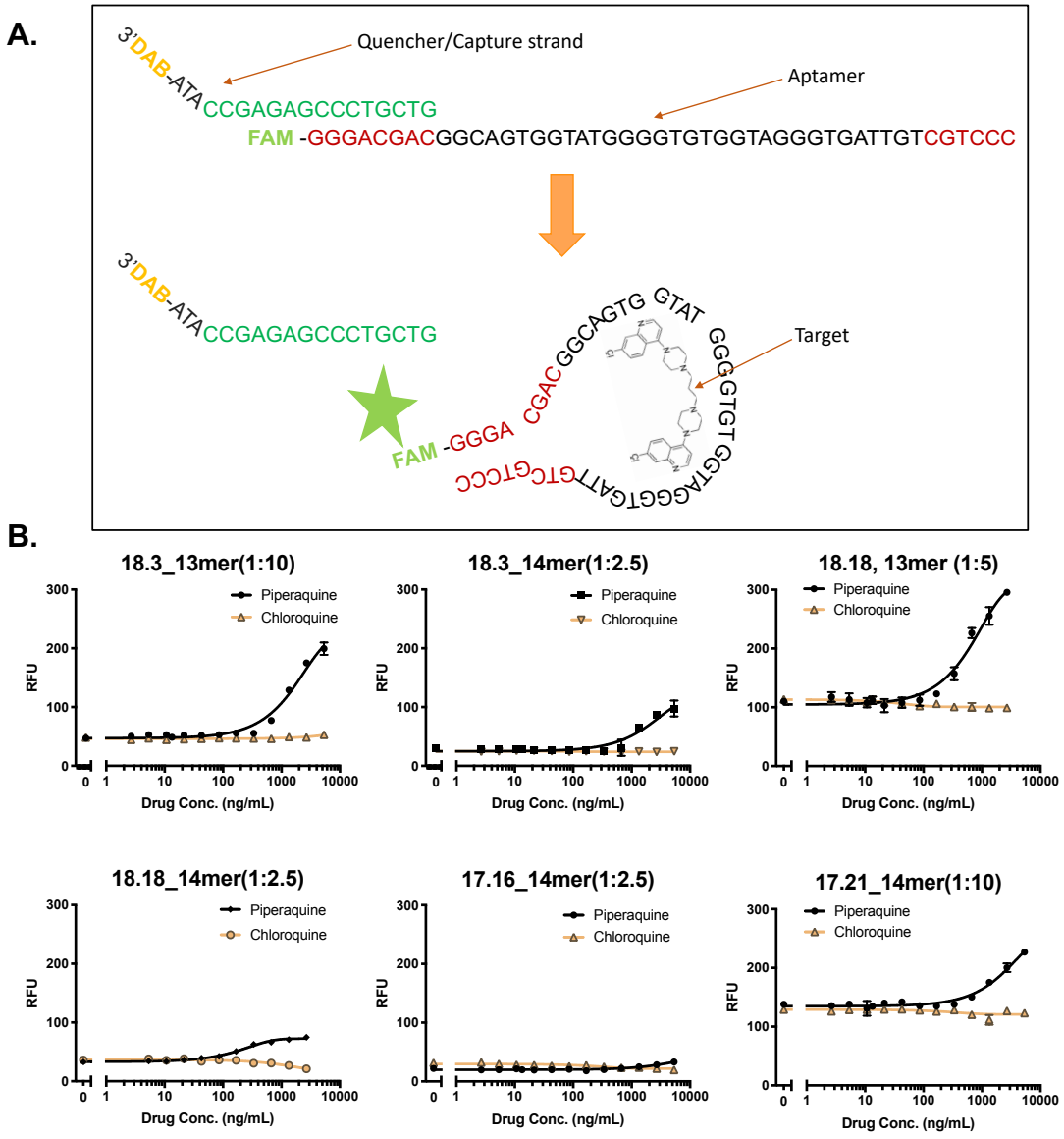


Figure 3.24: A. Reminder of fluorescent sensor mechanism. Aptamers of interest are tagged with a fluorophore (FAM) and their corresponding capture molecule is tagged with a quencher (DAB). Upon binding target, the aptamers release the quencher strand and an increase in fluorophore response is measured. **B.** Fluorescent-binding assay results for selected sequences from SELEX PQ1. The drug concentrations are reported on the X-axis and fluorescent response (RFU) is reported on the Y-axis. Each aptamer at its optimal quencher conditions was tested against a dilution curve of piperaquine and chloroquine. An increase in RFU response indicates aptamer-target binding. Aptamer 18.3 has detectable piperaquine binding around 500 ng/mL with the 13mer quencher and a much weaker response with the 14mer quencher. Aptamer 18.18 has detectable piperaquine binding around 200 ng/mL and again a much weaker response with the 14mer quencher. Aptamers 17.16 and 17.21 were only tested with 14mer quenchers since 13mers did not provide sufficient quenching and both show weaker binding than aptamers 18.3 and 18.18. No cross-reactivity to chloroquine is detected at the tested concentrations.

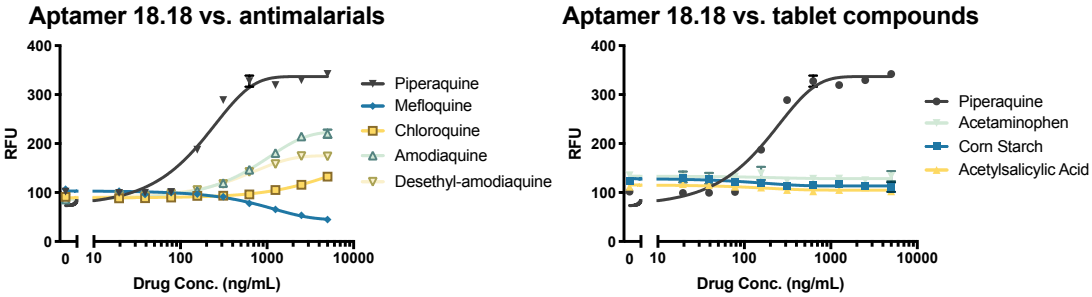


Figure 3.25: Specificity of aptamer 18.18. Aptamer 18.18 appears to bind amodiaquine and its active metabolite desethylamodiaquine at concentrations above 500 ng/mL. These concentrations are physiologically relevant. Amodiaquine is quickly converted to desethylamodiaquine which has a maximum physiological concentration around 800 ng/mL. Aptamer 18.18 also exhibited slight cross-reactivity to chloroquine above the physiologically relevant range of concentrations for chloroquine and its active metabolite desethylchloroquine. Aptamer sensor 18.18 shows no cross-reactivity to acetaminophen or acetysalicylic acid or to corn starch (a tablet filler).

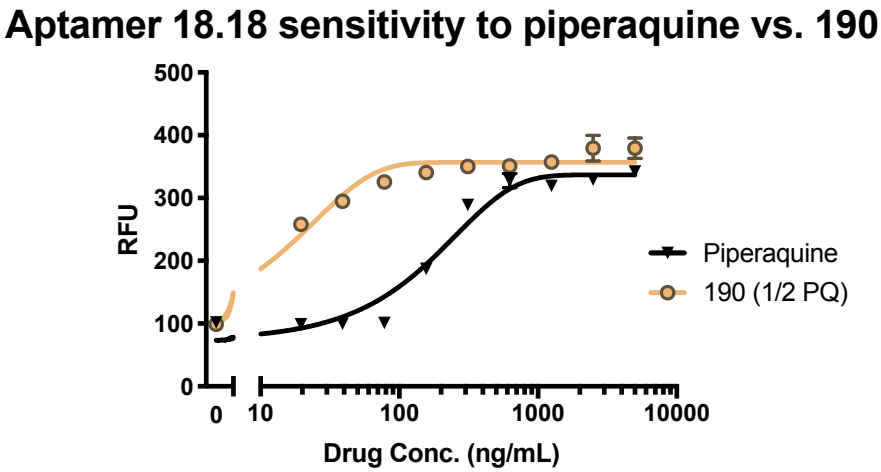


Figure 3.26: Aptamer 18.18 appears to have a higher affinity to molecule 190 as compared to the full piperaquine molecule.

negative selection step with diluted serum, and used the full piperaquine molecule as the positive selection target.

Two sensors from SELEX PQ2, called PQ4 and PQ19, were assessed for sensitivity and specificity via the fluorescent-binding assay using piperaquine as the positive target and mefloquine, chloroquine, and amodiaquine as negative targets. The decision to include more similarly structured compounds in the initial specificity testing in this round of sensor characterization was influenced by the discovery during sensor 18.18 testing that chloroquine alone cannot be used as an effective predictor of

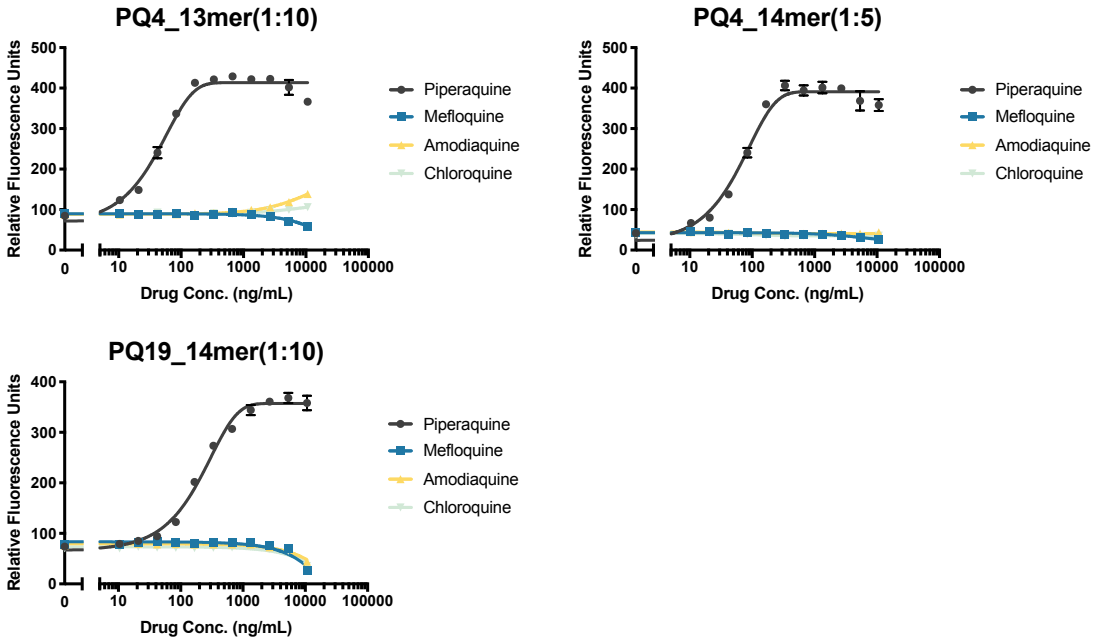


Figure 3.27: Fluorescent-binding assay results for selected sequences from SELEX PQ2. The drug concentrations are reported on the X-axis and fluorescent response (RFU) is reported on the Y-axis. PQ4 and PQ19 have comparable sensitivity and specificity. PQ4 was selected for further analysis due to lower background. Comparing the 1:10 13mer curve with the 1:5 14mer curve reveals an anticipated trade-off between improved sensitivity with the 13mer quencher and decreased background and cross-reactivity with the 14mer quencher. In the future, the choice of capture length could be optimized based on the intended application. Aptamer PQ4 with both 13mer and 14mer quenchers were further tested for function in serum.

cross-reactivity against other quinoline compounds. Dilutions of all drugs were tested from around 10,000 ng/mL to 10 ng/mL. The results are reported in Figure 3.27.

Two sensors from SELEX MQ1, called MQ2 and MQ10, were assessed for sensitivity and specificity via the fluorescent-binding assay using mefloquine as the positive target and piperaquine, amodiaquine, and chloroquine as the negative target. Dilutions of all drugs were tested from around 8,000 ng/mL to 8 ng/mL (dilutions were originally made in µM concentrations and then converted to ng/mL for consistency). The results are reported in Figure 3.28.

Biacore analysis of lumefantrine sequences

Three of the five lumefantrine sequences assessed via ITC were also assessed via Biacore binding analysis to confirm results. Table 3.27 shows the change in resonance

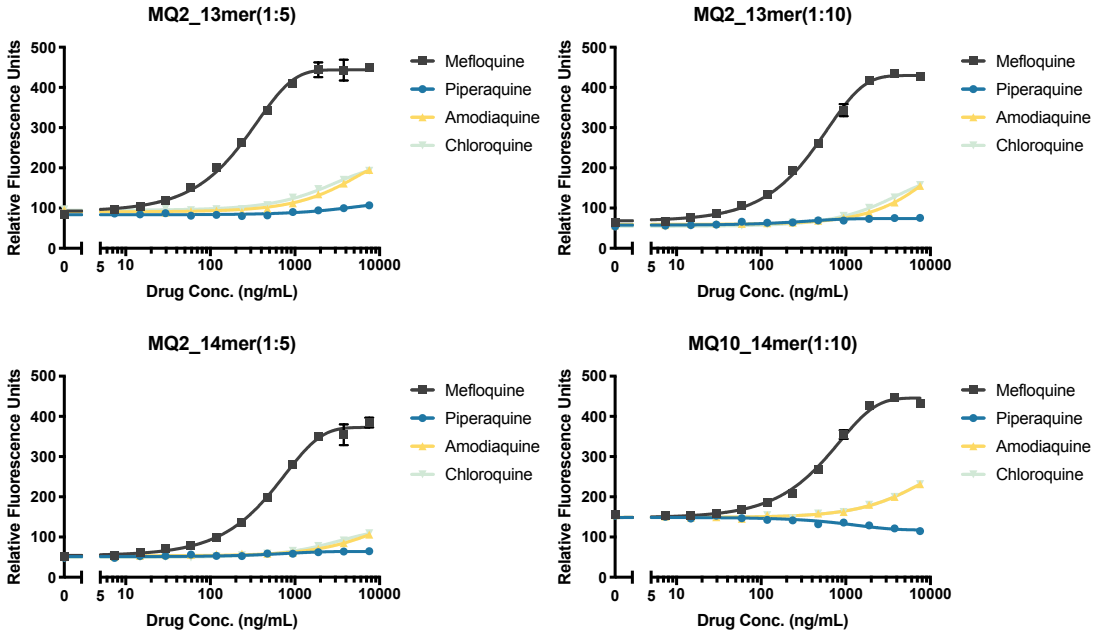


Figure 3.28: Fluorescent-binding assay results for selected sequences from SELEX MQ1. The drug concentrations are reported on the X-axis and fluorescent response (RFU) is reported on the Y-axis. Sequence MQ2 appears to have lower background and improved sensitivity over sensor MQ10. These graphs again show a tradeoff between sensitivity and specificity where sensitivity increases with fewer complementary bases (13mer) and specificity improves with more complementary bases (14mer) and increased concentration of quencher strand. Aptamer MQ2 with both 13mer and 14mer quenchers were further tested for function in serum.

units (RU) reported during blank injections, 50 µM lumefantrine injections, and the blank corrected lumefantrine injections. All injections were reference cell corrected by subtracting the ΔRU measured on reference cell from the test cell. If sequences bound lumefantrine, they would release during the drug injection at a higher rate than the blank injections resulting in a negative blank corrected ΔRU. Since no response was detected at the lumefantrine concentrations tested, the analysis was not continued. These results appear to confirm the ITC results from the previous section. Enriched sequences from the lumefantrine SELEX showed no significant target binding via ITC or Biacore SPR.

Biacore analysis of model kanamycin aptamer and SELEX tracking method

In order to validate the Biacore method used to assess lumefantrine sequences in which a loss of mass at the chip surface indicates aptamer release and thus

Aptamer	Blank (5% MeOH, B+W) (ΔRU)	Lumefantrine test (50 µM, 5% MeOH, B+W) (ΔRU)	Blank corrected ΔRU of 50 µM lumefantrine injections
LF1c8n2	-45	-33.3	11.7
LF1c8n4	-53.4	-38.4	15
LF2c7n2	-23.6	-14.3	9.3
LF2c7n4	-28.7	-19.8	8.9

Table 3.27: Biacore assessment of lumefantrine sequences. The results from a blank injection, a 50 µM lumefantrine injection, and the blank corrected values are reported. All injections were 300s long at a flow rate of 10 µL/min and all reported ΔRU values are the reference cell corrected values. If the aptamer sequences bound lumefantrine they would release from the immobilized capture oligo resulting in a net decrease in the ΔRU of the blank corrected values.

target binding, the method was repeated with a previously characterized kanamycin aptamer. Kanamycin aptamer 13_82 [141] was immobilized to the test cell of the Biacore chip via capture oligo and aptamer library was immobilized to the reference cell. After initial testing showed a reference cell corrected release of aptamer from the test cell during drug injections as compared to blank injections, a Biacore protocol was set to inject a kanamycin dilution curve over both the test and reference cell. Figure 3.29 shows a dose dependent response as varying concentrations of kanamycin were injected over the Biacore chip. The data was fit to a one-site specific binding model in Graphpad Prism:

$Y = \frac{B_{max}*X}{K_D+X}$; where B_{max}=the maximum specific binding measured in the same units as Y and K_D=the equilibrium constant in the same units as X.

Using this model, a K_D of 250.9 µM was reported. Original publication of the 13_82 kanamycin aptamer reported a K_D of 106 µM. The K_D reported here was believed to be within reasonable range of the previously reported value. Success with this model aptamer system suggests that the inability to observe a release of lumefantrine sequences during drug injections as compared to blank injections indicates a lack of sequence binding rather than an issue with the method.

After analysis of the lumefantrine sequences, a method was developed to measure the binding of library pools with low levels of enrichment. The goal of this method was to provide a quantitative way to assess SELEX progress and track enrichment of binding sequences across SELEX rounds. This would be helpful for future SELEX

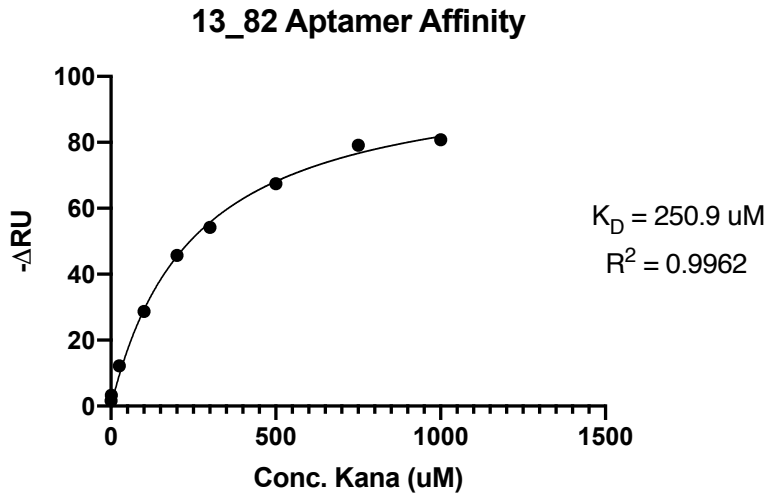


Figure 3.29: Biacore assessment of model kanamycin aptamer. Aptamer 13_82 was immobilized to the test cell and Lib3 was immobilized to the reference cell. The curve shown is the reference cell corrected curve. A decrease in mass on the chip surface is reported on the Y-axis in the form of -ΔRU. A one-site binding model in Graphpad Prism reported at K_D of 250.9 µM, within reasonable range of the previously reported value given that different instruments and drug stocks were used for the measurements.

experiments, providing information on the success of selection throughout the experiment and informing when a sufficient number of rounds had been performed so that the pool was enriched for binding sequences. The method was first tested using the model kanamycin aptamer, spiked into aptamer library at varying concentrations. The artificially "enriched" libraries were immobilized on the Biacore chip test cells and compared to a reference cell on which unenriched library was immobilized. As seen in Figure 3.30, a dose dependent response can be observed in a library with as low as 2% enrichment for binding sequences.

As described in the results section, the intention was to use this method to quantitatively track SELEX progress during the SELEX PQ1 experiment. However, this method was abandoned after significant difficulty synthesizing enough intermediate library to repeatedly reload library on the chip after drug injections. It was decided that small-scale elution profiles, although qualitative, provided enough information to track SELEX progress. Though, in the absence of small-scale elution profiles, it may be worth exploring more methods to synthesize and purify material from intermediate libraries to allow for SELEX tracking via this Biacore method.

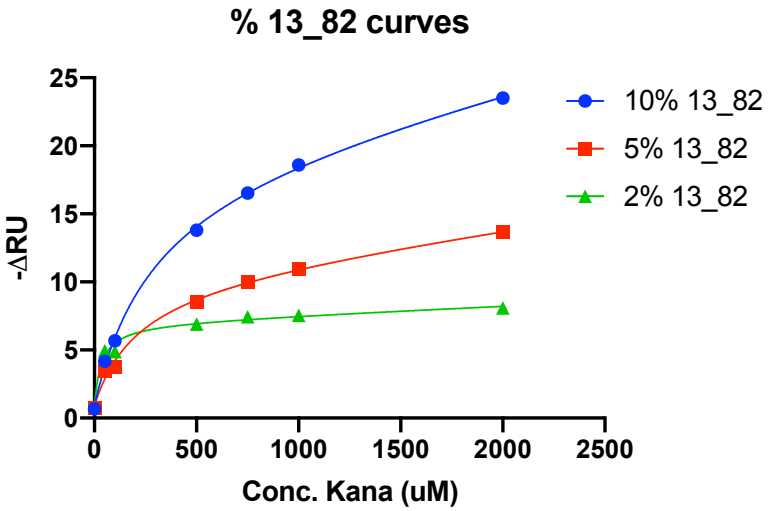


Figure 3.30: Biacore analysis of library pools artificially enriched for kanamycin binding sequences. Varying concentrations of kanamycin were injected over flow cells with enrichment of binding sequences ranging from 2-10%. Unenriched library was immobilized to the reference cell and the curves are reference cell corrected. There appears to be a dose dependent kanamycin response in all pools even (through slight) in the condition in which only 2% of sequences exhibit kanamycin binding.

Biacore characterization of aptamers PQ4 and MQ2

After aptamers PQ4 and MQ2 were identified as the most promising aptamers via the fluorescent-binding assay, they were further characterized via Biacore analysis. The performance of aptamer sensors described in Chapter 4 is affected by the binding interactions between aptamers and drug targets as well as between the aptamers and their capture (or quencher) oligos. While the fluorescent-binding assay provides a quick method for assessing aptamer sensitivity and specificity, it's output describes the aptamer sensor which depends on both aptamer-capture and aptamer-drug interactions. The following Biacore methods were used to assess the interactions between aptamers and their capture and drug targets separately.

Aptamers PQ4 and MQ2 aptamer-capture affinity measurements:

To characterize the binding between the most promising aptamers (PQ4 and MQ2) and their capture (or quencher) oligos, biotinylated capture oligo was immobilized on a Biacore chip and aptamer sequences were injected at varying concentrations. Note: the "capture" oligos are referred to as "quenchers" once the capture is tagged with a

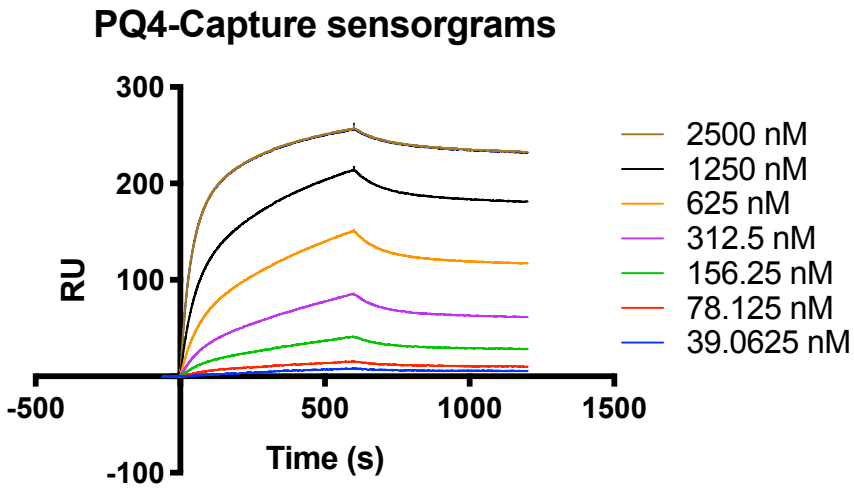


Figure 3.31: Biacore sensorgrams of PQ4 aptamer-capture affinity assay. Varying concentrations of PQ4 aptamer were injected over biotinylated 13mer capture for 600 seconds at a flow rate of 30 µL/minute followed by a 600s dissociation phase. NeutrAvidin was immobilized on the reference cell and all curves are reference cell corrected.

3' quencher molecule rather than a 3' biotin molecule. However, the sequences are identical and the binding characteristics are expected to be conserved. Figures 3.31 and 3.32 show the raw sensorgram results of the Biacore method to measure aptamer-capture binding interactions. The injection time was increased to 600s after initial tests in the hope of reaching equilibrium. However, as can be seen in both Figures 3.31 and 3.32, some of the concentration curves still do not flatten out. Due to a lack of material, the association time could not be further increased. This likely results in a slight underestimate of the binding affinity between aptamers and their captures.

Tables 3.28 and 3.29 show the results of a kinetic binding analysis performed on the sensorgram data from Figures 3.31 and 3.32. After analysis of the shape of the curves, a two-state reaction binding model was fit to the data. The binding interaction measured involves the hybridization of 13 bases from the aptamer to the capture oligo. It is hypothesized that there are some intermediate stages where not all of the bases are hybridized while the aptamer and capture orient themselves to allow for binding of all 13 bases. This would explain the fast and slow association and dissociation phases observed in the sensorgrams and the parameters listed in Tables 3.28 and 3.29. Analysis of the association and dissociation rates reports a K_D of 81.2 nM for the PQ4-capture interaction and a K_D of 132 nM nM for the

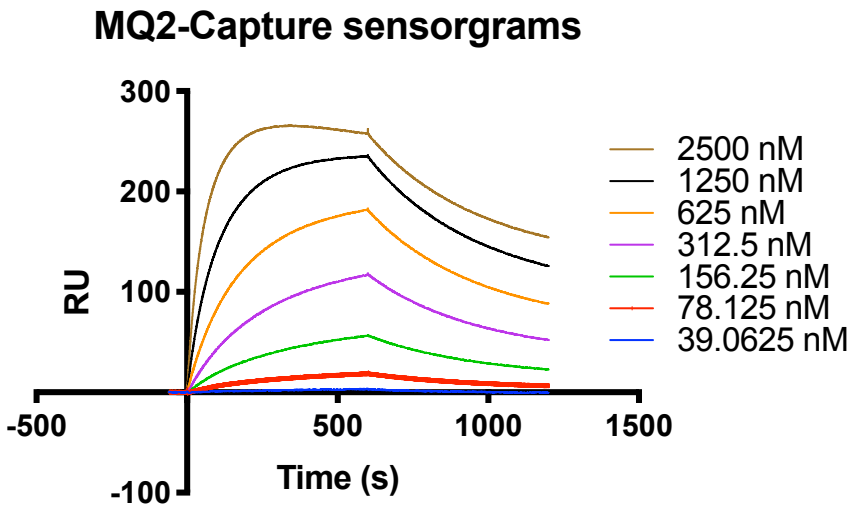


Figure 3.32: Biacore sensorgrams of MQ2 aptamer-capture affinity assay. Varying concentrations of MQ2 aptamer injected over 150 RU of biotinylated 13mer capture for 600 seconds at a flow rate of 30 µL/minute followed by a 600s dissociation phase. NeutrAvidin was immobilized on the reference cell and all curves are reference cell corrected.

	k_a1 (1/Ms)	k_d1 (1/s)	k_a2 (1/s)	k_d2 (1/s)	K_D (M)	Rmax (RU)	Chi² (RU²)
PQ4-Capture binding affinity analysis	2237	1.30E-02	3.17E-03	4.50E-05	8.12E-08	2485	191

Table 3.28: The sensorgram data shown in Figure 3.31 was fit to a two-state reaction binding model using kinetic fit analysis in the Biacore T100 evaluation software. The fit reports the on (K_a) and off (K_d) rates of the aptamer-capture interaction and reports a K_D of 81.2 nM.

MQ2-capture interaction. It was expected that the K_Ds would be similar since the measured interaction is between the same 13 bases for both aptamers. The observed differences in K_Ds could be due to secondary structure specific to one of the aptamers that might interfere with or improve hybridization.

	k_a1 (1/Ms)	k_d1 (1/s)	k_a2 (1/s)	k_d2 (1/s)	K_D (M)	Rmax (RU)	Chi² (RU²)
MQ2-Capture binding affinity analysis	5768	3.66E-03	1.34E-03	3.53E-04	1.32E-07	309.6	24.9

Table 3.29: The sensorgram data shown in Figure 3.32 was fit to a two-state reaction binding model using kinetic fit analysis in the Biacore T100 evaluation software. The fit reports the on (K_a) and off (K_d) rates of the aptamer-capture interaction and reports a K_D of 132 nM.

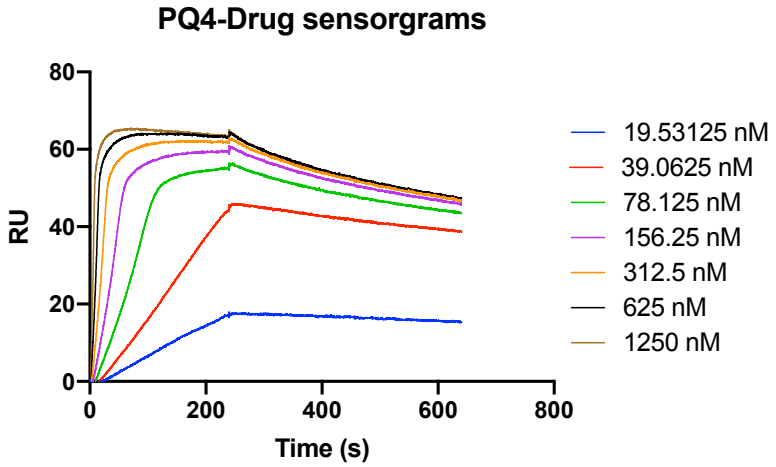


Figure 3.33: Biacore sensorgrams of PQ4 aptamer-drug affinity assay. Varying concentrations of piperaquine injected over biotinylated PQ4 aptamer for 250 seconds at a flow rate of 30 µL/minute followed by a 300s dissociation phase.

Aptamers PQ4 and MQ2 aptamer-drug affinity measurements:

In order to measure the binding characteristics of the aptamer to drug in isolation, the PQ4 and MQ2 aptamers were biotinylated and immobilized to the chip surface. Varying drug concentrations were injected over the chip surface and a change in mass was observed at the surface as drug bound to aptamer. The ΔRU measured in this assay was much smaller than that of the aptamer-capture assays due to the size of analytes. Figures 3.33 and 3.34 show the sensorgrams of the PQ4 and MQ2 aptamer-drug interactions. The sensorgrams reveal that both aptamers bind their drug targets with a rapid association rate. Analysis of the curve shape informed the decision to use a one-site binding model to obtain kinetic parameters for both aptamer-drug interactions. The curve fitting was performed using Biacore T100 evaluation software. Tables 3.30 and 3.31 report the kinetic binding parameters, goodness of fit, and the calculated K_D values for both aptamers.

The results in Tables 3.30 and 3.31 report that the PQ4 aptamer has about a 30-fold higher K_D than the MQ2 aptamer. This is evident also in the sensorgrams in Figures 3.33 and 3.34 (note the concentration of drug injected was different for the two aptamers). The PQ4 aptamer's higher affinity is also evident in the characterization of the sensors in Chapter 4 where the piperaquine sensors are more

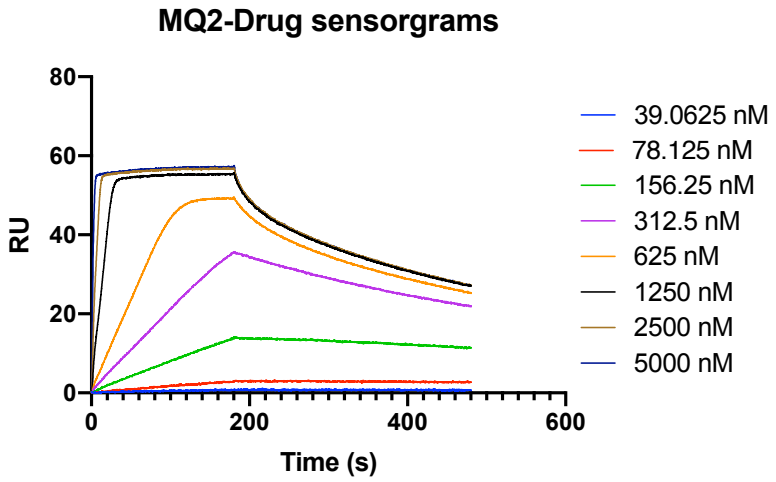


Figure 3.34: Biacore sensorgrams of MQ2 aptamer-drug affinity assay. Varying concentrations of mefloquine injected over biotinylated MQ2 aptamer for 200 seconds at a flow rate of 30 µL/minute followed by a 300s dissociation phase.

	k_a (1/Ms)	k_d (1/s)	K_D (M)	Rmax (RU)	Chi² (RU²)
PQ4-Drug binding affinity analysis	1.38E+06	2.47E-03	1.78E-09	62.61	5.76

Table 3.30: The sensorgram data shown in Figure 3.33 was fit to a one-site binding model using kinetic fit analysis in the Biacore T100 evaluation software. The fit reports the on (K_a) and off (K_d) rates of the aptamer-drug interaction and reports a K_D of 1.78 nM.

	k_a (1/Ms)	k_d (1/s)	K_D (M)	Rmax (RU)	Chi² (RU²)
MQ2-Drug binding affinity analysis	6.45E+04	3.38E-03	5.71E-08	50.72	9.39

Table 3.31: The sensorgram data shown in Figure 3.34 was fit to a one-site binding model using kinetic fit analysis in the Biacore T100 evaluation software. The fit reports the on (K_a) and off (K_d) rates of the aptamer-drug interaction and reports a K_D of 57.1 nM.

sensitive than the mefloquine sensors. However, both aptamers report satisfactory K_D values in the low nanomolar range. At this stage, SELEX was discontinued and these two aptamers were carried forward to Chapter 4 for sensor development.

3.4 Discussion

3.4.1 Overview

The selection of novel aptamers for the development of biosensors is a growing field. However, the selection of aptamers against small molecule targets is complex, facing a variety of challenges including small molecule immobilization and solubility. From 1990 (when the concept of *in vitro* aptamer selection was first published) through 2012, only 38 small molecule binding aptamers were published - mainly against highly soluble antibiotics [112]. As new SELEX methods were developed and optimized, the rate of SELEX success against small molecule targets improved, though it remains low [106]. This chapter describes the methods and results of two different SELEX protocols attempted against three small molecule antimalarial drug targets over the course of several years. As this work was performed in laboratories without previous experience in aptamers or aptamer selection, most the methods described in this chapter were adopted from the literature. Most of the techniques were learned through advice from authors and colleagues, failed attempts, and multiple repeats.

3.4.2 SELEX

The first SELEX method targeting lumefantrine binding aptamers was unsuccessful. None of the tested sequences showed any binding affinity to lumefantrine via ITC or Biacore SPR analysis. Upon initial review of the sequencing data from intermediate and final libraries of the SELEX LF1 and LF2 experiments, the trend towards enrichment was encouraging. However, after testing several enriched sequences and comparing enrichment to that observed in the SELEX PQ1, PQ2, and MQ1 experiments, it is hypothesized that the level of enrichment from the LF SELEX experiments could be attributed to a loss of diversity due to library handling or biases such as PCR bias or immobilization bias (more structured sequences may

not immobilize to the solid support as easily and are more likely to be lost in wash steps). After the results of the lumefantrine SELEX experiments proved fruitless, it was determined that before repeating SELEX, a method to track SELEX progress was needed. The lumefantrine SELEX had been performed blind, without tracking the library evolution to know when sufficient SELEX cycles had been performed to effectively identify sequences enriched for target binding. It is believed that the stringency of the lumefantrine SELEX experiments required more SELEX cycles to improve enrichment. It was at this time that the Biacore assay to track binding affinity of intermediate libraries was devised and tested with the kanamycin model aptamer.

Also, after this failed SELEX attempt, the survey described in Chapter 2 was conducted. This survey provided feedback on realistic applications of an aptamer-based antimalarial drug detection assay, on drug targets to prioritize, and it provided motivation to continue aptamer selection attempts. In 2016, a methods paper [142] was published describing a new protocol for the selection of aptamers against small molecule targets reporting high levels of success. Using this published protocol, several SELEX experiments were performed that successfully identified aptamers against piperaquine and mefloquine. This protocol included a method to track SELEX progress via the small-scale PCR of elution profiles from each cycle. The elution profile method is time consuming and only provides qualitative interpretation of bands on a gel to infer enrichment of the library pools. Thus, the Biacore method developed with the kanamycin model system was tried in conjunction with this protocol. However, as described in the results section, after many attempts to purify enough intermediate library to sequentially immobilize several rounds of aptamer for drug dilution testing, the method was abandoned. Although qualitative and laborious, the small-scale PCR elution profiles did allow for tracking information that effectively reported SELEX progress. Many more rounds of SELEX were performed while using the elution profile tracking method until it was decided that final library pools should be sequenced (>15 rounds for each of the PQ and MQ SELEX experiments, compared to 7 or 8 rounds completed for the LF SELEX

experiments without tracking). It seems clear that with the stringency of the SELEX protocols used in this research, closer to 15-20 rounds was required to achieve enough enrichment to identify binding sequences.

3.4.3 Sequencing

After each SELEX experiment, the final library pools were sequenced and sorted based on enrichment. For SELEX LF1 and LF2, library pools were sequenced via next generation sequencing (NGS) on an Illumina MiSeq system. To do this, the libraries were purified then sent to NIH research technologies branch where they were adapted and sequenced. NGS was appealing since it provides an in depth report of sequence enrichment and can be used to track enrichment across multiple SELEX rounds with little extra effort [146]. The depth of sequencing proved to be important here since the level of enrichment of these pools was so low that enrichment would not have been observed with other sequencing methods. However, sequencing via NGS was very slow (results took roughly 4 months). Alternatively, cloning and Sanger sequencing could provide results in 1-2 weeks. Sanger sequencing was used in the piperaquine and mefloquine SELEX experiments, where SELEX progress was tracked to ensure high levels of enrichment before sequencing. Via Sanger sequencing, only 20-50 clones were sequenced per SELEX experiment (targeting a minimum of 20 sequences). However, as can be seen in the sequence data, the pools were enriched enough so that even with this number of reads, enrichment trends could be observed.

3.4.4 Affinity analysis

After sequencing, the collected sequences from the piperaquine and mefloquine SELEX experiments were sorted using Multalin, a free online software to group similar sequences. The lumefantrine sequences were only sorted based on frequency. From the sorted sequences, several enriched sequences were chosen from each SELEX experiment for further analysis. The lumefantrine sequences were first assessed via ITC. No binding was detected for any of the sequences tested via ITC. However, there

were significant limitations to the ITC experiments including a lack of replicates and lumefantrine solubility concerns. Access to the ITC equipment was limited and during the allotted time, only enough aptamer had been produced to test each sequence once. This, in combination with concerns about lumefantrine solubility during drug injections, led to a desire to repeat testing of several of the sequences. Three of the enriched lumefantrine sequences tested via ITC were re-tested via Biacore SPR. In this method, the potential aptamers were immobilized to a Biacore chip via their biotinylated capture oligo, just as they had been during SELEX. Lumefantrine dilutions were injected over the chip with the goal of detecting a decrease in mass at the surface of the chip as aptamers released their capture oligo to bind target. However, after test injections of several concentrations of lumefantrine showed no difference in drug response between random aptamer library and selected aptamer sequences, the Biacore assay was stopped. Since this Biacore method is different from typical Biacore experiments in which ligand is immobilized to the chip and mass accumulates at the surface of the chip as an analyte binds ligand, it was decided that the method should be validated using a model aptamer system.

A previously published kanamycin aptamer selected from the same starting library as the lumefantrine sequences was obtained to use as a positive control to confirm the accuracy of the method. Repeating the same approach as was used for the lumefantrine sequences, the kanamycin aptamer reported dose a dependent loss of mass at the surface of the chip indicating sequence binding. Following positive initial results, the aptamer was tested against a dilution curve of kanamycin and a K_D was calculated. The calculated K_D was similar to the reported K_D of the kanamycin aptamer (250 µM versus 106 µM) from the literature, within the expected range of variation given that different instruments and drug stocks were used. This validated that the method was suitable, and it was accepted that the tested lumefantrine sequences do not exhibit lumefantrine binding properties.

The binding characteristics of the sequences selected from SELEX PQ1, PQ2, and MQ1 were first assessed via a fluorescent-binding assay. This screening approach was desirable as it reported aptamer binding characteristics and it also confirmed

that the aptamer sequence could be successfully adapted to a sensing platform. To create the fluorescent sensor, the SELEX capture oligo was converted to a quencher oligo by replacing the 3' biotin used for immobilization with a 3' quencher (in this case, DAB) and the aptamer to be tested was labeled with a 5' fluorophore (in this case, FAM). Next, an optimal ratio of aptamer:quencher was determined, as described in the results section. Both 13mer and 14mer quencher strands were tested at various concentrations to determine a combination in which about 80-90% of the fluorescent signal was quenched. Stronger quenching decreases assay sensitivity while weaker quenching results in high background. The quencher length and ratio can be optimized for different sensor applications but for this initial fluorescent-binding assay, a quenching of 80-90% was targeted. After quenching optimization, the sensors (aptamer and capture mixtures) were tested with dilutions of positive and negative drug targets to identify aptamers with the best sensitivity and specificity.

The initial results of testing the PQ1 sequences revealed that the most promising aptamer (18.18) had significant cross-reactivity to amodiaquine and its active metabolite desethylamodiaquine at physiologically relevant concentrations. For this SELEX experiment, chloroquine had been the only negative selection target used as a representative quinoline compound. The hope was that this would remove sequences that nonspecifically bound the quinoline moiety and would be sufficient to promote specificity to piperaquine. However, this did not appear to be the case. It was determined that the SELEX should be repeated using both chloroquine and amodiaquine as negative selection targets. Additionally, SELEX PQ1 had used molecule 190 as the positive selection target. Molecule 190 is half of the symmetrical piperaquine molecule and was synthesized to serve as a piperaquine target with improved solubility. It was hypothesized that sequences selected against molecule 190 would also bind the full piperaquine molecule and that perhaps two aptamers would bind each piperaquine molecule, increasing the sensitivity of the sensor and avoiding the solubility issues of the full piperaquine molecule. However, as shown in Figure 3.3, aptamer 18.18 had a much higher binding affinity to 190 than to full piperaquine. The reason for this is not entirely understood but it is hypothesized

that steric hindrance of the full molecule limits access of bases involved in aptamer binding. In an attempt to address these two issues, as well as the sensor's poor function in serum (described in Chapter 4), piperaquine selection was repeated (SELEX PQ2). This selection included choloroquine, amodiaquine, and diluted human serum in the negative selection steps and used the full piperaquine molecule (at lower concentrations due to solubility issues) as the positive target.

Selection against mefloquine followed the optimized conditions of SELEX PQ2, including all of the same negative selection targets. The resulting sequences from SELEX PQ2 and MQ1 were assessed via the fluorescent-binding assay and aptamers PQ4 and MQ2 were identified as the most promising sequences. To further characterize these aptamers, their binding affinity to drug targets and to their quencher strands was assessed via Biacore.

The fluorescent sensor curves are affected by both the aptamer binding affinity to its target as well as its affinity to the quencher oligo. Simply calculating a K_D of the fluorescent-binding curve would not accurately represent the K_D of the aptamer-drug interaction. The binding affinity of each aptamer directly to target and directly to its quencher strand were measured independently via Biacore SPR. Both aptamers reported a K_D to their capture oligos in the range of 80-130 nM. It makes sense that they would both be similar since the binding interaction measured in this experiment is between the same 13 complementary bases for each aptamer.

Analysis of the PQ4 and MQ2 aptamers to their drug targets revealed high affinity binding of both aptamers. The PQ4 aptamer has a higher target-binding affinity than the MQ2 aptamer, 1.78 nM and 57.1 nM respectively. This can be observed in the reported kinetic and binding parameters in Tables 3.30 and 3.31, the raw sensorgram data in Figures 3.33 and 3.34, and the sensor results in the following chapters.

3.4.5 Limitations and conclusion

A main limitation in this chapter was the inability to isolate lumefantrine binding aptamers. In the future, it would be nice to repeat the optimized SELEX method used for piperaquine and mefloquine for other antimalarial drugs of interest. Several

years were spent learning SELEX protocols, including the need for tracking library evolution during SELEX, and determining optimal methods to characterize selected aptamers. Now, these procedures could be repeated with new target molecules without much need for re-optimization. Developing a suite of antimalarial drug binding aptamers would likely improve the utility of the aptamer sensors.

In conclusion, after thorough literature searches and advice from authors (especially Kyung-Ae Yang), aptamers to both piperaquine and mefloquine were successfully selected. The sensitivity and specificity of these aptamers were screened via multiple techniques, reporting satisfactory binding characteristics. The most promising aptamers selected in this chapter were carried forward to Chapter 4 for sensor development.

4

Fluorescent Sensor Development

Contents

4.1 Introduction 110
4.1.1 Chapter 4 aims 111
4.2 Methods 111
4.2.1 Characterization of tablet sensors 112
4.2.2 Sensor function in serum versus buffer 115
4.2.3 Serum sensor troubleshooting 116
4.2.4 Characterization of serum sensors 125
4.3 Results 127
4.3.1 Characterization of tablet sensors 127
4.3.2 Sensor function in serum vs. buffer 132
4.3.3 Serum sensor troubleshooting results 134
4.3.4 Characterization of serum sensors 143
4.4 Discussion 153
4.4.1 Overview 153
4.4.2 Tablet sensors 154
4.4.3 Serum optimization 155
4.4.4 Serum sensors 156
4.4.5 Limitations and conclusion 158

4.1 Introduction

The goal of the work described in this chapter is to convert the piperaquine and mefloquine binding aptamers discovered in Chapter 3 into sensors with an easily

measurable readout reporting target concentration. Two applications of the sensors were tested and characterized, one designed for use with crushed tablets and one designed for use with human serum or plasma samples.

The clinical needs assessment survey described in Chapter 2 led to the development of two target product profiles. The target product for which there was more reported interest was a quantitative or semi-quantitative lab-based assay to allow local researchers in malaria endemic countries to measure ACT partner drugs from patient samples or from crushed tablets. This assay would ideally require only standardized lab equipment and use inexpensive materials and consumables. It could require access to a centrifuge for sample preparation and a fluorimeter for sample measurements. The second target product was a disposable, colorimetric, rapid assay to measure ACT partner drugs from finger stick blood samples in malaria clinics. This assay would require that all sample preparation be performed on the rapid assay and that the readout be visible by eye without the need for benchtop equipment. Development and optimization of the lab-based assay format was prioritized as the focus of this research. This chapter describes the experimental methods for optimizing the sensor function in buffer, optimizing the sensor function in human serum, and characterizing the optimized sensors for the analysis of both crushed tablets and human samples.

4.1.1 Chapter 4 aims

1. Optimize and characterize piperaquine and mefloquine aptamer tablet sensors.
2. Troubleshoot and optimize piperaquine and mefloquine aptamer serum sensors.
3. Characterize sensor function with crushed tablets and human samples.

4.2 Methods

The most promising aptamers from several SELEX experiments (aptamers PQ4 and MQ2) were characterized in Chapter 3 and have been carried forward for sensor development in this chapter. First, the sensor function against drug dilutions

Tablet sensors	
Piperaquine (PQ4)	
Aptamer	5'-FAM- CTCTCGGGACGACCACACGCTAGTTGCGCCGAATGGCCGTGAAAGTCGTCCC -3'
Quencher	5'-GGT CGT CCC GAG AG-DAB-3'
Ratio	1:5
Mefloquine (MQ2)	
Aptamer	5'-FAM- CTCTCGGGACGACGGCAGTCTATACCCCGTATCGCCGAAGGTTGTCGTCCC -3'
Quencher	5'-CGT CGT CCC GAG AG-DAB-3'
Ratio	1:5

Table 4.1: Tablet sensors. Details of the piperaquine and mefloquine tablet sensor components. Sensor solutions were prepared in selection buffer then mixed 1:1 with sample.

in buffer was characterized to report the potential of the assay to measure drug content of crushed tablets. For the tablet sensor, the most promising piperaquine aptamer (PQ4) and mefloquine aptamer (MQ2) were labeled with a FAM fluorophore and 14 base capture molecules were tagged with DAB quenchers (shown in Table 4.1). The 14mer quenchers were used instead of the 13mer quencher in order to maximize specificity. The range of detection and specificity of the tablet sensors are reported in this chapter.

Next, the PQ4 and MQ2 aptamer sensors were tested in drug-spiked human serum to assess the assay capacity to detect drugs from patient samples. Many optimization attempts are reported in this chapter. In the final optimized sensors, the PQ4 and MQ2 aptamers were labeled with an Alexa647 fluorophore and 13 base quencher molecules were tagged with Iowa Black (IAB) quenchers (shown in Table 4.2). The optimization of the assay in serum and characterization of the final sensor are described in this chapter. The sequences described in Tables 4.1 and 4.2 are referred to throughout this chapter as tablet sensors and serum sensors, respectively.

4.2.1 Characterization of tablet sensors

Based on the aptamer and quencher characterization in the previous chapter, 14mer quenchers were selected for use in the final tablet sensor components. Since genuine crushed tablets contain large amounts of drugs, the sensitivity of the sensor was not a concern and the tablet sensors were optimized instead for specificity. The 14mer quencher resulted in increased specificity but decreased sensitivity in

Serum sensors	
Piperaquine (PQ4)	
Aptamer	5'-ALEXA-CTCTCGGGACGACCACACGCTAGTTGCGCCGAATGGCCGTGAAAGTCGTCCC-3'
Quencher	5'-GTC GTC CCG AGA G-IAB-3'
Ratio	1:10
Mefloquine (MQ2)	
Aptamer	5'-ALEXA-CTCTCGGGACGACGGCAGTCTATACCCCGTATCGCCGAAGGTTGTCGTCCC-3'
Quencher	5'-GTC GTC CCG AGA G-IAB-3'
Ratio	1:5

Table 4.2: Serum sensors. Details of the piperaquine and mefloquine serum sensor components. Sensors were prepared in selection buffer and mixed 1:1 with diluted serum samples.

initial characterization experiments. Since aptamers were selected in a buffer in which dissolved tablets could be prepared (PBS, 2 mM $MgCl_2$, and low solvent concentrations), no optimization of matrix effects was required for the tablet sensors. The optimal sensors, listed in Table 4.1 are characterized to report their functional range and cross-reactivity in this section.

Sensor functional range

To assess the functional range of both the PQ4 and MQ2 tablet sensors, standard curves of piperaquine and mefloquine were prepared in selection buffer. Sensor solutions of PQ4 and MQ2 were prepared according to Table 4.1, heated in boiling water for five minutes, cooled to room temperature, and combined 1:1 with the drug dilutions (40 µL sensor + 40 µL sample). After 30 minutes of equilibration, the sample was transferred (75 µL) to a Corning black flat bottom 384 well plate and read at ex/em: 485/538. The functional range of the sensors, limits of detection (LOD), and limits of quantification (LOQ) are described in the results section.

Cross-reactivity

To assess cross-reactivity, the PQ4 and MQ2 sensor response to nine potentially cross-reactive compounds expected to be found in genuine or falsified antimalarial tablets was measured. These included other commonly used antimalarial drugs, acetaminophen, and calcium carbonate and corn starch which are tablet fillers. Stock solutions of these compounds were prepared according to Table 4.3. Serial dilutions

Compound	Concentration	Solvent
Piperaquine	535.5 µg/mL	5% MeOH/ H_2O
Mefloquine	378.3 µg/mL	2% MeOH/ H_2O
Chloroquine	1 mg/mL	H_2O
Amodiaquine	1 mg/mL	MeOH
Desethylamodiaquine	1 mg/mL	MeOH
Lumefantrine	1 mg/mL	MeOH
Primaquine	1 mg/mL	DMSO
Carboxyprimaquine	1 mg/mL	DMSO
Dihydroartemisinin	1 mg/mL	DMSO
Acetaminophen (paracetamol)	1 mg/mL	H_2O
Calcium carbonate	1 mg/mL	H_2O, 0.05M HCl
Corn starch	1 mg/mL	H_2O, heated

Table 4.3: Stock solutions of compounds for testing sensor cross-reactivity. The drugs were tested against both the tablet and the serum sensors. The metabolites were tested against the serum sensor only and the calcium carbonate and corn starch were tested against the tablet sensor only. Lumefantrine, amodiaquine, desethyl-amodiaquine, primaquine, carboxyprimaquine, and chloroquine were obtained as reference stocks from the WorldWide Antimalarial Resistance Network (WWARN) malaria drug reference material programme. Piperaquine (cat. no. C7874), mefloquine (cat. no. M2319), dihydroartemisinin (cat. no. D7439), acetaminophen (cat. no. A7085), calcium carbonate (cat. no. C6763), and corn starch (cat. no. S9679) were obtained from Sigma Aldrich. The purity of all compounds and standards was reported to be $\geq$ 98% with the exception of dihydroartemisinin ($\geq$ 97%) and corn starch (purity not specified).

(10,000 ng/mL to 20 ng/mL) of drug compounds in Table 4.3 (not including their metabolites), calcium carbonate, and corn starch were prepared in selection buffer. The sensors were prepared as previously described, mixed 1:1 with the compound dilution curves and read at ex/em: 485/538. The resulting cross-reactivity curves are shown in the results section.

Testing a crushed tablet

In order to confirm that the aptamer sensors can detect desired compounds from crushed tablets, a Eurartesim tablet (40 mg DHA/320 mg piperaquine tetraphosphate) was provided by NIH colleagues in Cambodia who obtained excess, expired research material from the Armed Forces Research Institute of Medical Sciences (AFRIMS) in Bangkok, Thailand. The tablet was manufactured by Sigma-Tau, Rome, Italy, Batch no. 150728, Mfg date: 06/2015, Exp. date: 05/2017). Note: the tablet was expired by the time it was obtained and tested (03/2019). Although this testing concerned the piperaquine component of the tablets, it should also be

noted that formulations of dihydroartemisinin with piperaquine have been shown to be particularly unstable in current preparations. Recent studies have reported dihydroartemisinin content falling below acceptable levels for active ingredients before shelf-life limits and suggest that the chemical instability of dihydroartemisinin make it an unsuitable artemisinin derivative for use in current preparations [147].

The tablet was crushed and dissolved following a previously published protocol for tablet quality testing [148]. The tablet was crushed using a mortar and pestle, transferred to a large volume flask, and dissolved in water, 2.5% MeOH, 12.5 µM HCl to a piperaquine concentration of 0.5 mg/mL. Due to the presence of insoluble tablet components, the dissolved tablet solution was non-homogenous with visible precipitates. An aliquot of the supernatant was collected, centrifuged to remove precipitates, and this stock was then further diluted to prepare a standard curve of predicted piperaquine concentration ranging from 5,000 ng/mL to 20 ng/mL. This was run against a laboratory prepared piperaquine standard curve to assess piperaquine content.

4.2.2 Sensor function in serum versus buffer

After initial testing in buffer, the performance of the 18.18, PQ4, and MQ2 aptamer sensors was assessed in drug spiked serum. Pooled human serum (Interstate Blood Bank, Memphis, TN) was stored at -80°C and thawed the day of testing. Drug dilutions were prepared by spiking drug stocks into the human serum in the range of 10,000 ng/mL to 20 ng/mL. Drug dilutions in selection buffer were prepared alongside serum dilutions for comparison. The buffer and serum drug dilutions were then incubated at 37°C for 30 minutes to allow protein and drug in serum samples to incubate at relevant *in vivo* binding conditions and then cooled to room temperature. Sensor solutions were prepared at the optimal conditions found in Chapter 3 (18.18 and MQ2 with 13mer quenchers at an aptamer:quencher ratio of 1:5 and PQ4 with a 13mer quencher at an aptamer:quencher ratio of 1:10). The sensor solutions were incubated in boiling water for five minutes and then cooled to room temperature. Once both the serum drug dilutions and the sensor solutions

were cooled to room temperature, they were combined 1:1 (40 µL sensor solution + 40 µL serum drug dilution), allowed to equilibrate for 30 minutes, and then 75 µL were transferred to a 384 black Corning flat bottom plate and read at the FAM optimized excitation/emission wavelength (485/538). All conditions were tested in triplicate. Aptamer 18.18 sensor results are included here because it was the first aptamer sensor tested in serum. Poor 18.18 sensor function in serum contributed to the decision to repeat SELEX PQ1 and to include diluted serum as a negative selection step in the subsequent selections (SELEX PQ2 and MQ1). All optimization of sensor function in serum described in the following sections was performed only with aptamers PQ4 and MQ2.

4.2.3 Serum sensor troubleshooting

This section describes attempts to optimize sensor function in serum. Aptamers PQ4 and MQ2 were tested under various conditions to study and improve sensor function in serum. It was hypothesized that the most likely causes of inhibited sensor function in serum compared to buffer were either fluorescent interference (quenching of serum proteins leading to decreased signal and/or serum protein autofluorescence leading to increased background) or drug-protein interactions that required the aptamer to compete with proteins to bind drug targets. The following tests aimed to elucidate the reasons for inhibited sensor function in serum and identify modifications to improve it.

Measuring the effects of serum carrier proteins

It has been reported that piperaquine and mefloquine are more than 90% bound to the serum proteins human serum albumin (HSA) and alpha-acid glycoprotein (AGP) *in vivo* [149–151]. This led to the hypothesis that competition to bind drug between aptamer and serum proteins may be contributing to the decreased sensor response observed in serum. Typical serum concentrations of HSA and AGP in malaria infected patients were found in the literature [152]. Typical serum concentrations of IgG [153] were used as a control for the effect of protein not

Protein	Physiologically relevant range
Human Serum Albumin (HSA)	30-50 mg/mL
Alpha-Acid Glycoprotein (AGP)	0.8-2 mg/mL
Gamma Globulin IgG	5-20 mg/mL

Table 4.4: Physiologically relevant ranges of proteins of interest as reported in the literature [152, 153]. HSA and AGP reportedly bind both piperaquine and mefloquine while IgG does not. All three proteins were obtained from Sigma Aldrich (HSA ($\geq$ 98% purity) cat. no. SRP6182, AGP ($\geq$ 99% purity) cat. no. G9885, IgG ($\geq$ 95% purity) cat. no. I4506).

anticipated to bind to piperaquine or mefloquine. These ranges are shown in Table 4.4. With the hope of better understanding the effects of these serum proteins on sensor function, the proteins were spiked into selection buffer to isolate their effects from the rest of the serum components.

Stock solutions of the maximum physiological concentration of each protein were prepared in selection buffer. These stock solutions were then serially diluted throughout the physiologically range for each protein. The protein dilutions were spiked with either piperaquine (0.5 µM) or mefloquine (2.5 µM) from drug stocks in Table 4.3. These drug concentrations were selected since they provide a high signal response in buffer for each sensor and would thus allow for the observation of signal inhibition. The drug/protein solutions were then incubated at 37°C for 30 minutes to mimic *in vivo* protein binding conditions and then cooled to room temperature. PQ4 and MQ2 sensors were prepared as previously described. The sensor solutions and drug/protein dilutions were then combined 1:1 (40 µL sensor + 40 µL sample), allowed to equilibrate for 30 minutes, and then transferred (75µL) to a Corning black flat bottom well plate and read at ex/em: 485/538. All conditions were tested in triplicate.

Adjusting pH

According to previous reports, varying serum pH can alter the fluorescent profile of serum proteins [154]. It was hypothesized that varying pH could reduce interference from protein autofluorescence and/or alter the binding efficiency of drug to plasma proteins, releasing more drug into serum to be bound by aptamer. With the hope

Sample Type	Serum																			
pH	6.5				7				7.75 (unaltered)				8				8.5			
[PQ] µM	0	0.1	0.25	2.5	0	0.1	0.25	2.5	0	0.1	0.25	2.5	0	0.1	0.25	2.5	0	0.1	0.25	2.5
Sample Type	Selection Buffer																			
pH	6.5				7				7.25 (unaltered)				8				8.5			
[PQ] µM	0	0.1	0.25	2.5	0	0.1	0.25	2.5	0	0.1	0.25	2.5	0	0.1	0.25	2.5	0	0.1	0.25	2.5

Table 4.5: Samples prepared to test the effect of pH on sensor function in serum and in selection buffer. Each sample and pH condition was tested with three piperaquine concentrations and a blank. Each condition was tested in triplicate.

of identifying a pH at which the aptamer sensor maintains function, but the serum effects are reduced, sensor function was assessed in drug spiked serum and buffer samples with altered pH. The PQ4 piperaquine sensor was tested at varying pH conditions first, with the intent of repeating the experiment with the mefloquine sensor if results appeared promising. The pH of human pooled serum (Interstate Blood Bank, Memphis, TN) and buffer were measured using pH strips (Healthywiser, Santa Monica, CA) rather than a pH meter in order to conserve sample. To estimate the final pH of serum under sensor conditions, the serum was diluted 1:1 in selection buffer before applying to the pH strips and the serum pH was measured to be 7.75. The unaltered pH of selection buffer was measured to be 7.25. Aliquots of serum and selection buffer were then adjusted to pH 6.5, 7, unaltered, 8, and 8.5 by the addition of 1N HCl or 1N NaOH, measured using pH strips. Serum and buffer samples from each pH group were spiked with piperaquine stock to create final concentrations of 0 µM, 0.1 µM, 0.25 µM, and 2.5 µM piperaquine as shown in Table 4.5.

Each drug concentration at each pH condition was incubated at 37°C for 30 minutes and cooled to room temperature. PQ4 sensor was prepared in selection buffer from 100 µM frozen oligonucleotide stocks. The sensor solution was incubated in boiling water for five minutes, then cooled to room temperature in the dark. Sensor solution was combined with each of the prepared samples from Table 4.5 (40 µL sensor + 40 µL sample), allowed to equilibrate for 30 minutes in the dark

and then transferred (75 µL) to a Corning black flat bottom 384 well plate and read at ex/em: 485/538. All conditions were tested in triplicate.

Adding surfactant/solvent

It was hypothesized that adding small amounts of surfactant or solvent to drug spiked serum may improve sensor function in serum by disrupting interactions between drug and serum proteins and releasing more drug into solution to be bound by the aptamer sensor. To test this, sodium dodecyl sulfate (SDS) and dimethyl sulfoxide (DMSO) were added to serum in low concentrations so as not to interfere with aptamer folding or binding characteristics.

First, SDS (Sigma Aldrich cat. no. 436143) was spiked into serum aliquots to prepare 0.05% SDS and 0.2% SDS. Drug dilutions of piperaquine and mefloquine were prepared in the two SDS conditions along with a serum control. Both piperaquine and mefloquine sensors were tested under these surfactant conditions to assess any differences in the effects on the two drugs. Serial dilutions of piperaquine and mefloquine in serum or serum/SDS were prepared.

Next, serum aliquots were spiked with DMSO (Sigma cat. no. D8418) to prepare solutions of 2% DMSO and 5% DMSO in serum. Drug dilutions of piperaquine and mefloquine were prepared in the DMSO conditions and the serum control.

PQ4 and MQ2 sensor solutions were prepared from frozen oligonucleotide stocks, incubated in boiling water for five minutes, and allowed to cool to room temperature. The sensor solutions and drug dilutions were then combined 1:1 (40 µL sensor + 40 µL sample), allowed to equilibrate for 30 minutes, and then transferred (75µL) to a Corning black flat bottom well plate and read at ex/em: 485/538. All conditions were tested in triplicate.

Increasing the sensor concentration

Throughout sensor characterization, sensor solutions were prepared at an aptamer concentration of 100 nM and a quencher concentration of typically 10x or 5x this aptamer concentration. For measurement, this sensor solution was mixed 1:1 (40 µL sensor + 40 µL sample) and fluorescent output was measured at a

final aptamer concentration of 50 nM. It was hypothesized that perhaps increasing the concentration of the sensor components would improve sensor readout. If sensor function is inhibited by competition with drug binding serum proteins, then a higher concentration of aptamer may be able to shift the equilibrium to allow more aptamer-drug binding without significantly increasing the background due to free, unbound aptamer.

To measure this, PQ4 and MQ2 sensor solutions at concentrations of 100 nM aptamer and 1 µM quencher were prepared from frozen oligonucleotide stocks as 1x standard sensor controls. PQ4 and MQ2 sensor solutions at concentrations of 200 nM aptamer and 2 µM quencher were prepared from frozen oligonucleotide stocks as a 2x sensor condition and at concentrations of 400 nM aptamer, 4 µM quencher as a 4x sensor condition.

Piperaquine and mefloquine dilutions in human pooled serum were prepared from frozen serum pools as previously described in Section 4.2.2. Serum drug dilutions were combined 1:1 (40 µL sensor + 40 µL sample) with each of the sensor conditions, allowed to equilibrate for ∼30 minutes, and then transferred (75µL) to a Corning black flat bottom well plate and read at ex/em: 485/538. All conditions were tested in triplicate.

Serum dilutions

It was hypothesized that simply diluting serum samples prior to mixing with sensors would decrease the serum effects enough to improve sensitivity. However, in diluting the serum samples, the drug content of the samples is diluted as well. To test this, drug dilutions of both piperaquine and mefloquine were prepared in pooled human serum as previously described. Samples from each concentration of both curves were left undiluted, diluted 1:3 in selection buffer (PBS, 2 mM $MgCl_2$), or diluted 1:5 in selection buffer. Dilution curves of mefloquine and piperaquine were prepared from the same drug stocks in selection buffer as a reference. All three serum dilution condition samples and buffer samples were incubated at 37°C for 30 minutes and then cooled to room temperature. Serum drug dilutions were combined 1:1 (40 µL sensor

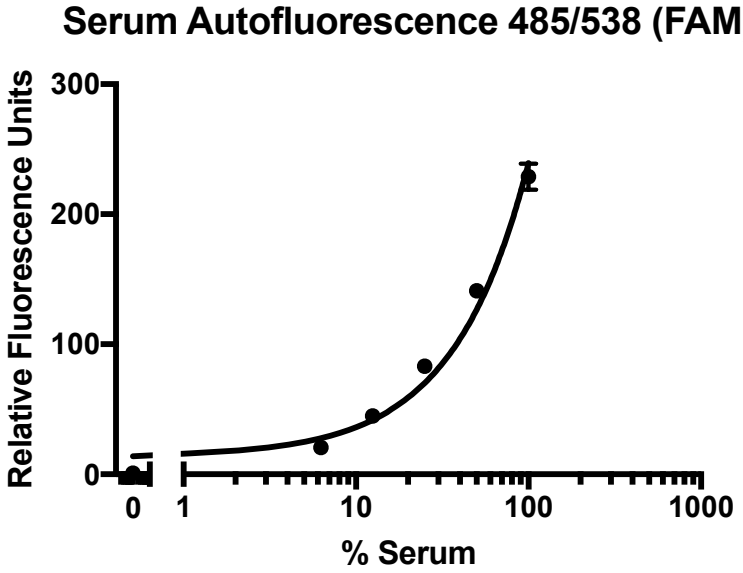


Figure 4.1: Serum autofluorescence at FAM ex/em wavelengths. At the typical serum concentration of 50% (which is the serum concentration after 1:1 mixing of sample with sensors) the background fluorescence (relative fluorescence units(RFU) is between 100 and 200 RFU. This suggests that the majority of increased background observed with the sensor in serum samples could be attributed to autofluorescence of proteins rather than nonspecific binding to serum proteins.

+ 40 µL sample) with each of the PQ4 and MQ2 sensors, allowed to equilibrate for 30 minutes, and then transferred (75µL) to a Corning black flat bottom well plate and read at ex/em: 485/538. All conditions were tested in triplicate.

Higher wavelength fluorophores

According to the literature, the autofluorescence and absorbance of many serum proteins are highest in the range of about 300-500 nm [154]. To assess serum autofluorescence that could contribute to high sensor background, the fluorescent response of serum dilutions in the absence of sensor was measured at the FAM excitation/emission wavelengths. Pooled human serum was serially diluted 4x in selection buffer and the fluorescent response at ex/em: 485/535 is shown here in Figure 4.1.

It was believed that serum protein autofluorescence and quenching of the fluorophore emission wavelength via protein absorption may be largely responsible for hindering sensor function in serum as compared to selection buffer. Thus, a

Fluorophore	Reported ex/em λ (nm)	Quencher	Quencher range (nm)
PQ4_FAM	485/535	13mer_Dabcyl	346-489 (max@479)
		13mer_Black hole Q1	480-580 (max@534)
PQ4_TYE563	549/563	13mer_Black hole Q2	560-670 (max@578)
PQ4_Cy5	648/668	13mer_Iowa Black-RQ	570-690 (max@656)
PQ4_Alexa647	645/665	13mer_Iowa Black-RQ	570-690 (max@656)

Table 4.6: Higher wavelength fluorophores and quenchers. New fluorophores were tested with selected quenchers whose absorbance range match their emission wavelengths. The FAM sensor was retested with the black hole quencher1 and compared to previous function where dabcyl (DAB) was used as the quenching molecule. New fluorophore-tagged aptamer sequences and quencher strands were synthesized and HPLC purified by IDT.

fluorophore with an excitation and emission wavelength in the 300-500 nm range would be more susceptible to interference due to the intrinsic autofluorescence of proteins, as well as interference due to the absorption of the excitation and emission signal by proteins in the matrix. The FAM fluorophore was originally chosen for sensor development due to previous reported success with this fluorophore [142]. The FAM fluorophore has obvious benefits such as a large Stokes shift and low cost. However, the excitation/emission wavelengths of 485/538 may not be ideal for minimizing serum protein effects.

Several new fluorophores and corresponding quenchers were selected for testing based on cost, excitation/emission wavelength, and Stokes shift (Table 4.6). In order to reduce costs during testing, the PQ4 sensor was first tested with new fluorophores with the plan to subsequently test the MQ2 sensor with new fluorophores if they improved PQ4 sensor function in serum.

First, the excitation/emission wavelength for each new fluorophore was optimized for our fluorimeter following the manufacturer's instructions. To maximize sensor sensitivity and decrease background effects, excitation and emission wavelengths should be optimized for each fluorimeter. Fluorophore labeled aptamer solutions were prepared in selection buffer at the typical final sensor concentration (50 nM). For each fluorophore, an excitation scan was performed from 30 nm below to 30 nm above the published excitation wavelength in increments of 1 nm while the emission

Fluorophore	Optimized ex/em λ (nm)	Cutoff filter (nm)
PQ4_FAM	485/538	515
PQ4_TYE563	537/567	550
PQ4_Cy5	642/672	665
PQ4_Alexa647	643/674	665

Table 4.7: Fluorimeter settings. Optimized excitation and emission wavelengths for higher wavelength fluorophores and quenchers. Conditions were optimized on a Molecular Devices Spectramax 190 microplate instrument, NIAID, Rockville, MD.

wavelength was held at the fluorophore's reported emission wavelength. From this scan, the excitation wavelength resulting in the peak RFU was recorded. Next, an emission scan was performed from 50 nm below to 50 nm above the reported emission wavelength in increments of 2 nm, with the excitation wavelength held constant at the previously determined optimal wavelength. From this second scan, the emission wavelength that resulted in the peak RFU was recorded. Lastly, the instrument's available cutoff filters that were between the selected excitation and emission wavelengths were applied for each fluorophore and the filter that provided the highest signal/noise ratio was selected. The optimized conditions are reported in Table 4.7.

Next, the new fluorophore sensors were optimized for ratios of aptamer:quencher as described previously for the FAM labeled aptamers and DAB labeled quenchers. Here only 13mer quenchers were assessed first.

Each fluorescently labeled aptamer sequence was tested with dilutions of the appropriate 13mer quencher to identify aptamer:quencher ratios that provided sufficient quenching of the fluorophore upon hybridization of aptamer and quenching strand. Stock solutions (100 µM) of the IDT synthesized fluorophore-labeled aptamer and quencher-labeled capture strands were prepared in DNAse/RNAse free water. A 100 nM solution of fluorophore-labeled aptamer was prepared in selection buffer from the 100 µM stock. A 1 µM quencher solution was prepared in selection buffer from 100 µM stock solutions and serially diluted seven times. These dilutions and a buffer blank were combined with the 100 nM fluorophore labeled aptamer solution

	Final [Aptamer] (nM)	Final [Quencher] (nM)	Ratio
1	50	0	1:0
2	50	7.8125	1:0.156
3	50	15.625	1:0.313
4	50	31.25	1:0.625
5	50	62.5	1:1.25
6	50	125	1:2.5
7	50	250	1:5
8	50	500	1:10

Table 4.8: Quencher optimization conditions for new fluorophores. Each aptamer sensor was tested against a dilution curve of the appropriate 13mer quencher strand. The tested concentrations and aptamer:quencher ratios are reported here.

1:1 (40µL aptamer + 40µL quencher) so that final concentrations of both aptamer and quencher were prepared as shown in Table 4.8.

The combined sensor and quencher mixtures were incubated in boiling water for five minutes, then cooled at room temp. The cooled sensing solutions were transferred (75µL) to a Corning flat bottom black 384 well plate. The dilutions were performed in triplicate and read at the optimal excitation/emission wavelengths for each fluorophore. Ratios of aptamer:quencher strand that provided ∼90% quenching were selected for further sensor analysis.

Next, the optimized sensors were tested in serum and buffer and compared to the original FAM-labeled sensor. Drug dilutions were prepared in pooled human serum and buffer as previously described, incubated at 37°C for 30 minutes, and cooled to room temperature. Sensor solutions were diluted from 100 µM stocks to prepare a 100 nM aptamer solution and corresponding optimized quencher concentration. The sensor solution was incubated in boiling water for five minutes then cooled to room temperature. The sensor solutions and drug dilutions were then combined 1:1 (40 µL sensor + 40 µL sample), allowed to equilibrate for ∼30 minutes, and then transferred (75µL) to a Corning black flat bottom well plate and read at the optimal excitation/emission wavelengths for each fluorophore. All conditions were tested in triplicate.

4.2.4 Characterization of serum sensors

Serum sensor optimization revealed that performance in serum could be significantly improved through diluting the serum 1:5 in buffer and replacing the FAM fluorophore and DAB quencher with an Alexa647 fluorophore and Iowa Black (IAB) quencher. Characterization of these optimized PQ4 and MQ2 sensors is described in this section. The sensors were characterized for their sensitivity, specificity, vulnerability to matrix effects, and were validated against an LC-MS reference standard drug detection method.

Limit of detection and limit of quantification

The limit of detection (LOD) and limit of quantification (LOQ) of both the piperaquine and mefloquine serum sensors were measured as well as their functional range. Blank serum samples were run 20 times with both the piperaquine sensor (PQ4) and the mefloquine sensor (MQ2). For PQ4, a solution of 100 nM PQ4 and 1 µM IAB_13mer was prepared in selection buffer, heated in boiling water for five minutes then cooled to room temperature. For MQ2, a solution of 100 nM MQ2 and 500 nM IAB_13mer were prepared in selection buffer and similarly heated and cooled. Once at room temperature, the sensor solutions were combined 1:1 with the drug dilution curves (40 µL sensor + 40 µL sample), allowed to equilibrate for 30 minutes in the dark and then transferred (75 µL) to a Corning black flat bottom 384 well plate and read at ex/em: 643/674.

The LOD was calculated as the average blank value plus 3x the standard deviation of blank. The LOQ was calculated as the average blank value plus 10x the standard deviation of blank. The plotted LOD and LOQ curves and their values are reported in Section 4.3.4.

Cross-reactivity

The PQ4 and MQ2 sensor response to 10 potentially cross-reactive compounds was assessed. These included commonly used antimalarial drugs and their active metabolites as well as acetaminophen, which is often taken to alleviate antimalarial

Sample name	Piperaquine concentration	Mefloquine concentration
LOQ	50 ng/mL	325 ng/mL
QC1	150 ng/mL	1,000 ng/mL
QC2	1,250 ng/mL	4,500 ng/mL
QC3	2,500 ng/mL	8,000 ng/mL
Hi	10,000 ng/mL	10,000 ng/mL

Table 4.9: Piperaquine and mefloquine quality control samples for accuracy and precision testing. The concentrations span the functional range of each sensor. Each of the five samples was tested in five replicates for four days.

symptoms. Stock solutions of these 10 compounds were prepared according to Table 4.3. The drug and metabolite stocks were spiked into pooled human serum (Interstate Blood Bank, Memphis, TN) and serially diluted from 10,000 ng/mL to around 20 ng/mL. The drug spiked serum samples were then diluted 1:5 in buffer. The sensor solutions were prepared as described for the LOD/LOQ calculations. All samples were tested in triplicate and the results are reported in Section 4.3.4.

Accuracy/Precision testing

To assess the accuracy and precision of the serum sensors, standard curves of both piperaquine and mefloquine were prepared in serum (10,000 ng/mL to 20 ng/mL) as well as five quality control (QC) samples (shown in Table 4.9). The QC sample concentrations ranged from the sensor limit of quantification to an upper limit of the standard curve for both piperaquine and mefloquine. The serum samples were diluted 1:5 in selection buffer, frozen at -80°C, and tested with fresh sensor solutions once per day for four days. Each day an aliquot of the standard curve as well as five replicates of the five quality control samples were thawed and run with the serum sensor as previously described. The inter, intra, and total assay variability was evaluated via an ANOVA test using Graphpad Prism software and reported in the results section.

Matrix effects

All previous sensor characterization had been performed in pooled human serum. To assess the background effects of varying serum samples, serum from five different individuals (Interstate Blood Bank, Memphis, TN) was tested against both the

piperaquine and mefloquine sensor. Serum samples from 10 individuals were diluted 1:5 in selection buffer as usual, and five samples were run against each sensor. The sensors were prepared as previously described. An ANOVA test was performed in Graphpad Prism to identify any significant difference between serum samples.

Validation against LC-MS reference standard

To further assess assay accuracy and to validate the assay results against a reference standard drug detection method, blinded QC samples were prepared by the Mahidol Oxford Research Unit (MORU) Pharmacology lab in Bangkok, Thailand and shipped to the NIH for testing with the aptamer sensor. These samples were also analyzed via LC-MS [78] in the pharmacology reference laboratory in Bangkok. LC-MS analysis was performed by trained technicians following routine procedures. The blinded plasma samples were shipped to the Laboratory of Malaria and Vector Research (LMVR) in Rockville, Maryland for analysis with the aptamer sensor. Samples were prepared and tested by Erin Coonahan. Serum samples were diluted 1:5 in selection buffer and run against either a piperaquine and a mefloquine standard curve. The PQ4 and MQ2 sensors were prepared as previously described. The blinded samples were run in five replicates, and the values of the blinded samples were interpolated from the standard curves. The accuracy of the aptamer assays as compared to LC-MS reference standard are described in the results section.

4.3 Results

4.3.1 Characterization of tablet sensors

Sensor functional range

To characterize the functional range, LOD, and LOQ of the piperaquine and mefloquine tablet sensors, drug dilutions were prepared in selection buffer and run against the tablet sensors as described in the methods sections. The limit of detection of each assay was calculated to be the blank mean value plus 3x the standard deviation of blank. The LOQ of each assay was calculated to be the blank mean value plus 10x the standard deviation of blank. These values are shown in

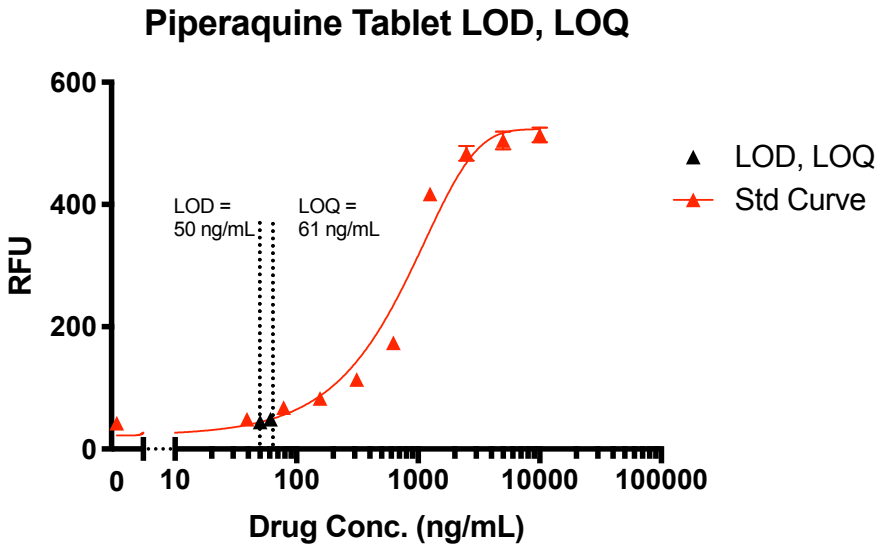


Figure 4.2: Piperaquine tablet sensor LOD and LOQ. The limit of detection and quantification are reported. The functional range of the piperaquine tablet sensor is around 60 ng/mL to 2500 ng/mL. Above 2500 ng/mL, the fluorescence response is saturated and would not allow for accurate quantitation of drug content.

Figures 4.2 and 4.3. The sensor functional ranges were defined to be between the LOQ value and the top of each standard curve (around 60 ng/mL (PQ4) or 300 (MQ2) to about 2500 ng/mL for both sensors). Therefore, to quantitatively assess drug content, tablet solutions should be diluted to target this range of concentrations.

Cross-reactivity

The specificity of tablet sensors was assessed by comparing their response to nine compounds including similarly structured antimalarial drugs, acetaminophen, and tablet fillers. The results are shown in Figures 4.4 and 4.5.

The piperaquine tablet sensor shows very good specificity with no concern for cross-reactivity to the tested compounds. The mefloquine tablet sensor shows cross-reactivity to chloroquine and amodiaquine at high levels. Although the sensor has a much higher response to mefloquine, a falsified tablet that was made from chloroquine or amodiaquine rather than mefloquine could provide a false signal. The response would be much lower than the reported concentration of mefloquine and should still flag any quality assurance testing. It is possible that a falsified tablet with very high chloroquine or amodiaquine content would not be able to be

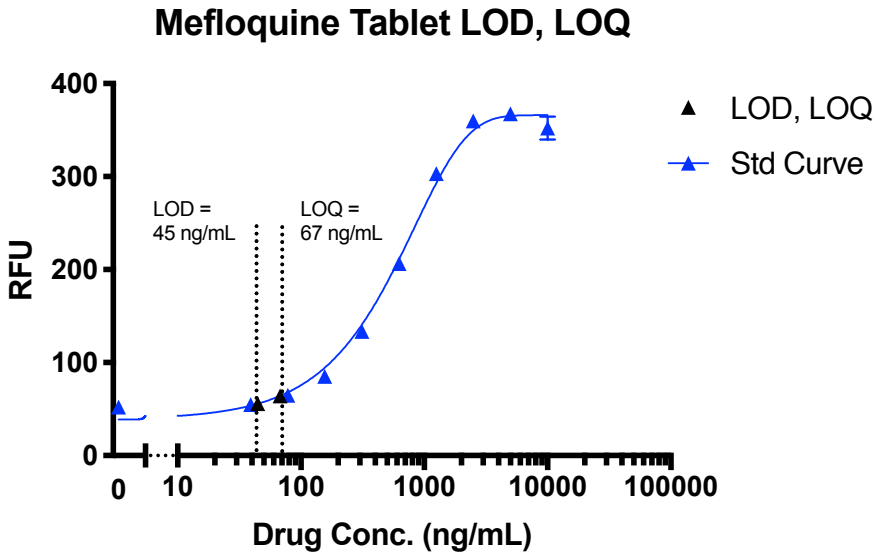


Figure 4.3: Mefloquine tablet sensor LOD and LOQ. The limit of detection and quantification are reported. The functional range of the mefloquine tablet sensor is around 300 ng/mL to 2500 ng/mL.

distinguished from a mefloquine-containing tablet. It seems unlikely that criminals would prepare a falsified mefloquine tablet that instead contained around 3-5x the reported mefloquine concentration of chloroquine or amodiaquine. However, this possibility cannot be ruled out.

Testing a crushed tablet

As described in the methods section, a Euartesim tablet was crushed, dissolved, and assessed with the piperaquine tablet sensor. The dilution curve of the predicted piperaquine concentration from the tablet is compared to the prepared piperaquine standard curve in Figure 4.6.

The measured piperaquine concentration of the tablet dilutions were interpolated from the piperaquine standard curve prepared from drug stock and plotted against the expected piperaquine concentration as reported by the tablet manufacturer (Figure 4.7).

The results of Figure 4.7, in which the aptamer assay found around 15% less piperaquine than reported in the Eurartesim tablet could be due to several factors. First, the discrepancy could be due to tablet solubility. Although a previously

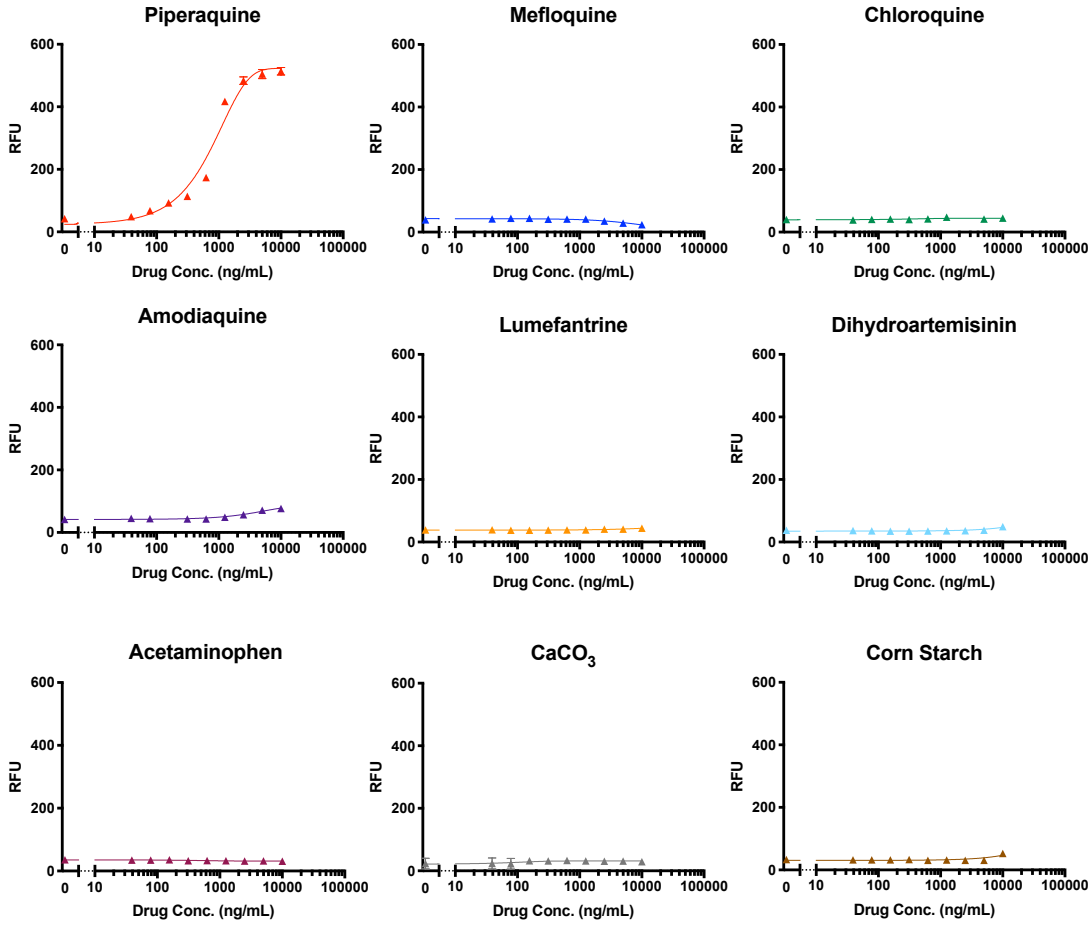


Figure 4.4: Piperaquine tablet sensor cross-reactivity. The piperaquine tablet sensor shows very high specificity. All concentrations were tested in triplicate

published protocol was followed to solubilize the tablet, insoluble contents resulted in a nonuniform solution with visible precipitates. The tablet solution was centrifuged to remove precipitates and the supernatant, which it was assumed contained all the piperaquine content, was tested against the aptamer sensor. Another possible explanation for the discrepancy is that the tablet was expired by two years and could contain less than the reported amount of piperaquine. Lastly, the shift could be due to accuracy of the aptamer assay which could have resulted in around 15% error in absolute values. In order to confirm this, the tablet solution would need to be tested with another reference standard drug detection method such as LC-MS or LC-UV. Without further testing, it is not possible to rule out whether the 15% shift in accuracy is due to incomplete solubilization of the tablet, aptamer assay

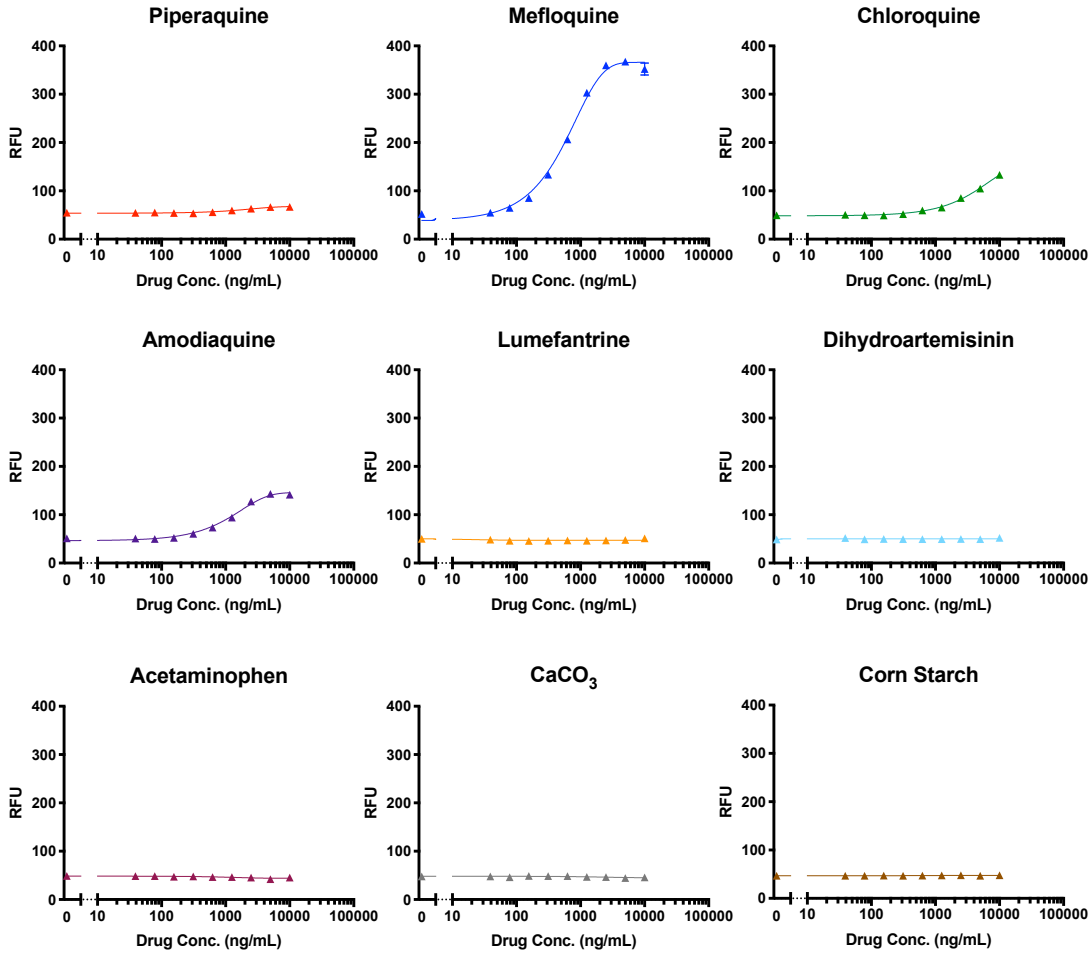


Figure 4.5: Mefloquine tablet sensor cross-reactivity. The mefloquine tablet sensor shows cross-reactivity to amodiaquine and chloroquine at high levels. There is no reported cross-reactivity to other antimalarial drugs or tablet fillers. All concentrations were tested in triplicate.

accuracy, or an actual deviation in reported tablet drug content. However, this experiment confirms that there are no tablet components in the Eurartesim tablets that significantly inhibit sensor function and suggests that the piperaquine tablet sensor could be used to identify falsified tablets. Unfortunately no mefloquine-containing tablets were obtained. Without testing a mefloquine containing tablet it is not possible to confirm the mefloquine sensor's function in real dissolved tablets. However, the positive results with the piperaquine sensor suggest that this sensor format is indeed compatible with crushed tablets.

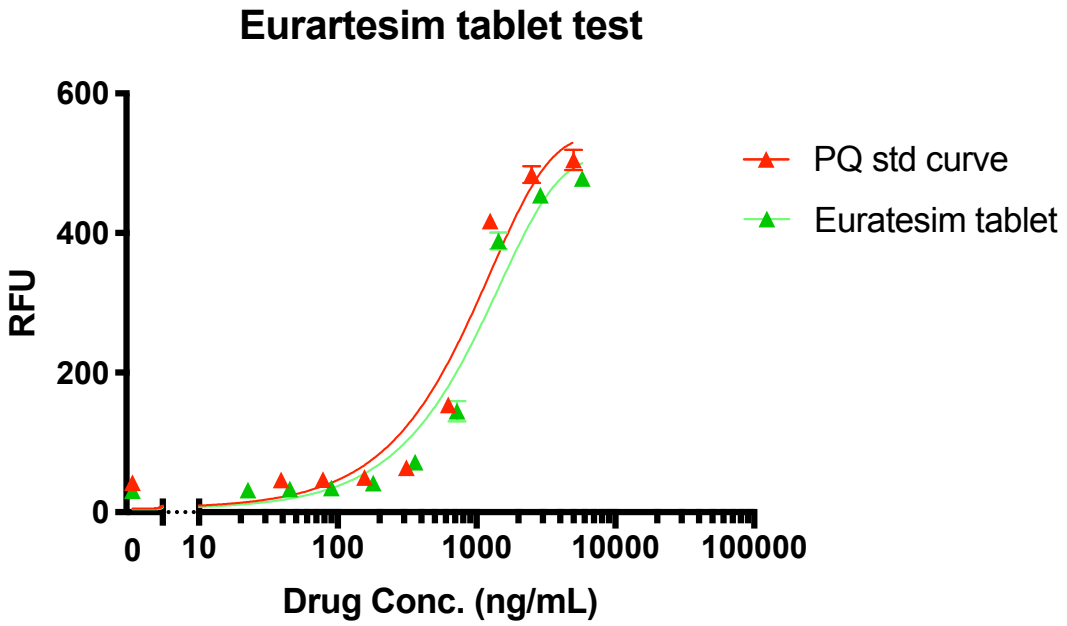


Figure 4.6: Piperaquine crushed tablet (Eurartesim) dilutions. A crushed Eurartesim tablet (40 mg DHA/320 mg piperaquine tetraphosphate) was dissolved and diluted to prepare a standard curve. The Eurartesim standard curve is compared to a piperaquine standard curve prepared from drug stock solution. Misalignment between the two curves represents deviations from the reported piperaquine content of the tablet.

4.3.2 Sensor function in serum vs. buffer

Initial sensor testing in serum

Aptamer sensor 18.18 was the first sensor to be tested in drug spiked serum. Dilutions of drug in selection buffer and serum were prepared and combined with the aptamer sensor at its previously determined quencher length and concentration (13mer quencher at a ratio of 1:5). All conditions were tested in triplicate (Figure 4.8).

The aptamer 18.18 drug response in serum was poor as compared to buffer. The reason for this was not yet understood but one hypothesis was that the aptamer may have cross-reactivity to serum proteins. These results, along with the cross-reactivity to amodiaquine and desethylamodiaquine exhibited by aptamer 18.18, and the lower response to whole piperaquine as compared to molecule 190 led to the decision to repeat SELEX PQ1. SELEX PQ2 was performed using whole piperaquine as positive target, including both amodiaquine and chloroquine as negative selection

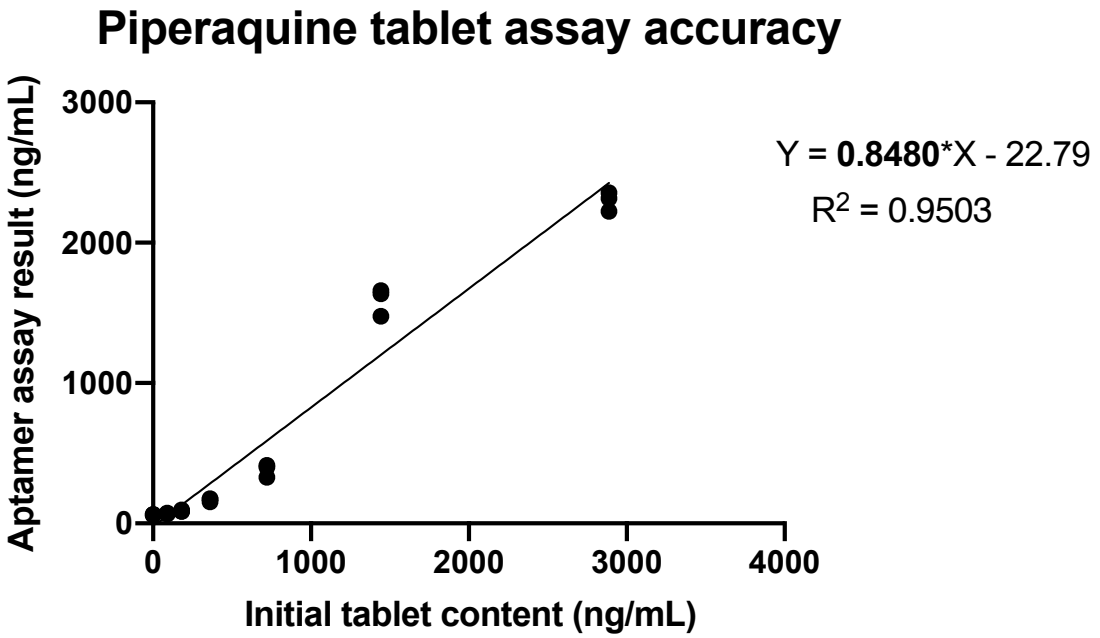


Figure 4.7: Test of piperaquine crushed tablet (Eurartesim, 40 mg DHA/320 mg piperaquine). Eurartesim dilutions predicted to be within the assay functional range were tested with the piperaquine tablet sensor in triplicate and drug content was interpolated from a piperaquine standard curve. The amount of piperaquine found by the aptamer assay is plotted against the reported initial amount of piperaquine expected from the manufacturer package insert datasheet, with the aptamer assay finding roughly 15% less than the reported amount of piperaquine. This data was intended to be interpreted as a proof of principle that crushed tablets are a potentially suitable medium for analysis with the aptamer assay. In order to understand assay accuracy, aptamer assay results should be compared to a reference standard and further statistical analysis is required. Red dotted lines indicate 95% confidence interval of the linear regression fit.

targets, and including diluted serum washes in an attempt to remove sequences that nonspecifically bind serum proteins (described in Chapter 3).

Aptamer sensors PQ4 and MQ2 resulting from SELEX PQ2 and MQ1, which both included negative selection against diluted serum, were assessed for function in serum compared to selection buffer. Since quencher conditions had been optimized in selection buffer, both quencher lengths (13mer and 14mer) were reevaluated for performance with drug dilutions in serum. All conditions were tested in triplicate and results are shown in Figure 4.9 and 4.10. These results show that the sensors in their current form do not perform adequately in serum and indicated that simply including a serum negative selection step during aptamer selection step would not resolve these issues. The next section describes the results from attempts to

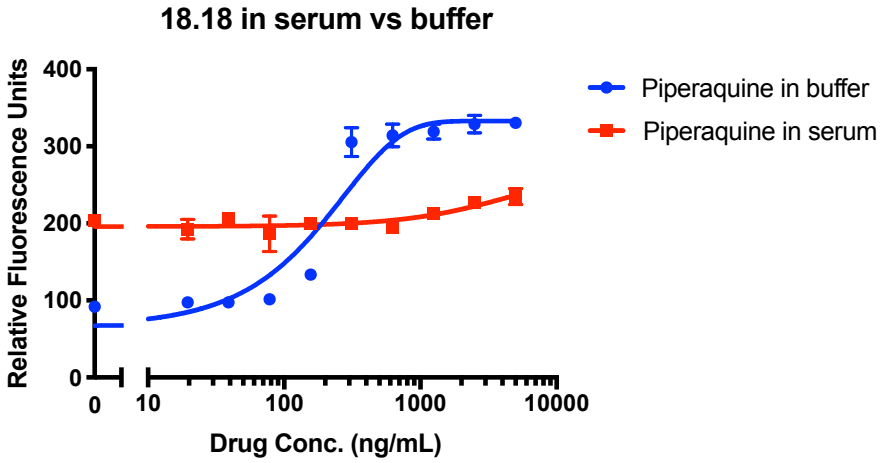


Figure 4.8: Aptamer sensor 18.18 in serum versus buffer. Sensor function is inhibited in serum as compared to selection buffer due to higher background signal and reduced sensor response to target.

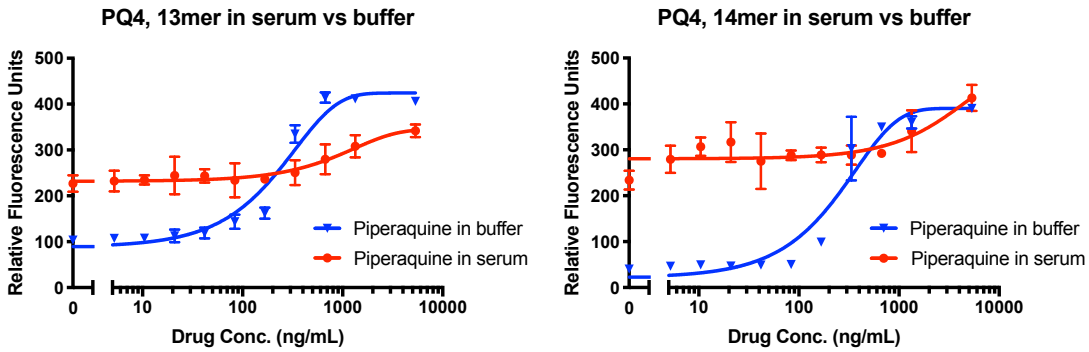


Figure 4.9: Aptamer sensor PQ4 in serum versus buffer. Piperaquine sensor performance in serum is inhibited as compared to buffer. The improved sensitivity of the 13mer quencher allows for a lower limit of detection in serum than the 14mer quencher.

understand and troubleshoot sensor function in serum.

4.3.3 Serum sensor troubleshooting results

Measuring effects of serum carrier proteins

To assess the effects of serum proteins expected to bind drug targets (HSA and AGP), these proteins were spiked into selection buffer with constant piperaquine or mefloquine content. Serum IgG was also tested as a control protein not expected to bind drug. All proteins were tested across their physiological ranges, listed below each graph in Figure 4.11 and 4.12.

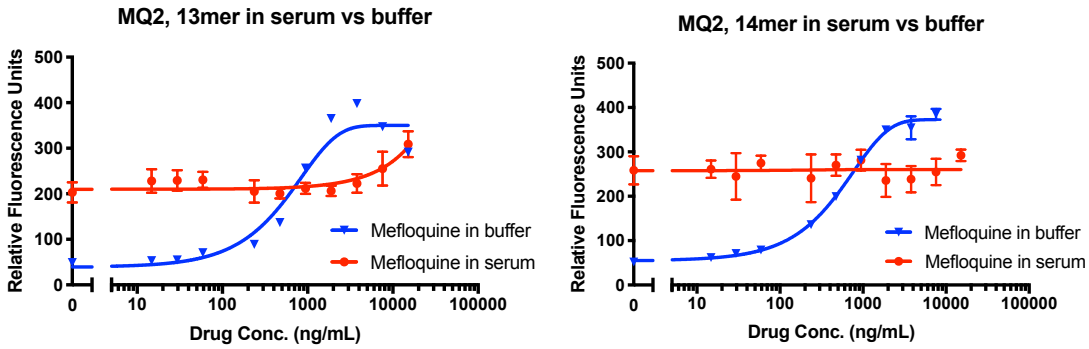


Figure 4.10: Aptamer sensor MQ2 in serum versus buffer. Mefloquine sensor function is inhibited in serum as compared to buffer. Again, the increased stringency of the 14mer quencher appears to further inhibit drug detection in serum.

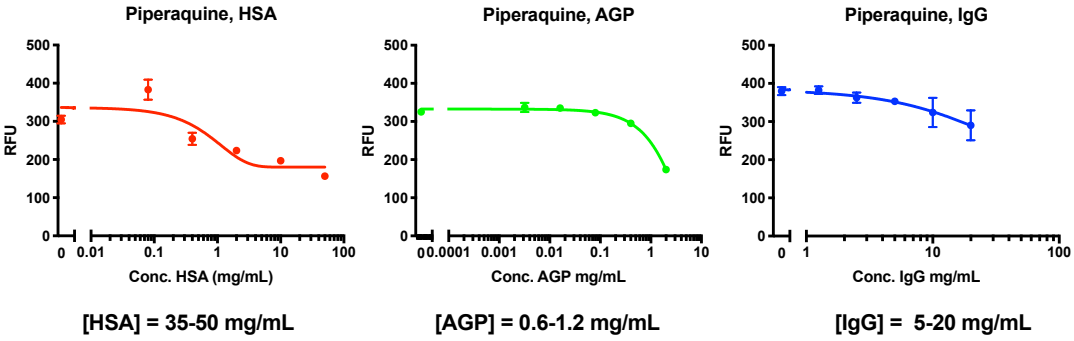


Figure 4.11: Serum protein effects on sensor PQ4. The effect of several serum proteins on the piperaquine sensor response in selection buffer is reported. Physiological ranges of selected proteins are shown below each graph.

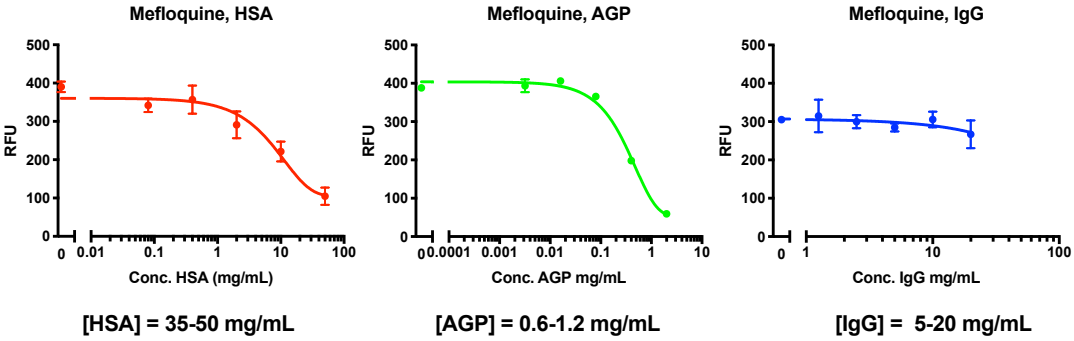


Figure 4.12: Serum protein effects on sensor MQ2. The effect of several serum proteins on the mefloquine sensor response in selection buffer is reported. Physiological ranges of selected proteins are shown below each graph.

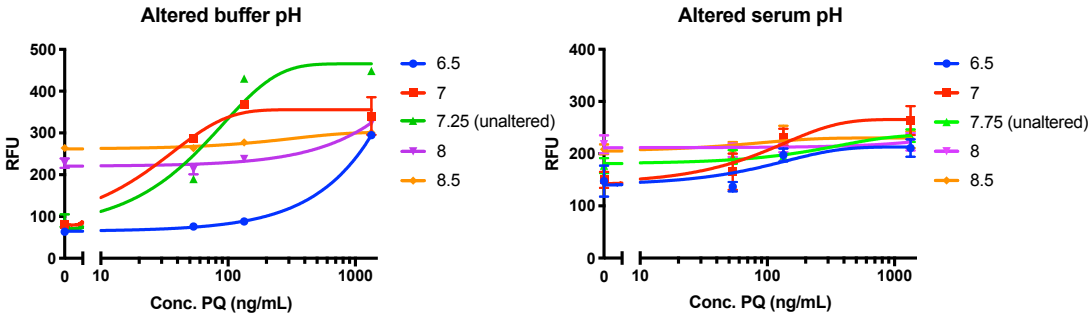


Figure 4.13: Effects of altering pH on sensor PQ4. Sensor function in both buffer and serum with altered pH is reported. High background in the pH 8 and 8.5 conditions suggest reduced hybridization between aptamer and quencher strand at higher pH. Drug dilutions ranging from around 1,000 to 50 ng/mL were tested in pH adjust buffer and serum.

Figures 4.11 and 4.12 show that all three proteins inhibit sensor function at the higher end of their physiologically relevant ranges. AGP seems to have the strongest inhibitory effects in these ranges, followed by HSA, and then IgG. However, this assay did not allow for interpretation of the mechanism of inhibition. It could be due to protein drug interactions as hypothesized and the fact the inhibition is greater in the proteins with reported drug binding than IgG supports this hypothesis. Though inhibition due to protein quenching cannot be ruled out. Further analysis would need to be done to confirm that HSA and AGP are inhibiting sensor function by competition for binding the drug targets in solution.

Adjusting pH

It was hypothesized that altering the pH of serum may improve sensor function by inhibiting protein-drug interactions while maintaining aptamer structure and binding ability. To test this, the piperaquine PQ4 sensor was tested in drug dilutions of buffer and serum at varying pH. The results are shown in Figure 4.13.

The pH adjusted buffer conditions were tested to assess the pH effect on sensor function in the absence of serum effects. In buffer, the sensor function was significantly hindered at pH 6.5, 8, and 8.5. A high background at pH 8 and 8.5 suggests that the aptamer and quencher annealing may be affected by the increased pH. Background is unaffected at pH 6.5, but the sensor response is

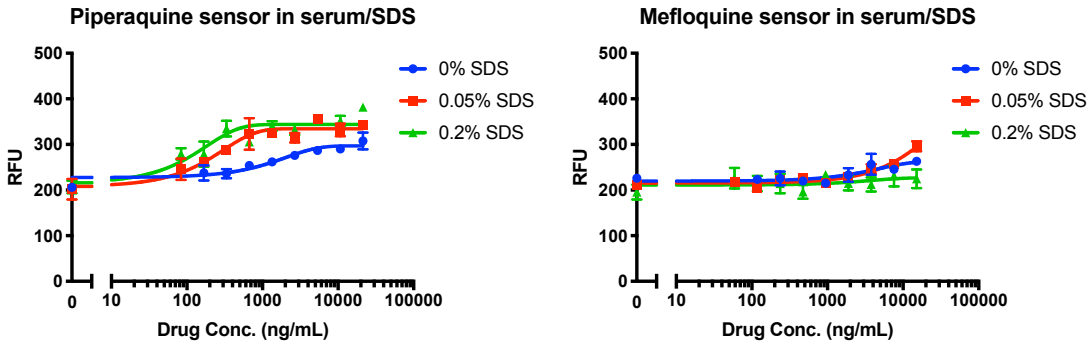


Figure 4.14: Effects of SDS in drug spiked serum on sensor function. Low concentrations of SDS were added to serum samples before testing with the piperaquine and mefloquine sensors. It appears that the SDS improved the response of the piperaquine sensor. However, the SDS made sample handling more difficult as seen in the increased variability of measurements and improved results were not observed in the mefloquine sensor.

inhibited, decreasing the limit of detection. Sensor function is mostly maintained at pH 7, however the magnitude of the fluorescent signal is slightly decreased. Overall, altering the pH did not improve sensor function in buffer and, in some cases, clearly inhibited it.

Similar effects of pH on sensor function are observed in the varying pH drug dilution curves in serum. Again, higher pH appears to increase background, although the background is higher for all conditions in serum as compared to selection buffer. pH 7 appears to retain function but no pH condition provided any significant improvement.

Adding surfactant/solvent

To assess the hypothesis that adding solvent or surfactant might release drug from serum proteins and improve sensor function, SDS and DMSO were added to drug dilutions in serum and tested with both the piperaquine and mefloquine sensors (Figures 4.14 and 4.15).

It appears that the tested concentrations of SDS improve piperaquine sensor function, shifting the limit of detection from the range of 1,000 ng/mL to around 100 ng/mL. However, the same effect is not observed in the mefloquine sensor. The addition of SDS to the serum resulted in increased bubbling during sample transfer

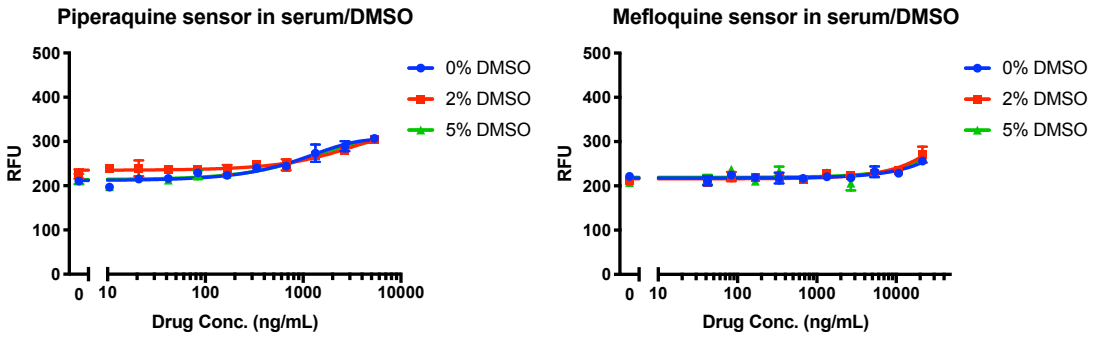


Figure 4.15: Effects of DMSO in drug spiked serum on sensor function. Low concentrations of DMSO were added to serum samples before testing with the piperaquine and mefloquine sensors. It appears that the DMSO has no effect on serum sensor function.

before reading on the fluorescent plate reader. This added complication during sample handling was undesirable and although SDS showed potential promise for improving sensor function, it was put on hold to revisit later if no other adjustments provided necessary improvements. It seems clear that the addition of DMSO at tested concentrations has no effect on sensor function.

Increasing the concentration of sensor

It was hypothesized that increasing the concentration of sensor, by increasing the amount of aptamer and quencher, in the solution that is combined with sample might improve the sensitivity of the sensors. An increased ratio of sensor:sample was tested for both the piperaquine and mefloquine sensor as shown in Figure 4.16. While increasing the ratio of sensor:sample does increase the magnitude of the sensor response, it does not appear to shift the curve to improve the limit of detection for either the piperaquine or mefloquine sensor. A higher concentration of aptamer and quencher also results in a higher signal background.

Serum dilutions

In order to decrease the matrix effects of serum, drug dilutions in serum were prepared and then diluted 1:3 and 1:5 in selection buffer. The hope was that simply diluting the serum might improve sensor function enough to overcome the effects of diluting the dug concentration in sample. The results are shown in Figure

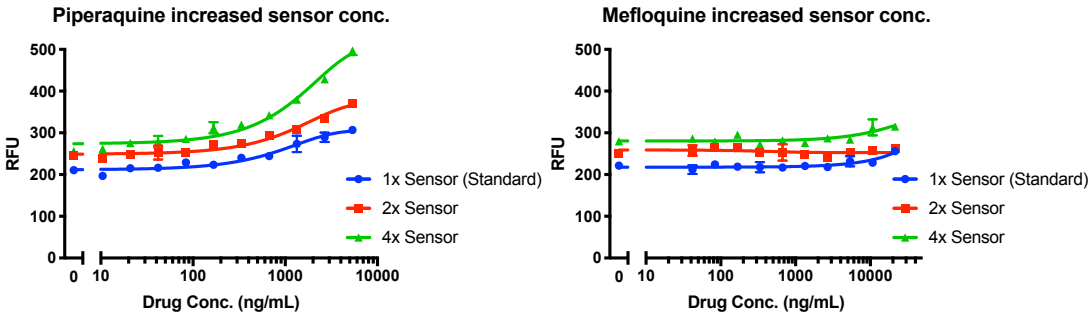


Figure 4.16: Effects of increased sensor concentration on serum sensor function. Doubling and quadrupling the amount of sensor mixed with serum samples increases the magnitude of the fluorescent response. However, since both the drug response and the level of background are increased, this approach does not seem to improve sensitivity.

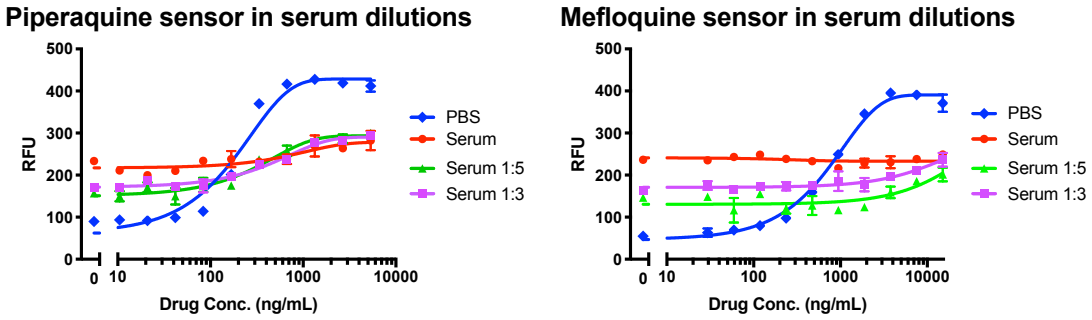


Figure 4.17: Effects of serum dilution on serum sensor function. Diluting drug spiked serum into selection buffer improves sensor function. Although the dilution of the spiked serum also decreases the drug content of the tested samples, the decreased matrix effects at these dilution conditions appear to outweigh the loss of sensitivity due to drug dilution. Dilution appears to improve sensor function by decreasing the initial background signal and by improving sensor response.

4.17. Diluting the drug spiked serum appears to reduce sensor background and increase sensor response to target.

Higher wavelength fluorophores

To try to decrease the effects of serum protein quenching and autofluorescence, fluorophores and corresponding quenchers across a range of excitation and emission wavelengths were tested (Table 4.6 in the methods section). First, the new fluorophores were tested with the piperaquine (PQ4) sensor with the goal of repeat testing only the most promising fluorphores with the mefloquine sensor. Before testing, the aptamer:quencher ratios needed to be optimized for these fluorophores.

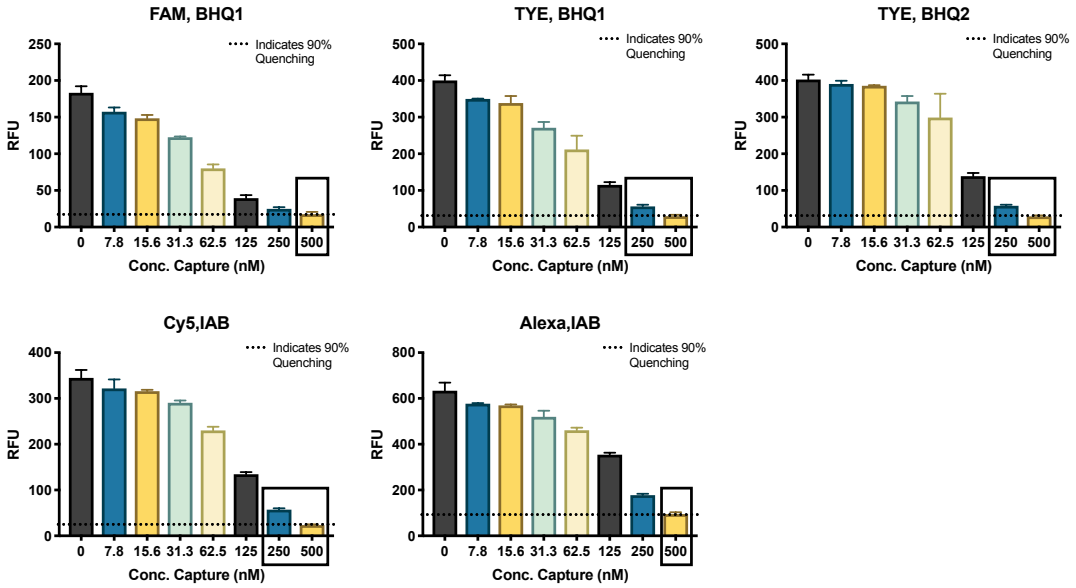


Figure 4.18: The dilution curves of PQ4 with new fluorophores and quenchers. Quencher concentrations are reported on the X-axis and relative fluorescent units (RFU) are reported on the Y-axis. The dotted line indicates 90% quenching and the box indicates the selected quencher concentrations.

Aptamer_Fluorophore	Selected 13mer quencher and ratio
PQ4_Cy5	IAB 1:8
PQ4_Alexa647	IAB 1:10
PQ4_TYE	BHQ1: 1:8
PQ4_FAM	BHQ1 1:10

Table 4.10: PQ4 optimized aptamer:quencher ratios for higher wavelength fluorophores. The selected ratios of each new fluorophore are reported here.

Quencher dilutions are shown in Figure 4.18 and selected aptamer:quencher ratios are shown in Table 4.10.

The new fluorophores with optimized quencher concentrations were then tested in drug spiked selection buffer and pooled serum. Figure 4.19 shows each of the new fluorophores in drug spiked serum and buffer. With all of new fluorophores, sensor function is still worse in serum as compared to buffer. However, the Alexa647 and Cy5 fluorophores are much more sensitive in both buffer and serum than the FAM fluorophore. Figure 4.20 shows all of the fluorophores in piperaquine spiked serum for comparison.

After fluorophore optimization with the PQ4 sensor, the Cy5 and Alexa647

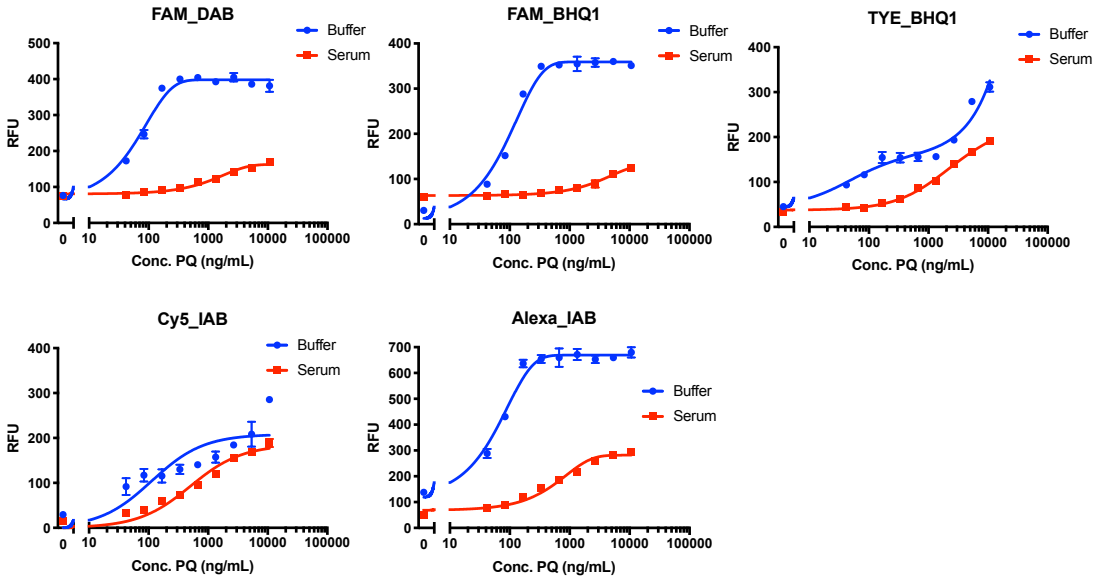


Figure 4.19: New fluorophores on the PQ4 aptamer with their optimized quencher ratios in piperaquine spiked serum and buffer. Quencher BHQ1 does not improve FAM sensor function over the DAB quencher. The TYE fluorophore appears to have improved sensor function in serum compared to the FAM fluorophore although function in serum is still inhibited compared to in buffer. Both Cy5 and Alexa fluorophores also appear to have improved sensor function in serum compared to FAM. However, compared to function in buffer, their performance in serum is still inhibited.

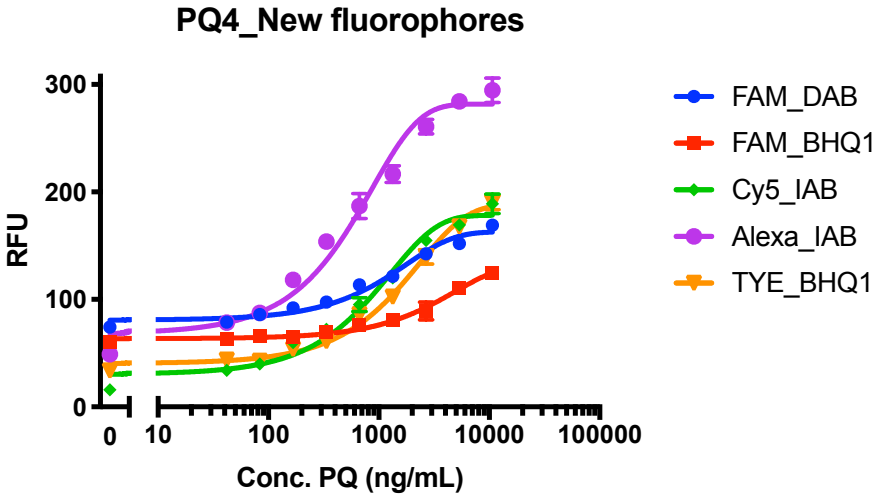


Figure 4.20: New fluorphore PQ4 sensors with their optimized respective quenchers in piperaquine spiked pooled human serum. Comparing side by side, it appears that the Alexa fluorophore has the strongest response in serum. The Cy5 and TYE fluorophores show similar results. The Alexa and Cy5 fluorophores were selected for further testing.

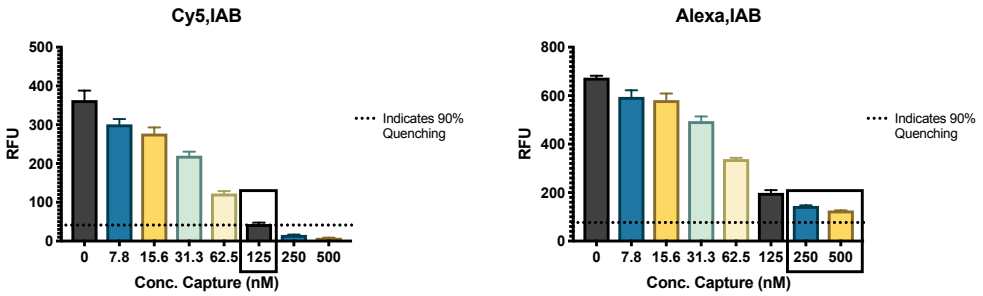


Figure 4.21: The dilution curves of MQ2 with new fluorophores and quenchers. Quencher concentrations are reported on the X-axis and relative fluorescent units (RFU) are reported on the Y-axis. The dotted line indicates 90% quenching and the box indicates the selected quencher concentrations.

Aptamer_Fluorophore	Selected 13mer quencher and ratio
MQ2_Cy5	IAB 1:2.5
MQ2_Alexa647	IAB 1:10, IAB 1:5

Table 4.11: MQ2 optimized aptamer:quencher ratios for higher wavelength fluorophores. The selected ratios of each new fluorophore are reported here.

fluorophores were selected to be tested with the mefloquine sensor. The MQ2 Cy5 and Alexa fluorophore tagged aptamers were assessed for optimal aptamer:capture ratios (Figure 4.21) then tested in mefloquine spiked serum (Figure 4.22).

The improvements in sensor function with the MQ2 sensor using higher wavelength fluorophores were not as obvious as with the PQ4 sensor. It was clear that further modifications would be necessary to improve the limit of detection of the MQ2 sensor to reach the desired target concentration of around 600 ng/mL (the average day seven plasma concentration). To further improve the sensitivity of the MQ2 sensor, the ratio of aptamer:quencher was adjusted from 1:10 to 1:5. Also, after the results of Figure 4.17, it was decided that serum samples would be diluted 1:5 before running with aptamer sensors to improve the function of both sensors in serum. The Alexa647 fluorophore was selected for use in the serum sensors and the new fluorophore in combination with the dilution step provide adequate sensitivity for both sensors as shown in the next section.

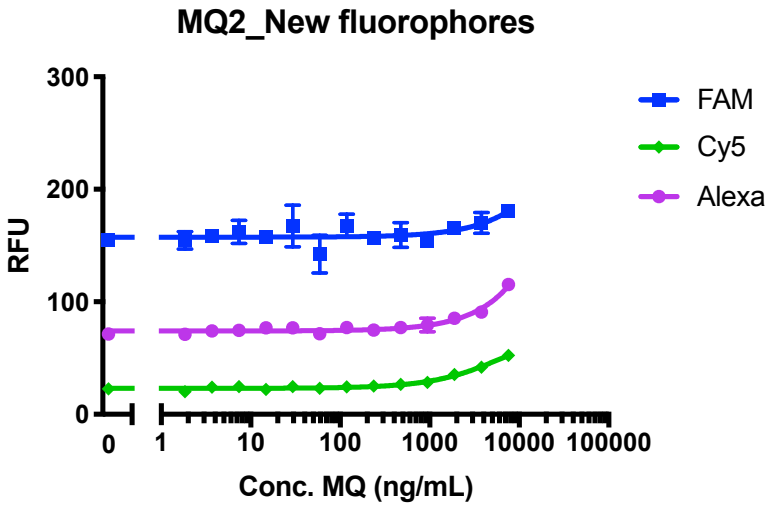


Figure 4.22: New fluorphore MQ2 sensors with their optimized respective quenchers in mefloquine spiked pooled human serum. It appears that the Alexa and Cy5 fluorophores have a slightly better response than the FAM fluorophore though the difference is not as marked as was observed with the PQ4 sensor.

4.3.4 Characterization of serum sensors

Limit of detection and limit of quantification

The functional range as well as limit of detection and limit of quantification of the optimized serum sensors was assessed. The goal for aptamer sensor sensitivity was to be able to detect drug seven days after treatment. The average day seven values for piperaquine and mefloquine are 50-70ng/mL and 500-600 ng/mL respectively. Serum drug dilution curves and blank replicates were diluted 1:5 in selection buffer and mixed with the Alexa647 PQ4 and MQ2 sensors to determine the sensor limits of detection and limits of quantification as described in the methods section. Although the mefloquine sensor is less sensitive than the piperaquine sensor, mefloquine has a higher average day seven plasma concentration. The piperaquine serum sensor LOD and LOQ were calculated to be 2 ng/mL and 50 ng/mL respectively (Figure 4.23). The mefloquine serum sensor LOD and LOQ were calculated to be 8 ng/mL and 325 ng/mL respectively (Figure 4.24). The upper end of the sensors' functional ranges are above maximum physiological drug concentrations.

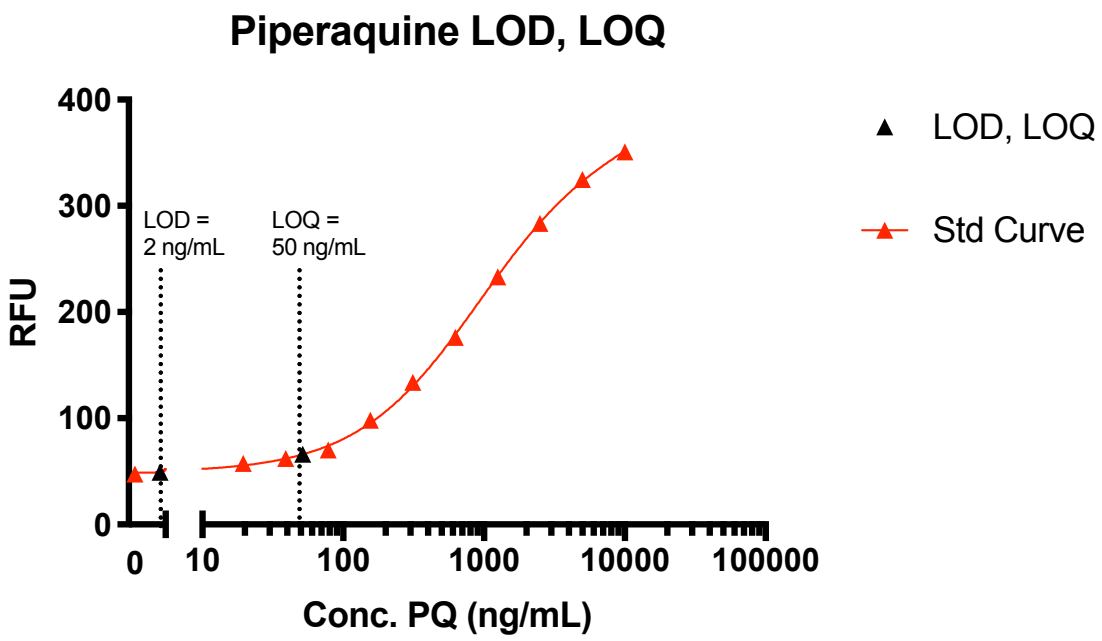


Figure 4.23: Piperaquine serum sensor LOD, LOQ. The LOD, calculated as average blank plus 3x standard deviation of blank and the LOQ, calculated as average blank plus 10x standard deviation of blank are plotted on a piperaquine standard curve.

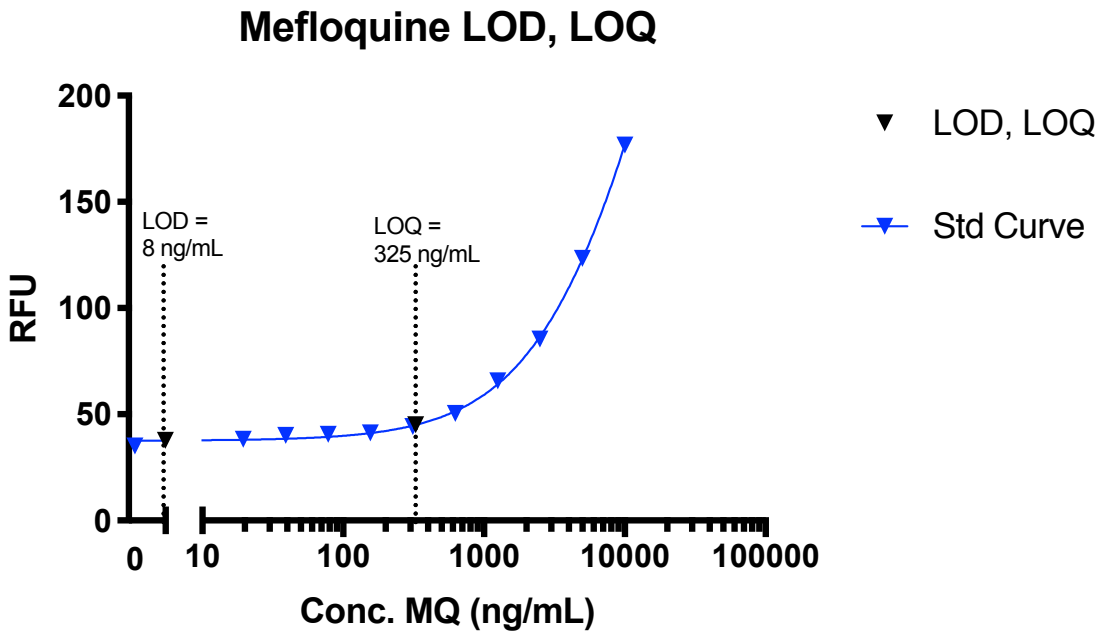


Figure 4.24: Mefloquine serum sensor LOD, LOQ. The LOD, calculated as average blank plus 3x standard deviation of blank and the LOQ, calculated as average blank plus 10x standard deviation of blank are plotted on a piperaqune standard curve. The limit of quantification is much higher for the mefloquine sensor than for the piperaquine sensor.

Cross-reactivity

The PQ4 and MQ2 serum sensors were assessed for their response to 10 potentially cross-reactive compounds including similarly structured antimalarial drugs and their major metabolites. All compounds were spiked into pooled human serum and tested against both sensors. The results are shown in Figures 4.25 and 4.26.

Increased cross-reactivity of the mefloquine sensor as compared to the piperaquine sensor is likely due in part to the inferior selectivity of the aptamer itself. It is also due to the lower ratio of capture to aptamer molecules used in the mefloquine sensor. In order to obtain sufficient sensitivity to mefloquine, a lower concentration of quencher was used. This also increases the response to other compounds to which the aptamer is cross-reactive. However, since the cross-reactivity is only detected at levels above physiologically relevant concentrations, it seems to be a worthwhile tradeoff to use less quencher oligo in order to improve the sensitivity of mefloquine detection.

Accuracy/Precision testing

To assess the accuracy and precision of PQ4 and MQ2 serum sensors, five QC samples ranging from the sensors' limits of quantification to the upper end of the assay functional range were prepared and tested in five replicates across four days, preparing fresh sensor each day as described in the methods section. The results are shown in Tables 4.12 and 4.13 and Figures 4.27 and 4.28.

Matrix effects

Pooled human serum was used during the majority of assay optimization and characterization. The serum of five different individuals was assessed with each sensor to ensure that matrix effects of serum from different individuals did not interfere with the assay results. The main concern was that samples with varying serum protein concentration such a bilirubin or with varying degrees of hemolysis would affect fluorescent background levels. In order to assess drug content of serum from varying individuals, serum samples will need to be compared to a laboratory

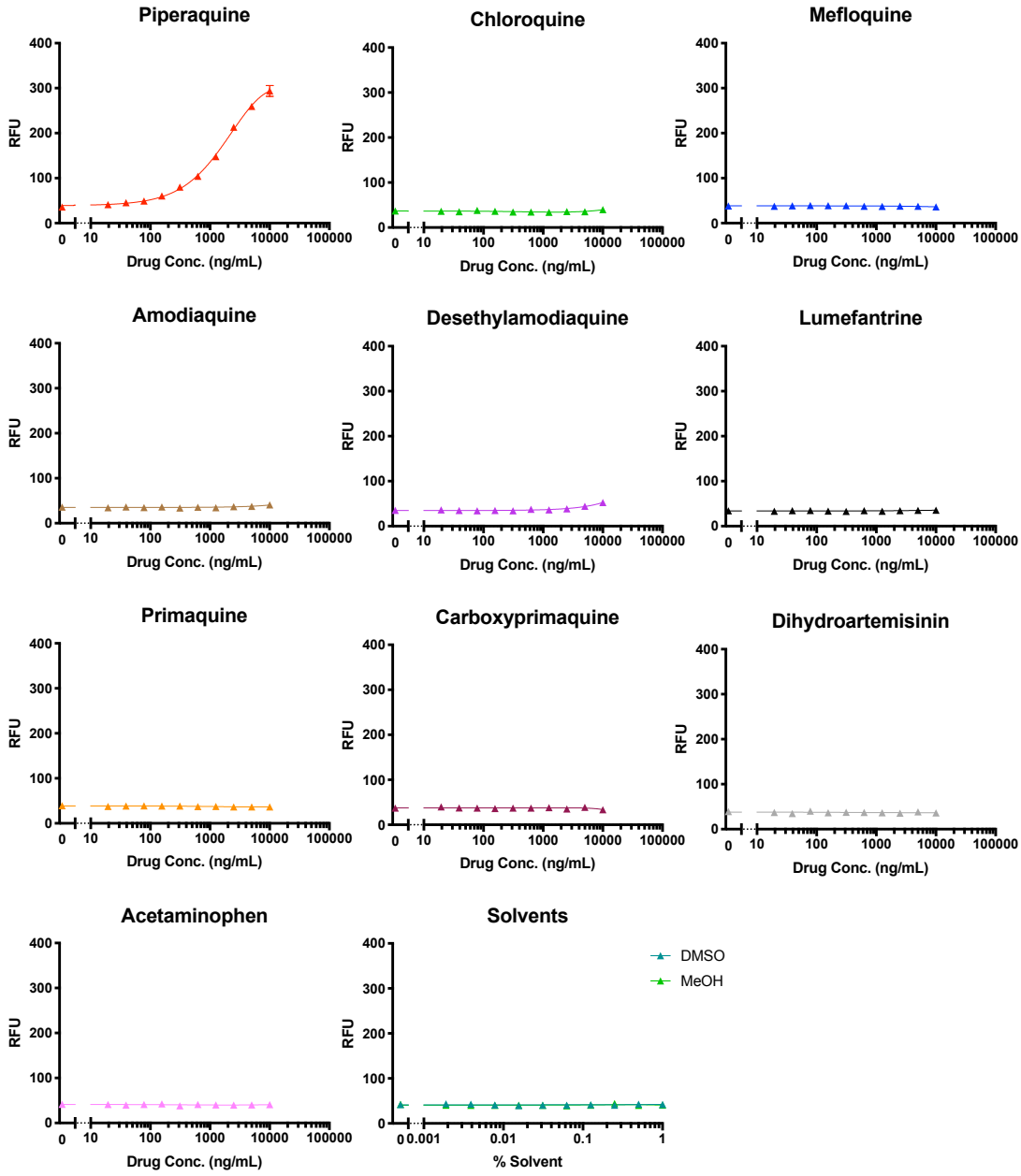


Figure 4.25: Piperaquine serum sensor cross-reactivity. The piperaquine serum sensor exhibits no cross-reactivity to the tested compounds at relevant levels. There appears to be a slight response to amodiaquine's active metabolite, desthethylamodiaquine, around 5,000 ng/mL and above, but this is much higher than the maximum physiological concentration of desethylamodiaquine which is around 500 ng/mL. In addition, the solvents used to create stock solutions of several compounds were tested to ensure they have no effect on sensor signal.

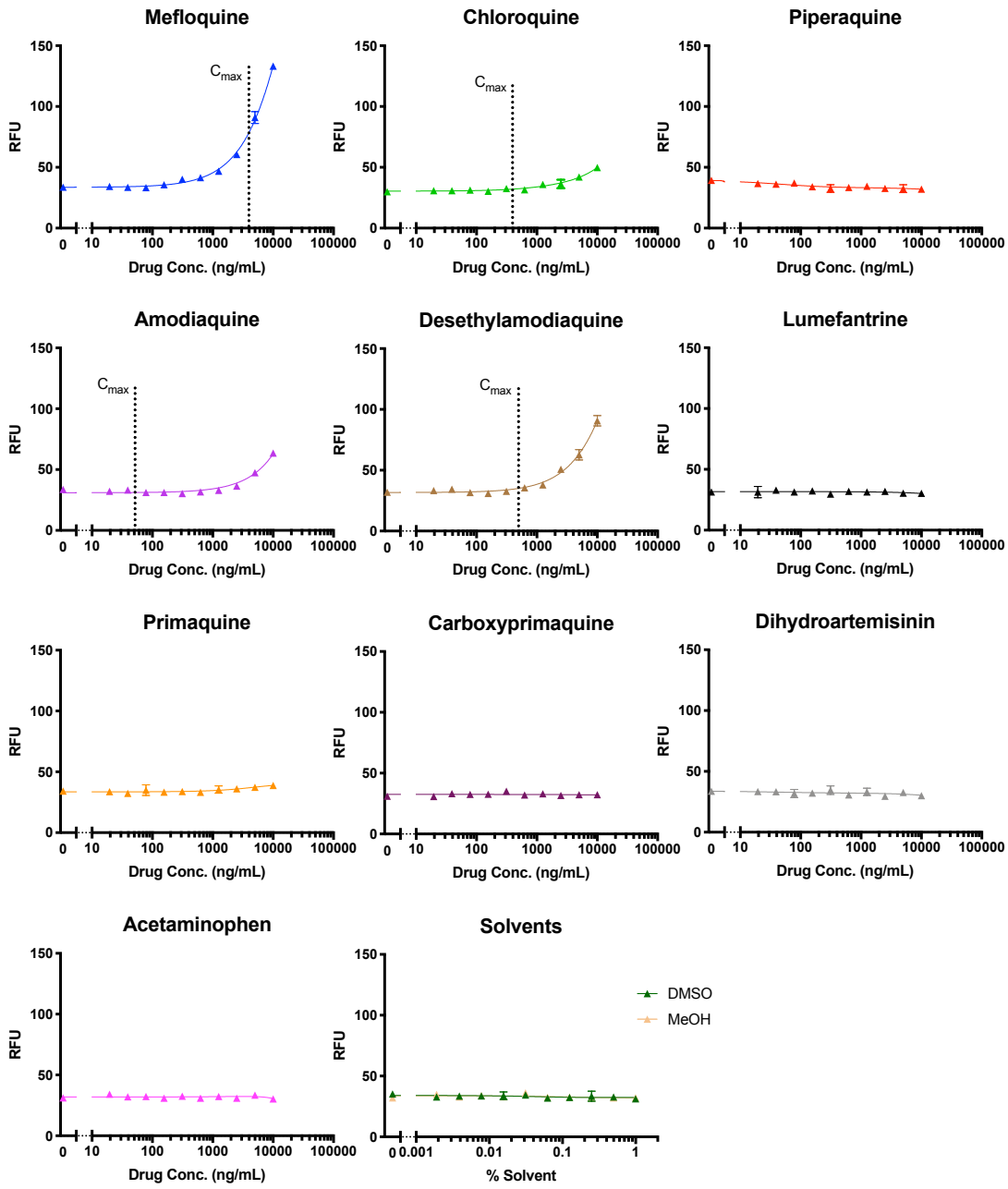


Figure 4.26: Mefloquine serum sensor cross-reactivity. The dotted lines indicate maximum physiological concentrations. Although there appears to be cross-reactivity to amodiaquine and its active metabolite desethylamodiaquine around 1,000 ng/mL, this is above the maximum physiological concentrations which are ∼50 ng/mL and ∼500 ng/mL respectively. Similarly, there is slight cross-reactivity to chloroquine at concentrations above 1,000 ng/mL, however the maximum physiological concentration of chloroquine is much lower, ∼400 ng/mL.

Added (ng/mL)	50	150	1250	2500	10,000
Reported (ng/mL)	48.99	153.92	1431.66	2781.04	10951.92
% Deviation reported verses added	-2.03	2.62	14.53	11.24	9.52
Inter-assay CV (%)	33.12	16.46	9.45	8.45	33.47
Intra-assay CV (%)	37.45	17.52	6.67	7.83	16.61
Total-assay CV (%)	36.80	17.36	7.18	7.93	21.37

Table 4.12: Piperaquine serum sensor accuracy and precision testing. The assay reports acceptable accuracy with % deviation below 15% across the tested sample range. However, the total assay variability is high at the low and high ranges. Total assay variability is above 15% at the 50 ng/mL, 150 ng/mL, and 10,000 ng/mL levels. 10,000 ng/mL is above physiologically relevant concentrations and is not a concern. However, for the lower ranges, it should be noted that although accurate, the assay has high variability so multiple replicates should be performed whenever possible.

Added (ng/mL)	325	1000	4500	8000	10,000
Found (ng/mL)	331.34	939.45	4950.24	8943.06	10469.21
% Deviation found verses added	1.95	-6.05	10.01	11.79	4.69
Inter-assay CV (%)	15.51	12.07	18.98	13.78	11.42
Intra-assay CV (%)	24.35	15.29	12.26	7.57	7.38
Total-assay CV (%)	23.18	14.82	13.55	8.84	8.15

Table 4.13: Mefloquine serum sensor accuracy and precision testing. Similar to the PQ4 assay, the MQ2 serum assay reports good accuracy but high variability at the lower range of tested concentrations. At 325 ng/mL the total assay variability is above 15%, so although the values average out to a value close to the accurate value, replicates must be performed to ensure accuracy.

standard curve. The goal of this experiment was to assess whether different serum samples have different baseline fluorescent levels that will interfere with their ability to be accurately assessed against a laboratory standard curve. The results are shown in Figure 4.29. An ANOVA test was performed in Graphpad Prism to identify any significant differences between serum sample blanks. A significant difference (P=0.028) was reported only between two samples in the piperaquine sensor test. The mean difference in fluorescent response was 6.8 RFU. This difference in background fluorescence would have very little effect on the reporting of high piperaquine concentration samples but could affect the accuracy of low concentration samples. For example, a difference of 7 RU at the very low end of the piperquine standard curve represents a 30 ng/mL difference in interpolated piperaquine concentration.

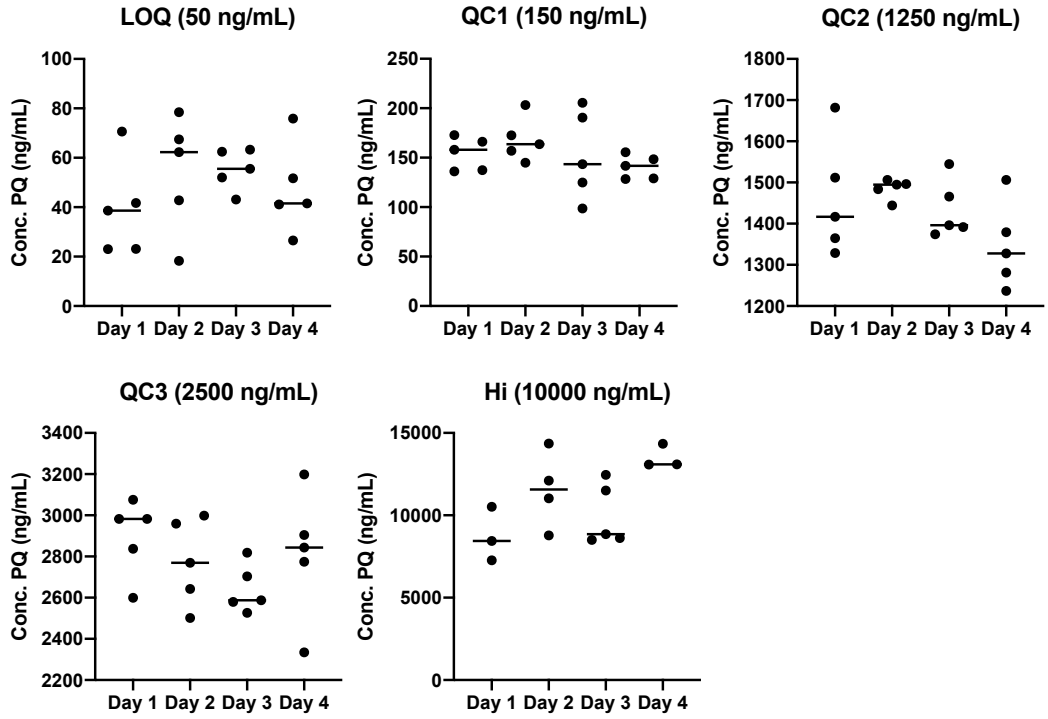


Figure 4.27: Piperaquine serum sensor accuracy and precision plots. All of the replicates from each QC sample from from each day of the accuracy and precision testing are reported to visualize assay accuracy and variability.

Assay validation against LC-MS reference standard

The accuracy of the aptamer sensors were validated against a reference standard LC-MS method for drug detection. Samples were prepared and analyzed via LC-MS at MORU in Bangkok, Thailand and then shipped to the NIH for analysis with the aptamer sensor. The samples were blinded during analysis with the aptamer sensor and results were compared to LC-MS reference standard values. The results are shown in Tables 4.14 and 4.15 and Figures 4.30 and 4.31. Both linear regression analysis and Bland Altman plots are included for interpretation of method agreement.

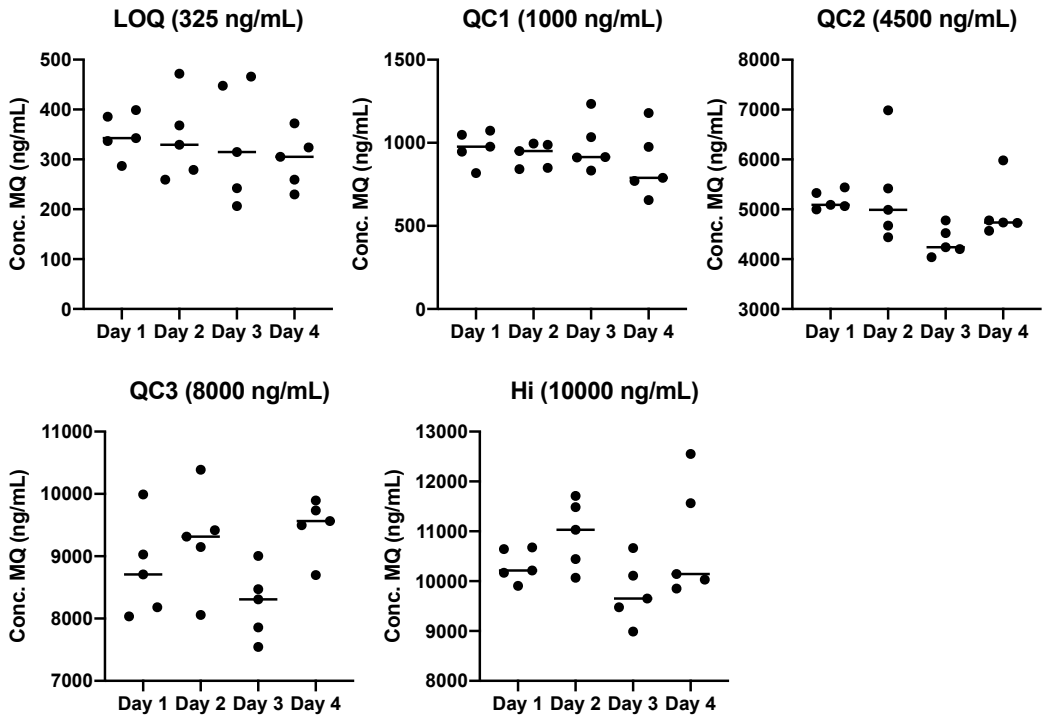


Figure 4.28: Mefloquine serum sensor accuracy and precision plots. All of the replicates from each QC sample from from each day of the accuracy and precision testing are reported to visualize assay accuracy and variability.

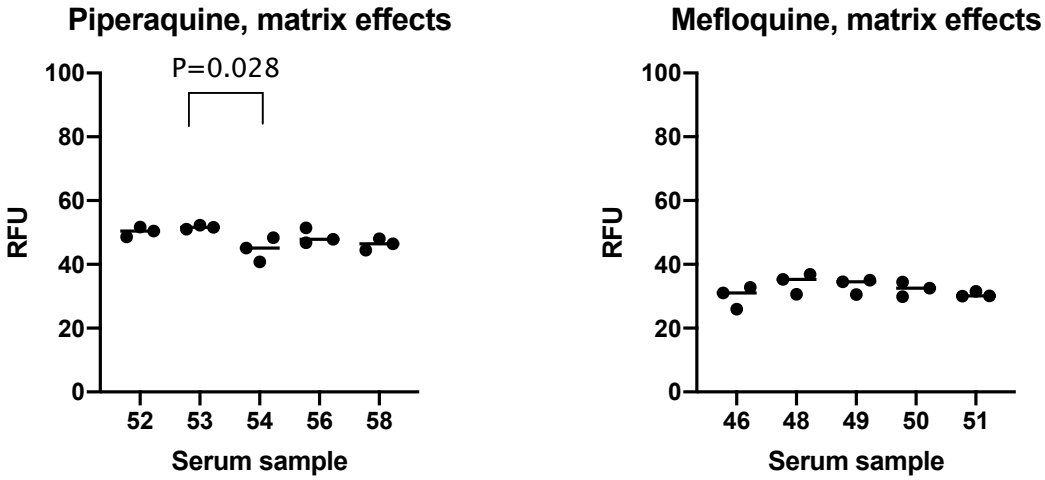


Figure 4.29: Piperaquine and mefloquine sensor matrix effects. The resulting fluorescent response of five blank samples tested against each sensor. Differences between samples were assessed via an ANOVA which reported a significant difference between only sample 53 and 54 in the piperaquine sensor test.

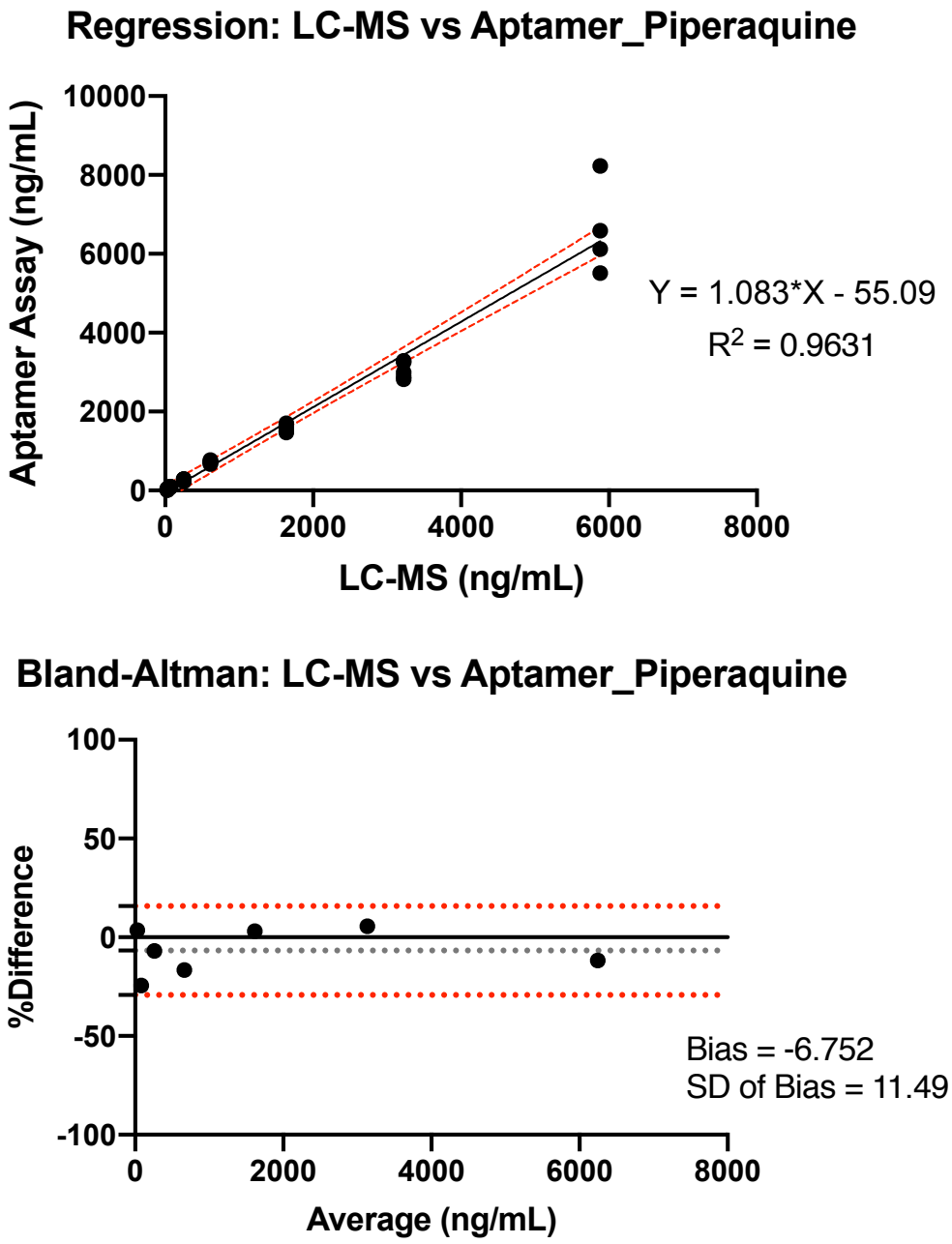


Figure 4.30: The piperaquine serum sensor results are plotted against the LC-MS reference standard results. The top figure shows the scatter plot of sample replicates and a linear regression fit. The bottom figure is a Bland Altman plot reporting the %Difference between the two methods across the sample range. The grey line indicates the determined bias between methods and the red lines indicate the 95% confidence interval of the bias. Since this interval crosses zero, it is concluded that there is no consistent bias between the two methods. Additionally, there is no visible trend in bias across the sample range. The highest piperaquine QC sample was omitted from the plot since 9,900 ng/mL is much higher than the physiological maximum concentration of piperaquine.

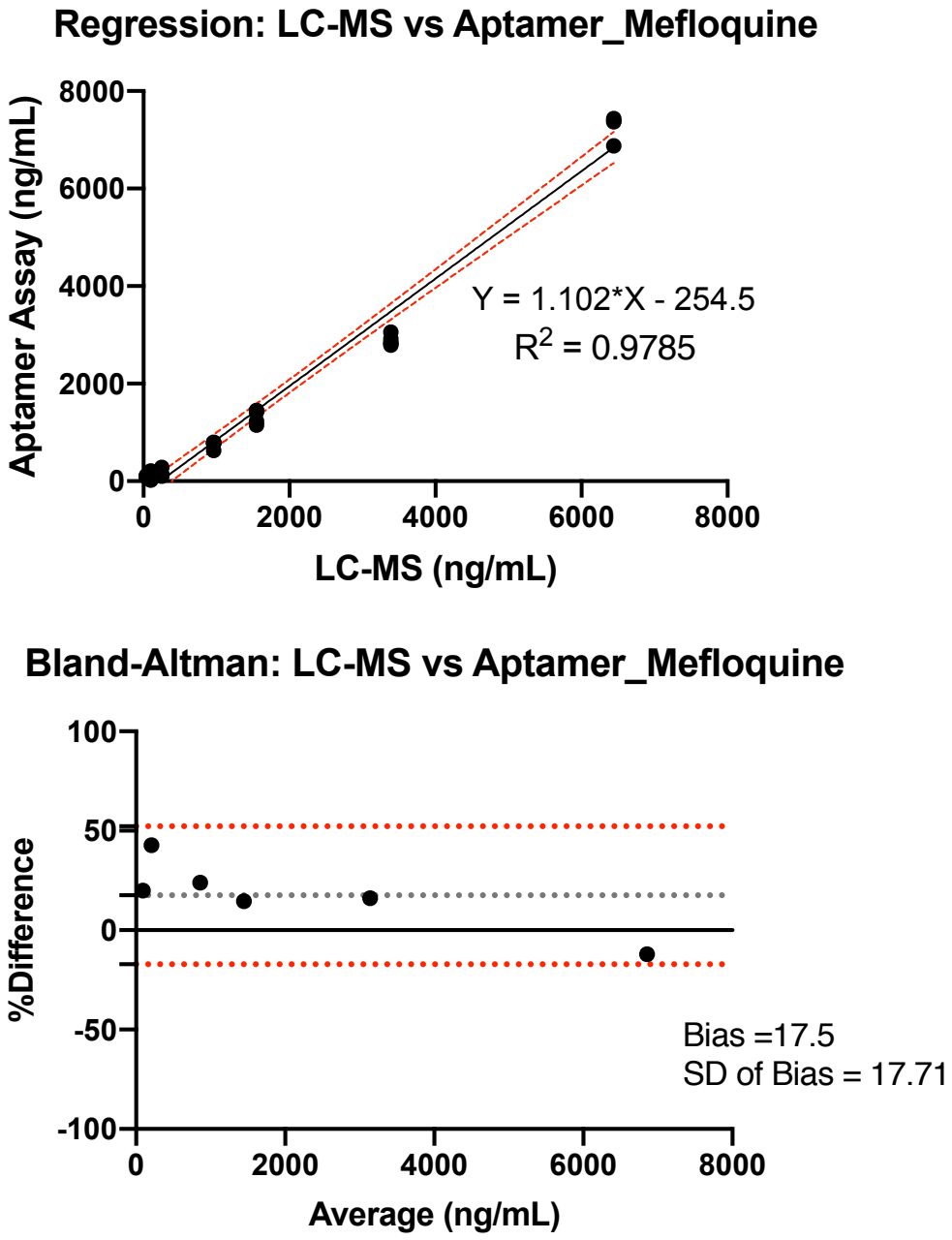


Figure 4.31: The mefloquine serum sensor results are plotted against the LC-MS reference standard results. The top figure shows the scatter plot of sample replicates and a linear regression fit. The bottom figure is a Bland Altman plot reporting the %Difference between the two methods across the sample range. The grey line indicates the determined bias between methods and the red lines indicate the 95% confidence interval of the bias. Since this interval crosses zero, it is concluded that there is no consistent bias between the two methods. Additionally, there is no visible trend in bias across the sample range. The serum sensor reports good accuracy compared to the LC-MS reference standard across all tested QC concentrations.

Sample	PQ 1	PQ 2	PQ 3	PQ 4	PQ 5	PQ 6	PQ 7	PQ 8
LC-MS value (ng/mL)	610	250	71	9901	1639	3226	5882	29
Aptamer value (ng/mL)	734.5	268.9	87.3	7097.1	1636.9	3192.8	7924.6	22.8
%CV (Aptamer)	5.1	10.3	5.1	10.8	6.3	7.2	28.4	63.6
% Deviation	20.5	7.6	22.2	-28.3	-0.2	-1.0	34.7	-21.8

Table 4.14: Piperaquine serum sensor validation against LC-MS reference standard. The accuracy of the aptamer assay compared to LC-MS reference standard is reported as well as the variation of the aptamer assay. High deviation is seen above 5,000 ng/mL but this is above the physiological maximum piperaquine concentration. High deviation is also seen at the low end of the QC sample range. However overall, the aptamer assay reports good accuracy across the range of tested concentrations.

Sample	MQ 1	MQ 2	MQ 3	MQ 4	MQ 5	MQ 6	MQ 7	MQ 8
LC-MS value (ng/mL)	877	219	32	8920	1610	3084	5983	85
Aptamer value (ng/mL)	756.2	162.7	99.2	6844.4	1339.1	2885.6	7267.6	82.7
%CV (Aptamer)	9.2	51.1	14.1	2.7	10.5	3.7	3.6	107.8
%Dev	-13.8	-25.8	211.0	-23.3	-16.8	-6.4	21.5	-2.8

Table 4.15: Mefloquine serum sensor validation against LC-MS reference standard. Similar to the piperaquine serum sensor, the mefloquine sensor shows higher deviation at the low and high ranges of the samples tested. The LOQ of the mefloquine assay is around 325 ng/mL and accuracy below this value, especially at the 32 ng/mL is not reliable. Again though, the accuracy is satisfactory from the assay LOQ to the physiological maximum mefloquine concentration.

4.4 Discussion

4.4.1 Overview

The results of this chapter show the development and characterization of aptamer sensors to detect piperaquine and mefloquine from dissolved tablets to assess medicine quality and from human serum to assess drug content in patient samples. The flexibility of the sensor format, in which the drug-binding aptamer releases from a short quencher DNA strand, allows for prioritization of either sensitivity or specificity depending on the application. For the tablet sensor, the longer quencher (14 complementary bases as opposed to 13) was employed. This increases the aptamer binding affinity to the quencher oligo, increasing competition for target binding and improving specificity. For the serum sensors, the 13mer quencher oligos were employed to maximize sensor sensitivity. Both sensors were characterized in their relevant sample matrices. Initial validation testing reports promising results,

however, further confirmation of assay function in relevant samples is needed.

4.4.2 Tablet sensors

Since tablets can be dissolved in a variety of desired buffers containing low solvent content (at low drug concentrations) it is possible to dissolve tablets in similar conditions to the ones in which the aptamers were selected. Thus, very little optimization was required for the tablet sensors. Specificity was the main concern since cross-reactivity to other substances found in falsified tablets would make the assay ineffective. In order to improve specificity, the tablet sensors used the 14mer quenchers. Characterization assays in Chapter 3 reported improved specificity for both PQ4 and MQ2 sensors with the 14mer quencher as compared to the 13mer quencher (Figures 3.27 and 3.28). The functional range of each sensor was defined as the LOQ through the top of the linear range of the standard curve. In order to accurately quantify drug content, dissolved tablets should be diluted to an expected range of concentrations that falls within the linear range of the sensor.

The PQ4 tablet sensor showed no cross-reactivity issues against five other antimalarial drugs, acetaminophen, calcium carbonate, or cornstarch. The last three compounds were included in the cross-reactivity testing as they have reportedly been found in falsified antimalarial tablets. However, the MQ2 sensor reported cross-reactivity to amodiaquine and chloroquine at concentrations around 1,000 ng/mL and above. As discussed in the results section, it seems unlikely that cross-reactivity to other antimalarial drugs at such high concentrations would be an issue for tablet quality testing, however, it cannot be ruled out. To confirm that no unexpected excipients or fillers interfere with the assay, a Euratesim tablet was dissolved and tested with the sensor. This served as a preliminary test to confirm that there were no major unforeseen cross-reactivity issues. However, since the tablet was not also assessed via another drug detection method, the accuracy of quantification cannot be determined. Overall, the experiments to characterize the tablet sensors suggest that they could be useful for assessing tablet quality. However, more tablets should be tested, including a mefloquine containing tablet

for the MQ2 sensor, and the results should be compared to a reference standard. Additionally, the potentially cross-reactive compounds tested in this research was not an exhaustive list. Many different compounds have been found in falsified antimalarial tablets, including a variety of undesired pharmaceutical compounds such as chloramphenicol, metronidazole, metamizole, and antimalarial compounds no longer approved for use [155]. These characterization assays serve as an initial assessment of the aptamer platform's ability to measure drug content from crushed tablets. If the platform is to be used for tablets, the next steps would be to further validate performance in more samples and to expand the repertoire of targets to detect other antimalarial drugs and commonly counterfeit compounds.

4.4.3 Serum optimization

The aptamer sensors, in the optimized formats from Chapter 3, were first tested for their performance in serum in Figures 4.8, 4.9, and 4.10. Comparing Figure 4.8 (from SELEX PQ1) to Figures 4.9 (SELEX PQ2) and 4.10 (SELEX MQ1), it seems clear that adding diluted serum to negative selection steps did resolve serum performance issues. This is likely because the serum performance was not hindered by cross-reactivity to serum proteins as was initially hypothesized. Further testing is necessary to determine if the inhibitory effects of serum proteins HSA and AGP on sensor performance are due to binding competition for drug or due to fluorescence quenching from the proteins. Once higher wavelength fluorophores resolved the sensor performance in serum, attempts to further elucidate the effects of these proteins on sensor function were abandoned. However, it would be interesting to further characterize protein-drug-aptamer interactions. Perhaps the aptamer is able to bind the protein-bound drug. Identifying the aptamer binding mechanisms via crystal structure determination would help clarify these interactions.

Several attempts to improve sensor function by interrupting potential drug-protein interactions included adjusting the pH, adjusting the sensor concentration, and adding SDS and DMSO. None of these adjustments significantly improved the sensor performance in serum. Simply diluting the drug spiked serum matrix

appeared to have the most promising effect on sensor function. Although this dilution step also dilutes the drug concentration in the sample, it appears that the effects of reducing serum content outweigh the drug dilution effects so that overall sensitivity is improved.

Finally, higher wavelength fluorophores were tested to address potential fluorescence interference from serum proteins. It was hypothesized that serum protein autofluorescence at the FAM excitation/emission wavelength likely contributed to high background levels observed in serum and that serum protein quenching at the FAM excitation and emission wavelengths likely contributed to the decreased sensor signal observed in serum. Several fluorophores with excitation/emission wavelengths spanning the 500-700 nm range were selected along with quencher molecules whose maximum absorbance aligned with each fluorophore's emission wavelength. The fluorophores and quenchers were selected from those available on the IDT website. This way, aptamer sensors and quenchers could be easily ordered by any lab interested in testing the sensors. The fluorophores were selected for their wavelength, their cost, and their Stokes shift. Ultimately, the Alexa647 fluorophore with a 13mer Iowa Black quencher was selected for use with both the PQ4 and MQ2 serum sensors. The PQ4 serum sensor used an aptamer:quencher ratio of 1:10 while the MQ2 serum sensor used an aptamer:quencher ratio of 1:5 in order to maximize sensitivity.

It appears that addressing the fluorescence interference of serum proteins was more effective than attempts to inhibit protein-drug interactions. However, the effects of protein-drug interactions may still inhibit sensor function. With higher wavelength fluorophores, sensor function in serum still less sensitive than in buffer.

4.4.4 Serum sensors

The final optimized serum sensors including higher wavelength fluorophores and a serum dilution step were characterized for sensitivity and specificity. The serum sensors were evaluated to ensure that their sensitivity allowed for detection around the targeted average day seven drug concentration values. Their cross-reactivity was

assessed and again, the piperaquine sensor showed no cross-reactivity issues. The mefloquine sensor showed some cross-reactivity above the physiological maximum concentration of chloroquine, amodiaquine, and desethylamodiaquine. Unlike with the tablet sensor, the cross-reactivity exhibited by the mefloquine serum sensor is not especially concerning since levels of these drugs above their maximum physiological concentrations should not be encountered. Specificity of the mefloquine sensor could be improved by increasing the concentration of quencher or by using a 14mer quencher instead of the 13mer quencher. However, it does not seem worth sacrificing sensitivity to address this cross-reactivity.

The serum sensors were further evaluated to describe their accuracy and precision as well as intra and inter assay variability. Five QC samples were prepared and repeatedly tested over four days. Both the PQ4 and MQ2 sensors report good accuracy across the range of tested concentrations. However, there is high variability at the low and high end of the tested concentrations. Since the standard curves begin to flatten out at these ranges, slight variations in RFU correlate to larger variations in reported concentrations. Values at the high end of the curve are above physiologically relevant concentrations and are not a concern. However, at the low end of the sensor functional ranges, concentrations are physiologically relevant and report variability above 15% (>30% at the LOQ value for piperaquine and >20% at the LOQ value for mefloquine). Thus, if the desired application requires accurate quantitative reports of drug content at the low end of the sensor functional ranges, it is recommended that multiple replicates are run. Since the values average out to be quite close to the accurate value, it can be concluded that the variation is random and that running replicates would increase the accuracy of the readout. If high accuracy at low drug concentrations is needed for an intended application, further optimization may be required. This could be achieved by performing a simple extraction of drug from serum. The solvent used for drug extraction could be evaporated and the extracted drug could be resuspended in buffer and mixed with aptamer sensor. This would decrease variability inherent in the serum samples.

To assess the effects of serum variations on sensor function, the serum from five donors was tested against the piperaquine sensor and serum from five different donors was tested against the mefloquine sensor. The background levels of these different serum samples were evaluated. The concern was that varying protein content would cause varying levels of fluorescence interference. Only two tested samples were reported to be significantly different and the mean RFU difference of these two samples was 6.8. This background difference would have very little effect on the reporting of high drug content samples, but it could skew the reporting of low drug content samples as discussed in the results section. It was anticipated that different serum samples (with varying protein content and hemolysis) would significantly affect background fluorescent levels. The 10 tested samples all appeared visually quite different, but the fluorescent values at the Alexa647 excitation/emission wavelengths were fairly consistent. It is hypothesized that much of this variability is avoided by using a fluorophore whose excitation/emission wavelengths are above typical autofluorescence and absorbance wavelength ranges of serum proteins.

Finally, the aptamer sensors were validated against the reference standard LC-MS method for drug detection from plasma. Blinded QC samples were evaluated via LC-MS and via the aptamer sensors. The results show very good agreement between the two methods. As expected, the values at the high and low end of the sensor functional range reported increased variability and decreased accuracy. For this reason, the highest piperaquine QC sample (which was much higher than physiologically relevant concentrations) was omitted from the analysis. The aptamer assays reported good accuracy compared to the reference standard LC-MS method between their LOQ values and the highest physiologically relevant concentrations.

4.4.5 Limitations and conclusion

A major limitation for the assay characterization is limited access to relevant samples. In order to confirm accurate reporting in crushed tablets and human serum and plasma, more testing is required. The tablet sensor would ideally be tested in more tablet formulations and compared to a reference standard method.

The serum sensor should be tested in relevant patient samples. The accuracy, precision, and cross-reactivity results are encouraging but accurate sensor function cannot be confirmed until more samples are tested.

The aptamer sensors were not expected to be as accurate or sensitive as LC-MS reference standard methods which require a drug extraction step, separation via chromatography columns, and evaluation via tandem mass spectrometry. The aptamer assay is more variable than LC-MS, especially at low concentrations, and is vulnerable to slight reporting bias from different serum samples. However, the assay is inexpensive, easy to use, and does not require extensive sample preparation or access to specialized equipment. The results in this chapter report the possibility of aptamer sensors as a promising new technology for drug detection from crushed tablets and from patient samples.

5 Conclusion

Contents

5.1 Overview 160
5.2 Cost analysis 161
5.3 Limitations and future work 161
5.4 Summary of findings 164

5.1 Overview

This thesis describes efforts to conduct a survey to collect feedback on the utility, realistic applications, and desired operational characteristics of a field-based assay to detect antimalarial drugs. The feedback collected in this survey informed the development of two aptamer-based fluorescent assays to detect piperaquine and mefloquine from crushed tablets and from human serum. The aptamers were selected using a capture-SELEX method in which an aptamer library was immobilized to a solid support via a short complementary capture oligonucleotide. Selected aptamers were adapted into fluorescent sensors in which aptamer-target binding causes the fluorophore-tagged aptamer to change structure, releasing from a complementary quencher strand. The resulting piperaquine and mefloquine sensors were optimized to detect drug from crushed tablets and from human serum. The sensors were

characterized to report their sensitivity and specificity and the serum sensor was validated against an LC-MS gold standard drug detection method.

5.2 Cost analysis

To ensure that the sensor cost meets the specifications listed in the target product profile from Chapter 2, the cost of all sensor consumables per sample are listed in Table 5.1. The aptamer and quencher components of each sensor cost less than $0.25 per sample and the buffer costs are negligible. However, each sample should be run in triplicate, so the cost per sample should be tripled to account for replicates. The most expensive consumable is the well plate and cost can be reduced by bundling more samples onto each plate. The fluorimeter is the most expensive component. While it is believed that fluorimeters are fairly common in research labs in malaria endemic countries as they are used for a wide variety of assays, the necessity of a fluorimeter may limit access to this assay. However, fluorimeters are becoming more accessible as technological advances report the development of portable, inexpensive, and even handheld fluorimeters. The only other equipment used for sensor preparation is a heat source to boil water for the five-minute sensor incubation (in our lab a microwaved is used).

5.3 Limitations and future work

To confirm the promising results of the tablet and serum sensor performance, further validation is required. The piperaquine tablet sensor was only tested with one crushed tablet as a proof of principle and the mefloquine sensor hasn't yet been tested with a crushed tablet. Both tablet sensors should be vetted with more testing and the results should be compared to a gold standard LC-MS or LC-UV method. The serum sensors performed well in the blinded QC samples and aptamer sensor results correlated well with LC-MS values. However, the serum sensor should be validated via testing with real patient samples.

Cost assessment						
Serum sensor costs per sample			**Tablet sensor costs per sample**			**Other costs**
Piperaquine – serum sensor			Piperaquine – tablet sensor			
Aptamer	$0.18		Aptamer	$0.03		
Quencher	$0.04		Quencher	$0.09		
Total	**$0.24**		**Total**	**$0.12**		
Mefloquine – serum sensor			Mefloquine – tablet sensor			
Aptamer	$0.09		Aptamer	$0.05		
Quencher	$0.01		Quencher	$0.09		
Total	**$0.10**		**Total**	**$0.14**		
Buffer reagents						**<$0.001**
Fluorescent plate						**$6.07 per 384 well plate**

Table 5.1: The cost of sensor consumables. This table shows the costs of all aptamer sensor reagents per amount required for each sample. The pricing information is based on the most recent orders from IDT and cost can vary slightly depending on synthesis and purification yield. The most significant expense is the 384 well plate and cost per sample is dependent on how many samples are run at a time. The 384 well plates were preferred because they reduce sample volumes but any plates compatible with fluorescent readings can be used. These costs do not include standard lab consumables such as tubes or pipet tips.

Additionally, more could be done to characterize aptamers MQ2 and PQ4, such as determining their exact drug-binding mechanisms. It is hypothesized that the bases involved in aptamer binding are those in the supposed 'binding pockets' depicted as open rings in the predicted Mfold structures of aptamer PQ4 and MQ2 (shown here again in Figure 5.1 for reference). It is hypothesized that, along with other hydrostatic interactions, these bases interact with the drug molecules via pi stacking between the conjugated rings of the bases and the quinoline structure of the drug molecules.

It would be very interesting to elucidate the crystal structures of drug-bound aptamers to determine which bases are involved in binding. It would also be interesting to explore how aptamer 18.18 has a higher affinity to molecule 190 than the full piperaquine, as this result was unexpected. However, solving the crystal structure of target-bound aptamers was not in the scope of this research. For the purpose of this research, priority was placed on characterizing the sensor function. However, in the future, as more aptamers to antimalarial drugs are

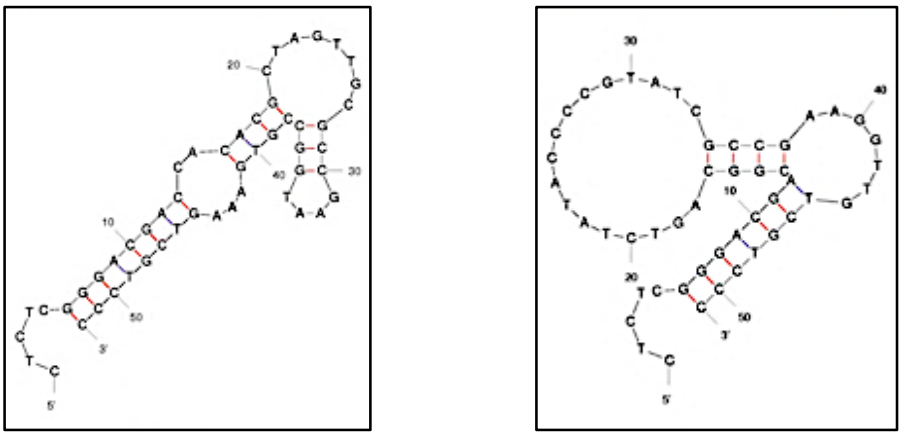


Figure 5.1: The Mfold predicted structures of PQ4 and MQ2.

developed, a better understanding of binding mechanisms could inform targeted selection and the development of improved sensors.

As discussed in Chapter 2, the initially envisioned sensor was a colorimetric dipstick assay that could be used at the point-of-care to detect previous treatment and inform future treatment. However, after discussions with malaria clinicians and researchers, it was understood that clinicians often do not have access to multiple therapies and information regarding previous treatment at the point-of-care would likely not impact future treatment. The results from the survey in Chapter 2 revealed that, instead, there was more interest in an affordable lab-based assay to assist research campaigns. The development of a quantitative lab-based assay was prioritized over a point-of-care drug detection assay in this research. However, future research will hopefully include the development of the colorimetric assay by adapting the fluorescent sensor to a dye-based platform. Initially when the assay was expected to have a colorimetric output, a smartphone application was developed to help interpret and store the results. With the help of Jai Balakumar, a student in the Oxford Computer Science department, a user interface was developed that would walk a user through the protocol of running point-of-care drug detection assay. The plan was to develop an algorithm to interpret the colorimetric results of the test, removing the variability of human interpretation. This automated interpretation

could address the difficulty reported in the survey with interpreting semiquantitative or quantitative assays in rural settings. However, since the colorimetric readout has not been developed, only the user-interface is complete. If future work results in the development of a colorimetric, point-of-care drug detection assay, this application could be further developed to allow for semi-quantitative interpretation. For example, one could imagine a use-scenario where monitoring of mass drug campaigns requires immediate results so that participants who do not have sufficient drug levels can be properly treated before they are lost to follow-up. A smart-phone application could interpret the assay results, walk a healthcare worker through any follow-up steps, and store data along with geographic information.

Another priority for future work is the selection of aptamers against other antimalarial drugs. Expanding the repertoire of available drugs for detection would likely increase the utility of the assay. The ability to detect lumefantrine and amodiaquine would allow for the detection of drugs most commonly used in Africa. While the detection of artemisinin derivatives is not a priority for the serum sensor due to its short half-life, detecting artemisinin components from crushed tablets would be useful. The majority of the work described in this thesis was the determination of optimal methods to select drug-binding aptamers as well as optimizing the performance of resulting aptamer sensors. Now that these methods have been determined, the platform could be adapted for other drug targets quite easily.

5.4 Summary of findings

To the best of our knowledge, this thesis research reports the first aptamers selected to specifically bind antimalarial drugs. It also reports the development of the first aptamer-based sensor to detect antimalarial drugs from crushed tablets or human serum. This work vetted and optimized protocols to select aptamers from aptamer libraries, improving positive and negative selection steps to hone aptamer sensitivity and specificity. Once suitable aptamers were identified, they were adapted into

simple fluorescent sensors. These sensors were then optimized and characterized in their relevant sample matrices.

The findings of this research could provide a new tool for researchers in malaria endemic countries to quickly and inexpensively collect drug use and adherence data from a study population. This assay could empower local researchers by enabling them to collect drug use data without having to ship frozen patient samples to an international lab for analysis. As the survey in Chapter 2 reports, researchers envision using this assay to monitor adherence during mass drug administration campaigns, to inform inclusion into research protocols, to assess drug toxicity, to survey drug use in a region, and in conjunction with molecular marker data to study emerging resistance. This sensor would not replace the highly sensitive and accurate LC-MS methods for plasma drug detection required for pharmacokinetic assessments of compounds. However, this assay could fill a current technology gap, allowing researchers to quickly and inexpensively collect data on drug use and tablet quality using standard equipment in their own laboratories.

References

1. World Health Organisation. *World malaria report 2018. World Health Organization.* tech. rep. (Geneva, 2018), 210. http://www.who.int/iris/handle/10665/275867.
2. Sergent, E., Sergent, E. & Parrot, L. *La découverte de Laveran : Constantine 6 novembre 1880* https://www.worldcat.org/title/decouverte-de-laveran-constantine-6-novembre-1880/oclc/12123606 (Masson, Paris, 1929).
3. Ross, R. On some peculiar pigmented cells found in two mosquitos fed on malarial blood. *British Medical Journal* **2,** 1786–1788. ISSN: 00071447 (1897).
4. Manson, P. On the nature and significance of the crescentic and flagellated bodies in malarial blood. *British Medical Journal.* ISSN: 00071447. doi:10.1136/bmj.2.1771.1306 (1894).
5. Miller, L. H. *et al.* Research toward malaria vaccines. *Science* **234,** 1349–1356. ISSN: 00368075 (1986).
6. World Health Organization. *World Malaria Report 2016* tech. rep. (WHO, Geneva, 2016). www.who.int/malaria.
7. Shretta, R. *et al. Malaria Elimination and Eradication* ISBN: 9781464805240. doi:10.1596/978-1-4648-0524-0/CH12. http://www.ncbi.nlm.nih.gov/pubmed/30212099 (The International Bank for Reconstruction and Development / The World Bank, Nov. 2017).
8. Ashley, E. A., Pyae Phyo, A. & Woodrow, C. J. *Malaria* Feb. 2014. doi:10.1016/S0140-6736(18)30324-6. https://www.sciencedirect.com/science/article/pii/S0140673613600240?via%7B%5C%%7D3Dihub.
9. Taylor, W. R., Hanson, J., Turner, G. D., White, N. J. & Dondorp, A. M. *Respiratory manifestations of malaria* Aug. 2012. doi:10.1378/chest.11-2655. https://www.sciencedirect.com/science/article/pii/S0012369212604644?via%7B%5C%%7D3Dihub.
10. Haldar, K. & Mohandas, N. Malaria, erythrocytic infection, and anemia. *Hematology / the Education Program of the American Society of Hematology. American Society of Hematology. Education Program,* 87–93. ISSN: 15204383 (2009).
11. Sriboonvorakul, N. *et al.* Acidosis and acute kidney injury in severe malaria. *Malaria Journal* **17,** 128. ISSN: 14752875 (Dec. 2018).
12. Wassmer, S. C. *et al.* Investigating the pathogenesis of severe malaria: A multidisciplinary and cross-geographical approach. *American Journal of Tropical Medicine and Hygiene.* ISSN: 00029637. doi:10.4269/ajtmh.14-0841 (2015).

13. World Health Organization. Guidelines For The Treatment of Malaria - 3rd edition. *www.who.int/malaria,* 1–313. ISSN: 00359203 (2015).

14. Plewes, K., Leopold, S. J., Kingston, H. W. & Dondorp, A. M. *Malaria: What's New in the Management of Malaria?* Mar. 2019. doi:10.1016/j.idc.2018.10.002. https://www.sciencedirect.com/science/article/pii/S0891552018300898?via%7B%5C%%7D3Dihub.

15. COATNEY, G. R. Pitfalls in a discovery: the chronicle of chloroquine. *The American journal of tropical medicine and hygiene.* ISSN: 0002-9637 (1963).

16. Cui, L. & Su, X. Z. *Discovery, mechanisms of action and combination therapy of artemisinin* Oct. 2009. doi:10.1586/ERI.09.68. http://www.ncbi.nlm.nih.gov/pubmed/19803708%20http://www.pubmedcentral.nih.gov/articlerender.fcgi?artid=PMC2778258.

17. Qinghaosu Antimalaria Coordinating Research Group. Antimalaria studies on Qinghaosu. *Chinese Medical Journal* **92,** 811–816. ISSN: 03666999 (1979).

18. White, N. J., Hien, T. T. & Nosten, F. H. *A Brief History of Qinghaosu* Dec. 2015. doi:10.1016/j.pt.2015.10.010. http://www.ncbi.nlm.nih.gov/pubmed/26776328%20http://www.pubmedcentral.nih.gov/articlerender.fcgi?artid=PMC4674626.

19. World Health Organization. *Guidelines for the treatment of malaria* tech. rep. (QHO, Geneva, 2006), 266. http://helid.digicollection.org/pdf/s13418e/s13418e.pdf%20http://apps.who.int/malaria/docs/TreatmentGuidelines2006.pdf.

20. Yeung, S. & White, N. J. *How do patients use antimalarial drugs? A review of the evidence* Feb. 2005. doi:10.1111/j.1365-3156.2004.01364.x. http://doi.wiley.com/10.1111/j.1365-3156.2004.01364.x.

21. White, N. J. & Nosten, F. Artemisinin-Based Combination Treatment of Falciparum Malaria. *The American Journal of Tropical Medicine and Hygiene* **77,** 181–192. ISSN: 0002-9637 (2018).

22. Price, R. N. Artemisinin drugs: novel antimalarial agents. *Expert Opinion on Investigational Drugs* **9,** 1815–1827. ISSN: 1354-3784 (2005).

23. Tarning, J. *et al.* Population pharmacokinetics and pharmacodynamics of piperaquine in children with uncomplicated falciparum malaria. *Clinical Pharmacology and Therapeutics* **91,** 497–505. ISSN: 00099236 (Mar. 2012).

24. Amaratunga, C. *et al.* Dihydroartemisinin–piperaquine resistance in Plasmodium falciparum malaria in Cambodia: a multisite prospective cohort study. *The Lancet Infectious Diseases* **16,** 357–365. ISSN: 14733099 (Mar. 2016).

25. Tarning, J. *et al.* Population Pharmacokinetics of Dihydroartemisinin and Piperaquine in Pregnant and Nonpregnant Women with Uncomplicated Malaria. *Antimicrobial Agents and Chemotherapy.* ISSN: 0066-4804. doi:10.1128/aac.05756-11 (2012).

26. Hoglund, R. M. *et al.* Population Pharmacokinetic Properties of Piperaquine in Falciparum Malaria: An Individual Participant Data Meta-Analysis. *PLoS Medicine.* ISSN: 15491676. doi:10.1371/journal.pmed.1002212 (2017).

27. Green, M. *et al.* Pharmacokinetics of mefloquine and its effect on sulfamethoxazole and trimethoprim steady-state blood levels in intermittent preventive treatment (IPTp) of pregnant HIV-infected women in Kenya. *Malaria Journal* **15,** 1–8. ISSN: 14752875 (Dec. 2016).

28. Ferreira, M. V. *et al.* Pharmacokinetics of mefloquine administered with artesunate in patients with uncomplicated falciparum malaria from the Brazilian Amazon basin. *Malaria Journal* **17,** 268. ISSN: 14752875 (Dec. 2018).

29. Kloprogge, F. *et al.* Lumefantrine and Desbutyl-Lumefantrine Population Pharmacokinetic-Pharmacodynamic Relationships in Pregnant Women with Uncomplicated Plasmodium falciparum Malaria on the Thailand-Myanmar Border. *Antimicrobial Agents and Chemotherapy* **59,** 6375–6384. ISSN: 0066-4804 (Oct. 2015).

30. Ezzet, F. & Karbwang, J. Population pharmacokinetics and therapeutic response of CGP 56697 (artemether + benflumetol) in malaria patients. *British Journal of Clinical Pharmacology* **46,** 553–561. ISSN: 03065251 (Dec. 1998).

31. Tarning, J. *et al.* Population Pharmacokinetic and Pharmacodynamic Modeling of Amodiaquine and Desethylamodiaquine in Women with Plasmodium vivax Malaria during and after Pregnancy. *Antimicrobial Agents and Chemotherapy.* ISSN: 0066-4804. doi:10.1128/aac.01242-12 (2012).

32. Davis, T. M., Hung, T. Y., Sim, I. K., Karunajeewa, H. A. & Ilett, K. F. *Piperaquine: A resurgent antimalarial drug* 2005. doi:10.2165/00003495-200565010-00004. http://link.springer.com/10.2165/00003495-200565010-00004.

33. European Medicines Agency. *Assessment report Eurartesim* tech. rep. (EMA, London, 2011), 129. www.ema.europa.eu.

34. Trenholme, G. M. *et al.* Mefloquine (WR 142,490) in the treatment of human malaria. *Science* **190,** 792–794. ISSN: 00368075 (Nov. 1975).

35. Wells, S., Diap, G. & Kiechel, J. R. The story of artesunate-mefloquine (ASMQ), innovative partnerships in drug development: Case study. *Malaria Journal* **12,** 68. ISSN: 14752875 (Feb. 2013).

36. Premji, Z. G. Coartem°: The journey to the clinic. *Malaria Journal* **8,** S3. ISSN: 14752875 (Dec. 2009).

37. Sirima, S. B. & Gansané, A. Artesunate–amodiaquine for the treatment of uncomplicated malaria. *Expert Opinion on Investigational Drugs* **16,** 1079–1085. ISSN: 1354-3784 (July 2007).

38. Medicines for Malaria Venture. *ASAQ Winthrop® (artesunate-amodiaquine) | Medicines for Malaria Venture* https://www.mmv.org/access/products-projects/asaq-winthrop-artesunate-amodiaquine (2019).

39. Goldberg, D. E., Slater, A. F., Cerami, A. & Henderson, G. B. Hemoglobin degradation in the malaria parasite Plasmodium falciparum: an ordered process in a unique organelle. *Proceedings of the National Academy of Sciences of the United States of America* **87,** 2931–5. ISSN: 0027-8424 (Apr. 1990).

40. Slater, A. F. *et al.* An iron-carboxylate bond links the heme units of malaria pigment. *Proceedings of the National Academy of Sciences* **88,** 325–329. ISSN: 0027-8424 (Jan. 2006).

41. Combrinck, J. M. *et al.* Insights into the role of heme in the mechanism of action of antimalarials. *ACS Chemical Biology* **8,** 133–137. ISSN: 15548929 (Jan. 2013).

42. Kokwaro, G., Mwai, L. & Nzila, A. Artemether/lumefantrine in the treatment of uncomplicated falciparum malaria. *Expert Opinion on Pharmacotherapy* **8,** 75–94. ISSN: 1465-6566 (Jan. 2007).

43. Wong, W. *et al.* Mefloquine targets the Plasmodium falciparum 80S ribosome to inhibit protein synthesis. *Nature Microbiology* **2,** 17031. ISSN: 20585276 (June 2017).

44. Mwai, L. *et al.* Genome wide adaptations of Plasmodium falciparum in response to Lumefantrine selective drug pressure. *PLoS ONE* **7** (ed Beeson, J. G.) e31623. ISSN: 19326203 (Feb. 2012).

45. Meshnick, S. R. Artemisinin: mechanisms of action, resistance and toxicity. *International journal for parasitology* **32,** 1655–60. ISSN: 0020-7519 (Dec. 2002).

46. Meshnick, S. R. *et al.* Iron-dependent free radical generation from the antimalarial agent artemisinin (qinghaosu). *Antimicrobial Agents and Chemotherapy.* ISSN: 00664804. doi:10.1128/AAC.37.5.1108 (1993).

47. Klonis, N. *et al.* Artemisinin activity against Plasmodium falciparum requires hemoglobin uptake and digestion. *Proceedings of the National Academy of Sciences* **108,** 11405–11410. ISSN: 0027-8424 (July 2011).

48. Wang, J. *et al.* Haem-activated promiscuous targeting of artemisinin in Plasmodium falciparum. *Nature Communications* **6,** 10111. ISSN: 20411723 (Dec. 2015).

49. Cowman, A. & Foote, S. Chemotherapy and drug resistance in malaria. *International Journal for Parasitology* **20,** 503–513. ISSN: 0020-7519 (July 1990).

50. MOORE, D. V. & LANIER, J. E. Observations on two Plasmodium falciparum infections with an abnormal response to chloroquine. *The American journal of tropical medicine and hygiene* **10,** 5–9. ISSN: 0002-9637 (Jan. 1961).

51. Hanboonkunupakarn, B. & White, N. J. *The threat of antimalarial drug resistance* 2015. doi:10.1186/s40794-016-0027-8. http://www.ncbi.nlm.nih.gov/pubmed/28883954%20http://www.pubmedcentral.nih.gov/articlerender.fcgi?artid=PMC5530994.

52. Murray, C. J. *et al.* Global malaria mortality between 1980 and 2010: A systematic analysis. *The Lancet* **379,** 413–431. ISSN: 01406736 (Feb. 2012).

53. Wellems, T. E., Walker-Jonah, A. & Panton, L. J. Genetic mapping of the chloroquine-resistance locus on Plasmodium falciparum chromosome 7. *Proceedings of the National Academy of Sciences of the United States of America* **88,** 3382–6. ISSN: 0027-8424 (1991).

54. Mita, T. *et al.* Limited geographical origin and global spread of sulfadoxine-resistant dhps alleles in plasmodium falciparum populations. *Journal of Infectious Diseases* **204,** 1980–1988. ISSN: 00221899 (Dec. 2011).

55. Roper, C. *et al.* Intercontinental spread of pyrimethamine-resistant malaria. *Science.* ISSN: 00368075. doi:10.1126/science.1098876 (2004).

56. World Health Organization. *WHO Malaria Report 2015* tech. rep. (WHO, 2015), 280. doi:ISBN9789241564403. arXiv: arXiv:1011.1669v3. http://www.who.int/malaria/visual-refresh/en/.

57. Dondorp, A. M. *et al.* Artemisinin Resistance in Plasmodium falciparum Malaria. *New England Journal of Medicine* **361,** 455–467. ISSN: 0028-4793 (July 2009).

58. Noedl, H. *et al.* Evidence of Artemisinin-Resistant Malaria in Western Cambodia. *New England Journal of Medicine.* ISSN: 0028-4793. doi:10.1056/nejmc0805011 (2008).

59. Dondorp, A. M. *et al.* The Threat of Artemisinin-Resistant Malaria. *New England Journal of Medicine* **365,** 1073–1075. ISSN: 0028-4793 (Sept. 2011).

60. WHO. *Global plan for artemisinin resistance containment. Acessible in http://www.who.int/malaria/publications/atoz/artemisinin_resistance_containment_2011.pdf* tech. rep. (Geneva, 2011), 93. http://www.wpro.who.int/mvp/artemisinin%7B%5C_%7Dresistance%7B%5C_%7Dcontainment%7B%5C_%7D2011.pdf.

61. Leang, R. *et al.* Efficacy of dihydroartemisinin-piperaquine for treatment of uncomplicated plasmodium falciparum and plasmodium vivax in Cambodia, 2008 to 2010. *Antimicrobial Agents and Chemotherapy* **57,** 818–826. ISSN: 00664804 (Feb. 2013).

62. Leang, R. *et al.* Evidence of Plasmodium falciparum Malaria Multidrug Resistance to Artemisinin and Piperaquine in Western Cambodia: Dihydroartemisinin-Piperaquine Open-Label Multicenter Clinical Assessment. *Antimicrobial Agents and Chemotherapy* **59,** 4719–4726. ISSN: 0066-4804 (Aug. 2015).

63. World Health Organization. *Artemisinin and artemisinin-based combination therapy resistance* tech. rep. April (2016), 1–8. https://apps.who.int/iris/bitstream/handle/10665/208820/WHO%7B%5C_%7DHTM%7B%5C_%7DGMP%7B%5C_%7D2016.5%7B%5C_%7Deng.pdf?sequence=1%7B%5C&%7DisAllowed=y%20http://apps.who.int/iris/bitstream/10665/208820/1/WHO%7B%5C_%7DHTM%7B%5C_%7DGMP%7B%5C_%7D2016.5%7B%5C_%7Deng.pdf?ua=1.

64. Woodrow, C. J. *et al.* Spread of Artemisinin Resistance in Plasmodium falciparum Malaria. *New England Journal of Medicine.* ISSN: 0028-4793. doi:10.1056/nejmoa1314981 (2014).

65. Imwong, M., Hien, T. T., Thuy-Nhien, N. T., Dondorp, A. M. & White, N. J. Spread of a single multidrug resistant malaria parasite lineage (PfPailin) to Vietnam. *The Lancet Infectious Diseases* **17,** 1022–1023. ISSN: 14733099 (Oct. 2017).

66. Ashley, E. A. & Phyo, A. P. Drugs in Development for Malaria. *Drugs* **78,** 861–879. ISSN: 1179-1950 (2018).

67. Tse, E. G., Korsik, M. & Todd, M. H. The past, present and future of anti-malarial medicines. *Malaria Journal.* ISSN: 14752875. doi:10.1186/s12936-019-2724-z (2019).

68. Dini, S. *et al.* Investigating the Efficacy of Triple Artemisinin-Based Combination Therapies for Treating Plasmodium falciparum Malaria Patients Using Mathematical Modeling. *Antimicrobial Agents and Chemotherapy* **62.** ISSN: 0066-4804. doi:10.1128/aac.01068-18. http://www.ncbi.nlm.nih.gov/pubmed/30150462%20http://www.pubmedcentral.nih.gov/articlerender.fcgi?artid=PMC6201091 (Nov. 2018).

69. Lowe, R. & Montagu, D. Legislation, regulation and consolidation in the retail pharmacy sector in low-income countries. *Southern Med Review* (2009).

70. Res, P. Social and cultural complexities of anti-malarial drug circulation: An ethnographic investigation in three rural remote communes of Cambodia. *Malaria Journal.* ISSN: 14752875. doi:10.1186/s12936-017-2082-7 (2017).

71. Banek, K., Lalani, M., Staedke, S. G. & Chandramohan, D. Adherence to artemisinin-based combination therapy for the treatment of malaria: A systematic review of the evidence. *Malaria Journal.* ISSN: 14752875. doi:10.1186/1475-2875-13-7 (2014).

72. Bruxvoort, K., Goodman, C., Patrick Kachur, S. & Schellenberg, D. *How patients take malaria treatment: A systematic review of the literature on adherence to antimalarial drugs* 2014. doi:10.1371/journal.pone.0084555. www.plosone.org.

73. Hodel, E. M. *et al.* Residual Antimalarial Concentrations before Treatment in Patients with Malaria from Cambodia: Indication of Drug Pressure. *The Journal of Infectious Diseases.* ISSN: 0022-1899. doi:10.1086/655779 (2010).

74. Hodel, E. M. *et al.* Residual antimalarials in malaria patients from Tanzania - Implications on drug efficacy assessment and spread of parasite resistance. *PLoS ONE* **4** (ed Myer, L.) e8184. ISSN: 19326203 (Dec. 2009).

75. Nwanyanwu, O. C. *et al.* Validity of mother's history regarding antimalarial drug use in Malawian children under five years old. *Transactions of the Royal Society of Tropical Medicine and Hygiene* **90,** 66–68. ISSN: 00359203 (1996).

76. Hildenwall, H. *et al.* Low validity of caretakers' reports on use of selected antimalarials and antibiotics in children with severe pneumonia at an urban hospital in Uganda. *Transactions of the Royal Society of Tropical Medicine and Hygiene* **103,** 95–101. ISSN: 00359203 (Jan. 2009).

77. Gallay, J. *et al.* LC–MS/MS method for the simultaneous analysis of seven antimalarials and two active metabolites in dried blood spots for applications in field trials: Analytical and clinical validation. *Journal of Pharmaceutical and Biomedical Analysis* **154,** 263–277. ISSN: 1873264X (May 2018).

78. Lindegardh, N., Annerberg, A., White, N. & Day, N. Development and validation of a liquid chromatographic-tandem mass spectrometric method for determination of piperaquine in plasma. *Journal of Chromatography B* **862,** 227–236. ISSN: 15700232 (Feb. 2007).

79. Silva, A. V., Mwebaza, N., Ntale, M., Gustafsson, L. L. & Pohanka, A. A fast and sensitive method for quantifying lumefantrine and desbutyl-lumefantrine using LC-MS/MS. *Journal of Chromatography B: Analytical Technologies in the Biomedical and Life Sciences* **1004,** 60–66. ISSN: 1873376X (Nov. 2015).

80. Chen, X., Deng, P., Dai, X. & Zhong, D. Simultaneous determination of amodiaquine and its active metabolite in human blood by ion-pair liquid chromatography-tandem mass spectrometry. *Journal of Chromatography B: Analytical Technologies in the Biomedical and Life Sciences* **860,** 18–25. ISSN: 15700232 (Dec. 2007).

81. Hilhorst, M. J. *et al.* A high-performance liquid chromatography-tandem mass spectrometry method for the determination of artemether and dihydroartemisinin in human plasma. *Journal of Chromatography B: Analytical Technologies in the Biomedical and Life Sciences* **965,** 45–53. ISSN: 1873376X (Aug. 2014).

82. Wiesner, L., Govender, K., Meredith, S. A., Norman, J. & Smith, P. J. A liquid-liquid LC/MS/MS assay for the determination of artemether and DHA in malaria patient samples. *Journal of Pharmaceutical and Biomedical Analysis* **55,** 373–378. ISSN: 07317085 (May 2011).

83. Hodel, E. M. *et al.* A single LC-tandem mass spectrometry method for the simultaneous determination of 14 antimalarial drugs and their metabolites in human plasma. *Journal of Chromatography B: Analytical Technologies in the Biomedical and Life Sciences* **877,** 867–886. ISSN: 15700232 (Apr. 2009).

84. Blessborn, D., Romsing, S., Bergqvist, Y. & Lindegardh, N. Assay for screening for six antimalarial drugs and one metabolite using dried blood spot sampling, sequential extraction and ion-trap detection. *Bioanalysis* **2,** 1839–1847. ISSN: 17576180 (Nov. 2010).

85. World Health Organization. WHO Global Surveillance and Monitoring System for substandard and falsified medical products. *WHO,* 1–73 (2017).

86. Tabernero, P., Fernández, F. M., Green, M., Guerin, P. J. & Newton, P. N. Mind the gaps - The epidemiology of poor-quality anti-malarials in the malarious world - Analysis of the WorldWide Antimalarial Resistance Network database. *Malaria Journal* **13,** 139. ISSN: 14752875 (Apr. 2014).

87. Nayyar, G. M., Breman, J. G., Newton, P. N. & Herrington, J. *Poor-quality antimalarial drugs in southeast Asia and sub-Saharan Africa* 2012. doi:10.1016/S1473-3099(12)70064-6.

88. WHO. *A study on the public health and socioeconomic impact of substandard and falsified medical products* tech. rep. (2017), 38. doi:/entity/medicines/regulation/ssffc/publications/se-study-sf/en/index.html. arXiv: 978-92-4-151343-2. http://apps.who.int/bookorders.%20http://apps.who.int/bookorders.%7B%5C%7D0Ahttps://www.who.int/medicines/regulation/ssffc/publications/se-study-sf/en/.

89. Chaccour, C., Kaur, H. & Del Pozo, J. L. *Falsified antimalarials: A minireview* 2015. doi:10.1586/14787210.2015.1015990. https://www.tandfonline.com/action/journalInformation?journalCode=ierz20.

90. Vickers, S. *et al. Field detection devices for screening the quality of medicines: A systematic review* 2018. doi:10.1136/bmjgh-2018-000725.

91. Ioset, J. R. & Kaur, H. Simple field assays to check quality of current artemisinin-based antimalarial combination formulations. *PLoS ONE* **4** (ed Pan, X.) e7270. ISSN: 19326203 (Sept. 2009).

92. Green, M. D. *et al.* Use of refractometry and colorimetry as field methods to rapidly assess antimalarial drug quality. *Journal of Pharmaceutical and Biomedical Analysis* **43,** 105–110. ISSN: 07317085 (Jan. 2007).

93. Batson, J. C. S. *et al.* Assessment of the effectiveness of the CD3+ tool to detect counterfeit and substandard anti-malarials. *Malaria Journal* **15,** 119. ISSN: 14752875 (Feb. 2016).

94. He, L. *et al.* Development of a colloidal gold-based lateral flow dipstick immunoassay for rapid qualitative and semi-quantitative analysis of artesunate and dihydroartemisinin. *Malaria Journal* **13,** 127. ISSN: 14752875 (Mar. 2014).

95. Weaver, A. A. & Lieberman, M. Paper Test Cards for Presumptive Testing of Very Low Quality Antimalarial Medications. *The American Journal of Tropical Medicine and Hygiene* **92,** 17–23. ISSN: 0002-9637 (June 2015).

96. Visser, B. J. *et al.* Assessing the quality of anti-malarial drugs from Gabonese pharmacies using the MiniLab®: A field study. *Malaria Journal* **14,** 273. ISSN: 14752875 (Dec. 2015).

97. Kaur, H., Green, M. D., Hostetler, D. M., Fernández, F. M. & Newton, P. N. *Antimalarial drug quality: Methods to detect suspect drugs* 2010. doi:10.2217/thy.09.84. www.futuremedicine.com.

98. Myers, N. M., Kernisan, E. N. & Lieberman, M. Lab on Paper: Iodometric Titration on a Printed Card. *Analytical Chemistry.* ISSN: 15206882. doi:10.1021/ac504269q (2015).

99. AD, E. & JW, S. In vitro selection of RNA molecules that bind specific ligands. *Nature* **346,** 818–22. ISSN: 0028-0836 (1990).

100. Tuerk, C. & Gold, L. Systematic evolution of ligands by exponential enrichment: RNA ligands to bacteriophage T4 DNA polymerase. *Science* **249,** 505–510. ISSN: 00368075 (Aug. 1990).

101. Morris, K. N., Jensen, K. B., Julin, C. M., Weil, M. & Gold, L. High affinity ligands from in vitro selection: complex targets. *Proceedings of the National Academy of Sciences* **95,** 2902–7. ISSN: 0027-8424 (Mar. 1998).

102. Mayer, G. *et al.* Fluorescence-activated cell sorting for aptamer SELEX with cell mixtures. *Nature Protocols.* ISSN: 17542189. doi:10.1038/nprot.2010.163 (2010).

103. Mosing, R. K. & Bowser, M. T. Isolating aptamers using capillary electrophoresis-SELEX (CE-SELEX). *Methods in Molecular Biology.* ISSN: 10643745. doi:10.1007/978-1-59745-557-2_3 (2009).

104. Lou, X. *et al.* Micromagnetic selection of aptamers in microfluidic channels. *Proceedings of the National Academy of Sciences* **106,** 2989–2994. ISSN: 0027-8424 (2009).

105. Nutiu, R. & Li, Y. Structure-switching signaling aptamers. *Journal of the American Chemical Society* **125,** 4771–4778. ISSN: 00027863 (2003).

106. Ruscito, A. & DeRosa, M. C. Small-Molecule Binding Aptamers: Selection Strategies, Characterization, and Applications. *Frontiers in Chemistry* **4,** 14 (2016).

107. Kim, Y. S. & Gu, M. B. Advances in aptamer screening and small molecule aptasensors. *Advances in Biochemical Engineering/Biotechnology.* ISSN: 07246145. doi:10.1007/10_2013_225 (2014).

108. Kusser, W. Chemically modified nucleic acid aptamers for in vitro selections: evolving evolution. *Reviews in Molecular Biotechnology* **74,** 27–38. ISSN: 13890352 (Mar. 2002).

109. Gold, L. *et al.* Aptamer-based multiplexed proteomic technology for biomarker discovery. *PLoS ONE* **5** (ed Gelain, F.) e15004. ISSN: 19326203 (Dec. 2010).

110. Ruff, K. M., Snyder, T. M. & Liu, D. R. Enhanced functional potential of nucleic acid aptamer libraries patterned to increase secondary structure. *Journal of the American Chemical Society* **132,** 9453–9464. ISSN: 00027863 (July 2010).

111. Mascini, M. *Aptamers in Bioanalysis* 1–313. ISBN: 9780470148303. doi:10.1002/9780470380772 (John Wiley & Sons, 2008).

112. McKeague, M. & DeRosa, M. C. Challenges and Opportunities for Small Molecule Aptamer Development. *Journal of Nucleic Acids* **2012,** 1–20. ISSN: 2090-0201 (2012).

113. Cheung, Y.-W. *et al.* Structural basis for discriminatory recognition of Plasmodium lactate dehydrogenase by a DNA aptamer. *Proceedings of the National Academy of Sciences* **110,** 15967–15972. ISSN: 0027-8424 (Oct. 2013).

114. D. Jayasena, S. Aptamers: An emerging class of molecules that rival antibodies in diagnostics. *Clinical Chemistry* **45,** 1628–1650. ISSN: 00099147 (1999).

115. Jenison, R. D., Gill, S. C., Pardi, A. & Polisky, B. High-resolution molecular discrimination by RNA. *Science.* ISSN: 00368075. doi:10.1126/science.7510417 (1994).

116. Shoji, A., Kuwahara, M., Ozaki, H. & Sawai, H. Modified DNA aptamer that binds the (R)-isomer of a thalidomide derivative with high enantioselectivity. *Journal of the American Chemical Society* **129,** 1456–1464. ISSN: 00027863 (2007).

117. Michaud, M. *et al.* A DNA aptamer as a new target-specific chiral selector for HPLC. *Journal of the American Chemical Society* **125,** 8672–8679. ISSN: 00027863 (2003).

118. Geiger, A., Burgstaller, P., von der Eltz, H., Roeder, A. & Famulok, M. RNA aptamers that bind L-arginine with sub-micromolar dissociation constants and high enantioselectivity. *Nucleic Acids Research* **24,** 1029–36. ISSN: 0305-1048 (Mar. 1996).

119. Vavvas, D. & D'Amico, D. J. *Pegaptanib (Macugen): Treating Neovascular Age-Related Macular Degeneration and Current Role in Clinical Practice* Sept. 2006. doi:10.1016/j.ohc.2006.05.008. http://www.ncbi.nlm.nih.gov/pubmed/16935210.

120. Zhou, J. & Rossi, J. *Aptamers as targeted therapeutics: Current potential and challenges* Mar. 2017. doi:10.1038/nrd.2016.199. http://www.nature.com/articles/nrd.2016.199.

121. Huang, Y. F. *et al.* Molecular assembly of an aptamer-drug conjugate for targeted drug delivery to tumor cells. *ChemBioChem* **10,** 862–868. ISSN: 14394227 (Mar. 2009).

122. Wang, R. *et al.* Automated modular synthesis of Aptamer-drug conjugates for targeted drug delivery. *Journal of the American Chemical Society* **136,** 2731–2734. ISSN: 00027863 (Feb. 2014).

123. Wan, W.-L., Liao, Z.-X., Chuang, E.-Y., Lin, C.-C. & Sung, H.-W. An aptamer-conjugated liposomal system containing a bubble-generating agent for tumor-specific chemotherapy overcoming multidrug resistance. *Nanomedicine: Nanotechnology, Biology and Medicine.* ISSN: 15499634. doi:10.1016/j.nano.2015.12.098 (2016).

124. Wang, Q. *et al.* Screening of DNA aptamers against myoglobin using a positive and negative selection units integrated microfluidic chip and its biosensing application. *Analytical Chemistry* **86,** 6572–6579. ISSN: 15206882 (July 2014).

125. Zhu, Q., Liu, G., Kai, M. & Miller, A. O. *DNA aptamers in the diagnosis and treatment of human diseases* Nov. 2015. doi:10.3390/molecules201219739. http://www.ncbi.nlm.nih.gov/pubmed/26610462%20http://www.pubmedcentral.nih.gov/articlerender.fcgi?artid=PMC6332121.

126. Wang, Y. *et al.* DNA aptamer evolved by cell-SELEX for recognition of prostate cancer. *PLoS ONE* **9** (ed D'Auria, S.) e100243. ISSN: 19326203 (June 2014).

127. Xu, J. *et al.* Molecular recognition of human liver cancer cells using DNA aptamers generated via cell-SELEX. *PLoS ONE* **10,** e0125863. ISSN: 19326203 (2015).

128. Li, X. *et al.* Evolution of DNA aptamers through in vitro metastatic-cell-based systematic evolution of ligands by exponential enrichment for metastatic cancer recognition and imaging. *Analytical Chemistry* **87,** 4941–4948. ISSN: 15206882 (May 2015).

129. Cheng, A. K., Sen, D. & Yu, H. Z. Design and testing of aptamer-based electrochemical biosensors for proteins and small molecules. *Bioelectrochemistry* **77,** 1–12. ISSN: 15675394 (Nov. 2009).

130. Wang, R. E., Zhang, Y., Cai, J., Cai, W. & Gao, T. Aptamer-based fluorescent biosensors. *Current medicinal chemistry* **18,** 4175–84. ISSN: 1875-533X (2011).

131. Alsager, O. A., Alotaibi, K. M., Alswieleh, A. M. & Alyamani, B. J. Colorimetric Aptasensor of Vitamin D3: A Novel Approach to Eliminate Residual Adhesion between Aptamers and Gold Nanoparticles. *Scientific Reports* **8,** 12947. ISSN: 20452322 (Aug. 2018).

132. Li, H. & Rothberg, L. Colorimetric detection of DNA sequences based on electrostatic interactions with unmodified gold nanoparticles. *Proceedings of the National Academy of Sciences* **101,** 14036–14039. ISSN: 0027-8424 (Sept. 2004).

133. Wei, H., Li, B., Li, J., Wang, E. & Dong, S. Simple and sensitive aptamer-based colorimetric sensing of protein using unmodified gold nanoparticle probes. *Chemical Communications* **0,** 3735–3737. ISSN: 13597345 (Sept. 2007).

134. Sharma, A. K., Kent, A. D. & Heemstra, J. M. Enzyme-linked small-molecule detection using split aptamer ligation. *Analytical Chemistry* **84,** 6104–6109. ISSN: 00032700 (July 2012).

135. Baker, B. R. *et al.* An electronic, aptamer-based small-molecule sensor for the rapid, label-free detection of cocaine in adulterated samples and biological fluids. *Journal of the American Chemical Society.* ISSN: 00027863. doi:10.1021/ja056957p (2006).

136. Li, B., Du, Y., Wei, H. & Dong, S. Reusable, label-free electrochemical aptasensor for sensitive detection of small molecules. *Chemical Communications.* ISSN: 13597345. doi:10.1039/b707057h (2007).

137. Stoltenburg, R., Reinemann, C. & Strehlitz, B. FluMag-SELEX as an advantageous method for DNA aptamer selection. *Analytical and Bioanalytical Chemistry* **383,** 83–91. ISSN: 16182642 (Sept. 2005).

138. Nutiu, R. & Li, Y. In vitro selection of structure-switching signaling aptamers. *Angewandte Chemie - International Edition* **44,** 1061–1065. ISSN: 14337851 (Feb. 2005).

139. Hamaguchi, N., Ellington, A. & Stanton, M. Aptamer beacons for the direct detection of proteins. *Analytical Biochemistry.* ISSN: 00032697. doi:10.1006/abio.2001.5169 (2001).

140. Weigl, B. H. *et al.* The value of clinical needs assessments for point-of-care diagnostics. *Point of Care* **11,** 108–113. ISSN: 1533029X (June 2012).

141. Stoltenburg, R., Nikolaus, N. & Strehlitz, B. Capture-SELEX: Selection of DNA aptamers for aminoglycoside antibiotics. *Journal of Analytical Methods in Chemistry* **1,** 415697. ISSN: 20908865 (Dec. 2012).

142. Yang, K. A., Pei, R. & Stojanovic, M. N. *In vitro selection and amplification protocols for isolation of aptameric sensors for small molecules* 2016. doi:10.1016/j.ymeth.2016.04.032. http://www.ncbi.nlm.nih.gov/pubmed/27155227%20http://www.pubmedcentral.nih.gov/articlerender.fcgi?artid=PMC4981533.

143. Shaikh, M. M., Bhutiya, P. L. & Chikhalia, K. H. Modified Sonogashira Coupling Strategy For the Functionalization of Substituted Quinoline. *ChemistrySelect.* ISSN: 23656549. doi:10.1002/slct.201700137 (2017).

144. Zuker, M. Mfold web server for nucleic acid folding and hybridization prediction. *Nucleic acids research* **31,** 3406–15. ISSN: 1362-4962 (July 2003).

145. Corpet, F. Multiple sequence alignment with hierarchical clustering. *Nucleic acids research* **16,** 10881–90. ISSN: 0305-1048 (Nov. 1988).

146. Cole, K. H. & Lupták, A. High-throughput methods in aptamer discovery and analysis. *Methods in Enzymology* **621,** 329–346 (Jan. 2019).

147. Jansen, F. H. The pharmaceutical death-ride of dihydroartemisinin. *Malaria journal* **9,** 212. ISSN: 1475-2875 (July 2010).

148. Maria Hodel, E., Kaur, H. & Terlouw, D. J. Stability of dihydroartemisinin-piperaquine tablet halves during prolonged storage under tropical conditions. *American Journal of Tropical Medicine and Hygiene* **96,** 338–340. ISSN: 00029637 (2017).

149. Ashley, E. A. *et al.* Comparison of plasma, venous and capillary blood levels of piperaquine in patients with uncomplicated falciparum malaria. *European journal of clinical pharmacology* **66,** 705–12. ISSN: 1432-1041 (July 2010).

150. Yusmaidie Aziz, M. *Piperaquine and Metabolites Bioanalysis and Pharmacokinetics* PhD thesis (2017). ISBN: 9789162902520. https://gupea.ub.gu.se/bitstream/2077/52861/4/gupea%7B%5C_%7D2077%7B%5C_%7D52861%7B%5C_%7D4.pdf.

151. Karbwang, J. & White, N. J. Clinical Pharmacokinetics of Mefloquine. *Clinical Pharmacokinetics* **19,** 264–279. ISSN: 0312-5963 (Oct. 1990).

152. Olafuyi, O., Coleman, M. & Badhan, R. K. The application of physiologically based pharmacokinetic modelling to assess the impact of antiretroviral-mediated drug-drug interactions on piperaquine antimalarial therapy during pregnancy. *Biopharmaceutics & Drug Disposition* **38,** 464–478. ISSN: 01422782 (Nov. 2017).

153. Gonzalez-Quintela, A. *et al.* Serum levels of immunoglobulins (IgG, IgA, IgM) in a general adult population and their relationship with alcohol consumption, smoking and common metabolic abnormalities. *Clinical and Experimental Immunology* **151,** 42–50. ISSN: 00099104 (Jan. 2008).

154. Wolfbeis, O. S. & Leiner, M. *MAPPING OF THE TOTAL FLUORESCENCE OF HUMAN BLOOD SERUM AS A NEW METHOD FOR ITS CHARACTERIZATION* tech. rep. (1985), 203–215. https://ac.els-cdn.com/S0003267000844220/1-s2.0-S0003267000844220-main.pdf?%7B%5C_%7Dtid=d469c8d2-70c6-4e5b-9c7f-609531a78a29%7B%5C&%7Dacdnat=1552420050%7B%5C_%7D286751325fff98082e388ba3a2492f5e.

155. Fernández, F. M. *et al.* Characterization of Solid Counterfeit Drug Samples by Desorption Electrospray Ionization and Direct-analysis-in-real-time Coupled to Time-of-flight Mass Spectrometry. *ChemMedChem* **1,** 702–705. ISSN: 1860-7179 (July 2006).